

Studies in strongly coupled quantum field theories and renormalization group flows

Thèse N° 9660

Présentée le 22 août 2019

à la Faculté des sciences de base
Laboratoire de physique théorique des particules
Programme doctoral en physique

pour l'obtention du grade de Docteur ès Sciences

par

Bernardo ZAN

Acceptée sur proposition du jury

Prof. F. Carbone, président du jury
Prof. R. Rattazzi, Prof. V. Rychkov, directeurs de thèse
Prof. E. Kiritsis, rapporteur
Dr A. Zhiboedov, rapporteur
Prof. J. Penedones, rapporteur

2019



Abstract

This thesis presents studies in strongly coupled Renormalization Group (RG) flows. In the first part, we analyze the subject of non-local Conformal Field Theories (CFTs), arising as continuous phase transitions of statistical models with long-range interactions. Specifically, we study the critical long-range Ising model in a general number of dimension: first we show that it is conformally invariant, and then we study in depth the different regimes of the theory. We find an example of an infrared duality, to our knowledge the first non-local example of such phenomenon.

The second part of the thesis deals with walking theories and weakly first order phase transitions, meaning Quantum Field Theories that show approximate scale invariance over a range of energies, in a general number of dimensions. We discuss several example in the high energy as well as the statistical mechanics literature, and show that these theories can be understood as an RG flow passing between two complex CFTs, i.e. non-unitary theories living at complex values of the couplings. Combining the conformal data of these complex CFTs and conformal perturbation theory, we describe observables of the walking theory. Finally, we give the explicit example of the two dimensional Potts model with more than four states.

Keywords: Quantum Field Theory, Conformal Field Theory, Phase Transitions, Long-range Interactions, Walking

Riassunto

In questa tesi ci occuperemo di alcuni flussi fortemente accoppiati del gruppo di rinormalizzazione (RG). Nella prima parte tratteremo l'argomento delle teorie di campo conformi (CFT) non locali, che descrivono transizioni di fase continue per modelli statistici con interazioni a lungo raggio. Nello specifico, studieremo il modello di Ising a lungo raggio al punto critico, in un numero di dimensioni generiche: mostreremo che è invariante conforme, e successivamente studieremo in dettaglio i vari regimi della teoria. Troveremo un esempio di dualità infrarossa, che, a nostra conoscenza, è il primo esempio non locale di tale fenomeno.

Nella seconda parte della tesi tratteremo l'argomento delle *walking theories* e le transizioni di fase debolmente di primo ordine in un numero generico di dimensioni. Queste sono teorie quantistiche di campo che presentano un'invarianza di scala approssimativa in un determinato intervallo di energie. Presenteremo diversi esempi sia nel campo della fisica delle alte energie che della meccanica statistica e mostreremo che queste teorie possono essere viste come un flusso di RG che passa in mezzo a due CFT complesse, teorie non unitarie con costanti di accoppiamento complesse. Utilizzando il *conformal data* delle CFT complesse e la teoria di perturbazione conforme, calcoleremo alcune osservabili della *walking theory*. Infine considereremo l'esempio esplicito del modello di Potts bidimensionale con più di quattro stati.

Parole chiave: Teorie Quantistiche di Campo, Teorie di Campo Conformi, Transizioni di Fase, Interazioni a Lungo Raggio, Walking

Foreword

This thesis is based on four published papers.

- Chapter 1 is based on:
M. F. Paulos, S. Rychkov, B. C. van Rees, and B. Zan, “Conformal Invariance in the Long-Range Ising Model,” *Nucl. Phys.* **B902** (2016) 246–291, [arXiv:1509.00008 \[hep-th\]](#)
- Chapter 2 is based on:
C. Behan, L. Rastelli, S. Rychkov, and B. Zan, “A scaling theory for the long-range to short-range crossover and an infrared duality,” *J. Phys.* **A50** no. 35, (2017) 354002, [arXiv:1703.05325 \[hep-th\]](#)
- Chapter 3 is based on:
V. Gorbenko, S. Rychkov, and B. Zan, “Walking, Weak first-order transitions, and Complex CFTs,” *JHEP* **10** (2018) 108, [arXiv:1807.11512 \[hep-th\]](#)
- Chapter 4 is based on:
V. Gorbenko, S. Rychkov, and B. Zan, “Walking, Weak first-order transitions, and Complex CFTs II. Two-dimensional Potts model at $Q > 4$,” *SciPost Phys.* **5** no. 5, (2018) 050, [arXiv:1808.04380 \[hep-th\]](#)

Some of the material presented here does not appear in the original papers, notably the discussion about holographic QCD in section 3.4.4 and the discussion on how to obtain OPE coefficients using crossing symmetry for the two dimensional Potts model in section 4.4.

Contents

Abstract (English)	iii
Abstract (Italian)	v
Foreword	vii
Introduction	1
I Non-local CFTs	9
1 Conformality of the critical Long Range Ising model	11
1.1 Introduction	11
1.2 Field-theoretical setup	14
1.3 Tests of conformal invariance	17
1.3.1 $\langle \phi \phi^3 \rangle$	19
1.3.1.1 Explicit computation	19
1.3.1.2 General argument	22
1.3.2 $\langle \phi^2 \phi^4 \rangle$	25
1.4 Conformal invariance of the gaussian phase	26
1.4.1 Direct argument	26
1.4.2 Argument from correlation functions	27
1.4.3 Caffarelli-Silvestre trick	27
1.5 Conformal invariance of the LRI critical point	29
1.5.1 Ward identities	29
1.5.2 Beyond perturbation theory	33
1.5.2.1 Virial currents	33
1.5.2.2 Conformality of LRI beyond perturbation theory	34
1.6 Discussion	35
2 The long-range to short-range crossover	39
2.1 Introduction	39
2.1.1 Our picture	41
2.1.2 Outline	43
2.2 Beta-function	43

Contents

2.2.1	Beta-function: $d = 2$	47
2.2.2	Beta-function: $d = 3$	49
2.2.3	Fixed point existence	50
2.3	Anomalous dimensions	51
2.3.1	Results: $d = 2$	53
2.3.1.1	χ, σ and \mathcal{O}	53
2.3.1.2	ε	55
2.3.1.3	$T_{\mu\nu}$	55
2.3.2	Results: $d = 3$	59
2.3.2.1	ε	59
2.3.2.2	$T_{\mu\nu}$	60
2.4	Infrared duality	61
2.4.1	All-order conjectures about the $\sigma\chi$ -flow	61
2.4.2	Duality interpretation	63
2.5	Discussion	65
II Walking theories		69
3	Walking, weak first order phase transitions and complex CFTs	71
3.1	Introduction	71
3.2	Walking as a mechanism for hierarchy	73
3.2.1	Tuning	73
3.2.2	Walking	74
3.2.2.1	Introducing complex CFTs	77
3.2.2.2	Naturalness of walking	78
3.3	Walking in statistical physics: 2d Potts model	78
3.3.1	Spin and cluster definitions	79
3.3.2	Phase transition	80
3.3.3	Symmetry	81
3.3.4	Weakly first-order phase transition at $Q \gtrsim 4$ and walking	82
3.3.5	Lessons and questions	84
3.4	Walking in high energy physics: 4d gauge theories	85
3.4.1	Walking and the electroweak phenomenology beyond the Standard Model	88
3.4.2	Light dilaton?	89
3.4.3	Other possibilities for the end of conformal window	91
3.4.4	The conformal window in holographic QCD	94
3.5	Deconfined criticality: a further example of walking?	95
3.6	Complex CFTs	97
3.6.1	Real vs complex QFTs	98
3.6.1.1	RG evolution	98
3.6.1.2	Correlation functions	99
3.6.1.3	Examples	100

3.6.2	Real vs complex CFTs	100
3.6.2.1	Examples	101
3.6.3	Complex CFTs and walking	103
3.7	Conclusions	106
4	The $Q > 4$ Potts model	107
4.1	Introduction	107
4.2	2d Potts model for $Q \leq 4$	108
4.2.1	Lattice transfer matrix and local operators	109
4.2.2	Symmetry	112
4.2.3	Height representation	112
4.2.4	Long cylinder partition function and the Coulomb gas	115
4.2.5	Torus partition function	117
4.2.6	Spectrum of primaries for $Q \leq 4$	119
4.3	Analytic continuation to $Q > 4$	124
4.4	Walking RG flow in $Q > 4$ Potts models	127
4.4.1	One-loop beta-function	129
4.4.2	Im-flip for other operators	132
4.4.3	Drifting scaling dimensions	133
4.4.4	Two-loop beta-function	137
4.4.5	General arguments about the real flow	139
4.4.6	The range of Q for which the walking behavior persists	139
4.5	Conclusions	141
	Conclusions and outlook	143
	III Appendices	145
	A Further facts about the Long Range Ising model	147
A.1	Relative normalization of the ϕ and ϕ^3 OPE coefficients	147
A.2	Selected prior work on the long-range Ising model	149
A.2.1	Physics	149
A.2.2	Rigorous results	150
	B Further facts about walking	151
B.1	Tuning and weakly first-order phase transitions	151
B.2	Walking vs BKT transition	153
B.3	Walking in large- N theories	155
	C Further facts about the Potts model	159
C.1	'Breakdown' of Landau-Ginzburg paradigm	159
C.2	First-order phase transition at large Q	160
C.3	Generalization to $d > 2$	161

Contents

C.4	Representations of S_Q and the operator spectrum	161
C.5	$Q = 4$ Potts model as an orbifold free boson	164
D	Technicalities	167
D.1	Integrals for γ_ε and γ_T	167
	Bibliography	171
	Acknowledgements	187

Introduction

The framework of Quantum Field Theory (QFT) is ubiquitous in modern theoretical physics. It is used in particle physics as a way of combining quantum mechanics and special relativity, with the Standard Model being its most famous successful example. QFT finds many applications in the context of condensed matter and statistical physics as well, as a way to describe collective excitations of systems with many degrees of freedom, both at zero and at finite temperature.

Studying a given QFT is in general a very hard problem. A clear exception are free theories, where all physical observables are easy to compute. Such theories are trivial, but serve as a first step to study theories where particles interact in a weak manner. These theories are close to being free, and we can find observables as perturbative series in terms of the small couplings of the theory. While there are weakly coupled QFTs which are relevant for real world applications, many systems are described by strongly coupled theories, where the couplings are in general of order one. Here, perturbation theory breaks down and we are back to the original question: what can we say about the observables of this QFT?

Symmetries can come to our rescue. The presence of a symmetry in a system leads to many constraints which can incredibly simplify its structure, and, therefore, our work. The example that is most relevant to this thesis is conformal symmetry.

The renormalization group and its fixed points

Looking at a system from different length (or energy) scales gives us potentially very different pictures. One of the most notorious examples in particle physics is Quantum Chromodynamics (QCD). At high energies, it is a theory of weakly interacting quarks and gluons, but, as we lower the energy scale the coupling becomes stronger and stronger. At low energies, it becomes a theory of hadrons.

The dependence of a QFT on the energy scale is the object of study of the Renormalization Group (RG). We can parametrize a theory by its couplings, and imagine that, by changing the energy scale, we set out a flow, called RG flow, in this coupling space. A special role is played by the fixed points of these RG flows: here the theory is scale invariant. This has many implications, among which is the absence of a characteristic length scale. This means, for

example, that a scale invariant theory cannot have massive particles in it, since the mass of this particle would define a characteristic length scale, i.e. its Compton wavelength.

Another surprising feature of these fixed points is that, very often, we get more symmetries than we asked for. These theories are often invariant under special conformal transformation as well, see figure 1. It has been shown that this always happens for unitary theories in two spacetime dimensions [5], and progress was made in four dimensions [6, 7], but there is no argument for theories living in a general number of dimensions. Yet, it is surprisingly common to have scale invariance implying conformal invariance, and if this is the case, our theory is a Conformal Field Theory (CFT).

We can imagine many UV-complete QFTs as flows that start from some CFT_{UV} and can, at low energy, either flow to another CFT_{IR} or to a gapped phase (which can be thought of as an empty CFT), see figure 2.¹ If CFT_{UV} is a free theory, then we can use perturbation theory to describe the RG flow close to it, but perturbation theory will break down once we get too far along the flow. There are some examples when the whole RG flow is short, and perturbation theory can be used to describe CFT_{IR} as well, such as the Wilson Fisher fixed point in $4 - \epsilon$ dimensions [9], but this is not the general case.

The success of the bootstrap

The idea that CFTs, due to their extended symmetry group, tend to be easier to study than generic QFTs was first brought forward by [10, 11], and indeed the vast power of conformal symmetry in two dimension was shown more than thirty years ago [12]. It was only ten years ago that the so-called conformal bootstrap approach was extended to higher dimension [13], with great success (see for example [14–16], and in general [17] for a review).

The bootstrap philosophy consists of imposing self consistency conditions on the theory, and ruling out regions of theory space which would violate these. To be more precise, one normally imposes unitarity and crossing symmetry of correlation functions; with very little input, such

¹Not all UV-complete QFTs are described by CFTs at high energy, as one can always start a flow from a scale invariant, but not conformally invariant, theory. An example of this would be Maxwell theory in $d = 3$ [8].

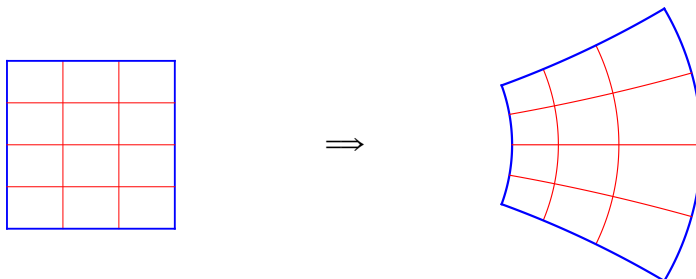


Figure 1 – The action of a special conformal transformation.

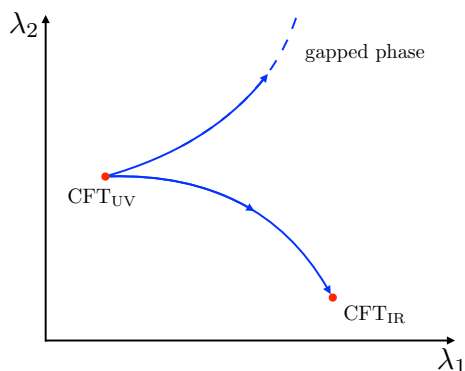


Figure 2 – Different RG flows in the space of couplings. A RG flow starting from a UV CFT can either flow to another CFT in the IR or to a gapped phase.

as the symmetries of the system, the number of relevant parameters and, potentially, some other data known about the system through other methods (such as Monte Carlo simulations), he or she can find very strong constraints on the theory itself.

The most notorious example of the success of the conformal bootstrap is its application to the most notorious statistical mechanics model, the Ising model. In two dimensions everything about the critical Ising model is known exactly since the 1980s [12]. In three dimensions, one can use the numerical bootstrap to gain access to the low-lying operators of the theory. These are the most important operators from a statistical mechanics point of view, since their dimension determines the critical exponents. As a result, the numerical bootstrap gives us the most precise determination of some of the three-dimensional Ising critical exponents to date [15]. But the numerical bootstrap approach is not the only one. For example, the lightcone bootstrap gives access to a different sector of a CFT, where it's possible to study the lowest twist operators, which are very important from a holographic point of view [18, 19].

Conformal perturbation theory

The moral of the bootstrap story is that if we focus on CFTs, there are approaches which allow us to systematically study even strongly coupled theories. Now, let's go back to considering RG flows starting from a CFT_{UV} . As mentioned earlier, if CFT_{UV} is a free theory, we can describe QFTs along this flow in the vicinity of CFT_{UV} by using perturbation theory. But now assume that CFT_{UV} is itself strongly interacting, but we know enough about it thanks to some bootstrap method. Can we say anything about QFTs in its proximity?

The answer to this question is affirmative, and the tool that we need is called conformal perturbation theory [20, 21]. This thesis studies two cases where it's possible to make predictions on strongly coupled QFTs by treating them as perturbations of known, strongly coupled, CFTs. The first part considers the case of CFTs with long range interactions, specifically the long range Ising model, while the second part is about walking theories, i.e. QFTs which are

approximately scale invariant over a large range of energies.

Long-range models and non-local theories

The most studied QFTs in the literature are local theories. If the theory we are considering has a lagrangian formulation, locality means having an action which is the integral of a local lagrangian density. More in general, a local theory has a spin-2 conserved local operator, the stress tensor. Let's consider an example from statistical physics: a spin model close to a continuous phase transition can be described by a QFT. This QFT is local if the model has short-range interactions, meaning that a given spin only interacts with spins within some finite distance from it. As an example, the Ising model has only nearest neighbor interactions and at its fixed point it is described by a local CFT. We could add next-to-nearest-neighbor interactions to the model as well, or next-to-next-to-nearest-neighbor interactions, and so on, and as long as we add only a finite number of these interactions this model at a fixed point will be described by a local CFT.

A substantially different situation arises if we have long-range interactions, meaning that a given spin interacts with spins arbitrarily far away in the system. What we will consider in the first part of the thesis will be the long-range Ising (LRI) model [22–24]. It is very similar to the usual Short Range Ising (SRI) model, with the only exception that all spins interact with each other, with the interaction decaying as a power of the distance. The model has a continuous phase transition at a critical value of the temperature, and here it is described by a non-local CFT.²

Non-local CFTs are interesting for several reasons. One of these reasons is the issue of 'scale vs. conformal' symmetry. As mentioned earlier, end points of local RG flows are scale invariant, but very often they are also conformally invariant. When trying to determine conformal invariance in the case of a local fixed point, the object of interest is the trace of the stress tensor: if it vanishes the theory is a CFT [5]. But in the case of non-local CFTs there is no stress tensor to begin with, and the question of conformality needs to be studied in a different way. This is what we will do in chapter 1, where we show that the LRI is indeed conformally invariant at the fixed point. In order to do so, we construct a higher dimensional defect field theory, which by itself is local and contains a stress tensor. Our LRI CFT can be obtained by restricting ourselves to the theory living on the defect only.

Another interesting characteristic of non-local CFTs is their abundance. Local CFTs are, in a sense, isolated. For example, one may wonder how many local CFTs with a given symmetry group and a given number of relevant operators exist in a certain number of dimensions. We believe the answer to be that there are few of them. For example, imposing crossing symmetry and unitarity in a \mathbb{Z}_2 symmetric local CFT in three dimensions, and requiring that we have only two relevant operators (one \mathbb{Z}_2 even and one \mathbb{Z}_2 odd), the numerical bootstrap finds an

²What here we call non-local CFTs are sometimes called conformal theories in the literature, with the word 'field' reserved exclusively for local theories.

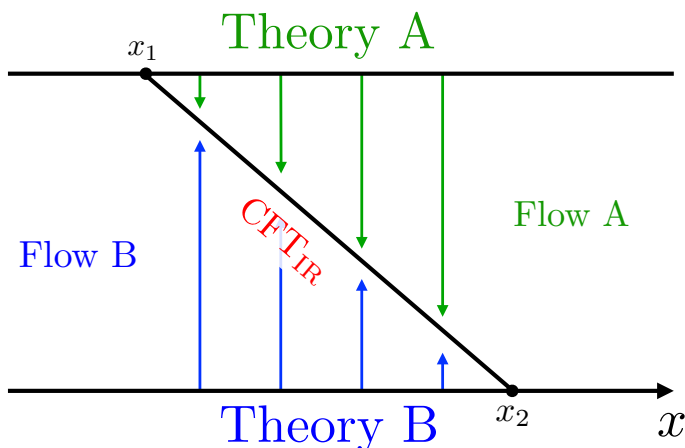


Figure 3 – Schematic representation of an IR duality: the same CFT_{IR} can be reached by perturbing two different UV theories. For $0 < x - x_1 \ll 1$ flow A is short and under perturbative control, while for $0 < x_2 - x \ll 1$ flow B is.

isolated region, an ‘island’, in the parameter space of the theory [15]. This island shrinks as one improves the numerics, and it’s reasonable to believe that in the limit of infinite computational resources, it shrinks to a point. This would mean that there is only one self-consistent theory with these characteristics.

The situation is very different when we discuss non-local theories. The simplest example are generalized free field (GFF) theories, which are a continuous family of non-local gaussian CFTs. In the context of interacting theories, the LRI model has one parameter that we can play with, the exponent of the power law decay of the interaction. For every value of this parameter, the model undergoes a continuous phase transition. The final picture is that of a family of non-local CFTs with the same symmetry group and the same number of relevant operators. Besides, there is an interesting dependence on the power law exponent that gives rise to qualitatively different regimes of the theory. This will be discussed at length in chapter 1 and 2. In general, it’s much easier to ‘construct’ a CFT without requiring locality. We show in chapter 2 that by coupling a local CFT and a GFF theory, we very easily get a continuous family of non-local interacting CFTs.

Finally, it is worth mentioning that studying non-local CFTs is a task which is made easier by an IR duality. This will be shown in chapter 2 for the LRI CFT, but the mechanism is likely to hold for other non-local CFTs, such as the long range $O(n)$ model. There is a non-trivial regime of the LRI CFT which can be reached as the IR fixed point of two very different RG flows. The first one is a Wilson-Fisher like flow which consists of perturbing a non-local gaussian action with a quartic interaction, while the second one is a flow which in the UV consists of two decoupled sectors, a GFF and the SRI CFT, which are perturbed by an operator which couples the two sectors.

The strength of a IR duality is that, depending on the situation, it is more convenient to think of our LRI theory as the IR fixed point of one flow rather than the other. In some cases, one of the flow will be a long flow (which means that the IR fixed point is not within reach of perturbation theory), but we can use the other flow, which is short, to make perturbative predictions on the theory. Examples of IR dualities are not so common: the most famous example is Seiberg duality in $\mathcal{N} = 1$ SUSY theories in $d = 4$ [25]. Our example is, to our knowledge, the first example of a non-local duality. We will use this duality by considering the flow which starts from a decoupled GFF and the SRI CFT: this CFT_{UV} is strongly coupled but a lot is known about it. By using conformal perturbation theory we will be able to make predictions on the observables of the LRI CFT such as the critical exponents.

Walking theories and complex CFTs

The second part of the thesis concerns walking theories. In general, the physics of a QFT depends strongly on the energy scale. The situation is very different in a CFT, where the couplings are independent on the scale. There are examples of QFTs where, in some energy range, the couplings depend on the scale only in a weak manner, and look approximately like a scale invariant theory. This can happen, for example, when we perturb a CFT by a weakly relevant deformation: at high energy this theory still looks almost scale invariant and the coupling constant of this deformation evolves slowly. We will refer to this scenario as “tuning”. There are cases, however, where some coupling constant evolves slowly but there are no CFTs nearby living at real values of this coupling. This phenomenon is what we refer to as walking.

Walking theories play a role in several physical systems, even though they sometimes appear with different names. The term walking was born in the high energy physics literature. Here we have QFTs where the beta function of some coupling is small in a range of energies. This means that there is a large hierarchy, i.e. a large separation between some scale Λ_{UV} where walking kicks in and some Λ_{IR} where walking stops. If our beta function is of order $O(\epsilon)$, with ϵ some small positive parameter, then we expect the separation of scales to behave like $\Lambda_{UV}/\Lambda_{IR} \sim \exp(const/\epsilon)$. We therefore have an exponentially large hierarchy.

Walking played a role in theories of physics beyond the Standard Model. Technicolor theories, where the role of the Higgs field is played by a fermion bilinear condensate, were introduced in order to account for the hierarchy problem (see for example [26]). However, these theories had the issue of introducing flavor changing neutral currents (FCNC), which are highly constrained by experimental results. Walking Technicolor theories were introduced as a better alternative to Technicolor theories [27–29]. A sector of the theory is almost scale invariant in some range of energies, and we can associate to every operator a scaling dimension, and that of the operator playing the role of the Higgs could be such that the problem of FCNC is made less severe. These models of beyond the Standard Model physics are currently not favored, but the issue of walking remains interesting from a QFT point of view.

The same walking phenomenon appears in statistical physics under the name of weakly first

order phase transitions. In this scenario, our lattice spacing a plays the role of the UV length scale ℓ_{UV} while the correlation length ξ plays the role of the IR scale ℓ_{IR} . The long range physics of a continuous phase transition is scale invariant, therefore it cannot have any characteristic scale: this means that $\xi = \ell_{IR} = \infty$. In a discontinuous phase transition, instead, the correlation length is finite and in general, $\xi/a \sim O(1)$. A weakly first order (WFO) phase transition has a finite but large correlation length, and $\xi/a \gg 1$. We have again a large separation of scales and the physics in the range between a and ξ is approximately scale invariant. An example of a system showing a WFO phase transition is the Q -states Potts model Q slightly larger than some critical value [30, 31].

WFO phase transitions are particularly hard to study numerically due to their large correlation length. When running a Monte Carlo simulation, one considers larger and larger lattices, and tries to extrapolate an answer for an infinitely large lattice. In general, to see that a phase transition is not continuous, one has to take a lattice whose linear size is at least of the order of than the correlation length. This means that in WFO phase transitions, very large lattices are needed and numerical simulation of these systems are computationally very intensive. As an example, a lot has recently been discussed about the Néel/VBS phase transition in $2 + 1$ dimensions, also known as deconfined quantum criticality [32]. Monte Carlo studies find evidence for a symmetric enhanced fixed point [33, 34], but this is ruled out by numerical bootstrap approaches [35]. The simplest resolution of the paradox is that we are not in the presence of a second order phase transition, rather of a WFO phase transition. If this is the case, then bootstrap bounds don't apply and there is no contradiction.

The fact that a walking QFT is approximately scale invariant suggests that it's close to some CFT. But in many cases, one can consider a flow which is described just by a single real coupling, and this flow cannot pass close to a real fixed point without actually ending up in it. Everything changes if we consider the full complex plane of this coupling: there could be fixed points at complex value of the coupling. We can imagine a walking theory as being close to a pair of complex conjugate fixed points which live close to the real axis of the coupling, and it's this proximity which explains the weak energy dependence of the theory in this regime.

At this point, it is convenient to take this fixed points at complex coupling seriously. We assume that they are complex CFTs, a term which will be made precise in chapter 3; they are a bit unusual in the sense that they are not unitary, but they are well defined (e.g. crossing symmetric) CFTs. Assume now that we know enough about these theories, for example the dimension of some low-lying operators and some of the OPE coefficients: when these fixed points are close to the real axis, we can use conformal perturbation theory to make predictions on the strongly coupled walking QFT.

Once one has in mind this picture of a walking QFT as a flow between two complex CFTs, it is easy to see another reason why walking is an interesting phenomenon. The hierarchy due to walking does not require tuning of the coefficients of the theory, since the flow is forced to pass in between the two complex CFTs, as there is nowhere else it could go. It's possible to achieve

Contents

a hierarchy also by starting from a theory with a weakly relevant operator, but this requires tuning the coefficient of this weakly relevant operator. From this point of view, walking is a more natural way to get this hierarchy.

Examples of walking and the interpretation of this phenomenon in terms of complex CFTs are explained in chapter 3, while the explicit case of the two dimensional Potts model with more than four states is worked out in detail in chapter 4.

Non-local CFTs **Part I**

1 Conformality of the critical Long Range Ising model

1.1 Introduction

Spin models with long-range interactions exhibit rich critical behavior with continuously varying exponents. Here we focus on the ferromagnetic long-range Ising model (LRI), with spin-spin interaction decaying as a power of the distance $\sim 1/r^{d+s}$.¹ The lattice Hamiltonian is given by

$$H_s = - \sum_{i,j} \frac{J}{|i-j|^{d+s}} S_i S_j, \quad (1.1.1)$$

where $S_i = \pm 1$ are the Ising spin variables, and $J > 0$ in the considered ferromagnetic case. We will assume $s > 0$ for the thermodynamic limit to be well defined. The space dimensionality d will be $d = 2, 3$. Formally our considerations will apply also to non-integer dimensions in the range $1 < d < 4$.

Forty years of theoretical considerations [22, 23, 36, 37] and Monte Carlo simulations [38] have established what we will refer to as the standard picture. The model (1.1.1) has a second-order phase transition for each $s > 0$. The critical theory is universal, i.e. independent of the short-distance details such as the choice of the lattice. It has however an interesting dependence on s (see Fig. 1.1). One distinguishes three critical regimes: (i) the mean-field Gaussian regime for $s < d/2$, (ii) the intermediate non-trivial regime for $s > d/2$ and up to a certain s_* (see below) and (iii) the short-range regime $s > s_*$. We warn the reader that we believe the standard picture to be dissatisfactory in the region $s \geq s_*$; this will be discussed at length in chapter 2.

To study the long-distance behavior, it's standard to replace the lattice model with a continuum field theory in the same universality class. Besides the usual quadratic and quartic local terms, the action includes a gaussian non-local term (with a negative sign for the ferromagnetic

¹The exponent s is usually denoted σ , but here we reserve letter σ for the short-range Ising spin field.

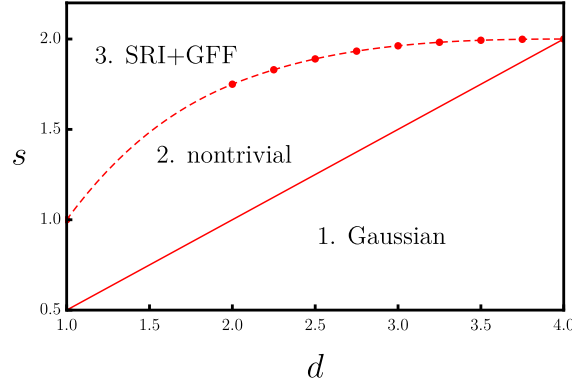


Figure 1.1 – The three phases for the LRI critical point. The boundaries are $s = d/2$ (straight solid) and $s = 2 - \eta_{\text{SRI}}(d)$ (curved dashed, interpolated using the known exact $\eta_{\text{SRI}}(d)$ for $d = 1, 2, 4$ and numerical values from the ϵ -expansion [39] and the conformal bootstrap [40] for a few intermediate d). Here we will be working near the boundary $s = d/2$.

interaction)²

$$S = - \int d^d x d^d y \frac{\phi(x)\phi(y)}{|x-y|^{d+s}} + \int d^d x [t\phi(x)^2 + g\phi(x)^4]. \quad (1.1.2)$$

The non-local term by itself describes mean field theory (MFT); it endows ϕ with dimension³

$$[\phi]_{\text{UV}} = (d-s)/2. \quad (1.1.3)$$

The quadratic term is always relevant and its coefficient t must be tuned to zero to reach the transition.

- (i) For $s < d/2$ the quartic term is irrelevant and the critical point is simply a gaussian theory described by the nonlocal action involving the “fractional Laplacian” operator $\mathcal{L}_s \equiv (-\partial^2)^{s/2}$:

$$S_0 \sim \int d^d x \phi \mathcal{L}_s \phi. \quad (1.1.4)$$

The field ϕ represents the spin density, and its scaling dimension is simply (1.1.3). Composite operators can be built out of ϕ by differentiations and taking normal-ordered products. Since the theory is gaussian, there are no anomalous dimensions.

- (ii) For $d/2 < s < s_*$, the quartic term becomes relevant and generates a renormalization group (RG) flow, reaching a fixed point in the IR. This critical point, believed to be in the same universality class as the critical point of the LRI lattice model, is a nontrivial, non-gaussian, theory. Interestingly, as it will be explained below, the dimension of ϕ at

²We will assume $0 < s < 2$, which includes the long-range to short-range crossover point s_* , see (2.1.1). This action is appropriate in this interval. Beyond $s = 2$ the local kinetic term $(\partial\phi)^2$ becomes relevant and would have to be added.

³Scaling dimensions of various fields X are denoted interchangeably by $[X]$ or Δ_X .

the fixed point is still given by the same formula (1.1.3). However, composite operators do get nontrivial anomalous dimensions.

- (iii) Finally, for $s > s_*$, the potential becomes strongly peaked at short distances. According to the standard picture, the critical point for $s > s_*$ is exactly the same as the short range Ising (SRI) fixed point. This relied on the observation that some of the critical exponents are the same as the SRI theory, see for example [38]. We will show in chapter 2 that the fixed point in the $s > s_*$ regime has a richer structure than the SRI one, and only some of the critical exponents coincide. The value at which there is a crossover is

$$s_* = d - 2\Delta_\phi^{\text{SRI}} \equiv 2 - \eta_{\text{SRI}}, \quad (1.1.5)$$

using the usual definition of the η critical exponent. The value of s_* can be inferred by requiring continuity of the dimension of the spin field at the crossover.

In this chapter we will be focussing on the region near the phase boundary $s = d/2$, i.e. away from $s = s_*$. We will work in an expansion in $\epsilon = 2s - d \ll 1$.

Problem of conformal invariance

As it will be briefly discussed in section 1.5.2.1, the SRI critical point enjoys the property of conformal invariance. The utility of this symmetry in 2d is long known, as it allows for an exact solution of the critical theory [12] via a method called the conformal bootstrap.⁴ In 3d, an exact solution is not yet known, but the conformal bootstrap has recently been used to get the world's most precise numerical determinations of the SRI critical exponents [41].⁵

What about the LRI critical point? In region 1 it's described by the nonlocal gaussian theory, whose conformal invariance is well known and will be reviewed in section 1.4.

Our main goal here will be to show that the LRI critical point is conformal in the non-gaussian region 2. This is harder to ascertain, and as far as we know, this issue has not been previously discussed. Here we will present a proof valid to all orders in perturbation theory. Having conformal symmetry also in this region is very interesting and useful, paving the way for the conformal bootstrap methods [49].⁶ Until now, the LRI critical point was studied using RG methods, both perturbative [22, 23, 36, 37] and nonperturbative [51].

Concerning region 3, contrary to the standard picture, we will show substantial evidence in chapter 2 that the theory is described by the SRI fixed point and a decoupled generalized free field. Conformal invariance of the two decoupled subsectors implies conformal invariance

⁴In fact, the 2d SRI critical point is invariant under the Virasoro algebra, which is an infinite-dimensional extension of the global conformal algebra. In this chapter, we will be working in general d and by conformal invariance we will mean global, finite dimensional, conformal invariance, unless specified otherwise. In 2d this is sometimes referred to as Möbius invariance.

⁵For prior work see [13, 14, 42–45]. An alternative technique has been developed in [46–48].

⁶Some work has already been done in [14], section 5.4, and [50].

of the full theory. See section 1.5.2.1 where we discuss conformal invariance of the SRI fixed point.

The remainder of this chapter is organized as follows. In the next section we discuss the basic setup of the epsilon expansion for the long-range Ising model. We then provide nontrivial evidence for conformal invariance by computing $\langle \phi \phi^3 \rangle$ and $\langle \phi^2 \phi^4 \rangle$ up to order ϵ^2 , as we find that these correlators vanish at the fixed point. This behavior does not follow from scale invariance alone but it is a necessary condition for conformal invariance, so we are led to believe that the LRI at criticality could actually be conformally invariant. The remainder of the chapter is dedicated to an all-orders proof of this claim. In section 1.4 we review the proofs of conformal invariance of the gaussian theory (see below for a definition). This sets the stage for the proof of conformal invariance of the LRI, which we present in section 1.5. In that section we also discuss the prospects for proving conformal invariance at the nonperturbative level. We end the chapter with some concluding remarks, and several technicalities have been relegated to the appendices.

1.2 Field-theoretical setup

In this work we will study the LRI critical point for $1 \leq d < 4$, inside the non-gaussian region 2, close to the boundary separating it from the gaussian region 1, i.e. for

$$s = (d + \epsilon)/2, \quad 0 < \epsilon \ll 1. \quad (1.2.1)$$

The UV dimension of the ϕ field is then

$$\Delta_\phi = (d - \epsilon)/4, \quad (1.2.2)$$

so that the quartic term ϕ^4 is a weakly relevant perturbation. The IR fixed point is then accessible in perturbation theory. As is standard [36, 37], we will setup a perturbative expansion using the analytic regularization scheme, where Feynman diagrams are considered analytic functions of ϵ . This is convenient since it allows one to evaluate integrals without introducing an explicit UV cutoff.

As mentioned in the introduction, the relevant action is

$$S = S_0 + \frac{g_0}{4!} \int d^d x \phi^4, \quad S_0 = \frac{\mathcal{N}_s}{2} \int d^d x \phi \mathcal{L}_s \phi. \quad (1.2.3)$$

The coefficient \mathcal{N}_s , whose precise value is unimportant, will be fixed so that the free ϕ two

⁷If d is close to 4, we should assume a stronger condition $\epsilon \ll 4 - d$, so that we stay closer to the boundary between the regions 1 and 2 than to that between 2 and 3. In the opposite case $\epsilon \gtrsim 4 - d$ the structure of perturbation theory is modified due to the presence of a weakly irrelevant operator $\partial^2 \phi$. See [36, 37] for a discussion.

point function is normalized to one:

$$\langle \phi(x)\phi(0) \rangle_{S_0} = |x|^{-2\Delta_\phi}. \quad (1.2.4)$$

Notice that the analytic regularization scheme is mass independent. So we can avoid introducing the mass term $m^2\phi^2$ into the action (1.2.3). In other words, in this scheme the flow which leads to the fixed point has $m^2 = 0$ all along the flow.

As usual in the field theoretical studies of critical phenomena, it will be extremely useful to view the theory (1.2.3) as regulating the theory with $\epsilon = 0$, where the interaction is marginal. As $\epsilon \rightarrow 0$, computations in theory (1.2.3) give poles in ϵ . These poles can be removed order by order in perturbation theory by multiplicatively renormalizing the terms in the action.⁸

The gaussian term in (1.2.3) is not renormalized, because it's nonlocal, while the divergences are local. In other words, the theory under consideration does not have wavefunction renormalization, and the bare and the renormalized field ϕ coincide. In particular, the anomalous dimension of ϕ vanishes. This implies that, to all orders in perturbation theory, the dimension of ϕ at the IR fixed point is equal to its UV dimension (1.2.2) [22, 23, 36].

On the other hand, the coupling constant does require renormalization. The bare coupling g_0 is expressed in terms of the finite, renormalized, coupling g as:

$$g_0 = Z(g, \epsilon) g \mu^\epsilon, \quad (1.2.5)$$

where μ is the renormalization scale and Z is the renormalization factor which starts with 1 and contains an ascending series of poles in ϵ :

$$Z(g, \epsilon) = 1 + \sum_{k=1}^{\infty} f_k(g) \epsilon^{-k}. \quad (1.2.6)$$

The coefficient $f_k(g)$ of the pole ϵ^{-k} is a power series in g starting from $O(g^k)$; it gets contributions from all loop orders larger than or equal to k .

The β -function of the theory can be expressed in terms of the single pole coefficient:

$$\beta(g) \equiv \partial g / \partial \log \mu = -\epsilon g + g^2 f_1'(g). \quad (1.2.7)$$

The story is exceedingly similar to the ϵ -expansion for the Wilson-Fisher (WF) fixed point (see e.g. the books [56, 57], or [58] for a concise treatment), with an extra simplification that there is no wavefunction renormalization.

⁸Multiplicative renormalizability is most familiar in local quantum field theory, but it holds also for nonlocal theories of the kind we are considering here, with the standard proof [52]. For the validity of Weinberg's convergence theorem [53] (that if all subdiagrams are superficially convergent, then the diagram is convergent) in this context see the discussion in [54], p.600. For the structure of divergences in theories with propagators involving arbitrary powers of x^2 (studied in the context of analytic regularization), see [55] and the discussion in [36].

Chapter 1. Conformality of the critical Long Range Ising model

Let us compute the β -function at the first nontrivial, one-loop, order. We need to determine the one-loop counterterm to the coupling. Consider the four point function of ϕ , which up to the second order in g is given by the sum of diagrams:

The $O(g^2)$ contribution will contain a $1/\epsilon$ pole coming from the region where the two ϕ^4 insertions are near each other. The contribution of this region can be easily extracted using the operator product expansion (OPE) of the gaussian UV theory:

$$\phi^4(x) \times \phi^4(0) \supset (72/|x|^{d-\epsilon}) \phi^4(0). \quad (1.2.8)$$

This OPE implies that the expansion of the functional integral to the second order will contain a short-distance contribution corresponding to the insertion of ϕ^4 times

$$72 \times \frac{1}{2} \times \frac{g^2 \mu^{2\epsilon}}{(4!)^2} \int_{|x| \ll 1} \frac{d^d x}{|x|^{d-\epsilon}} = 36 \frac{g^2}{(4!)^2} \frac{S_d}{\epsilon} + \text{finite}, \quad (1.2.9)$$

where $S_d = 2\pi^{d/2}/\Gamma(d/2)$ is the volume of the unit sphere in d dimensions. The $1/\epsilon$ pole is canceled by adding a coupling counterterm

$$\delta g = (36g^2/4!)(S_d/\epsilon). \quad (1.2.10)$$

Therefore the expansion of the single pole function $f_1(g)$ in (1.2.6) starts with

$$f_1(g) = Kg + O(g^2), \quad K = 3S_d/2. \quad (1.2.11)$$

The one-loop β -function is given by

$$\beta(g) = -\epsilon g + Kg^2 + O(g^3). \quad (1.2.12)$$

It has a zero at

$$g = g_* = \epsilon/K + O(\epsilon^2). \quad (1.2.13)$$

This zero corresponds to the LRI critical point that we want to study.⁹

Below we will be interested in the correlation functions of the composite operators ϕ^n . As usual, we will define the renormalized operators $[\phi^n] = [\phi^n]_{g,\mu}$ which remain finite in the limit $\epsilon \rightarrow 0$. They are related to the bare operators ϕ^n by rescaling factors subtracting poles in ϵ :

$$\phi^n = Z_n(g, \epsilon)[\phi^n]. \quad (1.2.14)$$

⁹ In $d = 1, 2, 3$ and for sufficiently small $\epsilon > 0$ the existence of this fixed point has been shown rigorously [59–62]. See also [63] for a series of rigorous results about the LRI phase transition. We are grateful to Abdelmalek Abdesselam and Pronob Mitter for communications concerning these works.

As indicated, the operators $[\phi^n]$ depend on the scale μ and on the value of the coupling g at this scale. On the other hand correlation functions of the bare operators don't depend on μ and g separately, but only on their combination g_0 . As usual, this gives a CS equation for the correlators of the renormalized operators. The anomalous dimension of $[\phi^n]$ is given by

$$\gamma_n(g) = Z_n^{-1} \partial Z_n / \partial \log \mu |_{g_0 = \text{const.}} . \quad (1.2.15)$$

Notice that since the dimension of ϕ is not integer, in the considered theory the ϕ^n operators don't mix with the operators where some ϕ 's are replaced by derivatives.¹⁰

As already mentioned above, this theory has no wavefunction renormalization. Therefore ϕ is a finite operator without any rescaling. So $Z_1 \equiv 1$ and $\gamma_1 \equiv 0$. The UV dimension of ϕ given in (1.2.2) will also be its IR dimension.¹¹

Let's compute the anomalous dimensions of ϕ^n , $n \geq 2$, at the lowest nontrivial order. The $1/\epsilon$ contribution to the correlation functions of ϕ^n will come from the nearby $(g/4!)\phi^4$ insertions. In this region we can use the OPE generalizing (1.2.8):

$$\phi^n(0) \times \phi^4(x) \supset [6n(n-1)/|x|^{d-\epsilon}] \phi^n(0) . \quad (1.2.16)$$

Integration in x gives a $1/\epsilon$ pole which must be canceled by rescaling the operator. We get

$$Z_n = 1 - K_n g / \epsilon + \dots, \quad K_n = n(n-1)S_d/4 \implies \gamma_n(g) = K_n g + O(g^2) . \quad (1.2.17)$$

At the IR fixed point we have

$$\gamma_n^* \approx K_n g_* = [n(n-1)/6]\epsilon + O(\epsilon^2) . \quad (1.2.18)$$

These are the same anomalous dimensions as in the usual ϵ -expansion for the WF fixed point (see e.g. [64]). Indeed, the answer at this order is controlled by the combinatorics of the Wick contractions in the gaussian UV fixed point, which is the same in the local free scalar theory and in the nonlocal theory defined by our S_0 . Of course, it's not true that all computations are the same between the two theories. We will see some examples below.

1.3 Tests of conformal invariance

How can we check if a certain model is conformally invariant or just scale invariant? The currently available data on the LRI amount to the anomalous dimensions of scaling operators, which are determined with RG methods and also measured on the lattice from two point

¹⁰This is true for generic d , while for integer d there can be some mixing for high n . E.g. $\Delta_\phi \approx 1/2$ in $d=2$, and one can trade 4 ϕ 's for 2 derivatives. This could become important for operators starting from ϕ^6 . In this chapter we will mostly work with operators up to ϕ^4 and we will ignore this.

¹¹This fact has also been established non-perturbatively for sufficiently small $\epsilon > 0$ for which the existence of the fixed point is rigorously known [61, 62], see note 9.

Chapter 1. Conformality of the critical Long Range Ising model

functions. These data cannot distinguish between scale and conformal invariance, because both predict the same functional form for the critical two point function:

$$\langle \mathcal{O}(x)\mathcal{O}(0) \rangle \propto |x|^{-2\Delta_{\mathcal{O}}}. \quad (1.3.1)$$

Here \mathcal{O} is a generic scalar operator of dimension $\Delta_{\mathcal{O}}$.

One celebrated prediction of conformal invariance is the form of a three point function [65], but this is harder to compute and to measure on the lattice than the two point function. We are not aware of any three point function data for the LRI critical point.

An easier discriminating variable is the two point function of two different operators. Scale invariance predicts that

$$\langle \mathcal{O}_1(x)\mathcal{O}_2(0) \rangle = c_{12}|x|^{-\Delta_1-\Delta_2}, \quad (1.3.2)$$

while conformal invariance implies [65] the stronger constraint that $c_{12} = 0$ unless $\Delta_1 = \Delta_2$. To be precise, this conclusion is reached if both operators are so-called primary operators, i.e. if they are not derivatives of other operators. If the \mathcal{O}_i are both of the form $(\partial^2)^{n_i}\mathcal{O}$ for the same operator \mathcal{O} , they will of course have a nonzero two point function. This trivial case is easy to monitor since the scaling dimensions are different by an even integer.

To summarize, conformal invariance implies that any two scalar operators whose dimensions are not different by an even integer must have a zero two point function, while scale invariance would allow such two point functions to be nonzero.

The goal of this section will be to study the following two point functions of different scalars at the critical point of the LRI:

$$\langle \phi(x)\phi^3(0) \rangle \text{ and } \langle \phi^2(x)\phi^4(0) \rangle. \quad (1.3.3)$$

Notice that we chose pairs of operators with the same parity under $\phi \rightarrow -\phi$. If the IR fixed point is only scale invariant but not conformal, these correlators could be nonzero.

We will consider these correlators in the perturbative setup of the previous section. As we will see, a nontrivial check requires to go to at least the second order in the coupling constant g , or in the parameter ϵ parametrizing the deviation from marginality. At $O(\epsilon^2)$, scale invariance alone then allows for both of the above correlators to be nonzero.

As a matter of fact, it turns out that the first correlator is a bit special, as it involves ϕ whose anomalous dimension is identically zero, as well as ϕ^3 which is related to ϕ via a "nonlocal equation of motion" (nonlocal EOM).¹² Using these facts, we will give an all-order argument that the correlator $\langle \phi\phi^3 \rangle$ vanishes at the IR fixed point. We will buttress the argument by an explicit second-order computation showing that the correlator vanishes at $O(\epsilon^2)$.

¹²We thank Riccardo Rattazzi who emphasized this to us.

We do not know any analogous general argument for the correlator $\langle \phi^2 \phi^4 \rangle$. This seems to be a truly generic correlator involving fields with unrelated anomalous dimensions. We will perform an explicit second-order computation for this correlator, finding that it also vanishes at $O(\epsilon^2)$.

These computations lead us to believe that the LRI critical point is in fact conformally invariant, and to look for a general proof of this fact. A proof that we found will be discussed in the rest of the chapter.

1.3.1 $\langle \phi \phi^3 \rangle$

By dimensional considerations, this correlator should behave in the IR as $C|x|^{-\Delta_\phi - \Delta_{\phi^3}}$. We recall that at the WF fixed point $C \neq 0$ because ϕ^3 is not a primary but is related to ϕ by the equations of motion: $\phi^3 \propto \partial^2 \phi$. In the conformal field theory (CFT) language, ϕ^3 is a descendant of the primary ϕ . At the LRI fixed point, we know for sure that ϕ^3 is not a descendant of ϕ since the dimensions don't match. So $C \neq 0$ would disprove conformal invariance, while $C = 0$ would be evidence in its favor.

We will first show that $C = O(\epsilon^3)$ by an explicit computation, and next present an argument that $C = 0$ to all orders in perturbation theory.

1.3.1.1 Explicit computation

We will now present an explicit computation of the correlation function $\langle \phi \phi^3 \rangle$ to the second order in the coupling. More precisely, we will consider the correlator

$$F(x, g, \mu) = \langle \phi(x) [\phi^3](0) \rangle, \quad (1.3.4)$$

where $[\phi^3] = [\phi^3]_{g, \mu}$ is the ϕ^3 rescaled by subtracting poles in ϵ as discussed in section 1.2.¹³ This correlator allows an expansion in powers of the renormalized coupling g without poles in ϵ . By dimensional reasons, it should have the form

$$F = f(\tau, g) |x|^{-\Delta_\phi - \Delta_{\phi^3}^{(0)}}, \quad (1.3.5)$$

where $\Delta_{\phi^3}^{(0)} = 3\Delta_\phi$ is the UV dimension of ϕ^3 and f is a function of dimensionless variables g and $\tau \equiv \mu|x|$.

We will have a Callan-Symanzik (CS) equation expressing the invariance of the theory under

¹³Note that since we don't take the limit $\epsilon \rightarrow 0$, operator renormalization is not strictly necessary. The rescaling factors $Z_n(g, \epsilon)$ are finite at finite ϵ , and the $1/\epsilon$ terms in them never even become large, since $g = O(\epsilon)$ all along the RG flow. The role of renormalization is rather that of convenience, as it allows to cleanly separate the $O(1)$ effects coming from the powers of g/ϵ from the effects suppressed by powers of g which are truly higher order. This makes the weakly coupled nature of the theory manifest.

Chapter 1. Conformality of the critical Long Range Ising model

simultaneous changes of g and μ leaving g_0 fixed:

$$[\mu\partial_\mu + \beta(g)\partial_g + \gamma_3(g)]F(x, g, \mu) = 0. \quad (1.3.6)$$

The only difference from the usual ϕ^4 theory is that the anomalous dimension of ϕ does not appear since it's identically zero. Substituting (1.3.5) into (1.3.6), we get an equation for f :

$$[\tau\partial_\tau + \beta(g)\partial_g + \gamma_3(g)]f(\tau, g) = 0. \quad (1.3.7)$$

At large distances $\beta(g) \rightarrow 0$ and $\gamma_3(g) \rightarrow \gamma_3(g_*)$, and Eq. (1.3.7) predicts

$$f(\tau, g) \approx C\tau^{-\gamma_3(g_*)}. \quad (1.3.8)$$

We thus rederived the result that at large distances the considered correlation function should go as $|x|^{-\Delta_\phi - \Delta_{\phi^3}}$ where $\Delta_{\phi^3} = \Delta_{\phi^3}^{(0)} + \gamma_3(g_*)$. This argument does not determine the value of C , which in particular may still turn out to be zero.

To determine the prefactor C , we have to match the CS equation to fixed-order perturbation theory. Recall that the full solution of Eq. (1.3.7) can be written in the form:

$$f(\tau, g) = \hat{f}(\bar{g}(\tau, g)) \exp \left[- \int_1^\tau d \log \tau' \gamma_3(\bar{g}(\tau', g)) \right], \quad (1.3.9)$$

where \bar{g} is the “running coupling” solving the following differential equation with a boundary condition at $s = 1$:

$$\tau \partial_\tau \bar{g} = -\beta(\bar{g}), \quad \bar{g}|_{\tau=1} = g. \quad (1.3.10)$$

In particular, at $\tau = 1$ the function $f(\tau, g)$ reduces to $\hat{f}(g)$. Once this latter function is fixed from perturbation theory, the prefactor C in (1.3.8) is found as

$$C = \hat{f}(g_*). \quad (1.3.11)$$

We will now show that this vanishes up to order e^2 .

For this we would like to extract \hat{f} up to the second order in g . Consider first the nonrenormalized correlator

$$F_0(x) = \langle \phi(x)\phi^3(0) \rangle, \quad (1.3.12)$$

which has no tree-level contribution. Up to the second order in the coupling it is given by the sum of two position-space diagrams:¹⁴

$$\begin{array}{c} \text{---} \bigcirc \text{---} + \text{---} \bigcirc \text{---} \end{array} \quad (1.3.13)$$

Both these diagrams are easily evaluated using the following basic integral (which in turn can

¹⁴The signs and combinatorial factors are left implicit.

be derived by going to momentum space):

$$\int \frac{d^d y}{|x-y|^A |y|^B} = \frac{w_A w_B}{w_{A+B-d}} \frac{1}{|x|^{A+B-d}}, \quad w_A = (4\pi)^{d/2} 2^{-A} \frac{\Gamma(\frac{d-A}{2})}{\Gamma(A/2)}. \quad (1.3.14)$$

Using this result, we obtain

$$F_0(x) = R_1 g_0 / |x|^{d-2\epsilon} + R_2 g_0^2 / |x|^{d-3\epsilon} + O(g_0^3), \quad (1.3.15)$$

where

$$R_1 = -\frac{w_{\frac{d-\epsilon}{2}} w_{3\frac{d-\epsilon}{2}}}{w_{d-2\epsilon}} \approx -\epsilon \pi^{d/2} \frac{\Gamma(-d/4) \Gamma(d/2)}{\Gamma(3d/4)},$$

$$R_2 = \frac{3}{2} \frac{w_{d-\epsilon}^2 w_{\frac{d-\epsilon}{2}} w_{\frac{3}{2}d-\frac{5}{2}\epsilon}}{w_{d-2\epsilon} w_{d-3\epsilon}} \approx 9\pi^d \frac{\Gamma(-d/4)}{\Gamma(3d/4)}. \quad (1.3.16)$$

The given approximate expressions are the leading ones in the small ϵ limit. Notice that $R_1 = O(\epsilon)$. This has a simple explanation: in the limit $\epsilon \rightarrow 0$ the interaction becomes exactly marginal, the integral defining R_1 becomes conformal, and it should give zero answer for a correlator of two fields of different scaling dimensions by the usual arguments based on conformal symmetry. To get a nontrivial check of conformal invariance, we have to go to the second order in ϵ , hence to the second order in g , which is what we are doing.

To get at the function \hat{f} , we need to replace the coupling g_0 by g via (1.2.5), (1.2.11):

$$g_0 = Z g \mu^\epsilon = [g + K g^2 \epsilon^{-1} + O(g^3)] \mu^\epsilon, \quad (1.3.17)$$

and to use the relation between ϕ^3 and $[\phi^3]$, see (1.2.14), (1.2.17). This gives the following expression for F to the second order in g :

$$F(x) = \{g R_1 \tau^\epsilon + g^2 [R_1 (K + K_3) \epsilon^{-1} \tau^\epsilon + R_2 \tau^{2\epsilon}]\} / |x|^{d-\epsilon}. \quad (1.3.18)$$

We see the structure is in agreement with (1.3.5). To extract \hat{f} we set $\tau = 1$ and obtain:¹⁵

$$\hat{f}(g) = g R_1 + g^2 [R_1 (K + K_3) \epsilon^{-1} + R_2] + O(g^3). \quad (1.3.19)$$

Since $R_1 = O(\epsilon)$ this expression is free of poles in ϵ : as we mentioned above the correlator and in particular \hat{f} should have a regular expansion in g without such poles. Using (1.3.19) and (1.3.9) we can compute the considered correlator at all distances with ϵ^2 accuracy.

Now using the values of the various constants appearing in (1.3.19), it's easy to see that to the order that we computed it can be rewritten as

$$\hat{f}(g) = -R_1 \epsilon^{-1} (-\epsilon g + K g^2) = -R_1 \epsilon^{-1} \beta(g), \quad (1.3.20)$$

¹⁵We have analyzed also the leading $\log \tau$ terms in the expansion of G around $\tau = 1$ and checked that they are consistent with what the solution (1.3.9) to the CS equation predicts.

Chapter 1. Conformality of the critical Long Range Ising model

This form of writing makes it manifest that $\hat{f}(g)$ vanishes at the IR fixed point.

1.3.1.2 General argument

We will now give a general argument that $C = 0$ to all orders in perturbation theory. The idea is to use the nonlocal EOM of the LRI field theory (1.2.3):¹⁶

$$\mathcal{N}_s \mathcal{L}_s \phi + \frac{g_0}{3!} \phi^3 = 0. \quad (1.3.21)$$

This can be used to express the correlators of ϕ^3 in terms of those of ϕ . In particular:

$$\langle \phi^3(x) \phi(0) \rangle \propto \mathcal{L}_s \langle \phi(x) \phi(0) \rangle. \quad (1.3.22)$$

This equation is subtle to use, because the fractional Laplacian is a nonlocal operator. We will therefore proceed cautiously.

First of all we have to understand in some detail the correlator $\langle \phi(x) \phi(0) \rangle$. Since ϕ does not acquire an anomalous dimension, its two point function has the form

$$\langle \phi(x) \phi(0) \rangle = \rho(x) |x|^{-2\Delta_\phi}, \quad (1.3.23)$$

where

$$\rho(x) = \hat{\rho}(\bar{g}(\tau, g)). \quad (1.3.24)$$

is a function of the running coupling \bar{g} which we introduced in the previous section. The function $\hat{\rho}$ can be determined by matching to perturbation theory. We will only need to know its rough structural properties.

Through $O(g^2)$ we have two diagrams:

$$\text{---} + \text{---} \bigcirc \text{---} \quad (1.3.25)$$

This implies that

$$\hat{\rho}(g) = 1 + Qg^2 + \dots, \quad Q = (\pi^d/6) \Gamma\left(-\frac{d}{4}\right) / \Gamma\left(\frac{3d}{4}\right). \quad (1.3.26)$$

We see that the function $\rho(x)$ approaches a constant at short and long distances:

$$\rho(x) \rightarrow \begin{cases} 1, & x \rightarrow 0, \\ \rho(g_*) = 1 + O(\epsilon^2), & x \rightarrow \infty. \end{cases} \quad (1.3.27)$$

In what follows we will also need the asymptotics of the approach to the long distance limit.

¹⁶Notice that it would be a non-permissible stretch of terminology to call ϕ^3 a “nonlocal descendant” of ϕ on the grounds of this equation. Descendants are defined as local derivatives of primaries, and we are not aware of any useful generalization of the descendant concept to nonlocal relations.

1.3. Tests of conformal invariance

From now on we will fix μ to be a scale μ_c at which the coupling $g \sim g_*/2$ is roughly halfway between the UV and the IR fixed points. The long distance asymptotic behavior of the running coupling \bar{g} is given by:

$$\bar{g} = g_* - O(\epsilon \tau^{-\beta'(g_*)}) \quad (\tau \gg 1), \quad (1.3.28)$$

where $\beta'(g_*) = \epsilon + O(\epsilon^2)$. It follows that $\rho(x)$ approaches the long distance limit as

$$\rho(x) = \rho(g_*) + O(\epsilon^2 \tau^{-\beta'(g_*)}). \quad (1.3.29)$$

We are now ready to compute the long distance behavior of the correlator $\langle \phi^3(x)\phi(0) \rangle$. According to Eq. (1.3.22) we need to evaluate the integral:

$$I = \int d^d y T(x-y) \langle \phi(y)\phi(0) \rangle, \quad (1.3.30)$$

where $T(x-y) \propto |x-y|^{-d-s}$ is the position space kernel of the fractional Laplacian, see eq. (1.1.4). Notice that this kernel is not absolutely integrable and at short distances it must be understood in the sense of distributions, as the Fourier transform of $|k|^s$.

We split the above integral into two parts $I = I_1 + I_2$, one against the long distance asymptotics of $\langle \phi\phi \rangle$ and the rest:

$$I_1 = \int d^d y T(x-y) \rho(g_*) |y|^{-2\Delta_\phi}, \quad (1.3.31)$$

$$I_2 = I - I_1 = \int d^d y T(x-y) [\rho(y) - \rho(g_*)] |y|^{-2\Delta_\phi}. \quad (1.3.32)$$

The first part I_1 vanishes at non-coincident points, $I_1 \propto \delta(x)$, by the definition of Green's function of the gaussian theory. As to I_2 , in the limit of very large x the leading asymptotics of the integral will come from large y , where we can use the asymptotics (1.3.29). We get:

$$I_2 \sim \int d^d y T(x-y) \epsilon^2 \tau^{-\beta'(g_*)} |y|^{-2\Delta_\phi}. \quad (1.3.33)$$

By dimensional analysis, this integral behaves $\propto |x|^{-\alpha}$ with

$$\alpha = s + 2\Delta_\phi + \beta'(g_*). \quad (1.3.34)$$

It's important that this exponent is larger than $\Delta_\phi + \Delta_{\phi^3}$:

$$\alpha - (\Delta_\phi + \Delta_{\phi^3}) = \beta'(g_*) + O(\epsilon^2), \quad (1.3.35)$$

using the known anomalous dimension of ϕ^3 , $\gamma_3(g_*) = \epsilon + O(\epsilon^2)$. This means that the constant C in the natural dimensional asymptotics of the studied correlator, see (1.3.8), has to vanish. The current argument establishes this fact to all orders in perturbation theory.

Chapter 1. Conformality of the critical Long Range Ising model

The above reasoning was made possible by two properties: the nonlocal EOM and the vanishing anomalous dimension of ϕ . Before leaving this section, we will similarly prove one more interesting fact: that $\gamma_3^* = \epsilon$ to all orders in perturbation theory. In other words the leading order result in (1.2.18) is in fact exact for $n = 3$.

We will use the nonlocal EOM to prove the following relation between the IR dimensions of ϕ and ϕ^3 :

$$\Delta_{\phi^3} = \Delta_\phi + s \quad (\text{IR}), \quad (1.3.36)$$

of which $\gamma_3^* = \epsilon$ is an immediate consequence. Eq. (1.3.36) looks similar to the relation $\Delta_{\phi^3} = \Delta_\phi + 2$ valid at the WF fixed point, also a consequence of the corresponding EOM. However, due to nonlocality, the proof is a bit more subtle for the LRI.

The idea is to use the nonlocal EOM twice, expressing $\langle \phi^3 \phi^3 \rangle$ in terms of $\langle \phi \phi \rangle$. This relation takes the form:

$$\langle \phi^3 \phi^3 \rangle = 36g_0^{-2} \mathcal{N}_s^2 \mathcal{L}_s \mathcal{L}_s \langle \phi \phi \rangle_{\text{pert}}, \quad \langle \phi \phi \rangle_{\text{pert}} \equiv \langle \phi \phi \rangle - \langle \phi \phi \rangle_{S_0}. \quad (1.3.37)$$

with the two \mathcal{L}_s 's acting on each of the arguments of $\langle \phi \phi \rangle_{\text{pert}}$. The subtlety here is that we have to subtract the gaussian two point function. This is easy to understand in perturbation theory. $\langle \phi \phi \rangle_{\text{pert}}$ is the sum of all diagrams in which each ϕ is connected to a vertex, like in the second diagram in (1.3.25). When we act with \mathcal{L}_s 's, the legs connecting ϕ 's to the vertices get cancelled, and we reproduce all diagrams for $\langle \phi^3 \phi^3 \rangle$. Were we to keep $\langle \phi \phi \rangle_{S_0}$, we would get an extra nonlocal contribution which does not correspond to any diagram. This is in contrast to what happens when using the equation of motion in the local ϕ^4 theory. In that case the contribution from the unperturbed propagator is zero at noncoincident points and we don't have to worry about it.¹⁷

Let us proceed now to the proof of (1.3.36). It will be convenient to work in momentum space. The asymptotics (1.3.29) of the function $\rho(x)$ means that the Fourier transform of $\langle \phi \phi \rangle_{\text{pert}}$ behaves at small momenta as:

$$\langle \phi(-k)\phi(k) \rangle_{\text{pert}} \sim |k|^{-s} [1 + O(|k|^{\beta^l(g^*)})]. \quad (1.3.38)$$

It's important that the proportionality coefficient here is nonzero (we computed that it's $O(\epsilon^2)$). When we act on this correlator once by the fractional Laplacian, multiplying by $|k|^s$, the leading term gives 1, which is a delta-function in the position space, and the subleading term determines the long-distance asymptotics. We thus reproduce the above result that $\langle \phi^3 \phi \rangle$ vanishes in the IR faster than its natural scaling. However, when we act by the fractional Laplacian twice, the leading result is nonanalytic $|k|^s$ and it is this result which determines the long-distance asymptotics. We conclude that the two point function $\langle \phi^3 \phi^3 \rangle$ behaves at long distances as $1/|x|^{d+s}$, which can be expressed as Eq. (1.3.36).

¹⁷One can also check that (1.3.37) has a smooth limit when $g_0 \rightarrow 0$, reducing to $\langle \phi^3 \phi^3 \rangle_{S_0}$ in this limit. This would not be the case were we to keep $\langle \phi \phi \rangle_{S_0}$.

1.3.2 $\langle \phi^2 \phi^4 \rangle$

In the previous section we studied the correlator $\langle \phi \phi^3 \rangle$ and found that it vanishes at the IR fixed point, consistently with conformal invariance. However, as we saw, the studied correlator was actually a bit special, since it involved two fields related by the nonlocal EOM of the LRI. One could wonder if the vanishing of this correlator is an accident. In this section we will study the correlator $\langle \phi^2 \phi^4 \rangle$, which as far as we can see is a truly generic correlator of our theory. We will find, by an explicit computation at $O(\epsilon^2)$, that this correlator also vanishes at the IR fixed point. We consider this a strong piece of evidence for the conformal invariance of the LRI critical point.

The computation proceeds similarly to $\langle \phi \phi^3 \rangle$, so we will be brief. The renormalized correlator

$$H(x, g, \mu) = \langle [\phi^2](x) [\phi^4](0) \rangle = h(\tau, g, \mu) |x|^{-\Delta_{\phi^2}^{(0)} - \Delta_{\phi^4}^{(0)}} \quad (1.3.39)$$

satisfies a CS equation which can be solved to give:

$$h(\tau, g, \mu) = \hat{h}(\bar{g}(\tau, g)) \exp \left\{ - \int_1^\tau d \log \tau' [\gamma_2(\bar{g}(\tau', g)) + \gamma_4(\bar{g}(\tau', g))] \right\}. \quad (1.3.40)$$

The function \hat{h} is determined by matching to perturbation theory. We have one diagram at $O(g_0)$ and three diagrams at $O(g_0^2)$:

$$(1.3.41)$$

The first two diagrams here are the same as in (1.3.13) times an extra propagator. The third diagram is new, but it can also be readily evaluated using Eq. (1.3.14) repeatedly. The final diagram is the hardest—it is analyzed in appendix A of [1].

The nonrenormalized correlator is thus given by

$$H_0(x) = \frac{P_1 g_0}{|x|^{3d/2 - 5\epsilon/2}} + \frac{(P_{2a} + P_{2b} + P_{2c}) g_0^2}{|x|^{3d/2 - 7\epsilon/2}} + O(g_0^3), \quad (1.3.42)$$

where we split the coefficients diagram by diagram. Taking into account signs and symmetry factors, we have (see (1.3.16)):

$$\begin{aligned} P_1 &= 8R_1, \\ P_{2a} &= 8R_2, \\ P_{2b} &= 4 \frac{w_{\frac{3}{2}(d-\epsilon)} w_{\frac{d-\epsilon}{2}} w_{d-\epsilon} w_{\frac{3}{2}d - \frac{5}{2}\epsilon}}{w_{d-2\epsilon} w_{\frac{3}{2}d - \frac{7}{2}\epsilon}} \approx 8\pi^d \frac{\Gamma\left(-\frac{d}{4}\right)}{\Gamma\left(\frac{3d}{4}\right)}, \end{aligned}$$

$$P_{2c} \approx 24\pi^d \Gamma\left(-\frac{d}{4}\right) / \Gamma\left(\frac{3d}{4}\right). \quad (1.3.43)$$

To pass from this result to the function \hat{h} , we need to perform the coupling and operator renormalization. We get:

$$\hat{h}(g) = gP_1 + g^2[P_1(K + K_2 + K_4)\epsilon^{-1} + P_{2a} + P_{2b} + P_{2c}] + O(g^3). \quad (1.3.44)$$

Putting in the values of all coefficients, we find that this expression is proportional to the one-loop beta function, similarly to (1.3.20). We conclude that $\hat{h}(g)$ vanishes at the IR fixed point at $O(\epsilon^2)$.

1.4 Conformal invariance of the gaussian phase

The nonlocal gaussian theory described by the action (1.1.4) is also conformal. This is widely known in high energy physics,¹⁸ and more recently has also been discussed from statistical physics perspective. In this section we will review this fact pedagogically, trying to bridge the gap between the two communities.¹⁹

1.4.1 Direct argument

We will start in the antichronological order. As pointed out in [66], the fractional Laplacian, just like the ordinary Laplacian, is covariant under conformal transformations. Namely if $x \rightarrow x'$ is a conformal transformation and

$$\phi'(x') = |\partial x' / \partial x|^{-\Delta_\phi/d} \phi(x) \quad (1.4.1)$$

with Δ_ϕ given in (1.1.3), then

$$\mathcal{L}'_s \phi'(x') = |\partial x' / \partial x|^{\Delta_\phi/d-1} \mathcal{L}_s \phi(x). \quad (1.4.2)$$

As a result the action (1.1.4) is invariant under conformal transformations. The proof of (1.4.2) is given in [66] and we will not repeat it here. As usual, covariance under translations, rotations, and dilatations is obvious, and a simple calculation establishes covariance under the inversion.

Notice that since we are dealing with a nonlocal theory, there is no reason to expect that in $d = 2$ the global conformal invariance of the action (1.1.4) gets enhanced to the full Virasoro invariance, and indeed this does not happen.²⁰

¹⁸There, this theory is sometimes referred to as Mean Field Theory or Generalized Free Field.

¹⁹Even though we won't discuss it, conformality of the gaussian phase can be shown using the AdS/CFT correspondence as well, see for example section 5.3 of [1].

²⁰Although it's not essential for this discussion, we would like to point out that there are also examples of *local* 2d theories which have global conformal but not Virasoro invariance. Once such theory is the "biharmonic scalar" with the Lagrangian $(\partial^2 \phi)^2$. Its stress tensor trace is of the form $\partial^\mu \partial^\nu Y_{\mu\nu}$ which is enough for global conformal invariance but not enough for an improvement to make it traceless and recover full Virasoro, since in 2d one needs

1.4.2 Argument from correlation functions

The previous argument shows the invariance of the action. Since the theory is gaussian, conformal covariance of the correlation functions follows. It's also easy to check the transformation properties of the correlation functions directly. This way of proving conformal invariance predates the previous one, see [68] and an analogous discussion for a nonlocal *vector* theory appeared in [69].

Let's start with the two point function of ϕ . It is given by $|x - y|^{-2\Delta_\phi}$, which indeed has the form of a two point function of a primary scalar of dimension Δ_ϕ . The N -point functions of ϕ are given by Wick's theorem, since the theory is gaussian. A moment's thought shows that since the two point function transforms as it should, the N -point functions will do so as well. So all correlation functions of ϕ are consistent with conformal symmetry.

The theory contains more operators, for example the normal ordered products $:\phi^n:$. Their correlation functions are defined by just leaving out the Wick contractions at coincident points, hence they will also be conformally covariant.

Although there are still more operators in addition to the ones considered above, all of them can be obtained by taking repeatedly the OPE of ϕ with itself. Correlation functions of these operators will inherit conformal transformation properties from the correlators of ϕ .²¹ Hence the theory is conformal.

1.4.3 Caffarelli-Silvestre trick

The idea of the previous argument is to rewrite the nonlocal gaussian theory as an equivalent higher dimensional theory whose conformal invariance is manifest. We will now present a second way to implement this idea, based on an observation of Caffarelli and Silvestre [70].

Consider a scalar field $\Phi = \Phi(x, y)$ where the extra coordinate y now takes values in the flat Euclidean space of $p = 2 - s$ dimensions. Hopefully the reader is not disturbed by the fact that p is in general fractional. In this space we consider the massless scalar field action:

$$S_{CS} = \int d^d x d^p y [(\partial_x \Phi)^2 + (\partial_y \Phi)^2]. \quad (1.4.3)$$

We will now show that this local action is equivalent to the nonlocal action (1.1.4).

Let $\phi(x)$ be the value of the field Φ on the d dimensional hyperplane $y = 0$:

$$\phi(x) = \Phi(x, 0), \quad (1.4.4)$$

and consider the effective action for ϕ obtained by integrating out the rest of the space.

$T_\mu^\mu = \partial^2 Y$ for the latter [5]. See [66, 67] for a discussion.

²¹See the argument in appendix B of [1].

Chapter 1. Conformality of the critical Long Range Ising model

To find it we have to solve the equations of motion of the higher-dimensional theory subject to the boundary condition (1.4.4). It's clear that we can restrict to the sector of fields radially symmetric in the y variable. In this sector the action becomes ($z = |y| > 0$):

$$S_{CS} = S_p \int d^d x dz z^{1-s} [(\partial_x \Phi)^2 + (\partial_z \Phi)^2]. \quad (1.4.5)$$

Recall that S_p is the unit sphere volume in p dimensions. The equation of motion is

$$\partial_x^2 \Phi + (1-s) \partial_z \Phi / z + \partial_z^2 \Phi = 0. \quad (1.4.6)$$

The solution decreasing at large z takes in momentum space the form:

$$\Phi(p, z) = \text{const.} (|p|z)^{s/2} K_{s/2}(|p|z) \phi(p). \quad (1.4.7)$$

For small z this has an expansion:

$$\Phi(p, z) = (1 + \text{const.} (|p|z)^s + \dots) \phi(p). \quad (1.4.8)$$

The ... terms are $O(z^2)$ compared to the shown ones and are subdominant in the range of interest $0 < s < 2$. We integrate by parts in (1.4.3), pick up the boundary term, and find

$$S_{CS} = -S_p \int d^d x z^{1-s} \Phi \partial_z \Phi|_{z \rightarrow 0} \propto \int d^d p \phi(p) |p|^s \phi(-p), \quad (1.4.9)$$

which is the nonlocal action (1.1.4) in momentum space.²²

It is now easy to complete the argument for conformal invariance. We started with a massless scalar theory in flat space (1.4.3), which is conformally invariant in an arbitrary number of dimensions. When we construct an effective theory by integrating out the space away from the $y = 0$ hyperplane, we are guaranteed to obtain a theory invariant under the subgroup of the $d + p$ dimensional conformal group which leaves invariant this hyperplane. This is precisely the d dimensional conformal group.

Concerning the prior history of the given argument, Caffarelli and Silvestre noticed that the equation of motion (1.4.6) gives rise to the fractional Laplacian and showed the equivalence of the two actions. They also noticed that (1.4.6) is nothing but the Laplace equations for functions radially symmetric in p extra coordinates. The Caffarelli-Silvestre description in the radially reduced sector was used by Rajabpour [66] to discuss some aspects of the nonlocal gaussian theory. Using the full $d + p$ dimensional description to argue for the conformal invariance of the theory seems to be done here for the first time.

²²The form of this effective action could also be predicted from the following argument. The free scalar Φ two point function depends on the distance as $\propto 1/r^{d+p-2}$. The same dependence is inherited by ϕ when we set $y = 0$, and we recover the expected two point function of the nonlocal scalar field of dimension $d - s$.

1.5 Conformal invariance of the LRI critical point

We will now present a proof that the LRI critical point is conformally invariant also in the nontrivial region 2.

The key idea is to rewrite our theory (1.2.3) as a *defect quantum field theory*. Namely, according to the discussion in section 1.4.3, we can rewrite the action as²³

$$S = \frac{1}{2} \int d^{\bar{d}} X (\partial_M \Phi)^2 + \frac{g_0}{4!} \int_{y=0} d^d x \Phi^4. \quad (1.5.1)$$

In the first term Φ is the free scalar Caffarelli-Silvestre field from section 1.4.3, defined on the $\bar{d} = d + p$ dimensional space $X = (x, y)$. The second term represents interaction living on the *defect*: the d -dimensional plane located at $y = 0$. The number of extra dimensions will be fractional in the case of interest (s near $d/2$), but in spite of this fact the theory (1.5.1) makes perfect sense, at least in perturbation theory.²⁴

In the theory (1.5.1) we will consider N -point functions of $\Phi(X)$, $G(X_1 \dots X_N)$. The correlators of the original theory (1.2.3) can be obtained by taking the $y \rightarrow 0$ limit.

The first part of the proof will be to derive broken scale and conformal Ward identities satisfied by the correlators $G(X_1 \dots X_N)$. We will then discuss how these Ward identities imply conformal invariance of the IR fixed point.

1.5.1 Ward identities

Crucially, the theory (1.5.1) is local and so its Ward identities can be derived by a variation of the usual method: the idea of the proof [58, 71–73] is to construct the Ward identities for scale and conformal invariance broken by the effects of the running coupling, and to show that the breaking effects disappear at the fixed point. Our derivation is along the lines of the simplified one of [58]. We start by considering the canonical stress tensor:

$$T_{MN} = \partial_M \Phi \partial_N \Phi - \frac{1}{2} \delta_{MN} (\partial_K \Phi)^2 - \delta_{MN}^{\parallel} \delta^{(p)}(y) \frac{g_0}{4!} \Phi^4. \quad (1.5.2)$$

The indices $M, N \dots$ will run over the full \bar{d} -dimensional space, $\mu, \nu \dots$ over the d -dimensional “parallel” subspace, and $m, n \dots$ over the p -dimensional “perpendicular” subspace. The δ_{MN}^{\parallel} is the Kronecker delta in the parallel subspace: $\delta_{MN}^{\parallel} = \delta_{\mu\nu}$ if both indices are parallel, and zero otherwise.

We don’t make a distinction between the bare and renormalized field Φ , because Φ does not get renormalized: since the interaction term is located on the defect, it cannot renormalize

²³Normalization of the first term is different from (1.2.3) where it was fixed via (1.2.4). This difference is unimportant for the proof of conformal invariance.

²⁴See section 1.5.2.2 for a nonperturbative discussion. An introduction to perturbative quantum field theory in non-integer dimensions can be found in [52].

Chapter 1. Conformality of the critical Long Range Ising model

the bulk kinetic term. The boundary kinetic term corresponds to an irrelevant operator and cannot be generated either.

The next step is to find the divergence and the trace of T_{MN} . Direct computation gives:

$$\partial^M T_{MN} = -E_N + \delta^{(p)}(y) D_N, \quad (1.5.3)$$

$$T^M_M = -\Delta_\phi E - \epsilon(g_0/4!) \delta^{(p)}(y) \Phi^4 + (1/2 - \bar{d}/4) \partial_K^2 \Phi^2, \quad (1.5.4)$$

where the E and E_N are operators proportional to the equations of motion of the theory

$$E = \Phi \{-\partial_K^2 \Phi + \delta^{(p)}(y)(g_0/3!) \Phi^3\}, \quad E_N = \partial_N \Phi \{-\partial_K^2 \Phi + \delta^{(p)}(y)(g_0/3!) \Phi^3\}, \quad (1.5.5)$$

and the object D_N is called the displacement operator. It is given by:

$$D_N = (g_0/3!) \Phi^3 \partial_n \Phi \quad \text{if } N = n \quad (1.5.6)$$

is a perpendicular index, and vanishes otherwise. This operator represents an infinitesimal movement of the defect in an orthogonal direction.

Correlation functions of the operators E and E_N are trivial: their insertions into n -point functions of φ produce a bunch of δ -function at coincident points, see Brown's (3.10), (3.28):

$$\begin{aligned} G(X_1 \dots X_n; E(X)) &= \sum_{i=1}^n \delta(X - X_i) G(X_1 \dots X_n), \\ G(X_1 \dots X_n; E_N(X)) &= \sum_{i=1}^n \delta(X - X_i) \frac{\partial}{\partial X_i^N} G(X_1 \dots X_n). \end{aligned} \quad (1.5.7)$$

One may wonder why we bother at all about the operators E and E_μ , since they have vanishing correlation functions at non-coincident points. Indeed, in the usual CFT language, they would not even qualify to be called operators. However, here we are working in perturbative quantum field theory, and in this situation it turns out to be both legitimate and useful to have access to E and E_μ . Legitimate because in the regularized theory the equations (1.5.7) make perfect technical, and not just formal, sense. Useful because the fastest derivation of the Ward identities uses these operators, as we will see momentarily.

Unlike Φ , the operator $\Phi^4|_{y=0} \equiv \phi^4$ appearing in (1.5.4) is not a finite operator; it will be related to a finite renormalized operator $[\phi^4]$ via a rescaling

$$\phi^4 = Z_4 [\phi^4]. \quad (1.5.8)$$

Contrary to what would happen in the local Wilson Fisher fixed point, in the LRI there is no other operator with which ϕ^4 could mix. The coefficient Z_4 is easy to compute. For any finite

1.5. Conformal invariance of the LRI critical point

correlation function we have

$$\begin{aligned}\frac{\partial}{\partial g}\Big|_{\mu=\text{const.}} \langle \dots \rangle &= \langle \dots \int d^d x \mu^\epsilon [\phi^4](x) \rangle, \\ \frac{d}{dg_0} \langle \dots \rangle &= \langle \dots \int d^d x \phi^4(x) \rangle.\end{aligned}\tag{1.5.9}$$

On the other hand, differentiating (1.2.5) with respect to $\log \mu$ we obtain the relation $\partial g_0 / \partial g = -\epsilon g_0 / \beta(g)$. It follows that:

$$Z_4 = -\beta(g) \mu^\epsilon / (\epsilon g_0),\tag{1.5.10}$$

and therefore

$$\frac{g_0}{4!} \phi_0^4 = -\frac{\mu^\epsilon}{4!} (\beta(g) / \epsilon) [\phi^4]\tag{1.5.11}$$

Plugging this into (1.5.4) we obtain:

$$T^M_M = -\Delta_\phi E + (\beta(g)/4!) \mu^\epsilon \delta^{(p)}(y) [\phi^4] + (1/2 - \bar{d}/4) \partial_K^2 \Phi^2.\tag{1.5.12}$$

We next consider the dilatation and special conformal currents:

$$\mathcal{D}_M = T_{MN} X^N, \quad \mathcal{C}_M^L = T_{MN} (2X^N X^L - \delta^{NL} X^2).\tag{1.5.13}$$

The divergence of the scale current is given by

$$\partial^M \mathcal{D}_M = -X^N (E_N - \delta^{(p)}(y) D_N) + T^M_M = -X^M E_M + T^M_M.\tag{1.5.14}$$

The term proportional to D_N is seen to vanish, since either N is a parallel index and then $D_N = 0$, or else it's a perpendicular index and then $X^N \delta^{(p)}(y) = 0$. Inserting these equation in an n -point function and integrating over the full space, we get

$$\int d^d x G(X_1 \dots X_n; -X^M E_M(X) + T^M_M(X)) = 0,\tag{1.5.15}$$

which allows us to obtain the scale Ward identity

$$\sum_{i=1}^n [X_i \cdot \partial_{X_i} + \Delta_\phi] G(X_1 \dots X_n) = \beta(g) \frac{\mu^\epsilon}{4!} \int d^d x G(X_1 \dots X_n; [\phi^4](x)).\tag{1.5.16}$$

Analogously let's analyze the divergence of the special conformal current

$$\partial^M \mathcal{C}_M^L = -(2X^N X^L - \delta^{NL} X^2) (E_N + \delta^{(p)}(y) D_N) + 2X^L T^M_M.\tag{1.5.17}$$

We would like to derive a Ward identity corresponding to special conformal transformations leaving the defect invariant, i.e. when $L = \lambda$ is a parallel index. The extra term proportional to D_N then drops out just as for the scale current, since D_N is nontrivial only if $N = n$ is a perpendicular index. Then $\delta^{n\lambda} = 0$, while $X^n X^\lambda$ vanishes when multiplied by $\delta^{(p)}(y)$.

Chapter 1. Conformality of the critical Long Range Ising model

Therefore, inserting this in a n -point function and integrating over space we have

$$\int d^{\bar{d}}x G(X_1 \dots X_n; -(2X^N X^L - \delta^{NL} X^2)E_N(X) + 2X^L T^M_M(X)) = 0. \quad (1.5.18)$$

and the Ward identity:²⁵

$$\begin{aligned} \sum_{i=1}^N \left[(2X_i^M X_i^\lambda - \delta^{M\lambda} X_i^2) \frac{\partial}{\partial X_i^M} + 2\Delta_\phi X_i^\lambda \right] G(X_1 \dots X_N) \\ = 2\beta(g) \frac{\mu^\epsilon}{4!} \int d^d x x^\lambda G(X_1 \dots X_N; [\phi^4](x)). \end{aligned} \quad (1.5.19)$$

Now, the correlators $G(X_1 \dots X_n)$ behave continuously in the limit $y \rightarrow 0$. This can be seen diagram by diagram in perturbation theory.²⁶ Thus, if one is primarily interested in the correlators at the defect, which are the correlators of the original theory, then one may set $y = 0$ in (1.5.16) and (1.5.19), obtaining restricted Ward identities satisfied by the correlators of the original theory (1.2.3):

$$\sum_{i=1}^N [x_i \cdot \partial_{x_i} + \Delta_\phi] G(x_1 \dots x_N) = \beta(g) \frac{\mu^\epsilon}{4!} \int d^d x G(x_1 \dots x_N; [\phi^4](x)), \quad (1.5.20)$$

$$\sum_{i=1}^N \left[(2x_i^\mu x_i^\lambda - \delta^{\mu\lambda} x_i^2) \frac{\partial}{\partial x_i^\mu} + 2\Delta_\phi x_i^\lambda \right] G(x_1 \dots x_N) = 2\beta(g) \frac{\mu^\epsilon}{4!} \int d^d x x^\lambda G(x_1 \dots x_N; [\phi^4](x)). \quad (1.5.21)$$

At this point, if one wishes, one may altogether forget about the construct of the extra dimensions. Notice however that without this construct, it would remain pretty mysterious why the nonlocal LRI theory should satisfy Ward identities which are almost identical in form to the ones satisfied by the local SRI.²⁷

These are the Ward identities expressing the breaking of scale and special conformal invariance by the running coupling. They are valid at all distances and for all λ . For the purposes of studying the IR fixed point, we have to go to large distances and to take the limit $\mu \rightarrow 0$, so that $\lambda(\mu) \rightarrow \lambda_*$. In this limit the beta-function multiplying the RHS of (1.5.20) and (1.5.21) vanishes. One is thus tempted to conclude that the IR fixed point is both scale and conformally invariant.

²⁵It's not hard to convince oneself that various boundary terms appearing when integrating by parts in the derivation of the Ward identities vanish by a good margin. We need an estimate of the decay of a correlation function of a group of ϕ 's and a widely separated T_{MN} for a theory which has not yet reached the fixed point, and for an unimproved T_{MN} . For a quick and dirty estimate, notice that there will be at least two propagators connecting T_{MN} to the ϕ 's, with two derivatives acting on them. This gives decay $\sim 1/|X|^{2\bar{d}-2}$, which is sufficient for $d > 1$ and $s < 2$. The ϕ^4 part of T_{MN} gives an even smaller contribution.

²⁶This is also closely related to the fact that Φ does not acquire anomalous dimension, and thus its bulk-to-defect OPE is non-singular (see a related discussion in section 6.3 in [1]).

²⁷It is possible that the Ward identities (1.5.20), (1.5.21) can be proved by endowing the LRI theory with some sort of nonlocal stress tensor operator. See [66] for steps in this direction for the gaussian case. Still, the most natural path to the nonlocal stress tensor lies through the Caffarelli-Silvestre construction.

While this conclusion will turn out to be correct, we believe that this last step of the argument merits somewhat more attention. There is a subtlety here. It's true that $\beta(\lambda) \rightarrow 0$ as $\mu \rightarrow 0$, but what about the integrals multiplying it? The integrals are μ -dependent because the operator $[\phi^4]$ is normalized at the scale μ . Could it be that the integrals grow in the $\mu \rightarrow 0$ limit, overcoming the $\beta(\lambda)\mu^\epsilon$ suppression? This issue seems to have been neglected in the literature. The proof that r.h.s. of (1.5.20) and (1.5.21) vanishes in the IR can be found in [1].

The main subtlety is that naive dimensional analysis fails when studying the integrals on the r.h.s. of (1.5.20) and (1.5.21), and it might look like they diverge when approaching the IR so that the complete r.h.s. of these equations is $O(1)$. However, one can express the integral in (1.5.20) as a derivative of a correlation function w.r.t. g and use the Callan-Symanzik equation to prove that the full r.h.s. vanishes in the IR. Once this is done, it's possible to show that the same happens for (1.5.21).

Therefore, we conclude that, in the IR correlation functions of the field ϕ are conformally invariant. In order to have a complete proof of conformal invariance, we should now turn our attention to composite operators. Correlation functions of composites can be related to those of the fundamental field by using the OPE. This is especially obvious for the bulk correlators, since one then needs only the bulk-to-bulk OPE, identical to that of the free theory. Composite operator correlators on the defect can be obtained from those away from the defect via the bulk-to-defect OPE. Alternatively, one can access such correlators via the OPE of fundamental fields on the defect. For more details, see section 6.3 and appendix B of [1].

1.5.2 Beyond perturbation theory

1.5.2.1 Virial currents

The question of scale invariance implying conformal invariance in a local theory,²⁸ as lucidly explained long ago by Polchinski [5], boils down to whether the trace of the stress tensor contains a total derivative term in addition to terms vanishing at the critical point or at non-coincident points:

$$T^\mu{}_\mu \supset \partial_\mu V^\mu \quad (?) \tag{1.5.22}$$

The operator V^μ is called a *virial current*. It must be a vector operator of scaling dimension exactly $D - 1$, to match the scaling dimension of $T_{\mu\nu}$. The appearance of $\partial_\mu V^\mu$ in $T^\mu{}_\mu$ does not contradict scale invariance, because the extra term vanishes when integrated over the full space, and does not disturb the scale Ward identity. However, the derivation of special conformal Ward identity requires integrating $T^\mu{}_\mu$ multiplied by x^λ , in the same way as (1.5.18). The extra term then does not go away *unless* V_μ is itself a total derivative, $V_\mu = \partial^\nu Y_{\mu\nu}$.

From a modern perspective, then, to check if a theory is conformally invariant it's enough to see if it contains a vector operator of dimension exactly $d - 1$ which is (a) a singlet under

²⁸See [74] for a review and in particular [6, 7, 75] for recent nontrivial progress in 4d.

Chapter 1. Conformality of the critical Long Range Ising model

all global symmetries, (b) not conserved, and (c) not a total derivative. In weakly coupled examples it can be seen by inspection whether such an operator exists. As Polchinski [5] pointed out, the φ^4 theory in $d = 4 - \varepsilon$ dimensions does not have any nontrivial V_μ candidate, and hence its IR fixed point must be conformally invariant to all orders in perturbation theory.

In the strongly coupled situation one can argue (see e.g. [8, 76, 77]) that the (a,b,c) requirements cannot *generically* be satisfied, and thus scale invariance *generically* implies conformal invariance. Indeed, what's the likelihood that there will be a dimension $d - 1$ vector which is not conserved, given that all non-conserved vectors generically acquire anomalous dimensions? This being pretty obvious, the real question is to what extent one can get rid of the genericity assumption.

To be concrete, let's take the critical SRI in $d = 3$ as an example. Very dramatic evidence for its conformal invariance comes from years of exploration using conformal bootstrap methods [13, 14, 16, 41–48]. These methods take conformal invariance as an assumption, which leads to a system of equations on the operator dimensions and OPE coefficients of the theory. The system is tightly constraining, and the fact that it has a solution which is in agreement with everything computed about the 3d Ising model using more pedestrian techniques is strong evidence for the validity of the assumption.

But is there any more direct evidence of conformality for the critical SRI? The question was recently approached using Monte Carlo methods in [78]. The dimension of the lowest spin 1 operator of the theory was measured, and it was found that $\Delta_V > 5$, well above the $d - 1 = 2$ required by a virial current. This is a very strong non-perturbative test of the conformality of the SRI fixed point.

1.5.2.2 Conformality of LRI beyond perturbation theory

Finally, we would like to discuss the prospects of a nonperturbative proof of conformal invariance of the LRI critical point.

First of all one would have to be convinced that the extra-dimensional defect QFT formulation (1.5.1) makes sense beyond perturbation theory.²⁹

Alternatively, one can try to get rid of the fractional dimensions altogether by restricting the $y > 0$ theory to the radially symmetric sector described by the reduced action (1.4.5), which is $d + 1$ dimensional. This action should still contain the conformal symmetry of the original action. The disadvantage of this formulation is the explicit dependence of the action on y . On the other hand it's manifestly nonperturbatively well defined.

Whatever the formulation one uses, one will be reduced to studying the Ward identities for the corresponding stress tensor operator. Analogously to section 1.5.2.1, one can ask: what if the

²⁹For a collection of recent work trying to make nonperturbative sense of various aspects of quantum field theory in fractional number of dimensions see [40, 79, 80].

stress tensor trace contains the following term:

$$T^M_M \supset \delta^{(p)}(y) \partial_\mu v^\mu (?), \quad (1.5.23)$$

where v_μ is a dimension $d - 1$ vector operator on the defect—a defect virial current. By assumption, v^μ is not identically conserved. Like in the discussion following the analogous Eq. (1.5.22), we see that unless v_μ is a total derivative its presence precludes conformal invariance of the correlation functions, while preserving their scale invariance.

So, can our theory contain a defect vector which has dimension exactly $d - 1$ and is not a total derivative? Generically, this appears unlikely (with or without the total derivative clause). In perturbation theory, there was no candidate for such an operator (and so it's not surprising that no such term is visible in (1.5.12)). To establish this rigorously and nonperturbatively appears as hard as the corresponding problem for the SRI.

We finally note that in the context of *boundary* rather than *defect* quantum field theory the question whether scale invariance implies conformality was recently discussed in [81].

1.6 Discussion

The general problem of scale versus conformal invariance is continuing to provide food for thought. In this chapter we have discussed this issue for the specific theory corresponding to the LRI at criticality. Since this model most notably does not have a local stress tensor, even the standard (genericity) arguments are invalid, leaving the question of scale versus conformal invariance hanging in midair.

In the first part of the chapter we have provided nontrivial evidence for conformal invariance of the LRI by showing that the $\langle \phi \phi^3 \rangle$ and $\langle \phi^2 \phi^4 \rangle$ two point functions vanish at criticality, at least up to terms of $O(\epsilon^3)$. In the second part we were able to *prove* conformal invariance at the critical point to all orders in perturbation theory. The salient point of the proof was the construction of the LRI model as a defect theory in an auxiliary higher-dimensional space; this allowed us to work with a higher-dimensional stress tensor and construct a proof analogous to the one used for the Wilson-Fisher fixed point. Much like the SRI, it is plausible that the LRI is also nonperturbatively conformally invariant.

What does our proof teach us about general long-range lattice models? First of all, the models that have an epsilon expansion starting from a generalized free theory, like the long-range $O(N)$ or Potts models, will be conformally invariant at their critical points to all orders by simple extensions of our proof.³⁰

In hindsight it is now also easy to cook up long-range models which will *not* be conformally invariant. The simplest one is based on a vector rather than a scalar. The gaussian long-range

³⁰Recall once again that in $1 + 1$ dimensions conformal invariance without a stress tensor implies a global $SO(3, 1)$ invariance, not the full Virasoro symmetry.

Chapter 1. Conformality of the critical Long Range Ising model

action then has two terms consistent with rotation invariance. Equivalently, the vector two point function also has two terms:

$$\langle B_\mu(x)B_\nu(0)\rangle = (a\delta_{\mu\nu} + bx^\mu x^\nu/x^2)/|x|^{2\Delta_B}. \quad (1.6.1)$$

This agrees with the two point function of a conformal primary vector for $b/a = -2$, and with that of a derivative of a scalar primary for $b/a = -2\Delta_B$. For all the other ratios this gaussian model will not be conformal [69].³¹ Let us now perturb the gaussian theory by a quartic local term $(B_\mu B^\mu)^2$ and flow to the IR fixed point. We conjecture that this fixed point will be an interacting scale invariant theory without conformal invariance. It would be interesting to check this by explicit epsilon expansion computations of two point functions, like we did in section 1.3.

In recent years the use of the conformal bootstrap has emerged as an excellent tool to analyze CFTs in various dimensions [13]. The main ingredients in this approach are the conformal block decomposition of four point functions and the associated crossing symmetry equations, which all follow directly from conformal invariance (see e.g. [76]). The present work therefore opens the door towards an analysis of the LRI using these methods. Such a completely non-perturbative analysis has since been carried out in [49].

With an eye towards the conformal bootstrap let us finally discuss the critical point of the LRI from the perspective of an ordinary CFT. Firstly, the LRI distinguishes itself from the more familiar, local, CFTs by the absence of a local stress tensor operator. Secondly, we expect a one-dimensional family of solutions to the crossing symmetry, parametrized by the exactly known scaling dimension of ϕ . Thirdly, our analysis uncovered an interesting fact that the second \mathbb{Z}_2 odd primary operator ϕ^3 is related to ϕ through the nonlocal EOM: $\phi^3 \propto \mathcal{L}_s \phi$. This fixes the scaling dimension of ϕ^3 to be $\Delta_\phi + s$. Curiously, this can be equivalently rewritten as

$$\Delta_{\phi^3} = d - \Delta_\phi. \quad (1.6.2)$$

This identifies ϕ^3 as the so-called ‘shadow’ operator of ϕ , which by definition transforms in a conformal representation with the same value of the quadratic Casimir as ϕ . The shadow operators often appear in discussions of conformal blocks (see e.g. [83]), but usually as a formal tool, since they do not belong to the local operators of the theory. On the contrary, Eq. (1.6.2) means that both ϕ and its shadow are good local operators of the LRI critical point.³²

One may wonder if the nonlocal EOM also implies an exact proportionality relation between

³¹One can also reproduce this theory *à la* Caffarelli-Silvestre from an auxiliary vector theory in a higher-dimensional space. The auxiliary theory action has two terms $(\partial_M B_N)^2$ and $(\partial_M B_M)^2$. As is well known, such a vector theory without gauge invariance (“theory of elasticity”) is not conformally invariant [8, 82].

³²Other examples of theories with pairs of operators satisfying the “shadow relation” $\Delta_1 + \Delta_2 = d$ can be found among SUSY CFTs. Namely, such a relation can emerge if \mathcal{O}_1 is a chiral primary of dimension d/n where n is an integer, and $\mathcal{O}_2 = (\mathcal{O}_1)^{n-1}$. We thank Leonardo Rastelli for sending us a list of such theories. One simple example is the $\mathcal{N} = 2$ 3d Ising model where $n = 3$. What sets LRI apart is that the shadow relation appears as a consequence of the nonlocal EOM.

the coefficients with which ϕ and ϕ^3 appear in any OPE. Unfortunately, this appears not to be the case. Using the nonlocal EOM *once*, we can easily relate the three point functions of ϕ^3 to those of ϕ . However, we then have to relate the normalizations of the ϕ and ϕ^3 two point functions. This requires using the nonlocal EOM twice, subtracting the unperturbed ϕ two point function as in (1.3.37). The final answer then depends on the relative normalization of $\langle\phi\phi\rangle$ and $\langle\phi\phi\rangle_{S_0}$, which is unknown in general. See appendix A.1.

Subsequently, a conformal bootstrap analysis of the three dimensional LRI CFT in the intermediate regime was carried out in [49]. Up to six correlators of the relevant primaries ϕ , ϕ^2 and ϕ^3 were considered, and, imposing conditions about the OPE coefficients such as those of appendix A.1,³³ the constraints on the space of theories were studied. A way of isolating the theory with a specific value of s is to fix the dimension of the first spin-2 operator, which is larger than 3 for $s < s^*$ due to non-locality of the theory. For generic values of s , no islands are found, contrary to what happens in the SRI CFT [15], but the allowed region has a kink in the $(\Delta_\phi, \Delta_{\phi^2})$ plane. Assuming, like it's customary, that the theory lives at the kink, we can read off the value of Δ_ϕ and Δ_{ϕ^2} , and, using the non-renormalization of ϕ , find which is the value of s we are studying. The results agree well with the perturbative expansions close to $s \sim d/2$ and $s \sim s^*$, which we will discuss in the next chapter.

We conclude this chapter with a brief comment about the limit $s \rightarrow s_*$. What happens with the nonlocal CFT describing the LRI critical point when we approach this limit from below? As we discussed in the introductions, for $s > s_*$ the standard picture predicts the LRI critical point to be in the SRI universality class. It would be simplest if all correlation functions continuously transitioned to the SRI ones in the limit. However, this seems problematic in the standard picture in view of the presence of ϕ^3 as a primary in the LRI CFT.

Consider for example the correlation function $\langle\phi\phi^2\phi\phi^2\rangle$. In the LRI, its conformal block decomposition is expected to contain the contributions of *two* relevant \mathbb{Z}_2 odd scalars: ϕ and ϕ^3 . On the other hand, in the SRI fixed point ϕ^3 is a descendant in the CFT describing the WF fixed point, while the second \mathbb{Z}_2 odd primary operator (ϕ^5) is irrelevant. It could be that ϕ^3 decouples in the $s \rightarrow s_*$ limit, but based on the discussion in appendix A.1 this also seems unlikely. This would lead to conclude that, according to the standard picture, there is a discontinuity in the transition from the LRI to the SRI correlation functions. However, in the next chapter, we will see a more natural picture predicting a continuous transition.

³³The author of [49] generalized the discussion of appendix A.1 to spinning fields.

2 The long-range to short-range crossover

2.1 Introduction

The primary goal of this chapter will be to elucidate the long-range to short-range crossover at $s = s_*$. As explained in the previous chapter, the crossover from the long-range to the short-range regime happens when the dimension of the long-range fixed point (LRFP) spin field, $[\phi]_{\text{LRFP}}$, decreasing with s , reaches the short-range Ising fixed point (SRFP) dimension $[\phi]_{\text{SRFP}}$ [23].¹ In other words, the dimension of $[\phi]$ varies continuously through the crossover. This fixes

$$s_* = d - 2[\phi]_{\text{SRFP}} = 2 - \eta \quad (2.1.1)$$

in terms of the SRFP critical exponent η . Although we use the word “crossover”, it’s important to emphasize that the transition happens sharply, at $s = s_*$.

However, while the crossover from the mean-field to the intermediate regime is well understood, some features of the long-range to short-range crossover remain puzzling in the standard picture. For s slightly above $d/2$, the quartic interaction is slightly relevant and one can study the flow perturbatively, as we did in the previous chapter. By contrast, a perturbative description of the long-range to short-range crossover is presently lacking. Sak [24] (see also Cardy’s book [21], section 4.3), proposed to analyze the SRFP stability in terms of the non-local perturbation

$$\mathcal{O}_{\text{Sak}} = \int d^d x d^d y \frac{\sigma(x)\sigma(y)}{|x-y|^{d+s}}, \quad (2.1.2)$$

where $\sigma \equiv \phi_{\text{SRFP}}$ is the SRFP spin field. This perturbation crosses from relevant to irrelevant precisely at $s = s_*$ [21, 24]. For $s < s_*$ the SRFP perturbed by \mathcal{O}_{Sak} should flow to the LRFP. The RG flow diagram summarizing the standard picture is shown in Fig. 2.1. If s is just slightly below s_* , Sak’s perturbation is weakly relevant, and in principle it should be possible to study the flow perturbatively. However, it is unclear how to adapt the rules of conformal perturbation theory to this non-local case. To the best of our knowledge this has not been done.

¹In this chapter, to avoid confusion, we will always specify whether we are talking about operators in the $d/2 < s < s_*$ critical LRI regime or in critical SRI by $[\mathcal{O}]_{\text{LRFP}}$ and $[\mathcal{O}]_{\text{SRFP}}$ respectively.

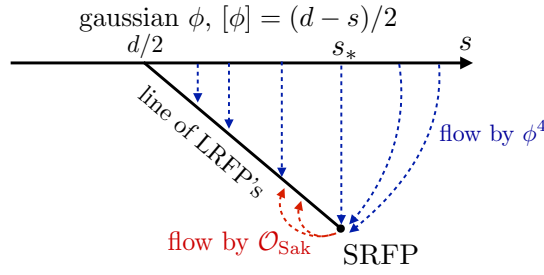


Figure 2.1 – RG flow diagram of the standard picture.

This lack of computability may be dismissed as a technical problem, but there are related conceptual puzzles. If the crossover is continuous, the spectrum of all operators, not just ϕ , should vary continuously. In particular, the number of operators should be the same on both sides of the crossover. However, for some LRFP operators no counterpart SRFP operators appear to exist.

One such operator is ϕ^3 . We have shown in chapter 1 that the dimension of this operator at the LRFP satisfies the “shadow relation”:

$$[\phi^3]_{\text{LRFP}} + [\phi]_{\text{LRFP}} = d. \tag{2.1.3}$$

This suggests that at the crossover point there should be a \mathbb{Z}_2 odd operator of dimension $d - [\phi]_{\text{SRFP}}$. This is puzzling, because the SRFP Ising contains, both in $d = 2$ and $d = 3$, a *single* relevant \mathbb{Z}_2 odd scalar.

Another puzzle involves the stress tensor operator. The SRFP has a local conserved stress tensor $T_{\mu\nu}$. Moving to the long-range regime, this operator is expected to acquire an anomalous dimension so that it’s no longer conserved. The divergence $V_\nu = \partial^\mu T_{\mu\nu}$ is thus a nontrivial operator at the LRFP. At the crossover point the dimension of this vector operator is exactly $d + 1$. Is there such an operator in SRFP? For $d = 2$ the SRFP is a solvable minimal model conformal field theory (CFT), and it’s easy to see by inspection that there is no such operator. For d close to 4 one can use the weakly coupled Wilson-Fisher description, and again there is no such operator. While in $d = 3$ its existence cannot be rigorously excluded by bootstrap studies, since \mathbb{Z}_2 -even operators of odd spin have not yet been probed in this approach, Monte Carlo simulations have put a lower bound on the dimension on the lightest spin 1, \mathbb{Z}_2 even, operator which seems to exclude its presence [78].

The puzzle of the missing V_μ can be stated more formally in terms of “recombination rules” of unitary representations of the $\mathfrak{so}(d + 1, 1)$ conformal algebra.² Now, the standard stress tensor of the SRFP is the lowest weight state (conformal primary) of the *shortened* spin-two representation $\mathcal{C}_{\ell=2}^d$, while the non-conserved spin-two operator of the LRFP is the conformal primary of the *long* spin-two representation $\mathcal{A}_{\ell=2}^\Delta$, with $\Delta \geq d$ for unitarity. When the unitarity

²It is common lore that SRFP is conformally invariant, in any d . See the discussion in section 1.5.2.1.

bound is saturated, the long spin-two representation decomposes into the semi-direct sum $\mathcal{A}_{\ell=2}^d \simeq \mathcal{C}_{\ell=2}^d \oplus \mathcal{A}_{\ell=1}^{d+1}$. In other terms, the shortened spin-two representation can become long only by recombining with (“eating”) an additional spin-one representation, $\mathcal{A}_{\ell=1}^{d+1}$, whose conformal primary V_μ is however missing in the SRFP.

In this chapter we will propose a modified theory of the long-range to short-range crossover, which will both resolve the puzzle of missing states and lead to concrete predictions of how the long-range exponents vary near the crossover point.

2.1.1 Our picture

The need to resolve the above-mentioned difficulties leads us to the following modified picture of the LRFP to SRFP crossover (referred to as “our picture” below). Like in the standard picture, the crossover in our picture does happen continuously and at $s = s_*$. However, and this is where we differ, we posit that LRFP crosses over not to SRFP, but to a larger theory, which consists from SRFP and a decoupled sector: the mean-field theory of a gaussian field χ . This larger theory will be referred to as “SRFP+ χ ”. The two point (2pt) function of χ will be taken unit-normalized: $1/|x|^{2\Delta_\chi}$.

Assuming our picture, we can construct the flow from the “SRFP+ χ ” theory to the LRFP by turning on the perturbation

$$g_0 \int d^d x \mathcal{O}(x), \quad \mathcal{O} = \sigma \cdot \chi. \quad (2.1.4)$$

The sign of g_0 is arbitrary since it can be flipped by the \mathbb{Z}_2^χ symmetry $\chi \rightarrow -\chi$. In fact the decoupled SRFP+ χ theory has an enlarged $\mathbb{Z}_2^\sigma \times \mathbb{Z}_2^\chi$ symmetry which is broken to the diagonal when the perturbation \mathcal{O} is turned on. This is as it should be, since the LRFP has only a single \mathbb{Z}_2 symmetry $\phi \rightarrow -\phi$. The enlarged symmetry of SRFP+ χ leads to selection rules, which will appear many times in the RG calculations below.

Connection to the standard picture is established by integrating out χ , which should generate precisely Sak’s non-local perturbation (2.1.2).³ This fixes the dimension $[\chi] = (d + s)/2$, so that

$$[\mathcal{O}] = [\chi] + [\sigma] = d - \delta, \quad \delta = (s_* - s)/2. \quad (2.1.5)$$

This crosses from relevant to irrelevant at the same location as before. We emphasize however that χ is not simply a theoretical construct introduced to represent \mathcal{O}_{Sak} , but is a physical field.

It should be possible to verify the existence of χ via lattice measurements. This is true even in the short-range regime $s > s_*$, where it is decoupled. The point is that it is decoupled from the SRFP scaling fields, but not from the lattice operators. It should thus be possible to detect χ by measuring the spin-spin correlation function $\langle S_i S_j \rangle$ on the lattice. At the critical point and at

³Notice that for real g_0 , the generated \mathcal{O}_{Sak} has ferromagnetic, negative, sign, as it should.

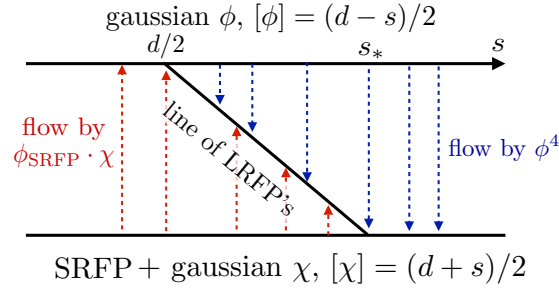


Figure 2.2 – RG flow diagram of our picture.

large distances, this function has a power law expansion of the form

$$\langle S_i S_j \rangle \sim \sum c_k / r^{2\Delta_k}, \quad r = |i - j|, \quad (2.1.6)$$

where Δ_k are the dimensions of \mathbb{Z}_2 -odd scalar operators. We predict that at the LRFP the dimension of χ should appear among Δ_k .

The existence of χ allows to resolve the difficulties concerning the crossover description. First of all, since χ and ϕ satisfy the shadow relation $[\chi] + [\phi] = d$, χ can be identified with ϕ^3 at the crossover point. This identification and its consequences will be discussed in detail below. We will also see that using χ one can construct a vector operator playing the role of V_μ . Finally, since \mathcal{O} is a local operator, we will be able to use the well-developed framework of conformal perturbation theory to compute the long-range critical exponents near the crossover point.

The RG flow diagram of our picture is shown in Fig. 2.2. We predict that in the intermediate regime $d/2 < s < s_*$ the LRFP is the common IR endpoint of two distinct RG flows:

1. Flow (1.1.2) from the mean field theory, which is weakly coupled near the lower end of the intermediate regime ($\epsilon \rightarrow 0$). We will call this “ ϕ^4 -flow”.
2. Our newly proposed flow emanating from the SRFP+ χ theory, which is weakly coupled near the crossover ($\delta \rightarrow 0$). We will call this “ $\sigma\chi$ -flow”.

In quantum-field theoretic parlance, this situation – when the same IR theory can be reached from two different UV descriptions – is referred to as “infrared duality”. A famous example is the Seiberg duality which establishes the IR equivalence of UV-distinct $\mathcal{N} = 1$ supersymmetric gauge theories [25]. Another example is the particle/vortex duality between the XY model and the $U(1)$ Abelian Higgs model in 3d, both flowing to the same $O(2)$ Wilson-Fisher critical point [84, 85]. The novelty of our example is that the IR fixed point does not have a local stress tensor.

2.1.2 Outline

We will start by investigating the structure of the LRFP close to the crossover ($\delta \ll 1$). In this region our $\sigma\chi$ -flow provides a weakly coupled description of the LRFP, allowing a number of explicit computations. In section 2.2 we compute the beta-function, at the leading nontrivial order, and establish the fixed point existence. In section 2.3 we compute the leading anomalous dimensions for the most interesting operators. In particular, we demonstrate that the stress tensor acquires anomalous dimension, and exhibit the eaten operator V_μ , thus resolving the paradox of missing states. These two sections include also a self-consistent presentation of necessary conformal perturbation theory techniques.

We start section 2.4 with some all-order results for the $\sigma\chi$ -flow, established by analogy with the ϕ^4 -flow. We then show that the results about the LRFP obtained from the ϕ^4 -flow and the $\sigma\chi$ -flow match together beautifully, providing compelling evidence for the infrared duality. At this high point, we conclude.

Appendix A.2 is an (admittedly incomplete) review of our favorite works on the long-range Ising model, both in the physics and the mathematics literature. Appendix D.1 evaluates some integrals arising in the conformal perturbation theory calculations.

2.2 Beta-function

According to our proposal, the LRFP can be described as the IR fixed point of the $\sigma\chi$ -flow. This description is weakly coupled for $\delta \ll 1$, when the $\sigma\chi$ perturbation is weakly relevant. This allows to compute the LRFP critical exponents in terms of the SRFP conformal data, known exactly in $d = 2$ [12], and with an impressive precision in $d = 3$ thanks to the recent progress in the numerical conformal bootstrap.

The standard framework to describe CFTs with turned on weakly relevant local perturbations is conformal perturbation theory (see e.g. [20, 86] for $d = 2$ and [21, 87] for general d). As usual in quantum field theory, we consider the perturbative expansion of observables in the bare coupling constant in a regulated theory, and then add counterterms to cancel the dependence on the short-distance regulator. The order n perturbative correction to an observable Ξ is given by

$$\frac{g_0^n}{n!} \int d^d x_1 \dots d^d x_n \langle \mathcal{O}(x_1) \dots \mathcal{O}(x_n) \Xi \rangle. \quad (2.2.1)$$

In general, this integral is divergent when points x_i collide. A convenient way to regulate is by point splitting, restricting integration to the region where all $|x_i - x_j| > a$ (short-distance cutoff). If Ξ is a local operator, there will also be divergences where x_i approach Ξ , but those are associated not with the running of the coupling but with the renormalization of Ξ . They will be discussed and interpreted separately below.

The first quantity we need is the beta-function. Let $g = a^\delta g_0$ be the dimensionless coupling at

the cutoff scale. The beta-function has the form

$$\beta(g) \equiv \frac{dg}{d \log(1/a)} = -\delta g + \dots, \quad (2.2.2)$$

where $-\delta g$ is the classical term and \dots are the quantum corrections.

The order g^2 correction to the beta-function is proportional to the 3pt function coefficient $C_{\mathcal{O}\mathcal{O}\mathcal{O}}$. This is well known and sufficient for most applications [20, 21, 86]. However, in our case $C_{\mathcal{O}\mathcal{O}\mathcal{O}}$ vanishes, because \mathcal{O} is odd under the \mathbb{Z}_2^χ symmetry $\chi \rightarrow -\chi$. Analogously all even-order contributions to $\beta(g)$ will vanish as well.

The lowest nonvanishing contribution will appear at order g^3 , at that's the only one we will use in this work. So we will have:

$$\beta(g) = -\delta g + \beta_3 g^3, \quad (2.2.3)$$

neglecting the higher order terms. We will now review how one computes the coefficient β_3 . We aim to discuss the fixed point properties at the leading nontrivial order in δ . For this we may neglect the dependence of β_3 on δ , so we will compute it in the limit $\delta = 0$.⁴ We will also specialize to the case $C_{\mathcal{O}\mathcal{O}\mathcal{O}} = 0$ of interest to us, as this simplifies some details. See [88, 89] for prior work involving third-order corrections. Our discussion owes a lot to [90], which covers also the general case $C_{\mathcal{O}\mathcal{O}\mathcal{O}} \neq 0$.

For $\delta = 0$ the coupling g is marginal and its running is related to the logarithmic short-distance divergence of (2.2.1). At order g^3 , we are interested in the divergence where three points come close together. In this region we can use the ‘triple operator product expansion (OPE)’:

$$\mathcal{O}(0)\mathcal{O}(x_2)\mathcal{O}(x_3) \sim f(x_2, x_3)\mathcal{O}(0). \quad (2.2.4)$$

It's easy to see that $f(x_2, x_3)$ is nothing but the 4pt correlation function:⁵

$$f(x_2, x_3) = \langle \mathcal{O}(0)\mathcal{O}(x_2)\mathcal{O}(x_3)\mathcal{O}(\infty) \rangle. \quad (2.2.5)$$

This is similar to the well-known relation between the usual OPE of two operators and the 3pt function. To check (2.2.5), use (2.2.4) in the r.h.s. and the fact that $\langle \mathcal{O}(0)\mathcal{O}(\infty) \rangle = 1$.

Using (2.2.4), we see that the divergence of the integral with three \mathcal{O} insertions is equal to the integral with one \mathcal{O} insertion times a divergent coefficient, computed by integrating the 4pt function:

$$\int_V d^d x_1 d^d x_2 d^d x_3 \langle \mathcal{O}(x_1)\mathcal{O}(x_2)\mathcal{O}(x_3)\mathcal{O}(\infty) \rangle = AV \log(1/a) + \dots \quad (2.2.6)$$

Integration is over the region $|x_i - x_j| > a$ with all three points belonging to a finite region of

⁴To compute higher order corrections, we would have to keep δ nonzero and set up a minimal subtraction scheme. This will not be carried out in this work, although see the all-order discussion in section 2.4.1.

⁵As usual $\mathcal{O}(\infty) = \lim_{x \rightarrow \infty} |x|^{2\Delta_{\mathcal{O}}} \mathcal{O}(x)$.

volume V , which serves as an IR cutoff. The IR cutoff is needed since we are interested only in the short-distance part of the divergence.

The divergence at $O(g^3)$ can thus be canceled, and the cutoff dependence removed, by a variation of the $O(g)$ term, adjusting the bare coupling by $-A \log(1/a) \times (g^3/3!)$. Therefore, the beta-function is given, to this order, by $\beta(g) = \beta_3 g^3$ with

$$\boxed{\beta_3 = -A/3!}. \quad (2.2.7)$$

To isolate the coefficient A , we use translational invariance to fix one of the points, say x_3 , to 0. The volume factor V cancels, and we are left with an integral of the function $f(x_1, x_2)$. We then separate the integration over the overall ‘size’ of the pair of points (x_1, x_2) and over their relative position. Rescaling the pair by, say, $|x_1|$, and using the fact that f has dimension $2d$ we have

$$\int d^d x_1 d^d x_2 f(x_1, x_2) = \int d^d x_1 d^d x_2 \frac{1}{|x_1|^{2d}} f\left(\frac{x_1}{|x_1|}, \frac{x_2}{|x_1|}\right) = S_d \int \frac{d|x_1|}{|x_1|} \int d^d y f(\hat{e}, y), \quad (2.2.8)$$

where \hat{e} is an arbitrary unit length vector and $S_d = 2\pi^{d/2}/\Gamma(d/2)$ is the volume of the unit sphere in d dimensions. The log divergence $\sim \log(L/a)$ now arises from integrating over $a < |x_1| < L$, which is basically the pair size. So we conclude

$$A = S_d \int d^d y f(\hat{e}, y) \quad (\text{naive}). \quad (2.2.9)$$

As written this expression is naive, since the y integral must be defined with care. In principle, the y integral in (2.2.8) was meant to be computed with a UV cutoff $a/|x_1|$. If the y integral were convergent, we could simply extend the integration to the whole space, as this does not affect the logarithmic divergence that we are after. However, the integral is not in general convergent, and this complicates matters.

The complication can be traced to the fact that, in the above discussion, we neglected that the integral (2.2.6) contains power divergences on top of the log divergence. These power divergences have nothing to do with the running of g . Instead, they renormalize coefficient of the relevant operators appearing in the OPE $\mathcal{O} \times \mathcal{O}$. In our case there are two such operators, the unit operator and the SRF energy density operator ε .⁶ The unit operator coefficient is unimportant, while that of ε has to be anyway tuned to zero to reach the fixed point, as this corresponds to tuning the temperature to the critical temperature. The bottom line is that the power divergences need to be subtracted away.

There are two methods to do this, which give equivalent, although not manifestly identical, final results. Method 1 subtracts the divergent terms, given by the relevant operators, from the integrand f . Method 2 computes the integral (2.2.9) with a cutoff and drop the terms that diverge when the cutoff is sent to zero. In both case we are just dropping power divergences of

⁶Another low-dimension scalar operator in the $\mathcal{O} \times \mathcal{O}$ OPE is χ^2 , but this one is irrelevant since $s > 0$.

Chapter 2. The long-range to short-range crossover

the integral (2.2.8), and we are not changing the coefficient of the logarithm divergence. Once one of these methods has been employed, the integral is convergent.

Method 1. We subtract from the integrand f in (2.2.8) the singularities associated with the two relevant operators in the limits $x_1 \rightarrow 0$, $x_2 \rightarrow 0$, $x_1 \rightarrow x_2$. The subtraction terms have to be chosen so that they fully subtract the power divergence but do not modify the logarithmic divergence. The following simple choice satisfies these constraints:

$$\begin{aligned} f &\rightarrow \tilde{f} = f - r_1 - r_\varepsilon, \\ r_1 &= \frac{1}{|x_1|^{2d}} + \frac{1}{|x_2|^{2d}} + \frac{1}{|x_1 - x_2|^{2d}}, \\ r_\varepsilon &= (C_{\sigma\sigma\varepsilon})^2 \left(\frac{1}{|x_1|^{2d-\Delta_\varepsilon}|x_2|^{\Delta_\varepsilon}} + \frac{1}{|x_2|^{2d-\Delta_\varepsilon}|x_1|^{\Delta_\varepsilon}} + \frac{1}{|x_1 - x_2|^{\Delta_\varepsilon}|x_1|^{2d-\Delta_\varepsilon}} \right). \end{aligned} \quad (2.2.10)$$

Here $C_{\sigma\sigma\varepsilon}$ is the SRFP OPE coefficient: $\sigma \times \sigma = \mathbb{1} + C_{\sigma\sigma\varepsilon}\varepsilon + \dots$. The crucial point is that these subtraction terms themselves only have power divergences. This is obvious for r_1 . For r_ε , notice that the $d^d x_1 d^d x_2$ integral of each term factorizes into a product of two integrals each of which has only power divergences. So the logarithmic divergence is not modified by the subtraction procedure.

The regulated expression for A is then obtained by $f \rightarrow \tilde{f}$ in (2.2.9):

$$A = S_d \int d^d y \tilde{f}(\hat{e}, y). \quad (2.2.11)$$

This integral is now convergent, although not absolutely convergent. The lack of absolute convergence is due to the presence of relevant or marginal operators with nonzero spin in the $\mathcal{O} \times \mathcal{O}$ OPE. These are $\partial_\mu \varepsilon$ and the stress tensor $T_{\mu\nu}$. Since these operators have nonzero spin, their contributions vanish when integrated over the angular directions. So the integral has to be understood in the sense of principal value, introducing and then removing spherical cutoffs around 0, \hat{e} and ∞ . These cutoffs are remnants of the original cutoffs on $|x_2|$ and $|x_1 - x_2|$, since y is the rescaled x_2 .

Method 2. In this method we start by splitting the integration region of (2.2.6) into three parts. We consider one region in which x_{12} is the shortest distance:

$$\mathcal{R}_{12} = \{x_1, x_2, x_3 : |x_{12}| < |x_{13}|, |x_{12}| < |x_{23}|\}, \quad (2.2.12)$$

and the two other regions \mathcal{R}_{23} and \mathcal{R}_{13} , given by permutations of the three points. It is clear that these three regions contribute equally to the integral (2.2.6), so we can focus on \mathcal{R}_{12} . As before, we set one of the points to zero and we rescale x_1 and x_2 by $|x_1|$. The logarithmic divergence arises when integrating over $|x_1|$. We obtain

$$A = 3S_d \int_{\mathcal{R}} d^d y f(\hat{e}, y), \quad (2.2.13)$$

where

$$\mathcal{R} = \{y : |y| < 1, |y| < |y - \hat{e}|\} \quad (2.2.14)$$

is the rescaled \mathcal{R}_{12} . Integral (2.2.13) is not convergent when integrating y around 0 due to the presence of relevant operators being exchanged. These divergences, associated with the renormalization of the operator, need to be subtracted away. This can be again done by computing the integral with a UV cutoff and by dropping terms that diverge when the cutoff goes to zero.

Although Eqs. (2.2.11) and (2.2.13) are not manifestly identical, the logic of their derivation shows that they should give identical answers (and they do, in all cases we checked). In practical computations, both ways of proceeding have advantages and disadvantages. Method 2 fully takes advantage of the symmetry among $0, 1, \infty$, while the integrands in Method 1 do not respect this symmetry (it is broken by the subtraction terms). Still, if one were to aim for analytic expressions, Method 1 seems preferable. The shape of the integration region in Method 2 makes it hard to compute the integral analytically. However, Method 2 will prove useful and yield more precise results when the integral needs to be evaluated numerically. Besides, in $d = 3$, where the correlation function is not known exactly but will be constructed approximately from the bootstrap data, Method 2 allows to consider the conformal block expansion in the s-channel only, without any need to deal with the t- and u-channel decomposition.

We adopted Method 2 as the principal method for the beta-function computation both in $d = 2$ and $d = 3$, since as we will see the integrals have to be computed numerically. While Method 1 is less precise for the numerical evaluation, we still checked that it gives the same results within its reduced precision.

2.2.1 Beta-function: $d = 2$

The 2d SRFP is the minimal model CFT $\mathcal{M}(3, 4)$ [12] and everything about it is known exactly. In particular, we have $\Delta_\sigma = 1/8$, $\Delta_\epsilon = 1$, $C_{\sigma\sigma\epsilon} = 1/2$. The 4pt function of σ is given by

$$\langle \sigma(0)\sigma(1)\sigma(z)\sigma(\infty) \rangle = \frac{|1 + \sqrt{1-z}| + |1 - \sqrt{1-z}|}{2|z|^{1/4}|1-z|^{1/4}}. \quad (2.2.15)$$

Comparing the notation to (2.2.11), here we have fixed \hat{e} at 1 on the real axis, while $y = z$ runs over the full complex plane. In spite of the appearance the 4pt function is smooth across $z \in (1, +\infty)$.

The 4pt function of χ is gaussian, given by the sum of three Wick contractions. In the same kinematics,

$$\langle \chi(0)\chi(1)\chi(z)\chi(\infty) \rangle = 1 + \frac{1}{|z|^{2\Delta_\chi}} + \frac{1}{|1-z|^{2\Delta_\chi}}, \quad \Delta_\chi = 2 - \Delta_\sigma = 15/8. \quad (2.2.16)$$

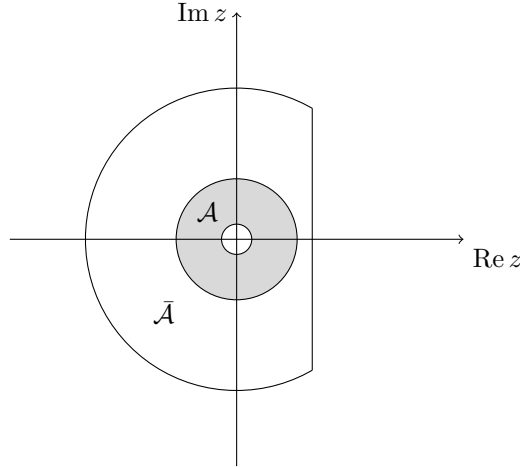


Figure 2.3 – The integration region \mathcal{R} .

The 4pt function of \mathcal{O} is given by the product of (2.2.15) and (2.2.16):

$$F(z, \bar{z}) = \left[1 + \frac{1}{|z|^{\frac{15}{4}}} + \frac{1}{|z-1|^{\frac{15}{4}}} \right] \frac{|1 + \sqrt{1-z}| + |1 - \sqrt{1-z}|}{2|z|^{\frac{1}{4}}|z-1|^{\frac{1}{4}}}. \quad (2.2.17)$$

We were not able to evaluate the integral of $F(z)$ analytically, so we will report the results of the numerical evaluation. We employ Method 2, so that we have to integrate over the region \mathcal{R} .

As discussed after Eq. (2.2.9), the integral is not convergent around 0. If we expand $F(z, \bar{z})$ around $z = 0$, we encounter several terms responsible for the non-convergence. The terms $|z|^{-4}$ and $|z|^{-2}$ correspond to contributions of the identity operator and energy density ε respectively. Other terms, such as $z/|z|^3$ and $z^2/|z|^4$ (+h.c.), are the contributions of $\partial_\mu \varepsilon$ and $T_{\mu\nu}$ in the $\mathcal{O} \times \mathcal{O}$ OPE; however, they will vanish upon angular integration.

To deal with the divergences, we remove from the region \mathcal{R} a small disk $|z| < a$ around the origin, and divide the rest into two regions: the annulus \mathcal{A} ($a < |z| < r_0$) centered around zero and its complement $\bar{\mathcal{A}}$, see Fig. 2.3. Here r_0 is arbitrary subject to $a < r_0 < 1/2$. In \mathcal{A} we expand $F(z)$ functions as a series in z and \bar{z} up to some high order. We can then drop the terms that vanish upon angular integration, and we integrate exactly the remaining terms. The power-divergent, as $a \rightarrow 0$, part of the answer is dropped. In the complement of the annulus we integrate $F(z)$ numerically. The so regulated integral over \mathcal{R} is then:

$$I_{d=2} = \int_{\mathcal{R}} d^2 z F(z, \bar{z}) = -0.403746\dots \quad (2.2.18)$$

All the shown digits are exact, and we checked that the result is stable against changes of r_0 . This implies

$$\beta_3 = -3(2\pi)I_{d=2}/3! = 1.268404 \quad (d = 2). \quad (2.2.19)$$

2.2.2 Beta-function: $d = 3$

The $d = 3$ SRFP is not yet exactly solved; however, high precision results are available thanks to the progress of the numerical conformal bootstrap [14–16, 41, 44]. Recently, the approximate critical 3d Ising 4pt function extracted from the bootstrap data was used in [90] to study the random bond Ising critical point. It was also used in [91] to qualify the non-gaussianity of the 3d Ising model.

Here we proceed analogously and will use the OPE coefficients $C_{\sigma\sigma\mathcal{O}}$ and dimensions $\Delta_{\mathcal{O}}$ of the lowest lying operators (such that $\Delta_{\mathcal{O}}$ is smaller than some cutoff in the spectrum Δ_*) to construct an approximate 4pt function for the σ field:

$$\langle \sigma(0)\sigma(\hat{e})\sigma(y)\sigma(\infty) \rangle \simeq \frac{1}{|x|^{2\Delta_\sigma}} \sum_{\mathcal{O}: \Delta_{\mathcal{O}} < \Delta_*} C_{\sigma\sigma\mathcal{O}}^2 g_{\Delta_{\mathcal{O}}, \ell_{\mathcal{O}}}(z, \bar{z}), \quad (2.2.20)$$

where $g_{\Delta, \ell}$ are the conformal blocks. Let us fix $\hat{e} = (1, 0, \dots, 0)$. Then z is the complex coordinate related to y by

$$z = y_1 + i|y_\perp|, \quad y_\perp = (y_2, \dots, y_d). \quad (2.2.21)$$

The 4pt function only depends on $|y_\perp|$ because of rotation invariance around the x_1 axis. The usual conformal cross ratios u, v are $u = |z|^2, v = |1 - z|^2$. Instead of z , it will be convenient to work with the radial coordinate ρ [92]

$$\rho(z) = \frac{z}{(1 + \sqrt{1 - z})^2}. \quad (2.2.22)$$

In three dimensions, the conformal blocks are not known exactly; however, they can be computed efficiently as a series in r and $\eta = \cos\theta$, where $\rho = r e^{i\theta}$, using a recursion relation [93, 94]. The conformal block expansion converges for $r < 1$ [95], while in the integration region \mathcal{R} the maximum value of r is $2 - \sqrt{3} \simeq 0.27 < 1$, so our series expansion will converge exponentially fast.

When approximating the 4pt function, we have to take into account three different sources of error:

1. We do not know the OPE coefficients and the operator dimensions exactly, as they are obtained through the numerical conformal bootstrap. The uncertainty due to this will turn out to be subleading;
2. We compute the conformal blocks as a series expansion in r . Here we did it up to order $O(r^{12})$, which provided sufficient accuracy, but it would be straightforward to compute them to a higher order;
3. We know the dimensions and the OPE coefficients of primary operators only up to a dimension Δ_* . The error introduced is of order r^{Δ_*} [95]. We use data from the numerical conformal bootstrap on operators up to dimension $\Delta_* = 8$.

Chapter 2. The long-range to short-range crossover

We will focus on the last source of error, since it will be the dominant one. The error one introduces when truncating the conformal block expansions of a 4pt function of identical scalars σ to some dimension Δ_* was estimated in [95] (see also [96]) to be

$$\left| \sum_{\mathcal{O}: \Delta_{\mathcal{O}} \geq \Delta_*} C_{\sigma\sigma\mathcal{O}}^2 g_{\Delta_{\mathcal{O}}, \ell_{\mathcal{O}}}(z, \bar{z}) \right| \lesssim \frac{2^{4\Delta_{\sigma}}}{\Gamma(4\Delta_{\sigma} + 1)} \Delta_*^{4\Delta_{\sigma}} |\rho(z)|^{\Delta_*}. \quad (2.2.23)$$

This error estimate is essentially optimal for real $0 < z < 1$, when the 4pt function is in a reflection positive configuration, and all conformal blocks are positive. This corresponds to the configuration with $\eta = 1$ in the ρ plane. For configurations with $\eta < 1$, conformal blocks decrease in absolute value by unitarity, and hence the same estimate (2.2.23) applies, although it's no longer optimal. When we integrate the 4pt function over the η coordinate, we will not be in a reflection positive configuration, but we will nonetheless bound the truncated operators contribution by its largest possible value, obtained for $\eta = 1$. Clearly, the obtained error estimate will be overly conservative, since it does not take into account cancelations due to the varying sign of contributions of operators with spin.

Once we have constructed the approximated 4pt function, we integrate it in the region \mathcal{R} .⁷ We follow the procedure outlined in appendix C of [90]: this consists in expanding the 4pt function as a power series in r and η , then integrating over r and dropping the diverging contributions of the identity and the energy operator. Finally we series-expand again with respect to η and we integrate the result exactly.

The data concerning the operator dimensions up to $\Delta_* = 8$ and their OPE coefficients can be found in Table 2 of [16] (our $C_{\sigma\sigma\mathcal{O}} = f_{\sigma\sigma\mathcal{O}}$ given in that table). The OPE coefficients given there are in the normalization for which the small r limit of the conformal block is $g_{\Delta, \ell} \simeq \frac{\ell!}{(\nu)_{\ell}} (-1)^{\ell} C_{\ell}^{\nu}(\eta) (4r)^{\Delta} + \dots$, where C_{ℓ}^{ν} is a Gegenbauer polynomial, $\nu = \frac{d}{2} - 1 = 1/2$ and $(\nu)_{\ell}$ is the Pochhammer symbol. Using these values, we obtain $I_{d=3} = -1.950 \pm 0.005$. The error is dominated by the truncation error, which we estimate by integrating (2.2.23).⁸ The g^3 term of the beta-function is then

$$\beta_3 = 12.26 \pm 0.03 \quad (d = 3). \quad (2.2.24)$$

2.2.3 Fixed point existence

If $0 < \delta \ll 1$, the flow that we are studying will reach a fixed point at

$$g^2 = g_*^2 = \delta / \beta_3. \quad (2.2.25)$$

This fixed point is naturally identified with LRF. Notice that for our picture to be correct, we must have $\beta_3 > 0$ (otherwise the fixed point at real g does not exist). The sign of β_3 was not

⁷In r and η coordinates, the region \mathcal{R} is given by $0 < r < r_*(|\eta|)$ and $-1 < \eta < 1$, with $r_*(\eta) = 2 + \eta - \sqrt{\eta^2 + 4\eta + 3}$.

⁸For comparison, if we only use operators up to $\Delta_* = 6$, we obtain the same central value but with a much larger error estimate: $I_{d=3} = -1.95 \pm 0.08$. This confirms that the error estimate is overly conservative.

manifest in the above calculations, since the regulated integrals are not sign-definite.⁹ Still, we have seen that β_3 is positive in both $d = 2$ and $d = 3$. This provides a nontrivial check on our picture.

That $\beta_3 > 0$ means that the operator $\sigma\chi$ is marginally irrelevant at the crossover. The flow at the crossover will be affected by logarithmic corrections to scaling due to $\sigma\chi$. One must be aware of this fact when interpreting Monte Carlo simulation data in the crossover region. See the discussion in appendix A.2.1.

2.3 Anomalous dimensions

When deforming a CFT with a local perturbation, operators renormalize and acquire anomalous dimensions. Let us recall how these are computed in conformal perturbation theory. As usual, we require observables to be cutoff independent. To find the anomalous dimension of a local operator $\Phi(x)$, assumed unit-normalized, we look at an observable with one insertion of Φ , $\langle\Phi(0)\Xi\rangle$. Perturbative corrections will be given by

$$\frac{g^n}{n!} \int d^d x_1 \dots d^d x_n \langle\Phi(0)\mathcal{O}(x_1)\dots\mathcal{O}(x_n)\Xi\rangle. \quad (2.3.1)$$

We regulate the integral by point splitting, with a short distance cutoff a , like in section 2.2. There we dealt with the divergences and cutoff dependence which appear when operators \mathcal{O} approach each other. Those were taken care of by renormalization of the coupling, leading to the nontrivial beta-function. Now we are interested in the additional divergences, in particular the logarithmic ones, which appear when operators \mathcal{O} collide with Φ .

We define a renormalized operator Φ_R , whose correlation functions remain finite in the $a \rightarrow 0$ limit. This is related to the bare operator by

$$\Phi = Z_\Phi(g, a)\Phi_R. \quad (2.3.2)$$

The anomalous dimension of Φ will then be given by¹⁰

$$\gamma_\Phi = -\frac{1}{Z_\Phi} \frac{\partial Z_\Phi}{\partial \log(1/a)}. \quad (2.3.3)$$

The above discussion was general, but now let us specialize to the flow which interests us, namely SRFP $+\chi$ perturbed by (2.1.4). We are ultimately interested in $\delta > 0$ small, but at the leading order we can compute the anomalous dimension for $\delta = 0$, when it's related to the log divergence as above. Moreover, order g corrections will vanish thanks to the Z_2^χ

⁹As a curiosity we notice that if it were not for the subtraction terms which had to be introduced in the process of disentangling short-distance divergences, then A would be positive, and β_3 negative.

¹⁰Compared to equation (1.2.15), there is an extra minus sign here. The reason behind this is that we are regulating the theory in a different way, *i.e.* point splitting, compared to what we did in the previous chapter.

Chapter 2. The long-range to short-range crossover

symmetry of the unperturbed theory, since $\Phi\mathcal{O}\Phi$ will be odd no matter if Φ is even or odd, and hence $C_{\Phi\mathcal{O}\Phi} = 0$. We will therefore be interested in the anomalous dimension to order g^2 . The computation of this anomalous dimension parallels the beta-function computation. To extract the short-distance divergence giving rise to the cutoff dependence of Φ , we consider the ‘triple OPE’

$$\Phi(0)\mathcal{O}(x_1)\mathcal{O}(x_2) \sim h(x_1, x_2)\Phi(0), \quad (2.3.4)$$

where h is the 4pt function

$$h(x_1, x_2) = \langle \Phi(0)\mathcal{O}(x_1)\mathcal{O}(x_2)\Phi(\infty) \rangle. \quad (2.3.5)$$

If the short-distance logarithmic divergence is

$$\int_V d^d x_1 d^d x_2 \langle \Phi(0)\mathcal{O}(x_1)\mathcal{O}(x_2)\Phi(\infty) \rangle = B \log \frac{1}{a} + \dots \quad (2.3.6)$$

the renormalized operator will be made cutoff-independent by the choice

$$Z_\Phi = 1 + \frac{g^2}{2} B \log \frac{1}{a} + O(g^3). \quad (2.3.7)$$

It follows that at the fixed point, where $g = g_*$, the operator Φ will acquire an anomalous dimension of

$$\gamma_\Phi = -\frac{g_*^2}{2} B + O(g_*^3). \quad (2.3.8)$$

As before, we rescale the two integration points x_1 and x_2 by $|x_1|$. The logarithmic divergence of the integral (2.3.6) is then

$$B = S_d \int d^d y \langle \Phi(0)\mathcal{O}(y)\mathcal{O}(\hat{e})\Phi(\infty) \rangle \quad (\text{naive}). \quad (2.3.9)$$

Just like for the beta-function, this “naive” answer needs to be regulated because of short-distance power divergences which we neglected.

Excluding the case $\Phi = \mathcal{O}$, the OPE $\Phi \times \mathcal{O}$ does not contain the unit operator and the stress tensor. Nor does it contain Φ since $C_{\Phi\Phi\mathcal{O}} = 0$. Assuming all other operators in the OPE have dimension larger than Φ , the above integral is convergent near 0 and ∞ . Let us proceed under the above assumptions, otherwise minor obvious modifications will be required.

The integral does present power divergences for y close to \hat{e} . These divergences are due to the unit operator and ε in the $\mathcal{O} \times \mathcal{O}$ OPE. As already mentioned in the beta-function discussion, they do not have anything to do with the critical point physics. We have to subtract and drop these divergences, but we have to do this in a way which does not modify the log divergence influencing the anomalous dimension of the operator Φ . We have again two different ways to proceed, with minor modifications compared to the beta-function computation.

Method 1. We subtract the contributions of the relevant operators at the level of Eq. (2.3.6),

so that the logarithmic divergences are unchanged. Just as (2.3.9), (2.3.6) diverges only when $x_1 \rightarrow x_2$, while it is finite for x_i close to 0 and to ∞ . Given that the relevant operators appearing in the $\mathcal{O} \times \mathcal{O}$ OPE are the identity and the ε operator, we can use the subtraction

$$\langle \Phi(0)\mathcal{O}(x_1)\mathcal{O}(x_2)\Phi(\infty) \rangle \rightarrow \langle \Phi(0)\mathcal{O}(x_1)\mathcal{O}(x_2)\Phi(\infty) \rangle - \frac{1}{|x_1 - x_2|^{2d}} - \frac{C_{\Phi\Phi\varepsilon}C_{\mathcal{O}\mathcal{O}\varepsilon}}{|x_1 - x_2|^{2d-\Delta_\varepsilon}|x_1|^{\Delta_\varepsilon}}. \quad (2.3.10)$$

Then we rescale the points by $|x_1|$, we obtain the following regulated expression for the logarithmic divergence coefficient:

$$B = S_d \int d^d y \left[\langle \Phi(0)\mathcal{O}(y)\mathcal{O}(\hat{e})\Phi(\infty) \rangle - \frac{1}{|y - \hat{e}|^{2d}} - \frac{C_{\Phi\Phi\varepsilon}C_{\mathcal{O}\mathcal{O}\varepsilon}}{|y - \hat{e}|^{2d-\Delta_\varepsilon}} \right]. \quad (2.3.11)$$

Method 2. We split again the integration region of (2.3.6) into three smaller subregion. This will make the numerical evaluation of the integral simpler. Clearly, the contribution of the integration region with x_1 close to zero, $|x_1| < |x_2|$ and $|x_1| < |x_1 - x_2|$, is the same as that of the region with x_2 close to zero. However, the contribution of the region where x_1 and x_2 are close together will be different. By the same logic as for (2.2.13), we obtain a regulated expression for (2.3.9):

$$B = S_d \int_{\mathcal{R}} d^d y \{ 2\langle \Phi(0)\mathcal{O}(y)\mathcal{O}(\hat{e})\Phi(\infty) \rangle + \langle \mathcal{O}(0)\mathcal{O}(y)\Phi(\hat{e})\Phi(\infty) \rangle \}. \quad (2.3.12)$$

The integration region \mathcal{R} is the same as in the previous section. The first term is finite since y is separated from \hat{e} . The second term has powerlike divergences, but no log divergences, for y close to 0; we make it finite by dropping the divergent terms.

2.3.1 Results: $d = 2$

We will now apply the developed formalism to determine the anomalous dimension of a few selected operators, first in $d = 2$ and then in $d = 3$.

2.3.1.1 χ, σ and \mathcal{O}

The arguments and the results of this section work for any dimension, so we keep d general. We will see in section 2.4.1 that the anomalous dimensions of the three operators we consider here can be discussed to all orders. As a check, we will reproduce here the lowest-order versions of those results using the general formalism.

We consider first the field χ . It clearly plays a very special role the $\sigma\chi$ -flow, being described by a non-local action in the UV. As a consequence, we expect that χ does not get anomalous dimension to all orders in δ . This is similar to what happens for the ϕ field in the ϕ^4 -flow. Here we will check, by an explicit computation, that the anomalous dimension of χ vanishes at order g^2 .

Chapter 2. The long-range to short-range crossover

To see this, observe that the integral (2.3.6), with $\Phi = \chi$ and $\mathcal{O} = \sigma\chi$, only has power divergences, and no logarithmic divergences. Indeed its integrand is

$$\frac{1}{|x_1 - x_2|^{2\Delta_\sigma}} \left(\frac{1}{|x_1|^{2\Delta_\chi}} + \frac{1}{|x_1|^{2\Delta_\chi}} + \frac{1}{|x_1 - x_2|^{2\Delta_\chi}} \right). \quad (2.3.13)$$

The integral only has power divergences by the same argument as that given for the beta-function subtraction terms (2.2.10). If we were to apply Method 1 to this integral, we would end up with an identically vanishing integrand. Notice that in this case the OPE $\Phi \times \mathcal{O}$ contains an operator σ with dimension $\Delta_\sigma < \Delta_\Phi$, So more subtraction terms are needed than the ones given in Eq. (2.3.11). After these subtractions, the integrand is identically zero.

Next we consider the field σ . It is also special, because it acts as a source for χ , and so the classical equation of motion (EOM) of χ sets a linear non-local relation between the two. In quantum theory, this non-local EOM implies that the IR dimensions of σ and χ satisfy the shadow relation:

$$\Delta_\chi + \Delta_\sigma = d. \quad (2.3.14)$$

This should be compared with the shadow relation (2.1.3) for the ϕ^4 -flow. The two relations suggest that in the IR limit of the two flows, ϕ has to be identified with σ , and ϕ^3 with χ . This fits nicely our proposed IR duality and will be discussed further in section 2.4.2.

Here we will check the shadow relation at the leading order in g . The anomalous dimension of the spin field σ can be reduced by a trick to the g^3 term of the beta-function, which we already computed. Let us consider the original integral (2.3.6) for $\Phi = \sigma$. It's easy to see that this integral (multiplied by the overall volume) is exactly one third of the integral (2.2.6) in the beta-function calculation. Indeed, the integrand in both cases involves the 4pt function of σ multiplied by a correlation function of χ , which has one term in the first case and three terms in the second one. These three terms all contribute equally, and so we obtain $B = A/3$. This fact is not manifest the expressions provided by Methods 1 and 2, but we checked it numerically. Given $B = A/3$, the anomalous dimension of σ is found to be:

$$\gamma_\sigma = \delta + O(\delta^2). \quad (2.3.15)$$

This checks the shadow relation at the lowest order.¹¹

Finally, we discuss the operator $\mathcal{O} = \sigma\chi$ which drives the flow. By the general RG arguments, the anomalous dimension of this operator should be given by:

$$\gamma_{\mathcal{O}}(g) = \beta'(g). \quad (2.3.16)$$

¹¹We notice that, as a consequence of the discussed RG equations, the 2pt function $\langle \sigma\sigma \rangle$ at the crossover ($\delta = 0$) exhibits a $1/\log r$ suppression in presence of the marginally irrelevant $\sigma\chi$ perturbation. See appendix B of [2].

Using the leading beta-function expression, at the fixed point this becomes

$$\gamma_{\mathcal{O}}(g_*) = 3\delta, \quad (2.3.17)$$

up to order g^2 corrections. As expected, \mathcal{O} becomes irrelevant at the IR fixed point:

$$[\mathcal{O}]_{\text{LRFP}} = d + 2\delta + O(\delta^2), \quad (2.3.18)$$

Eq. (2.3.17) can also be obtained in the formalism of the previous section. It follows by noticing that $B = A$ for the renormalization of \mathcal{O} .

2.3.1.2 ε

To compute the anomalous dimension of ε , we need to use the result from the Ising minimal model (see e.g. [97])

$$\langle \varepsilon(0)\sigma(z)\sigma(1)\varepsilon(\infty) \rangle = \frac{|1+z|^2}{4|z||1-z|^{1/4}}. \quad (2.3.19)$$

To obtain the correlation function $\langle \varepsilon \mathcal{O} \mathcal{O} \varepsilon \rangle$ we multiply (2.3.19) by $\langle \chi(z)\chi(1) \rangle$. This time we will use Method 1, and we will be able to carry out the integration analytically. We need to subtract the divergent terms due to the relevant operators, as shown in (2.3.11). The ε subtraction term is absent since, thanks to the Kramers-Wannier duality, $C_{\varepsilon\varepsilon\varepsilon} = 0$ in two dimensions. We obtain the integral

$$\int d^2z \frac{1}{|1-z|^4} \left(\frac{|1+z|^2}{4|z|} - 1 \right), \quad (2.3.20)$$

to be computed with circular cutoffs around 0, 1 and infinity. Careful evaluation shows that this integral is zero, see appendix D.1 for the proof. Unfortunately, the only proof we found was by brute force, and it would be nice to find an underlying reason. We also checked this result by numerical evaluation. Numerically, this was also previously observed in [90], Eqs. (6.14) and (5.28), in an unrelated computation which led to the same integral.

Therefore the anomalous dimension of ε vanishes at order g_*^2 , while order g_*^3 will be zero by the \mathbb{Z}_2 selection rules. Therefore

$$\gamma_{\varepsilon} = O(g_*^4) = O(\delta^2) \quad (d=2). \quad (2.3.21)$$

2.3.1.3 $T_{\mu\nu}$

We now come to the discussion of the stress tensor operator, the source of some paradoxes discussed in the introduction. The LRFP is a non-local theory, and we do not expect it to contain a conserved local stress tensor operator. Let us examine this issue from the RG point of view. The UV theory SRFP+ χ consists of two decoupled sectors. The SRFP is a local theory, with a conserved local stress tensor which we call $T_{\mu\nu}$. The χ sector is non-local, without a

Chapter 2. The long-range to short-range crossover

local stress tensor.¹² When we perturb the UV theory with the operator $\sigma\chi$, the two sectors are no longer decoupled and locality of the SRFP is lost. This implies that, at the IR fixed point, the operator $T_{\mu\nu}$ will acquire an anomalous dimension. We will still call it $T_{\mu\nu}$ and will sometimes refer to it as the ‘stress tensor’, but it has to be kept in mind that this operator will not be conserved at the IR fixed point.

We will compute the $T_{\mu\nu}$ anomalous dimension in two ways, first directly and then using the multiplet recombination which will clarify the puzzle of missing states.

For the direct computation, it is sufficient to consider only one tensor component, say $T \equiv T_{zz}$, as all the components will acquire the same anomalous dimension. The stress tensor in the UV is conventionally normalized as

$$\langle T(z, \bar{z}) T(0) \rangle = \frac{c}{2} \frac{1}{z^4}. \quad (2.3.22)$$

In the case of the two dimensional Ising model, the central charge is $c = \frac{1}{2}$. The 4pt function $\langle T(0)\sigma(z)\sigma(1)T(\infty) \rangle$ is then recovered in the standard way using the Ward identity twice on the 2pt function of σ . For the 4pt function involving two \mathcal{O} insertions we obtain:

$$\langle T(0)\sigma\chi(z)\sigma\chi(1)T(\infty) \rangle = \frac{1}{|1-z|^4} \left(\frac{1}{4} + \frac{(1-z)^2(z^2+30z+1)}{256z^2} \right). \quad (2.3.23)$$

Although the stress tensor is not a scalar operator, the discussion of section 2.3 on how to compute the anomalous dimensions still applies. We aim for an analytic result and use Method 1. Since $C_{TT\epsilon} = 0$ in $d = 2$, we only need to subtract the contribution of the identity in (2.3.11). Note that since the stress tensor is not unit-normalized, subtracting the contribution of the identity means subtracting $(4|z-1|^4)^{-1}$. The resulting integral can be evaluated exactly:

$$\int d^2z \frac{1}{(1-\bar{z})^2} \frac{(z^2+30z+1)}{256z^2} = -\frac{15}{128}\pi. \quad (2.3.24)$$

There is a subtlety in this computation related to the contribution of the region near $z = 1$. This is explained in appendix D.1.

Eq. (2.3.8) as written is valid for the unit-normalized operators. To make up for the fact that T is not, we need to multiply its r.h.s. by an extra factor $2/c$. Finally, we obtain:

$$\gamma_T = \frac{15}{32}\pi^2 g_*^2 + O(g_*^4) \approx 3.65\delta + O(\delta^2) \quad (d=2), \quad (2.3.25)$$

where we used (2.2.25) and (2.2.19).

We will now recompute the same anomalous dimension using the recombination of multi-

¹²This is easy to check explicitly. The χ sector being gaussian, all local operators are normal-ordered products of χ and its derivatives, and by inspection there is no spin 2, dimension d operator which could play the role of a local stress tensor.

plets.¹³ As we will see, this method requires only the integration of a 3pt function fixed by a Ward identity, and gives γ_T as a function of Δ_σ and of the central charge c for arbitrary d . So we switch to general d until the end of this section.

The stress tensor at the SRFP satisfies conservation equation $\partial^\mu T_{\mu\nu} = 0$, meaning that some of his descendants are zero. As we say, it belongs to a short multiplet. The same operator taken to the IR, to the LRFP, which is a non-local theory, is not expected to be conserved: $\partial^\mu T_{\mu\nu} \propto V_\nu \neq 0$. In other words, the stress tensor multiplet becomes long by eating the V_ν multiplet. The vector V_ν must exist in the UV theory as well; this was puzzling in the standard picture. The puzzle is neatly resolved in our picture, since this multiplet can be easily constructed with the help of the χ field. Namely, we have:

$$V_\nu = \sigma(\partial_\nu \chi) - \frac{\Delta_\chi}{\Delta_\sigma} (\partial_\nu \sigma) \chi. \quad (2.3.26)$$

This is clearly a vector field and of dimension $d + 1$ at the crossover point. The relative coefficient between the two terms is fixed by requiring that V_ν be a (non-unit normalized) vector primary at the crossover. For this it is sufficient to check that the 2pt function of V_ν and of the descendant $\partial_\nu(\sigma\chi)$ vanishes.

Since V_μ given above is the only candidate to be eaten, at the IR fixed point we expect

$$\partial^\mu T_{\mu\nu} = b(g) V_\nu, \quad (2.3.27)$$

where $b(g) \rightarrow 0$ as $g \rightarrow 0$.

We will be interested in the first nontrivial order: $b(g) = b_1 g + O(g^2)$. The value of b_1 can be determined by studying the 2pt function of V_μ with $T_{\mu\nu}$, computed at first order in perturbation theory. It will be more convenient to utilise the descendant $\partial^\mu T_{\mu\nu}$, as this will allow us to use the Ward identity. On the one hand from multiplet recombination (2.3.27) we expect at the lowest order in g_* :

$$\langle \partial^\mu T_{\mu\nu}(x) V_\rho(y) \rangle_g \approx b_1 g_* \langle V_\nu(x) V_\rho(y) \rangle_0. \quad (2.3.28)$$

Here and below we mark with subscript g the IR fixed point correlators, while with subscript 0 the correlators in the UV theory SRFP+ χ . The 2pt function of V_μ entering this equation can be computed explicitly given its definition:

$$\langle V_\mu(x) V_\nu(0) \rangle_0 = 2d \frac{\Delta_\chi}{\Delta_\sigma} \frac{I_{\mu\nu}(x)}{|x|^{2d+2}}, \quad I_{\mu\nu}(x) = \delta_{\mu\nu} - 2 \frac{x_\mu x_\nu}{x^2}. \quad (2.3.29)$$

Notice that this functional form is consistent with the conformal primary nature of V_μ .

On the other hand perturbation theory predicts for the correlator in the l.h.s. of (2.3.28)

$$\langle \partial^\mu T_{\mu\nu}(x) V_\rho(y) \rangle_g = g_* \int d^d z \langle \partial^\mu T_{\mu\nu}(x) V_\rho(y) \mathcal{O}(z) \rangle_0. \quad (2.3.30)$$

¹³For recent discussions of multiplet recombination in various CFT contexts see e.g. [64, 98–100].

Chapter 2. The long-range to short-range crossover

The 3pt function that we need to integrate is the sum of two factorized terms:

$$\begin{aligned} \langle \partial^\mu T_{\mu\nu}(x) V_\rho(y) \mathcal{O}(z) \rangle_0 &= \langle \partial^\mu T_{\mu\nu}(x) \sigma(y) \sigma(z) \rangle \langle \partial_\rho \chi(y) \chi(z) \rangle_0 \\ &\quad - \frac{\Delta_\chi}{\Delta_\sigma} \langle \partial^\mu T_{\mu\nu}(x) \partial_\rho \sigma(y) \sigma(z) \rangle \langle \chi(y) \chi(z) \rangle_0. \end{aligned} \quad (2.3.31)$$

When the 3pt functions in the r.h.s. are expressed using the Ward identity¹⁴ of the unperturbed theory, we get terms proportional to $\delta(x-y)$ and to $\delta(x-z)$. We assume that $x \neq y$, so only $\propto \delta(x-z)$ terms are important. They yield a non-zero contribution when we integrate over z . We obtain

$$\begin{aligned} \int d^d z \langle \partial^\mu T_{\mu\nu}(x) V_\rho(0) \mathcal{O}(z) \rangle_0 \\ = -\langle \sigma(x) \partial_\nu \sigma(0) \rangle \langle \partial_\rho \chi(x) \chi(0) \rangle + \frac{\Delta_\chi}{\Delta_\sigma} \langle \partial_\nu \sigma(x) \partial_\rho \sigma(0) \rangle \langle \chi(x) \chi(0) \rangle = 2\Delta_\chi \frac{I_{V\rho}(x)}{|x|^{2d+2}}. \end{aligned} \quad (2.3.32)$$

Using (2.3.28), (2.3.29), (2.3.30), the value of b_1 is fixed:

$$b_1 = \Delta_\sigma / d. \quad (2.3.33)$$

Now let us compute the anomalous dimension of $T_{\mu\nu}$. The 2pt function normalization customary for d dimensional CFT is [101] (see also [102])

$$\langle T_{\mu\nu}(x) T_{\rho\sigma}(0) \rangle = \frac{c_T}{2S_d^2} \frac{1}{|x|^{2\Delta_T}} \left[I_{\mu\rho}(x) I_{\nu\sigma}(x) + (\mu \leftrightarrow \nu) - \frac{2}{d} \delta_{\mu\nu} \delta_{\lambda\sigma} \right], \quad (2.3.34)$$

In this normalization, and assuming the Ward identities are normalized as in note 14, the free massless scalar has $c_T = d/(d-1)$.

Eq. (2.3.34) follows just from conformal invariance and the fact that $T_{\mu\nu}$ transforms as a rank 2 symmetric traceless primary. So it's valid both at the SRFP in the UV, and at the LRFP in the IR.¹⁵ In the UV we have $c_T = c_T^{\text{SRFP}}$ and $\Delta_T = d$, corresponding to the conserved local stress tensor. In the IR both c_T and Δ_T receive $O(g_*^2)$ corrections. At the intermediate distances there is some interpolating behavior which will not be important.

Let $\Delta_T = d + \gamma_T$ in the IR, where γ_T is the anomalous dimension. The quantity of interest is the 2pt function of the divergence of $T_{\mu\nu}$ at the LRFP which can be found by an explicit differentiation of (2.3.34). This vanishes for $\gamma_T = 0$, consistent with the fact that $T_{\mu\nu}$ is

¹⁴In this general d argument we normalize the stress tensor so that the Ward identity takes the form $\langle \partial^\mu T_{\mu\nu}(x) \mathcal{O}_1(x_1) \dots \mathcal{O}_n(x_n) \rangle = -\sum_i \delta(x-x_i) \partial_\nu^{x_i} \langle \mathcal{O}_1(x_1) \dots \mathcal{O}_n(x_n) \rangle$. Notice that it's not the same as the normalization usually used in 2d.

¹⁵This argument relies on conformal invariance of the LRFP, discussed in the previous chapter. It's also possible to see without invoking conformal invariance that the tensor structure of the 2pt function is preserved along the RG flow. This follows from the fact that the rescaling needed to make the operator finite depends only on the indices of the operator and not on any other insertions in the correlation function. It's part of the same argument which shows that all tensor components get the same anomalous dimension.

conserved in the UV, and for nonzero γ_T is given by:

$$\langle \partial^\mu T_{\mu\nu}(x) \partial^\rho T_{\rho\sigma}(0) \rangle_g \approx \frac{c_T}{S_d^2} \gamma_T \left(d + 1 - \frac{2}{d} \right) \frac{I_{V\sigma}}{|x|^{2d+2}}, \quad (2.3.35)$$

In (2.3.35) we dropped terms higher order in g_*^2 . One such higher order term is the correction to c_T which will not play any role, so in all subsequent equations $c_T = c_T^{\text{SRFP}}$.

At the same order, using the recombination of multiplets equation (2.3.27), we expect:

$$\langle \partial^\mu T_{\mu\nu}(x) \partial^\rho T_{\rho\sigma}(0) \rangle_g \approx b_1^2 g_*^2 \langle V_\nu(x) V_\sigma(0) \rangle_0. \quad (2.3.36)$$

From the last two equations, the 2pt function of V_μ , and the value of b_1 we find the lowest-order anomalous dimension of the stress tensor:

$$\gamma_T = \frac{2S_d^2}{c_T} \frac{\Delta_\sigma(d - \Delta_\sigma)}{d^2 + d - 2} g_*^2 + O(g_*^4). \quad (2.3.37)$$

Let us now specialize to $d = 2$. In the usual 2d normalization, the 2d critical Ising has central charge 1/2, half that of the free massless scalar. As mentioned, $c_T = \frac{d}{d-1} = 2$ for the free massless scalar in the normalization of (2.3.34) and of note 14, and so $c_T = 1$ for the 2d Ising in the same normalization. It is then easy to see that (2.3.37) agrees with the result (2.3.25) obtained via the integration of the 4pt function.

2.3.2 Results: $d = 3$

The anomalous dimensions of χ , σ and \mathcal{O} were already discussed in section 2.3.1.1 for any d .

2.3.2.1 ε

Recall that order g_*^2 anomalous dimension of the energy operator was zero in $d = 2$, for mysterious reasons unexplained by any obvious symmetry. As we will see this does not happen in three dimensions. We set up a numerical computation for this anomalous dimension using the CFT data from the numerical conformal bootstrap. In order to compute the 4pt function $\langle \varepsilon \sigma \sigma \varepsilon \rangle$, we will need the operator dimensions and the OPE coefficients of the operators appearing in the $\sigma \times \sigma$, $\sigma \times \varepsilon$ and $\varepsilon \times \varepsilon$ OPEs. For operators up to $\Delta_* = 8$, these can be found in Table 2 of [16]. We will use Method 2. We construct the 4pt function in the region where one ε is close to one \mathcal{O} and the region where the \mathcal{O} 's are close together:

$$\langle \varepsilon(0) \sigma(z) \sigma(1) \varepsilon(\infty) \rangle = \frac{1}{|z|^{\Delta_\sigma + \Delta_\varepsilon}} \sum_{\mathcal{O}: \Delta_{\mathcal{O}} < \Delta_*} C_{\sigma\varepsilon\mathcal{O}}^2 g_{\Delta_{\mathcal{O}}, \ell_{\mathcal{O}}}^{\Delta_{\varepsilon\sigma}, \Delta_{\sigma\varepsilon}}(z, \bar{z}), \quad (2.3.38)$$

$$\langle \sigma(0) \sigma(z) \varepsilon(1) \varepsilon(\infty) \rangle = \frac{1}{|z|^{2\Delta_\sigma}} \sum_{\mathcal{O}: \Delta_{\mathcal{O}} < \Delta_*} C_{\sigma\sigma\mathcal{O}} C_{\varepsilon\varepsilon\mathcal{O}} g_{\Delta_{\mathcal{O}}, \ell_{\mathcal{O}}}^{0,0}(z, \bar{z}). \quad (2.3.39)$$

Chapter 2. The long-range to short-range crossover

Here $g_{\Delta_{\mathcal{O}}, \ell_{\mathcal{O}}}$ with upper indices are the conformal blocks for the external scalars with unequal dimensions, which we compute via recursion relations from [45]. The operators entering the sum in the first (resp. second) equation are \mathbb{Z}_2 odd (resp. even). In both cases, we will be integrating over the region \mathcal{R} defined in section 2.2.

Once again, the largest error contribution when approximating the 4pt function will come from the truncation of the spectrum at dimension Δ_* . The same line of reasoning used to obtain the truncation error for four identical scalar in [95] will go through in the case of equation (2.3.38). Analyzing the proof in [95], it's possible to see that the truncation error will be given by (2.2.23) with the change $\Delta_{\sigma} \rightarrow (\Delta_{\sigma} + \Delta_{\varepsilon})/2$ in all occurrences in the r.h.s.

For equation (2.3.39), however, we cannot map the 4pt function onto a reflection positive configuration, and therefore we cannot find a bound on the contribution of the truncated operators in the same way. We need to first use Cauchy's inequality so that the tail of $\langle \sigma \sigma \varepsilon \varepsilon \rangle$ can be bounded by the tails of $\langle \sigma \sigma \sigma \sigma \rangle$ and $\langle \varepsilon \varepsilon \varepsilon \varepsilon \rangle$. At this point we can use again the result of [95], and we obtain

$$\left| \sum_{\mathcal{O}: \Delta_{\mathcal{O}} > \Delta_*} C_{\sigma \sigma \mathcal{O}} C_{\varepsilon \varepsilon \mathcal{O}} g_{\Delta_{\mathcal{O}}, \ell_{\mathcal{O}}}^{0,0}(z, \bar{z}) \right| \lesssim \frac{2^{2\Delta_{\sigma} + 2\Delta_{\varepsilon}}}{\sqrt{\Gamma(4\Delta_{\sigma} + 1)\Gamma(4\Delta_{\varepsilon} + 1)}} \Delta_*^{2\Delta_{\sigma} + 2\Delta_{\varepsilon}} |\rho(z)|^{\Delta_*}. \quad (2.3.40)$$

Truncating the CFT data up to $\Delta_* = 8$,¹⁶ and carrying out the integration in the region \mathcal{R} , we obtain a nonzero value, unlike in $d = 2$. The order g_*^2 anomalous dimension is

$$\gamma_{\varepsilon} \approx 3.3g_*^2 + O(g_*^4) \approx 0.27\delta + O(\delta^2) \quad (d = 3), \quad (2.3.41)$$

where in the second equality we used (2.2.25) and (2.2.24). The total truncation error on the coefficient 3.3, estimated as above, is ± 0.5 . So we are confident that ε gets a nonzero anomalous dimension in $d = 3$ already at the lowest order allowed by the \mathbb{Z}_2 selection rules.

2.3.2.2 $T_{\mu\nu}$

In $d = 3$ the data needed to compute the 4pt function $\langle T \sigma \sigma T \rangle$ are not yet available. So we cannot compute the anomalous dimension of $T_{\mu\nu}$ using the formalism of section 2.3. However, we can still use the general d expression (2.3.37) obtained by using the recombination method.

Using the spin field dimension $\Delta_{\sigma} = 0.5181489(10)$ [15] and the central charge $c_T/c_T^{\text{free}} = 0.946539(1)$ [44, 90] with the free scalar central charge $c_T^{\text{free}} = d/(d-1) = 3/2$, we get

$$\gamma_T = 28.60555(6)g_*^2 + O(g_*^4) \approx 2.33\delta + O(\delta^2) \quad (d = 3). \quad (2.3.42)$$

¹⁶Beware of the changes in normalization of OPE coefficients between [16] and [45, 90], explained in appendix A.3 in [16].

2.4 Infrared duality

2.4.1 All-order conjectures about the $\sigma\chi$ -flow

We have seen in the previous chapter how many nontrivial facts about the ϕ^4 -flow can be proved to all orders in the ϵ -expansion. Here we will give a parallel discussion for the $\sigma\chi$ -flow. Arguing by analogy, we will motivate a number of all order results in the δ -expansion. In the next section we will see how it all fits together with the infrared duality.

Compared to the standard perturbation theory of a Lagrangian field theory, whose structural properties are well-understood to all orders, conformal perturbation theory is an underdeveloped subject. The usual discussion starts from perturbing a CFT by a weakly relevant operator \mathcal{O} of scaling dimension $d - \delta$, where $\delta \ll 1$. To define perturbation theory, one needs a regulator, and point splitting is a natural choice. However point splitting is awkward to implement at higher orders. Dimensional regularization or analytic regularization in δ are not viable in general, because the CFT may exist or be tractable only for a fixed spacetime dimension, and because the relevant perturbation usually exists only for a fixed, physical value of δ . This is unlike Lagrangian perturbation theory, where correlation functions can be analytically continued to arbitrary d .

Fortunately, the case of the $\sigma\chi$ -flow is better than this generic situation, since the dimension of χ is a continuously varying parameter – the gaussian action which governs the dynamics of χ is defined for any Δ_χ . So in our case we can consider analytic continuation in δ as a way to regulate integrals. This provides a potential pathway to an all-order discussion.

We will now discuss how things might plausibly work out in this all-order perturbation theory. The results will be in agreement with the finite order computations that we performed in sections 2.2, 2.3 using the point-splitting regulator, and with further subsequent checks. Still, our all-order discussion of the $\sigma\chi$ -flow will not reach the level of rigor which was possible for the ϕ^4 -flow.

The basic object to study are the correlators of χ , defined in perturbation theory by series-expanding the interaction, evaluating the correlation functions in the factorized theory, and integrating using the above-mentioned analytic regulator. Some integrals will produce poles in δ . We conjecture that, to all orders, such poles can be removed by defining the renormalized coupling g related to the bare coupling by the usual relation:

$$g_0 = Z_g(g, \delta) \mu^\delta g \tag{2.4.1}$$

(the function Z_g is of course different from that of the ϕ^4 -flow). This conjecture seems reasonable because SRFP does not contain any marginal operator. Our computations in sections 2.2, 2.3 can be seen as a low-order test. It would be nice to find a full proof.¹⁷

¹⁷We are grateful to David Simmons-Duffin for discussions and for sharing his unpublished notes on all-order conformal perturbation theory.

Chapter 2. The long-range to short-range crossover

Assuming the conjecture, we can derive analogues of the all-order ϕ^4 -flow statements by an almost verbatim repetition of the arguments.

A part of the conjecture is that the gamma-function of χ is zero. This is motivated in the same way as for ϕ in the ϕ^4 flow. Namely, that poles in δ correspond to short-distances divergences of the integral for $\delta = 0$, the divergences are local, and the action of χ is non-local, so it can't be renormalized. We then obtain that the anomalous dimension of χ at the fixed point is identically zero. This is an all-order generalization of the lowest-order result in section 2.3.1.1.

For future use, notice that if χ is unit-normalized in the UV, then in the IR we will have

$$\langle \chi(x)\chi(0) \rangle = \frac{1 + \kappa(\delta)}{|x|^{2\Delta_\chi}}, \quad (2.4.2)$$

It's clear that κ has an expansion in even powers of g so $\kappa(\delta) = O(\delta)$ for small δ . In fact from the lowest order diagram we can easily obtain (using (1.3.14)):

$$\kappa = g_*^2 \pi^d \frac{\Gamma\left(\frac{d}{2} - \Delta_\sigma\right)\Gamma\left(\Delta_\sigma - \frac{d}{2}\right)}{\Gamma(\Delta_\sigma)\Gamma(d - \Delta_\sigma)} + O(g_*^4). \quad (2.4.3)$$

This is negative, similarly to how $\rho(\epsilon)$ starts out negative for small ϵ .

We can argue that the IR fixed point of the $\sigma\chi$ -flow should be conformally invariant. Indeed, we can derive the broken conformal Ward identities for the $\sigma\chi$ -flow by the same Caffarelli-Silvestre trick. We can then show that these Ward identities imply the conformal invariance in the IR.

We also have a non-local EOM:

$$\int d^d y \frac{1}{|x-y|^{2(d-\Delta_\chi)}} \chi(y) = C' \sigma(x). \quad (2.4.4)$$

From this we can see that the shadow relation $\Delta_\sigma + \Delta_\chi = d$ holds at the IR fixed point, generalizing the lowest-order result in section 2.3.1.1.

Finally, we can repeat verbatim the calculation of appendix A.1. Given (2.4.2), we obtain

$$\frac{\lambda_{12\bar{\sigma}}}{\lambda_{12\bar{\chi}}} = \hat{M}_3 \sqrt{\frac{1 + \kappa(\delta)}{\kappa(\delta)\hat{M}_2}}, \quad (2.4.5)$$

where \hat{M}_2 and \hat{M}_3 are the “shadow” quantities obtained from (A.1.8) and (A.1.4) replacing Δ_ϕ with $\Delta_\chi = d - \Delta_\phi$.

2.4.2 Duality interpretation

We have seen that the both ϕ^4 -flow and $\sigma\chi$ -flow have a conformally invariant IR fixed point. The dimensions of two operators at the fixed point are exactly known (one by non-renormalization, another by the shadow relation):

$$[\phi] = (d - s)/2, \quad [\phi^3] = (d + s)/2, \quad (2.4.6)$$

and

$$[\chi] = (d + s)/2, \quad [\sigma] = (d - s)/2. \quad (2.4.7)$$

The ϕ^4 -flow relations have been proved to all orders in $\epsilon = 2s - d \ll 1$, near the crossover to mean field.¹⁸

Under the reasonable assumption of renormalizability, the $\sigma\chi$ -flow relations hold to all orders in $\delta = (s_* - s)/2 \ll 1$, near the crossover to short range.

The most natural interpretation of these results is that there is only one CFTs for each s , which describes the fixed points of both flows (infrared duality). The fields ϕ, ϕ^3 for the first flow have to be identified in the IR with σ, χ for the second flow (up to proportionality coefficients). Finally, the above equations for the IR field dimensions are valid *exactly* and not just in perturbation theory. Indeed, if there were nonperturbative corrections, say, to the first set of equations, they would presumably become largest near the short-range crossover, but this is where the second set of equations becomes accurate and shows that there are no corrections.

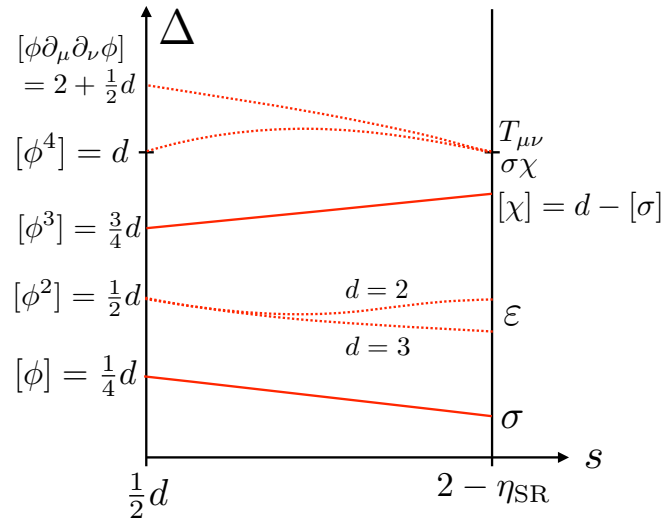


Figure 2.4 – The dependence of dimensions of several important operators on s .

¹⁸The fact that the anomalous dimension of ϕ is zero can also be seen from the realization of LRFP as a defect CFT via the Caffarelli-Silvestre trick, reviewed in section 1.4.3. It follows from the bulk equations of motion together with the assumptions of conformal invariance and bulk-to-defect OPE. See the discussion around Eq. (4.34) in [48]. We are grateful to Pedro Liendo and Marco Meineri for emphasizing this connection to us.

Chapter 2. The long-range to short-range crossover

See Fig. 2.4 for the predicted dependence of the most important LRF operator dimensions on s between the mean-field and the short-range crossovers. The solid lines joining ϕ to σ and χ to ϕ^3 are straight lines. The other lines are known only approximately in the ϵ and δ expansion around the crossovers. The shown shape of the lines is the simplest consistent with these asymptotics. The line joining ϕ^2 to ϵ deserves a comment. We have $[\phi^2] = (d - \epsilon)/2 + \gamma = d - \epsilon/6 + O(\epsilon^2)$ near the mean-field crossover, so that the line starts going linearly down. In $d = 3$ it joins to $\Delta_\epsilon \approx 1.41 < d/2$ with the negative first derivative, see (2.3.41). However, in $d = 2$ it rises back up to $\Delta_\epsilon = 1 = d/2$ and has a zero first derivative at the crossover, see (2.3.21).

As a further check of the duality, we will show that the relations (A.1.10) and (2.4.5) for the OPE coefficients can be made compatible with each other. We must have

$$\frac{\lambda_{12\phi^3}}{\lambda_{12\bar{\phi}}} \equiv \frac{\lambda_{12\bar{\chi}}}{\lambda_{12\bar{\sigma}}}. \quad (2.4.8)$$

It's not trivial that the two sides can agree, because the dependence on $\Delta_{1,2}$ must match. Fortunately it does, thanks to the following identity,

$$M_3 \hat{M}_3 = M_2 = \hat{M}_2. \quad (2.4.9)$$

Equation (2.4.8) holds provided that ρ and κ obey, at the same value of s , the relation:

$$\frac{\kappa(\delta)}{1 + \kappa(\delta)} = \frac{1 + \rho(\epsilon)}{\rho(\epsilon)}. \quad (2.4.10)$$

This leads to nontrivial predictions for the behavior of the two functions near the mean-field and short-range crossovers. Since as we have seen $\kappa(\delta) = O(\delta)$ for small δ , we conclude that the normalization of the 2pt function of ϕ must vanish linearly in s close to the short-range crossover:

$$1 + \rho(\epsilon) = O(s_* - s). \quad (2.4.11)$$

The same vanishing of the 2pt function normalization has been previously argued in [103], via a completely different argument.¹⁹

Analogously, we must have

$$1 + \kappa(\delta) = O((2s - d)^2) \quad (2.4.12)$$

when approaching the crossover to the mean-field regime. In this case the vanishing is expected to be quadratic since $\rho(\epsilon) = O(\epsilon^2)$.

In summary, we have accumulated strong evidence for a novel IR duality: the ϕ^4 -flow and the $\sigma\chi$ -flow end in the same IR fixed point. Unlike all previously studied examples of IR dualities, our theories lack a local stress tensor. Non-locality, which is an essential feature of

¹⁹See also appendix B of [2] for a discussion of the $\langle\phi\phi\rangle$ correlator precisely at the crossover, where it exhibits a logarithmic suppression with respect to the naive scaling. This suppression is derived via RG, but it can also be thought of as a remnant of the vanishing of the normalization (2.4.11) [103].

our construction, comes with a surprising bonus: remarkable computation power! One of its immediate consequences is the non-renormalization theorem for Δ_ϕ and Δ_χ . The non-local equations of motions were then used to show that Δ_{ϕ^3} and of Δ_σ obey shadow relations at the IR fixed point, and that OPE coefficients involving the shadow pairs must come in precise ratios. In the paradigmatic examples of IR dualities (such as 4d Seiberg duality and 3d mirror symmetry), it is supersymmetry that gives analytic control. Curiously, we were able to achieve significant analytic control in our non-supersymmetric setting, thanks precisely to the non-local nature of the problem.

2.5 Discussion

In this chapter we have proposed and studied a new compelling picture for the long-range to short-range crossover. Prior to our work, the understanding of this crossover was incomplete at best. Some of its qualitative features – in particular its continuous nature – had been anticipated, but doubts remained, as evidenced by some recent controversies in the literature (see appendix A.2). Other important features of the crossover were completely missed, in particular the fact that the crossover happens not to the SRFP, but to the SRFP plus a decoupled gaussian field.

Crucially, our new qualitative picture allowed us to advance greatly the quantitative side of the story, hitherto non-existent. We obtained a number of predictions for the critical exponents near the crossover, which in principle can be confirmed by Monte Carlo simulations and, perhaps, experiments. Hopefully this would convince the remaining skeptics that the crossover is continuous.

The infrared duality between the ϕ^4 and $\sigma\chi$ -flows is essential to our picture. All our findings support this idea. Notably, we have seen that both flows contain in the IR a pair of operators $(\mathcal{O}_1, \mathcal{O}_2)$ satisfying the shadow relation $\Delta_1 + \Delta_2 = d$. We argued that these relations are true to all orders in perturbation theory, and in view of the duality the simplest assumption is that they are also valid non-perturbatively. The shadow relation and the related results about the normalization of OPE coefficients (see section 2.4.2) prove useful in the analysis of the LRFP using the conformal bootstrap [49].²⁰

While in this chapter we have focused on the long-range *Ising* model, it's clear that most of the learned lessons are quite general. For example, the extension to the $O(N)$ case is straightforward. Still more generally, our $\sigma\chi$ -flow construction can be used with any CFT in place of the SRFP. Just pick a scalar CFT operator, call it σ again, of dimension Δ , and couple it to a non-local gaussian field χ of dimension $d - \Delta - \delta$, $\delta \ll 1$. One then needs to compute the quantum correction to the beta-function. Naively, there is a 50% chance that the quantum

²⁰The 3d LRFP is also expected to have a \mathbb{Z}_2 line defect operator, analogous to the SRFP line defect [104, 105] and continuously connected to it. This may explain why some ongoing bootstrap studies [106] do not succeed in isolating the 3d SRFP line defect. We thank Dalimil Mazáč for this remark.

Chapter 2. The long-range to short-range crossover

correction has the right sign to yield a stable IR fixed point.²¹ We will then obtain a continuous family (parametrized by δ) of non-local conformally invariant theories which are deformations of the original local CFT. It will be unitary if the original CFT was unitary and if χ is above the unitarity bound. The generic prediction of this construction is the non-renormalization of χ and the IR shadow relation $\Delta_{\sigma, \text{IR}} + \Delta_\chi = d$.

This demonstrates that, while we expect local CFTs to be generically isolated, non-local conformal theories can easily form continuous families. While this observation by itself is not new, the above general construction seems new. Another known way to construct such continuous families is to put a UV-complete massive theory in a fixed AdS background. Varying masses and couplings of the bulk theory, we obtain a continuous family of boundary theories which have conformal invariance but no local stress tensor (since the metric is non-dynamical). See e.g. [107].

We would like to finish with a brief discussion of the $d = 1$ case, which has so far been excluded from our considerations. The $d = 1$ short-range Ising model does not have a phase transition, and so the physics of long-range to short-range crossover is bound to be very different from $d = 2, 3$. The only scale-invariant phase of the $d = 1$ short-range Ising model occurs at zero temperature, where all correlation functions are constant. This corresponds to the commonly assigned exact critical exponent $\eta = 1$, see e.g. [108] (recall that $\Delta_\phi = -1/2$ is the scalar field engineering dimension in $d = 1$). Applying naively the general d -dimensional formula (2.1.1) for the crossover location, we expect it to happen at $s = 2 - \eta = 1$. This matches nicely with what is known about the long-range Ising model in $d = 1$. First of all, since the work of Dyson [109] it is rigorously known that the model has a phase transition for $0 < s < 1$. This transition is continuous in this range, as is also rigorously known ([110], Corollary 1.5). The transition disappears for $s > 1$, which is where we expect the short-range phase.

The borderline case $s = 1$ is special: the phase transition exists, but it's discontinuous, in the sense that the magnetization has a nonzero limit for $\beta \rightarrow \beta_c^+$, as was argued by Thouless [111] and later proved rigorously [112]. This phase transition is topological, driven by dissociation of kink-antikink pairs [111, 113, 114].²² For $s = 1$ ($1/|x|^2$ spin-spin interaction), kinks interact logarithmically. As temperature is raised, defect operators representing kinks become relevant, kinks proliferate, and the model disorders. So, the theory at $s = 1$ and $\beta = \beta_c$ has marginally relevant operators (kinks).

RG equations for the one dimensional LRI at leading order in $s - 1$ were written down in [115], and a comparison of results from this approach with critical exponents obtained through Monte Carlo simulations can be found in [116], figure 20, and shows good agreement in the

²¹One might wonder what goes wrong if we get an IR fixed point for negative value of g_*^2 , i.e. imaginary values of g_* . After all, due to the \mathbb{Z}_2 symmetry, all observables depend on g_*^2 only, and therefore will be real. However, we can see from (2.3.37) that the lowest spin 2 operator would be below the unitarity bound, and we would end up with a non-unitary theory.

²²The work of Thouless [111] foreshadowed later work by Berezinski and by Kosterlitz and Thouless on the BKT phase transition in two-dimensional $O(2)$ models, driven by dissociation of vortex-antivortex pairs.

region close to $s = 1$. However, a description in terms of QFT is missing, and it's not clear how to improve the results of [115] beyond leading order.

Walking theories **Part II**

3 Walking, weak first order phase transitions and complex CFTs

“But the beauty is in the walking – we are betrayed by destinations.”

Gwyn Thomas

3.1 Introduction

Walking is a somewhat mysterious behavior which can conjecturally be exhibited by some four-dimensional (4d) gauge theories. In a walking gauge theory, the gauge coupling is supposed to run slowly at intermediate energies, where the theory is approximately scale invariant, while at low energies the coupling starts running fast again, leading to confinement and chiral symmetry breaking. Originally this has been dreamed of in the context of technicolor scenarios of electroweak symmetry breaking [27–29].

A number of curious opinions about walking can be found in the literature. Walking is supposed to happen just below the end of the conformal window [117]. It is believed by some that walking theories contain a naturally light pseudo-dilation in the spectrum [28]. There are doubts if walking may naturally occur in theories with a small number of colors [118]. We warn the reader that only the first of these three opinions will find a confirmation in our analysis. The above definition of walking itself also needs revision, since as we will see it's not the gauge coupling which walks. We collected here this mix of opinions to stress that, at least to us, walking appears a rather controversial subject where much confusion lingers. This is also due to the fact that probing this scenario directly by lattice Monte Carlo simulations remains a hard task.

In this chapter, we will first improve understanding of walking by drawing intuition from a much simpler example of this behavior, belonging to the realm of statistical physics: the Q -state Potts model in 2d. This model is known to have a conformal phase for $Q < 4$, and a first-order phase transition at $Q > 4$. For $Q \gtrsim 4$, the transition is *weakly* first-order: the

Chapter 3. Walking, weak first order phase transitions and complex CFTs

correlation length is much larger than the lattice spacing. This was understood by statistical physicists in the 1980s [30, 31] in terms almost identical to walking (one difference being that the Potts model has a strongly relevant singlet scalar whose coefficient is tuned to zero to reach the transition). As far as we know, the connection between walking and weakly first-order phase transitions is being made here for the first time in the high energy physics literature.¹

Our second goal is to demystify the *fixed points at complex coupling*, often invoked in discussions of walking. We will formalize these fixed points as *complex conformal field theories (CFTs)*, a concept that we introduce. Complex CFTs are non-unitary, but they are sufficiently different from other commonly occurring non-unitary CFTs that they deserve a separate name. For example, 2d complex CFTs have a complex central charge c . In spite of this and other unusual features, we will argue that complex CFTs are nonperturbatively well defined. We will discuss, in general terms, how this new language can be used to describe some aspects of walking.

The chapter is structured as follows. In section 3.2 we present walking from renormalization group (RG) point of view: as a general mechanism for generating hierarchies in quantum field theory (QFT). We also briefly review a more common mechanism known as tuning. In the same section we give a first introduction to the concept of complex CFTs.

Sections 3.3, 3.4 and 3.5 focus on concrete systems exhibiting walking. In section 3.3 we discuss how walking is realized in the 2d Q -state Potts model, including a detailed introduction to this lattice model for the benefit of high energy physicists. Section 3.4 discusses various aspects of walking in 4d gauge theories. In particular, we explain why we don't believe in the parametrically light pseudo-dilaton. We also discuss walking in holographic models of QCD in the Veneziano limit. Finally in section 3.5 we discuss a recent example of walking that emerged in condensed matter physics, in the context of "deconfined criticality".

Section 3.6 is devoted to complex CFTs. We build upon intuitive understanding of the difference between RG flows in the space of real vs complexified couplings, towards a more formal definition of the concept of a complex QFT and a complex CFT. We explain how the real vs complex classification differs from the more familiar unitary vs non-unitary classification. In particular we give examples of non-unitary but real theories. Finally we come back to the connection between complex CFTs and walking. We present a computational paradigm, a kind of conformal perturbation theory, which allows to compute certain properties of walking RG flows in terms of CFT data of complex CFTs. In this chapter we only discuss general features of this paradigm. In chapter 4 we will show its usefulness by studying the walking behavior of the 2d Potts model at $Q > 4$. We will see that it allows for many concrete applications, tests, and predictions.

In section 3.7 we conclude. Appendix B.1 reminds that not all weakly first-order phase

¹In condensed matter/statistical physics this connection is not forgotten, as we will see in section 3.5. Walking is one of two known mechanisms which can explain weakness of a first-order phase transition, the other one being tuning, see section 3.2.1 and appendix B.1.

transitions are explainable by walking, some being due to tuning. Appendix B.2 explains the difference between the physics of walking and the BKT transition. Appendix B.3 discusses features of conformal window and walking in 4d gauge theories arising in the large N limit. Appendix C contains further details about the Potts model, in particular in $d > 2$.

3.2 Walking as a mechanism for hierarchy

This section will define walking using the language of RG, without specializing to any particular microscopic description. Walking is one of two known robust mechanisms for generating hierarchy in QFT, the other one being the much more familiar ‘tuning’. The question of hierarchies being of extreme importance, this explains why one should a priori be interested in walking.

Hierarchy is a separation of scales. A hierarchy in quantum field theory means that the theory contains two distance scales $\ell_{UV} \ll \ell_{IR}$ (or equivalently two energy scales $\Lambda_{UV} \gg \Lambda_{IR}$), the physics being approximately scale invariant in the intermediate range between them. The scale ℓ_{UV} can be thought of as a short-distance cutoff. The scale ℓ_{IR} in high energy physics is usually related to the inverse mass of some particle, while in statistical physics it is the correlation length.

Hierarchies are a familiar feature of theories with a logarithmically running coupling, such as the usual QCD. Although the coupling runs slowly, and one may be tempted to say poetically that it ‘walks’,² in our technical classification this is actually an example of a (mild) tuning and not of walking, see below.

3.2.1 Tuning

Tuning mechanism for hierarchies is completely standard and utterly familiar to QFT practitioners, but let’s review it anyway to set the stage. From many available prior discussions, ours will stay closest to [13, 119].

In this mechanism a hierarchy results from the fact that an RG trajectory describing the QFT starts close to a CFT and remains close to it for a long time. We can thus think of the RG flow in terms of the perturbing operators added to the CFT. For the flow to stay close to the CFT, we should worry in particular about the coefficients of all *relevant* perturbations, which must be assumed small.

Assuming for simplicity that there is just one relevant operator, the arising hierarchy is controlled by the size of its coefficient. At some UV scale where the microscopic theory

²Frank Wilczek used to say “You must walk before you run!” in his colloquia, referring to the QCD gauge coupling.

is matched onto the CFT plus a perturbation, the theory is described by

$$\text{CFT} + c \Lambda_{\text{UV}}^{d-\Delta} \int d^d x \mathcal{O}_\Delta(x), \quad (3.2.1)$$

where \mathcal{O}_Δ is a scalar operator of scaling dimension $\Delta < d$, and $c \ll 1$.³ The necessity to take $c \ll 1$ is why this scenario is called “tuning”. Then assuming the coupling c does not flow to a fixed point, the relation between the UV scale and the IR scale, at which the departure from the CFT becomes significant, is⁴

$$\Lambda_{\text{IR}} \sim c^{\frac{1}{d-\Delta}} \Lambda_{\text{UV}}. \quad (3.2.2)$$

In applications of this scenario in high energy physics, there is, justifiably, much preoccupation with how “natural” the implied tuning is. If the operator \mathcal{O}_Δ transforms non-trivially under some global symmetry present in the CFT, the assumption of a small coefficient c is considered “technically natural” in QFT jargon, because $c = 0$ would be preserved by RG evolution. Put another way, the smallness of this coefficient can be explained by requiring that the symmetry be approximately preserved in the microscopic description of our theory. This is just ‘t Hooft’s naturalness criterion [120] restated in the CFT language.

A more problematic case is when \mathcal{O}_Δ is a full singlet of the CFT global symmetry group. In this case a fully natural hierarchy is never possible. However there is a way to turn a *mild tuning* into a large hierarchy, provided that \mathcal{O}_Δ is *weakly relevant*, that is if $d - \Delta \ll 1$ [119]. To see this, notice that if both c and $d - \Delta$ are somewhat small, say 0.1, then Eq. (3.2.2) predicts the hierarchy $\Lambda_{\text{UV}}/\Lambda_{\text{IR}} \sim 10^{10}$.

The above-mentioned QCD example can be seen as a limiting case of the latter situation when $\Delta \rightarrow d$ and the operator is marginally relevant. In this case the relation between the IR scale (Λ_{QCD}) and the UV cutoff is exponential in the inverse of the bare gauge coupling. But to enjoy this exponential hierarchy, we must still assume that the gauge coupling is somewhat small at the cutoff, hence mild tuning.

In condensed matter/statistical physics context, the tuning mechanism explains the weakness of some first-order phase transitions, see appendix B.1.

3.2.2 Walking

We will now discuss walking which is our main interest. In this case the CFT picture is a bit more complicated, and it is convenient to present first a more intuitive picture based on the RG. We consider an RG flow of a coupling λ , of unspecified origin, and a singlet under the

³By d we denote the full number of dimensions, which includes time if we work in Minkowski signature.

⁴We don’t keep track of factors of 4π , which would be useful in practical applications of this sort of naive dimensional analysis.

global symmetry. We assume that the beta-function near $\lambda = 0$ takes the form ($t = \log E$)

$$\beta(\lambda) = \frac{d\lambda}{dt} = -y - \lambda^2 + O(\lambda^3), \quad (3.2.3)$$

where y is a small parameter, and the higher order terms are assumed to have $O(1)$ coefficients so that Eq. (3.2.3) is trustworthy at $|\lambda| \lesssim 1$. While the choice of $\lambda = 0$ may seem special, there is no loss of generality here, as we can first assume that the beta-function takes this form with $\lambda - \lambda_0$ instead of λ in the r.h.s., and eliminate λ_0 by a shift.⁵

Of course describing the flow in terms of just one coupling is an idealization. What we imagine is that all other couplings characterizing the flow are irrelevant, and so their effect on the flow of λ can be neglected.⁶

Assuming that the coupling λ is real, physics described by the beta-function (3.2.3) is very different depending on the sign of y . Suppose first that $y < 0$. Then we have two real fixed points $\lambda_{\pm} = \pm\sqrt{|y|}$ (see Fig. 3.1). The λ_+ fixed point is a UV fixed point in the sense that it cannot be reached by flowing from short distances. The λ_- fixed point is an IR fixed point as it can be reached flowing both from the UV fixed point and also from large negative λ , provided that in this range the microscopic description happens to match approximately the RG flow described by the above beta-function.

Concerning the CFTs describing these fixed points, the operator \mathcal{O}_{λ} to which λ couples will have dimension

$$\Delta_{\pm} = d + \beta'(\lambda_{\pm}) \approx d \mp 2\sqrt{|y|}. \quad (3.2.4)$$

For $|y| \ll 1$ this dimension is weakly relevant at the λ_+ fixed point. This CFT can be used to realize the mildly tuned hierarchy scenario of the previous section, flowing out in the positive λ direction.

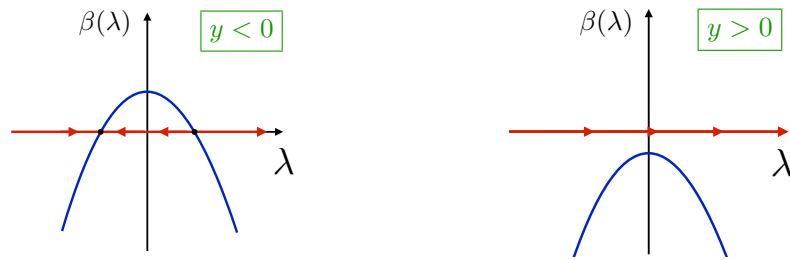


Figure 3.1 – Structure of RG flow for real coupling for $y < 0$ (left) and $y > 0$ (right).

Suppose instead that $y > 0$. Then there is no fixed point at real λ , at least not within the region of validity of the assumed approximate beta-function. A flow starting at $\lambda \sim -1$ will eventually

⁵Even more generally the λ^2 term could be $A(\lambda - \lambda_0 - By)^2$, and we can set $A \rightarrow 1$, $\lambda_0 \rightarrow 0$, $B \rightarrow 0$ shifting and rescaling λ .

⁶It is also possible that a few of them are relevant and then have to be finetuned small. This is what happens in the Potts model where one has to finetune the temperature, see section 3.3.4.

Chapter 3. Walking, weak first order phase transitions and complex CFTs

go through to $\lambda \sim 1$, but for small y it will slow down and linger around $\lambda \sim 0$. How much the flow lingers can be estimated by computing the RG time of passage:

$$\Delta t \sim - \int_{-1}^1 \frac{d\lambda}{\beta(\lambda)} \sim \frac{\pi}{\sqrt{y}}. \quad (3.2.5)$$

One can also use the exact solution of the beta-function equation neglecting $O(\lambda^3)$ terms:

$$\lambda(t) = -\sqrt{y} \tan[\sqrt{y}(t - t_0)]. \quad (3.2.6)$$

If we call Λ_{UV} the scale where the flow emerges from a microscopic description at $\lambda \sim -1$, and Λ_{IR} the scale where the flow plunges into the unknown at $\lambda \sim 1$, we obtain:

$$\Lambda_{UV}/\Lambda_{IR} \sim e^{\Delta t} \sim \exp(\pi/\sqrt{y}), \quad (3.2.7)$$

a huge ratio of scales if y is small. We will refer to (3.2.7) as ‘walking scaling’.⁷

Given the hierarchy, we expect that the flow in the intermediate range of energies should be approximately scale invariant, so it should be close to a CFT. But to which CFT? For $y < 0$ we had two CFTs, but for $y > 0$ there are no CFTs in sight.

One way out is to argue that the flow remains close to the CFT which describes the $y = 0$, $\lambda = 0$ point, where the fixed points join and disappear.⁸ This proposal is certainly viable and physically reasonable, and it allows to compute some quantities characterizing the flow at $y > 0$, expanding around the $y = 0$ point. However, there are some puzzling features with this way of thinking and computing.

One puzzle is what to do when the global symmetry of the problem depends on y . In the concrete examples of the Potts model and of the 4d gauge theories, the global symmetry will be S_Q and $SU(N_f) \times SU(N_f) \times U(1)$ respectively, with Q and N_f continuous functions of y . Certainly there are limitations for expanding a theory with, say, S_5 symmetry around a theory with S_4 symmetry, and yet in the above proposal that’s what we would have to do.

Another puzzle is that the above discussion does not have a built-in criterion for determining the range of validity of the obtained expansions. One might think that it is $|y| \ll 1$, but this is too naive and can’t be true because y is just an arbitrary parameter, not a physically significant quantity. And indeed the naive criterion with $y = Q - 4$ is violated by the 2d Potts model (see section 3.3.5). We need a better criterion.

⁷Ref. [117] refers to the functional form of this equation as ‘BKT scaling’, since this is also the form of the correlation length in Berezinskii-Kosterlitz-Thouless (BKT) transition. We review the physics of BKT transition in appendix B.2. In our opinion, there are more differences than similarities between BKT transition and walking, and so we propose to avoid terminology ‘BKT scaling’ when discussing walking in this chapter and in the future.

⁸This point of view would be close to [30, 31] where the walking scenario was first elucidated, see section 3.3.4.

3.2.2.1 Introducing complex CFTs

To achieve some peace with the above puzzles, let us reconsider the fate of the fixed points at $y > 0$. Of course the fixed points don't just disappear completely, but they *go to the complex plane*, see Fig. 3.2. While this is often said, as far as we know until now there has not been any concrete attempt to assign physical meaning to these complex fixed points. This is precisely what we would like to do. We posit that these fixed points should be viewed as nonperturbatively defined non-unitary CFTs of a novel type, which we call *complex CFTs*. To the pair of complex conjugate fixed points there will correspond a pair of complex conjugate CFTs, called \mathcal{C} and $\bar{\mathcal{C}}$.

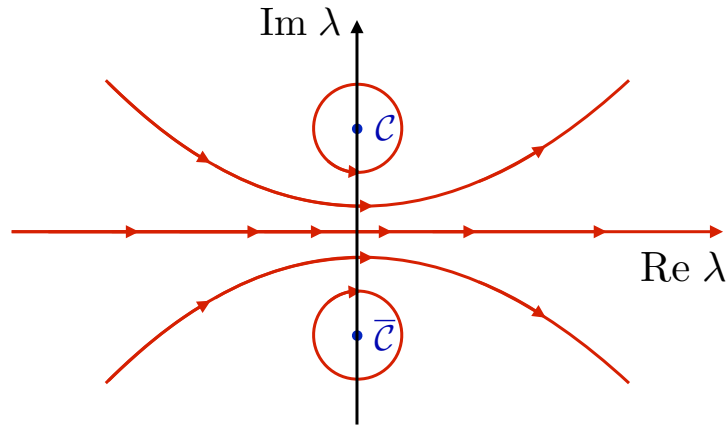


Figure 3.2 – Structure of RG flow in the complex coupling plane, in the approximation of dropping the higher order terms in (3.2.3). Notice that including those terms will generically change the nature of RG flow trajectories around \mathcal{C} and $\bar{\mathcal{C}}$, since the RG eigenvalue will then acquire a small real part $O(y^2)$, making the flow spirally in- or unwinding. See 4 for an example.

We will argue that these complex CFTs control the walking flow in the same way as the CFT appearing in (3.2.1) controls the tuned flow. It is around them that one should more properly expand the flow, and not around the CFT at $y = 0$. Doing so we readily resolve the first puzzle, since \mathcal{C} and $\bar{\mathcal{C}}$, living at the same value of the y parameter, have the same global symmetry as the physical RG flow along the real axis.

Having recourse to \mathcal{C} and $\bar{\mathcal{C}}$ also allows to determine the criteria for the walking behavior more sharply. For small $y > 0$ let us compute the fixed point dimension Δ of the CFT operator \mathcal{O}_λ to which λ couples. The fixed points being at $\lambda_* = \pm i\sqrt{y}$, we get similarly to (3.2.4)

$$\Delta = d + \beta'(\lambda_*) = d \mp 2i\sqrt{y} + O(y^2). \quad (3.2.8)$$

Notice that the dimension is complex (and complex conjugate for \mathcal{C} and $\bar{\mathcal{C}}$), which will be a hallmark of complex CFTs. Notice as well that Δ is close to marginality, with the leading deviation imaginary and small. As we will see, it is this smallness of the imaginary part of the near-marginal operator dimension which is necessary for walking, and not the smallness of y by itself. Suppose then that we have some nonperturbative access to $\text{Im } \Delta$, for example

because we solved \mathcal{C} and $\bar{\mathcal{C}}$. Then there is no need to expand around $y = 0$. Instead, using the nonperturbative solution, we can simply determine the range of y for which $|\text{Im} \Delta| \ll 1$ holds. This statement will be justified by means of conformal perturbation theory in section 3.6.3 and in 4.

3.2.2.2 Naturalness of walking

As for the tuning scenario, we would like to make an assessment of how natural the walking mechanism is.

We have seen that walking needs a complex CFT \mathcal{C} (and its complex conjugate $\bar{\mathcal{C}}$) with an operator whose dimension has the real part close to marginality (d) and the imaginary part small. An assumption of having such a CFT at our disposal certainly represents some “finetuning in theory space”, just like the assumption of having a CFT with a weakly relevant deformation in the mild tuning scenario. In fact we have seen that both these assumptions can be realized within a one-parameter family of RG flows, close to a special parameter value where a UV and an IR fixed points collide, and on two opposite sides of this value.

However, apart from this theory space finetuning, there is no further coupling finetuning required in the walking scenario (provided that all other couplings but λ are irrelevant). Indeed, we can start the flow *anywhere* on the negative real axis of λ , which represents 50% of the a priori possible initial coupling values. It will then inexorably be drawn to λ near 0. Basically, the flow is forced to pass between the ‘pillars of Hercules’ \mathcal{C} and $\bar{\mathcal{C}}$, because it has nowhere else to go.

This situation can be contrasted with the mild tuning scenario, where we had to buy *both* finetuning in theory space, and a mild coupling finetuning $c \ll 1$. From this point of view, walking seems less finetuned than mild tuning.

The just-given discussion only considered the naturalness of the basic walking scenario associated with the running of λ . There is an additional finetuning price if relevant singlet operators are present, whose coupling has to be tuned to zero, as for the Potts model.

3.3 Walking in statistical physics: 2d Potts model

Although we borrowed the term ‘walking’ from the physics of 4d gauge theories, historically the first example of walking has been observed in the 2d Q -state Potts model. This model is one of best known models of statistical physics, see [121, 122] for reviews, but it’s not as widely known to high energy physicists as it deserves. We therefore start with a mini-review. Generalizations to $d > 2$ will be discussed in appendix C.3.

3.3.1 Spin and cluster definitions

Consider a square lattice in 2d (other lattices are also possible). It will be important that the Potts model has two lattice definitions: either as a model of random spins living on lattice sites, or as a model random clusters, that is connected sets of lattice bonds. The two definitions agree for integer $Q \geq 2$, with the second definition providing an analytic continuation to non-integer Q 's.

In the spin definition, we put on every lattice site i a discrete variable $s_i \in \{1, 2, \dots, Q\}$. The partition function is the sum over spin configurations:

$$Z_{\text{spin}} = \sum_{\{s_i\}} e^{-H[\{s_i\}]}, \quad (3.3.1)$$

with the lattice Hamiltonian (we include $\beta = 1/T$ into the Hamiltonian) being the sum of nearest-neighbor interaction terms which energetically prefer for the spins to be identical (called the ferromagnetic case):

$$H[\{s_i\}] = -\beta \sum_{\langle ij \rangle} \delta_{s_i, s_j}. \quad (3.3.2)$$

For $Q = 2$ this reduces, up to a constant shift, to the Ising model Hamiltonian. This model has a discrete global symmetry S_Q (the permutation group).

Let us now discuss the cluster definition of the Potts model, due to Fortuin and Kasteleyn [123]. On the same lattice we consider random subsets of lattice bonds X . The probabilistic weight for a given subset X to occur is defined as

$$w(X) = v^{b(X)} Q^{c(X)}, \quad v = e^\beta - 1, \quad (3.3.3)$$

where $b(X)$ is the total number of bonds in X , and $c(X)$ is the total number of *clusters*—connected components in the graph which has all lattice sites as vertices and bonds from X as edges. Isolated sites also count as clusters (see Fig. 3.3). The partition function is then given by:

$$Z_{\text{cluster}} = \sum_X w(X). \quad (3.3.4)$$

The factor $v^{b(X)}$ in (3.3.3) simply means that each lattice bond is included or not into X with independent probabilities p and $1 - p$ where $p = v/(1 + v)$. This basic factorized probability distribution is then modified by the factor $Q^{c(X)}$. The number of clusters $c(X)$ is a nonlocal characteristic of X , so definition (3.3.3) is nonlocal. In particular, unlike for spins, it is not given in terms of a local Hamiltonian.⁹

For integer $Q \geq 2$ the two partition functions Z_{spin} and Z_{cluster} agree [123]. To see this one

⁹However some semblance of locality can be introduced by introducing the height representation, as we will review in 4.

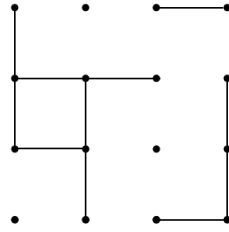


Figure 3.3 – An example of a random subset X of bonds on a 4×4 square lattice. Here $b(X) = 11$ and $c(X) = 6$. Notice that isolated points count as clusters.

perform a power-series expansion of Z_{spin} in ν , which is the high-temperature expansion. Using the identity

$$e^{\beta\delta_{s_i,s_j}} = \nu\delta_{s_i,s_j} + 1, \quad (3.3.5)$$

this expansion maps term by term onto Z_{cluster} , with the factor $Q^{c(X)}$ arising from contracting delta-functions. In other words, for integer $Q \geq 2$ each high-temperature expansion cluster may have one of Q “colors”.

On the other hand, the cluster definition is more general as it is applicable for continuously varying Q . It is worth mentioning that the model is reflection positive for integer Q while for non-integer Q it is not (see e.g. [124]). In this chapter we will focus on real $Q > 0$.

We note in passing that the cluster definition can also be used to extract nontrivial physics from integer values of $Q = 0, 1$ where the spin definition would seem to be trivial. Namely, $Q = 1$ defines bond percolation, and the limit $Q \rightarrow 0^+$ corresponds to spanning trees and forests [123].

3.3.2 Phase transition

Consider first the integer- Q Potts model defined in terms of spins. At low temperatures it has an ordered phase with Q degenerate ground states where S_Q is spontaneously broken and one spin value is preferred. At high temperatures we have a disordered phase where there is just one state and the spin distribution is S_Q -symmetric. These two phases are separated, for each Q , by an order-disorder phase transition at some critical temperature $\beta = \beta_c$.¹⁰ The phase transition can be detected by fixing one spin (s_0) and measuring the probability that a distant spin is in the same state:

$$p(r) = \mathbb{P}[s_r = s_0] - 1/Q, \quad (3.3.6)$$

where we subtract the trivial probability $1/Q$ which would arise for uncorrelated spins. An order parameter distinguishing the two phases is the value p_∞ of this probability in the limit $r \rightarrow \infty$, zero in the disordered phase and positive in the ordered one.

Consider then the same phase transition within the cluster definition. At high temperatures

¹⁰The exact value of $\beta_c = \log(1 + \sqrt{Q})$ is known in 2d from self-duality. See [121], including the discussion of how the duality acts in terms of the random cluster model.

we have $\nu \ll 1$ and the clusters tend to be very small. At low temperatures huge clusters occupy most of the lattice: a nonzero magnetization in the spin definition corresponds to clusters extending all across the infinite lattice in the cluster formulation. One basic cluster observable is the probability $\tilde{p}(r)$ that two lattice sites separated by distance r lie in the same cluster, as well as an order parameter $\tilde{p}_\infty = \lim_{r \rightarrow \infty} \tilde{p}(r)$. Using the high-temperature expansion, it's not hard to show that $p(r) = (1 - 1/Q)\tilde{p}(r)$ for integer Q , and so the two order parameters p_∞ and \tilde{p}_∞ are equivalent (see e.g. [125]).

Finally let us discuss the order of the transition. We can define the correlation length ξ from the rate of approach $\tilde{p}(r) - \tilde{p}_\infty \sim e^{-r/\xi}$. The transition is first-order or continuous depending if ξ remains finite or becomes infinite at $\beta = \beta_c$. An equivalent definition of the transition order is in terms of phase coexistence. At a first-order transition we expect that the ordered and disordered states will coexist, while at a continuous transition there is just one state.

It can be argued using $1/Q$ expansion that the transition is first-order at $Q \gg 1$ (see appendix C.2). In general we expect a critical value of Q so that the transition is continuous for $Q \leq Q_c$ and first-order for $Q > Q_c$. In the 2d case considered here, it is known that $Q_c = 4$ [126]. The phase transition for $Q \leq Q_c$ is described by a CFT. Much is known about this CFT as a function of Q , as we will see below and in 4.

Although the Potts model is usually studied on the square lattice, it is believed that the CFT describing the phase transition does not depend on the lattice type. E.g. 2d Potts models on the square and triangular lattice, as long as they have the same Q , should give rise to the same CFT (see e.g. [127, 128]).¹¹ This property can be stated by saying that parameter Q does not get renormalized. For integer Q this can be argued by symmetry, but for non-integer Q the question of symmetry appears more subtle (see the next section).

3.3.3 Symmetry

As mentioned, for integer $Q \geq 2$ the Potts model has discrete global S_Q symmetry. Knowing the symmetry is very useful for many reasons, for example because it allows us to identify the microscopic model with the CFT describing its fixed point. Potts models with the same symmetry will belong to the same universality class and their critical point will be described by the same CFT. We can change the lattice (e.g. from square to triangular), or we can add other interactions (e.g. next-to-nearest-neighbor). As long as symmetry is preserved, the CFT should remain the same.

Moving to non-integer Q , the precise mathematical meaning of symmetry is unclear. As mentioned above there is evidence that the critical point does not depend on the lattice,

¹¹We thank Jesper Jacobsen for the following exact solvability argument which provides additional evidence. At the critical temperature, the triangular lattice Potts model can be solved mapping it onto a six-vertex Kagomé lattice model ([129], chapter 12). Using the star-triangle relation, the latter model can be transformed to a square-lattice model ([129], chapter 11). This transformation shows that correlation functions along a certain line are the same in the triangular and square Potts model, so that in particular the critical exponents are the same.

and this asks for a symmetry explanation. However, the group S_Q certainly does not make mathematical sense for non-integer Q . Let us specify our requests for the symmetry in non-integer Q : it should allow a unique identification of Q , it should explain which perturbations of the cluster model preserve the universality class, and it should hopefully work for any d .¹²

We will proceed assuming that the concept of symmetry makes sense for any Q , even if it's not yet been properly defined for non-integer Q .

3.3.4 Weakly first-order phase transition at $Q \gtrsim 4$ and walking

Baxter [126] has computed the free energy of the 2d Potts model for any Q at the critical temperature, reducing to a 6-vertex model. From his exact solution it follows that latent heat L at the transition is zero for $Q \leq Q_c = 4$ (continuous transition) and positive at $Q > Q_c$ (first-order transition). Baxter's solution implies that the latent heat vanishes exponentially quickly for $Q \rightarrow Q_c^+$, as

$$L \sim \exp\left(-\frac{\pi^2}{2\sqrt{\delta}}\right), \quad \delta = Q - Q_c. \quad (3.3.7)$$

First-order phase transitions with small latent heat (in natural units) are called weak, and the 2d Potts for $Q \gtrsim Q_c$ is an example of this.

Another robust characteristic of a weak first-order (WFO) transition is that the correlation length ξ , while remaining finite, becomes very large in the units of lattice spacing. The critical 2d Potts correlation length was computed exactly in [131]. For $Q \rightarrow Q_c^+$ the correlation length becomes exponentially large:

$$\xi \approx \xi_0 \exp\left(\frac{\pi^2}{\sqrt{\delta}}\right), \quad (3.3.8)$$

with ξ_0 approximately constant in this limit.

For a lattice model, to have the correlation length much larger than the lattice spacing is an example of a hierarchy, in the sense of section 3.2. This property of the 2d Potts model at $Q \gtrsim 4$ was explained 40 years ago by Nauenberg, Scalapino, and Cardy [30, 31] as a consequence of walking, in what was perhaps the first evocation of this mechanism in physics.¹³

Let us review this explanation and the evidence in its favor. The key assumption is that the RG evolution is described by Eq. (3.2.3), with parameter y a monotonic function of Q . $Q = Q_c$ corresponds then to $y = 0$, and one assumes that near this point y has approximately linear dependence on δ :

$$y = C\delta + O(\delta^2). \quad (3.3.9)$$

¹²We note in this respect that in 2d, quantum algebra $U_q sl(2)$ with $q + q^{-1} = Q^{1/2}$ plays an important role in the Temperley-Lieb approach to the partition function of Q -state Potts model [130]. This seems to be an inherently 2d phenomenon and in addition intimately related to the integrability properties of the model.

¹³They did not actually use the term 'walking'. It seems that the mechanism does not have a standard name in statistical physics. Sometimes it is referred to as 'pseudo-critical behavior' [33, 132, 133].

3.3. Walking in statistical physics: 2d Potts model

The constant C must be positive, so that $y > 0$ (no fixed point at real λ) corresponds to $Q > Q_c$. The value of C can be readily fixed by demanding that the hierarchy (3.2.7) reproduce the exactly known correlation length asymptotics (3.3.8). One gets¹⁴

$$C = 1/\pi^2. \quad (3.3.10)$$

Consider then what happens for $Q < Q_c$. It is convenient to enlarge the coupling space of the Potts model by considering the *dilute Potts model*. In this model the Potts spins or clusters live only on a part of the lattice, while the rest is occupied by vacancies.¹⁵ One can also think that vacancies are generated by RG transformations and represent disordered spin configurations [127].

Now, it is known that the dilute Potts model has for $Q < Q_c$ two fixed points. One of them is the same as the critical point of the usual non-dilute Potts model. The other fixed point is tricritical, obtained by tuning both the temperature and the chemical potential for the vacancies. Ref. [127] first found these fixed points by means of an approximate RG transformation, and showed that they annihilate at $Q = Q_c$. This picture of two fixed points at $y < 0$ annihilating at $y = 0$ agrees with section 3.2.2 (see Fig. 3.4(b) below). We therefore identify the more stable $\lambda = \lambda_-$ fixed point as the critical and $\lambda = \lambda_+$ as the tricritical Potts model.

In fact, much is known about the CFTs describing these fixed points, and this can be used to further check and complete the walking RG picture.¹⁶ Here we will use the two lowest singlet operators ε and ε' , referred to as the leading and subleading temperature perturbations. Their dimensions are known exactly for $Q < Q_c$ [138–140], with the following asymptotics at $Q \rightarrow Q_c^-$:

$$\Delta_\varepsilon = \frac{1}{2} \mp \frac{3}{4\pi} \sqrt{|\delta|} + O(\delta), \quad (3.3.11)$$

$$\Delta_{\varepsilon'} = 2 \mp \frac{2}{\pi} \sqrt{|\delta|} + O(\delta). \quad (3.3.12)$$

(The upper sign corresponds to the tricritical fixed point.) Operator ε' is close to marginality and should be identified with the operator \mathcal{O}_λ , whose dimension is predicted by RG in (3.2.4). Using (3.3.9) and (3.3.10), we see that the RG prediction (3.2.4) agrees with the exact result (3.3.12).

Operator ε is strongly relevant, and its coupling (denoted ϕ in [30, 31]) must be finetuned to zero to reach the phase transition. This is a particularity of the Potts model compared to the

¹⁴This step was not done in [30, 31] because the correlation length asymptotics was not known at the time. They arrived at the same value of C via the exactly known energy operator dimensions and the latent heat asymptotics, see below.

¹⁵This is also called the Blume-Emery-Giffiths model [134, 135]. For a cluster definition applicable at non-integer Q see [136].

¹⁶The operator spectrum of both CFTs is fully known, some of it via exact lattice solution à la Baxter, and the rest via Coulomb gas [137]. The OPE coefficients are known fully for $Q = 2, 3, 4$ and partially for other Q 's. We will review and use this information in 4.

Q	5	6	7	8	9	10
ξ/a	2512.2	158.9	48.1	23.9	14.9	10.6

Table 3.1 – The 2d Potts model correlation length in units of lattice spacing on the square lattice at the first-order phase transition for $Q = 5 - 10$, computed from [131], Eq. (4.46).

basic scenario in section 3.2.2 and to walking in gauge theories. Small deviations of ϕ from zero are governed by an RG equation of the leading form

$$d\phi/dt = -(a + b\lambda)\phi + \dots \quad (3.3.13)$$

The fixed point dimension of ε is then given by

$$\Delta_\varepsilon = 2 - (a + b\lambda_\pm) + O(\delta). \quad (3.3.14)$$

Demanding agreement with (3.3.11) allows us to fix the two constants a, b :

$$a = \frac{3}{2}, \quad b = \frac{3}{4}. \quad (3.3.15)$$

The RG equation (3.3.13) is also important when studying the WFO regime $y > 0$. The running of ϕ must be taken into account when computing the latent heat (which is the derivative of free energy w.r.t. ϕ). The computation of [30, 31] finds an exponentially small latent heat of the same form as (3.3.7). Precise agreement in the exponent is obtained for $a = 3/2$ as in (3.3.15), providing yet another consistency check of this picture.

3.3.5 Lessons and questions

We see that the 2d Potts model presents a remarkable opportunity for testing the idea of walking. Not only some aspects of it are exactly solvable, it's also relatively easy to study via Monte Carlo simulations. The key assumption is that the same RG equations (3.2.3), (3.3.13) apply on both sides of $Q = Q_c$ provided that we make the parameter y depend on $Q - Q_c$ as in (3.3.9). Coefficients in these equations can be fixed demanding the consistency with the exactly known critical exponents at $Q < Q_c$. Solving the same equation for $Q > Q_c$, one obtains approximate results for the correlation length and latent heat in the phase where the transition is weakly first-order, which can be checked against the exact solution on the lattice.

What is the range of Q for which walking behavior persists? Looking at Table 3.1, we see large correlation lengths up to $Q \lesssim 10$. Eq. (3.3.8) works pretty well in this whole range, provided that one allows the coefficient ξ_0 to vary by 30%, from 0.13 to 0.19 (while ξ itself varies by factor 250). Naively this is puzzling, as it may seem that the expansion in $Q - Q_c$ has an unexpectedly large range of validity. However, as mentioned in section 3.2.2, the true criterion for walking should involve nonperturbative information about complex CFTs, rather than $Q - Q_c$. See section 3.6.3 for a general discussion and 4 for details specific to the 2d Potts.

3.4 Walking in high energy physics: 4d gauge theories

Slowly running or walking coupling was first introduced in particle physics in the context of technicolor models of electroweak symmetry breaking [27–29]. These models later received the name “walking technicolor” (WTC). Here we focus on the simplest setup where walking is supposed to occur. Connection to the electroweak phenomenology will be commented upon in section 3.4.1 below.

This simple setup is the 4d gauge theory with gauge group $SU(N_c)$ and N_f massless fermions in the fundamental representation. We will denote $x = N_f/N_c$ and assume $x < x_{\text{AF}} = 11/2$ so that the theory is asymptotically free. It is believed that in an interval of x below x_{AF} ,

$$x_c < x < x_{\text{AF}}, \quad (3.4.1)$$

this theory flows at long distances to a CFT called the Banks-Zaks (BZ) fixed point [141–143]. The interval (3.4.1) is called the conformal window.

The BZ fixed point is weakly coupled near x_{AF} but is strongly interacting near x_c . To consider the weakly coupled $x \rightarrow x_{\text{AF}}$ limit we can formally consider N_f to be a continuously varying parameter. It’s not clear if this makes full sense non-perturbatively.¹⁷ If we wanted to be conservative, we could restrict N_f to be an integer, but then we would have to take large N_c . For simplicity, we will not keep track of large N_c counting. In any case, it is believed that the conformal window is non-empty also for finite N_c . There is evidence for that from various theoretical considerations and from lattice Monte Carlo simulations, see e.g. [144] for a review.¹⁸

On the other hand, for $x < x_c$ there is no fixed point, the theory instead flowing to a confining phase with spontaneously broken chiral symmetry. So the fixed point must disappear as x approaches x_c from above. One possibility is that the fixed point annihilates with another fixed point; see Fig. 3.4(a). This is the scenario advocated in [117], where the new fixed point is called QCD* (see also [149]). One necessary condition for this scenario is that QCD* have the same global symmetry $SU(N_f) \times SU(N_f) \times U(1)$ as the BZ fixed point with which it is annihilating.

Fixed point annihilation appears to us the simplest scenario which explains fixed point

¹⁷On the other hand, the Potts model with Q states discussed above can be defined non-perturbatively for continuously varying Q , although it’s unitary only for integer Q .

¹⁸Here we are focusing on 4d gauge theories, but a similar story is believed to hold in 3d gauge theories coupled to N_f massless fermions. The difference is that in this case conformal window exists both for the abelian and nonabelian gauge theories, and that it extends all way to $N_f = \infty$. The lower boundary of the conformal window is not known in 3d just like in 4d. A natural possibility is that the 3d conformal window terminates via fixed point annihilation, as discussed below for the 4d case. See [145, 146] for recent discussions and references to prior work. The present-day lattice QCD community is neglecting the 3d case, with a few notable exceptions such as [147, 148]. We find this neglect regrettable and methodologically wrong. Not only is the 3d conformal window interesting in its own right and has multiple connections to contemporary condensed-matter physics, see section 3.5, it is certainly easier than the 4d case, and should be solved first as a warmup.

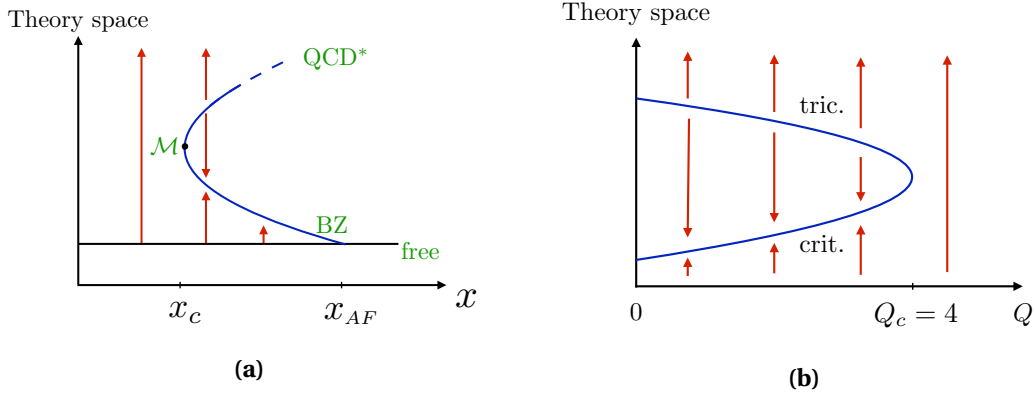


Figure 3.4 – *Left*: schematic view of the space of existing fixed points of 4d gauge theories as a function of $x = N_f/N_c$. The trivial fixed point (free) exists for any x . The line of BZ fixed points branches off from the free theory line at $x = x_{AF}$. At some smaller $x = x_c$ it annihilates with the line of QCD* fixed points. This latter line should exist for x close to x_c but it's not a priori clear where it starts. *Right*: schematic view of the space of fixed points for the 2d Potts model. No theory merges with the free theory, at least in the range $Q > 0$ we are interested in.

disappearance and confining behavior below x_c . In what follows we assume that this scenario is realized. We will comment on other logical possibilities in section 3.4.3 below.

We call \mathcal{M} the common endpoint of the BZ and QCD* branches:

$$\mathcal{M} = \text{BZ}(x_c) = \text{QCD}^*(x_c). \quad (3.4.2)$$

Let us look more carefully at how the annihilation happens. For x slightly larger than x_c there is an RG flow that connects BZ and QCD*. Close to \mathcal{M} this RG flow is very short and consequently can be described within conformal perturbation theory around QCD*. Call \mathcal{O} the operator that induces this flow, and λ the corresponding coupling constant. Since the flow degenerates when we approach \mathcal{M} , \mathcal{O} should become marginal at $x = x_c$:

$$\Delta_{\mathcal{O}} = d \quad (x = x_c). \quad (3.4.3)$$

It is the first robust prediction of this scenario.

Next, let's discuss the beta-function. The request of two fixed points for $x > x_c$ and no fixed points for $x < x_c$ naturally leads to the beta-function of the by now familiar form (3.2.3), where $y \approx C\delta$ for small $\delta = x - x_c$. This can be compared to Eq. (3.3.9) for the Potts model where $\delta = Q - Q_c$. However, the precise value of C is not known for the 4d gauge theory case, only its sign is fixed: $C < 0$, to have a conformal phase for $x > x_c$ (the opposite of that of the Potts model).

At this point much of the discussion of section 3.2.2 carries over. For example for x slightly above x_c the dimension of \mathcal{O} should have characteristic square root behavior (3.2.4). This square root behavior was emphasized recently in [146]. On the other hand, for x slightly below

x_c , we will have walking behavior resulting in the hierarchy (3.2.7).^{19 20}

Let us point out some important differences between the scenario we are describing and the descriptions of walking that have appeared previously in the particle physics context. First, unlike in the first references on WTC, we see that it would be misleading to think of the slow coupling λ as the gauge coupling constant g . The gauge coupling controls the flow next to the free theory. Near \mathcal{M} , the flow is strongly coupled, and λ is one particular linear combination of infinitely many couplings which happens to control the fixed point annihilation. Here we agree with Ref. [117] which did not postulate relation between λ and the gauge coupling. Further insight into the distinction between g and λ can be gained by considering theories with large- N counting, see appendix B.3. As we explain there, in this case \mathcal{O} has to be a double-trace operator, so it cannot even mix with the operator controlling the gauge coupling, $\text{tr}FF$, at the leading order.

On the other hand, our discussion differs from Ref. [117] in that they specialized early on to the large N_c limit, as well as used the holographic analogy. An important role in their discussion is played by an operator of dimensionality $d/2$ present at the fixed point \mathcal{M} in addition to the marginal operator \mathcal{O} . In the old WTC literature, it also often stated that the $\bar{\psi}\psi$ operator has scaling dimension $d/2 = 2$ at the onset of the walking regime (see e.g. [152]). Our discussion on the other hand tried to separate the general phenomenon of walking from its large N limit which may have special features. The operator of dimensionality $d/2$ is one of such features, as we discuss in appendix B.3. We do not find any support for the existence of such an operator in a generic case. In fact in the Potts model in two dimensions no operator of dimension one is present in the spectrum at $Q = 4$ when two fixed points annihilate, see 4.

We would also like to stress that walking is not a finetuned scenario. First, as we argued in section 3.2.2.2, walking does not involve any finetuning price whatsoever as far as the initial conditions of RG flow are concerned. One may be worried about finetuning in theory space, i.e. how close x should be taken to x_c . By analogy with $Q - 4$ for the 2d Potts model, we believe that walking may occur for x deviating from x_c by $O(1)$. In particular, in our opinion there seems to be no reason preventing walking to occur for some integer N_f even if N_c is small.

Finally, we would like to contrast the hierarchy appearing due to walking in massless QCD at $x \lesssim x_c$ with a different sort of hierarchy which would appear in the BZ regime (3.4.1) if we perturbed the massless QCD with a fermion mass term. Suppose we add a very small equal mass for all fermions. The resulting theory would first go close to a BZ fixed point, sit near it while the fermion mass term keeps growing, and finally flow out to a gapped phase. This hierarchy generation is classified as the tuning scenario of section 3.2.1; it is technically natural

¹⁹This scaling in the context of gauge theories is also known as ‘‘Miransky scaling’’ [150].

²⁰We thank Igor Klebanov for pointing out that beta-function of the walking form (3.2.3) was also obtained in [151] for orbifolds of $\mathcal{N} = 4$ Super Yang-Mills (SYM) theory. In their case the parameter $y = -D\lambda$, where λ is ’t Hooft coupling and D is a combination of dynamical characteristics of the theory. If $D < 0$, one can reach the walking regime by dialing λ small. The existence of a dialable coupling λ makes this example somewhat similar to the BKT transition discussed in appendix B.2. It should be contrasted with the theories discussed in this chapter where a symmetry parameter is varied to reach the walking regime.

tuning because the mass term breaks chiral symmetry. We included it here to emphasize that this is not what walking is about.

3.4.1 Walking and the electroweak phenomenology beyond the Standard Model

We would like to make here a few comments concerning connections between walking and electroweak phenomenology. As is well known, WTC was originally hypothesized in the hope of making less severe the problem of flavor changing neutral currents present in technicolor models of electroweak symmetry breaking. It is not our goal here to review this story in detail. For a review in the context of RG flows we refer to [119]. Relevantly for us, WTC models contain a sector which exhibits the walking regime of RG flow in a range of energies above the electroweak scale. This allows, in this range of energies, to classify operators belonging to the “walking” sector according to their (approximate) scaling dimensions. In particular, this sector is assumed to contain an operator with the quantum numbers of the Higgs field (in explicit models it is a fermion bilinear operator $\bar{\psi}\psi$). Various phenomenological constraints then require that this operator has dimension close to one and at the same time does not behave as a free field.

A proposal made in [119] was that we can treat the walking theory as a strongly interacting unitary CFT perturbed by a weakly relevant operator resulting in a slow RG flow, called “conformal technicolor” scenario. Subsequently, Ref. [13] pointed out that unitary CFTs with restrictions on operator dimensions required to make conformal technicolor scenario phenomenologically viable can be constrained from first principles using the conformal bootstrap techniques. The resulting constraints were fully worked out in [153], with rather pessimistic conclusions: the generic scenario was found inconsistent.²¹

There is however a loophole. Conformal technicolor scenario of [119] is a meaningful scenario, but it should not be considered as an equivalent formulation of walking. Indeed, according to our classification in section 3.2.1 it belongs to “mild tuning”. Walking is radically different in that there are no unitary fixed points. For this reason, strictly speaking, conformal bootstrap results derived in [13] and [153] under the assumption of unitarity cannot be used to rigorously bound the approximate scaling dimensions in the walking regime.

One may be wondering how serious this loophole actually is. After all, even in the walking scenario the flow passes near a CFT, which while not being exactly unitary can be described as “almost unitary” since imaginary parts of operator dimensions have to be small for the walking behavior to take place, Eq. (3.2.8). Can bootstrap bounds get significantly relaxed in presence of such small violations of unitarity? There is no immediate answer to this question, and this problem should be considered open. One related example where bounds seem to get relaxed will be discussed in section 3.5.

²¹However, consistency could be saved by making special assumptions about the structure of the flavor sector on top of admitting some tuning.

In retrospect, it's fortunate that the loophole was not noticed at the time of writing [13], since otherwise the conformal bootstrap methods may not have been developed, and those methods since then found many other applications [17].

3.4.2 Light dilaton?

Finally, let us mention that since the early days the presence of a parametrically light "pseudo-dilaton" is believed to be present in WTC models [28]. This is supposed to be a resonance with quantum numbers 0^{++} , and its parametric lightness means that it's much lighter than the other massive technihadrons (e.g. the technirho), the mass ratio going to zero as one approaches x_c from below. This belief is a popular subject of the lattice studies, see e.g. [154]. We therefore find it necessary to comment on this issue.

In our opinion, walking behavior is not by itself a sufficient condition for the presence of the pseudo-dilaton, that is a pseudo-Goldstone boson of spontaneously broken scale invariance, but it requires further assumptions.²² The presence of a Goldstone boson requires *spontaneous* breaking of a symmetry, while walking behavior corresponds to a small, in some sense, but *explicit* breaking.²³ It is the possibility of spontaneous breaking of conformal symmetry which represents an extra assumption. To have this possibility, we need a CFT with a moduli space of vacua, which is a phenomenon logically completely independent of walking.

Consider for example the CFT \mathcal{M} describing the annihilation point of the BZ and QCD* branches. This is certainly a special theory, as evidenced by the fact that it contains a marginal operator \mathcal{O} . If it had a moduli space, there would be room for realizing a light pseudo-dilaton scenario at $x < x_c$. However, does \mathcal{M} have a moduli space of vacua? We do not actually believe that this is the case.

Let us recall what is known about CFTs with a moduli space. In known examples the moduli space is parametrized by giving expectation values to scalar fields. The simplest example is the free massless scalar ϕ in $d > 2$ dimensions, where we can give an arbitrary expectation value to ϕ .²⁴ Passing to the interacting case, all known interacting CFTs with a finite number of degrees of freedom having a moduli space are supersymmetric. One example is the $\mathcal{N} = 1$ supersymmetric QCD which will be discussed in section 3.4.3 below. The key to the existence of the moduli space of supersymmetric theories is the nonrenormalization theorem for the superpotential. For non-SUSY theories we generically expect that flat directions, even if present in the UV Lagrangian, are lifted by quantum effect so that the IR fixed point has no

²²See [155] for the only known to us field-theoretical construction of a naturally light pseudo-dilation, which involves a host of dynamical assumptions very different from the situation at hand.

²³This is especially apparent from our description of walking as a perturbation of a (complex) CFT by an operator, which will be introduced in section 3.6.3. Addition of this operator to the action explicitly breaks the symmetry.

²⁴Notice that this theory in 4d also contains a marginal operator ϕ^4 . But it would of course be a logical fallacy to conclude that any 4d theory with a marginal operator, like \mathcal{M} , should have a moduli space. There are many examples of supersymmetric CFTs which have a conformal manifold (i.e. exactly marginal deformations), but do not have a moduli space of vacua. A very simple example is discussed in [156].

moduli space.

Constructions based on holography often lead to large- N ‘CFTs’ which appear to possess a moduli space of vacua, usually parametrized by a radial location of a brane. Notice however that only in supersymmetric cases (like the $\mathcal{N} = 4$ super Yang Mills) do these constructions correspond to UV complete theories. In non-SUSY cases these ‘CFTs’ are at best effective theories and it’s usually not known if they can be UV completed. Non-supersymmetric small- N CFTs are not expected to have weakly coupled gravitational duals.

A related example of how moduli space can be a large N artefact is as follows. A non-holographic non-SUSY model having a moduli space of vacua in the strict $N = \infty$ limit was discussed in [157]. However, it was shown [158, 159] that this moduli space does not survive at finite N .

To summarize, we don’t see any theoretical evidence for the presence of the light pseudo-dilaton in the walking regime of non-SUSY gauge theories. However, we do find the lattice investigations of gauge theories near the end of the conformal window intriguing, notwithstanding the issue of the light dilaton. It is a hard subject and should be done with care [144].

For completeness let us discuss what happens for the 2d $Q > 4$ Potts model. In this case the spectrum of massive excitations close to the end of ‘conformal window’, i.e. for $Q = 4 + \epsilon$, is known exactly from integrability [160]. It consists solely of kink-like excitations with masses of order of the infrared strong coupling scale. Of course when $\epsilon \rightarrow 0^+$ these excitations become massless, but this happens for all the IR excitations in the model simultaneously, so that the mass-ratios stay finite. We believe that this is what should happen near the end of the conformal window in QCD as well (except for the goldstone bosons which should stay exactly massless of course). We have not seen any evidence to the contrary.²⁵

It should be said that in 2d the general belief is that moduli space of vacua is impossible even for supersymmetric CFTs, due to infrared effects not unlike those which prevent the spontaneous breaking of global continuous symmetry in 2d via the Coleman-Mermin-Wagner theorem.²⁶ This goes towards showing once more that walking and spontaneous breaking of conformal invariance are logically independent phenomena.

²⁵Recent Ref. [161] studied $SU(3)$ gauge theory with $N_f = 8$ massless fermions in the fundamental via lattice Monte Carlo. They assign it close to, but somewhat below, the end of the conformal window and look for signs of light pseudodilaton. In the volumes they study, pseudoscalars π as well as the scalar 0^{++} have mass ≈ 0.5 (in the units in which $m_\rho = 1$). We take it as a sign that their simulations are still far from the infinite-volume limit in which m_π/m_ρ should go to zero. We conservatively predict that as one goes to larger volumes $m_{0^{++}}/m_\rho$ will plateau, and there will be no light pseudodilaton. We thank Anna Hasenfratz for discussions.

²⁶In the literature on 2d SUSY CFTs one uses the term ‘moduli space’ in a different meaning, to denote the conformal manifold, i.e. the space of all exactly marginal deformations.

3.4.3 Other possibilities for the end of conformal window

The above discussion was based on the simplest assumption [117] that the BZ line of fixed points terminates by annihilating with another line called QCD* and then moves to the complex plane. Let us now discuss what are possible other ways for the transition from the BZ regime at x near x_{AF} to the chiral symmetry breaking (χ SB) regime for $x < x_c$.

One could imagine a possibility that the BZ fixed point, which appears by splitting off the free theory, disappears by the inverse of this process, i.e. by merging with another free theory. As we will see below this is likely inconsistent with the χ SB phase for $x < x_c$, but it's instructive to discuss this anyway. We can imagine the RG flow happening in the space of all theories having $G = SU(N_f) \times SU(N_f) \times U(1)$ global symmetry. In this theory space there are special points: free gauge theories. The beta-functions vanish at free theory points, and we may imagine that they are rather generic vector fields in the bulk of the theory space. Under this genericity assumptions, the fixed points can naturally appear or disappear through two processes: split off or merge with a free theory,²⁷ or pair create and annihilate in the bulk of the theory space. (See below for a third process involving global symmetry enhancement.) The genericity argument can be made mathematically precise in the context of bifurcation theory for finite-dimensional families of vector fields [146].

Disappearance via merging is realized in $\mathcal{N} = 1$ supersymmetric QCD (see Fig. 3.5). The extent of the conformal window in this theory is exactly known: $3/2 < x < 3$.²⁸ The BZ-like fixed point disappears at $x = 3/2$ via merging with another free gauge theory, with a different number of colors $N'_c = N_f - N_c$, a manifestation of Seiberg duality [25]. In the SUSY case for x just below $3/2$ there is no chiral symmetry breaking, the theory instead flowing to a free magnetic phase. On the other hand in the non-SUSY case we expect chiral symmetry breaking below x_c . Therefore the non-SUSY BZ fixed point cannot disappear via merging with free theory, and SUSY intuition is not a good guidance for this particular question.²⁹

On the other hand one could ask if the QCD* line could merge with a free theory at some $x_* > x_c$, which may or may not be equal to x_{AF} . If so we could get QCD* as an RG fixed point flowing from that free theory, which would be weakly coupled for x near x_* . This problem is

²⁷Ref. [117] also considered a possibility which they call “running off to infinite coupling”. We prefer to use a terminology which is invariant under reparametrizations of the coupling space. What matters is not whether the coupling is finite or infinite, but whether the point where the topology of the RG flow changes is a truly special point of the coupling space, e.g. if it corresponds to a free theory in terms of some dual variables, as it happens for the $\mathcal{N} = 1$ SQCD discussed below.

²⁸In connection with the discussion in section 3.4.2, we note that the SUSY CFT describing the IR fixed point allows spontaneous breaking of conformal invariance, as it has a moduli space of vacua of complex dimension $2N_f N_c - (N_c^2 - 1)$.

²⁹Ref. [162] studied the conformal window of non-SUSY gauge theories in perturbation theory around x_{AF} and used the criterion $\Delta_{\bar{\psi}\psi} = 1$ (unitarity bound) for the lower end of the conformal window. This was inspired by the SUSY case, where $\bar{\psi}\psi$ becomes free scalar at the lower end as a consequence of merger with free theory. Since as we described in the non-SUSY case there is no merger with free theory, their criterion is inadequate in the non-SUSY case. Moreover, whatever the criterion, we believe perturbation theory is inadequate to describe the lower end of conformal window where anomalous dimensions become $O(1)$. We thank Robert Shrock for an email about his work.

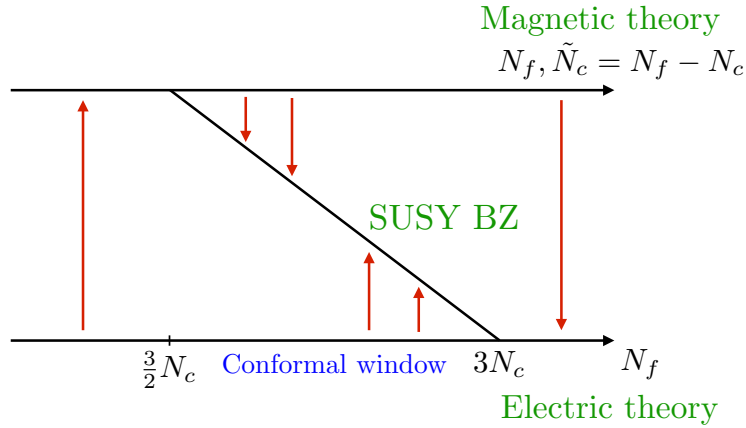


Figure 3.5 – Conformal window for the $\mathcal{N} = 1$ SUSY case. In this case the BZ-like fixed point disappears by merging with another free theory. Compare with Fig. 3.4 in the non-SUSY case.

constrained by the requirements that QCD* should have the same symmetry as BZ, that it should have exactly one relevant singlet scalar operator, and also by ’t Hooft anomaly matching. Ref. [117] tried a few RG flows but they either did not manifestly have the requisite symmetry, or did not yield a fixed point. So this problem is open.

The final possibility that we would like to mention involves global symmetry enhancement. Namely, imagine that the BZ fixed point, when moving around in the theory space as a function of x collides for $x = x'$ with a fixed point BZ' which is interacting but which has a strictly larger global symmetry $G' \supset G$. In such a situation we can have an exchange of stability, i.e. the BZ fixed point is stable for $x > x'$, while BZ' is stable for $x < x'$. This can happen naturally at a point of the BZ' line where some operator which breaks G' to G crosses marginality. A well-known example of this phenomenon is the collision between the cubic and the $O(N)$ fixed points of multifield scalar theories in $4 - \epsilon$ dimensions, which pass through each other interchanging stability at some $N_c = 4 + O(\epsilon)$ ([163] and [164], section 11.3).

Notice that the collision with free theories discussed above can also be viewed as an example of symmetry enhancement, since free theories possess higher spin symmetries. In this case, in perturbation theory the fixed point ‘goes through’, but the fixed point coupling on the other side has a bad sign. E.g. if we tried to formally continue BZ fixed point to $x > x_{AF}$ we would find a theory at negative squared gauge coupling g_*^2 . In a related case of trying to continue the Wilson-Fisher fixed point of $\lambda\phi^4$ to $4 + \epsilon$ dimensions we would find a theory with negative λ_* . The common lore is that these fixed points are not well defined nonperturbatively. Indeed from the path integral point of view it’s hard to believe that they make sense. So in this case we speak of fixed point merger as opposed to intersection.

On the contrary, if BZ collides with BZ', we may indeed expect an intersection, because an interacting BZ' is not expected to be as fragile as free theories, and the line of BZ fixed points

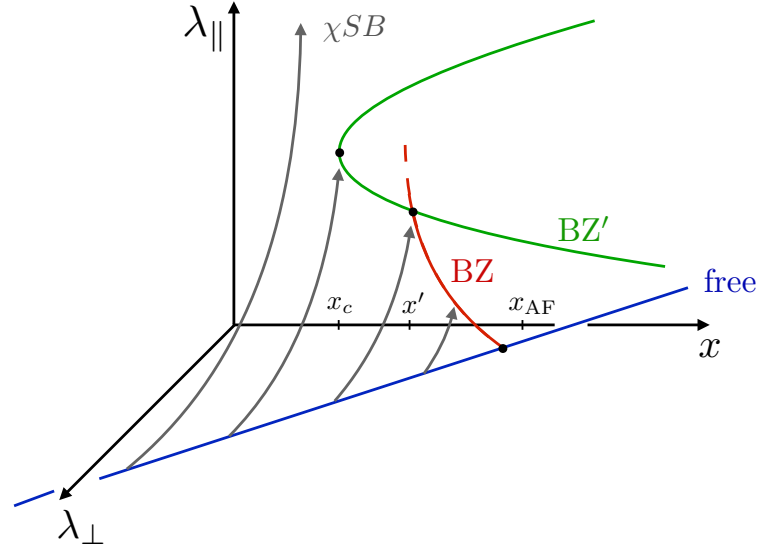


Figure 3.6 – The non-minimal scenario. We call collectively by λ_{\parallel} the couplings which preserved G' symmetry, and by λ_{\perp} the couplings which break G' to G . The line of fixed points BZ' lives at $\lambda_{\perp} = 0$. The RG flow lines lie in planes of constant x .

should make sense on its both sides.³⁰

Fig. 3.6 illustrates the considered non-minimal scenario. In it we see the line of BZ' fixed points, of uncertain origin, which interchanges stability with BZ line at $x = x'$. For $x_c < x < x'$ the flow from free theory leads to BZ' (and thus we have symmetry enhancement in IR to G'). At x_c the line of BZ' fixed points disappears by annihilation with a line of CFTs analogous to QCD* (but with symmetry G'). The BZ line of CFTs with symmetry G continues to exist at $x < x'$, but is unstable (contains a relevant G -singlet scalar). Being unstable, it does not affect the IR properties of RG flows originating in free theory at $x < x'$ and in principle it may continue to exist even for $x < x_c$.

Admittedly this scenario is a bit contrived, which is why we prefer the minimal scenario described in section 3.4. However, it can eventually be probed by Monte Carlo simulations. Notice that in the non-minimal scenario approximate symmetry enhancement to G' should appear even in the walking regime just below x_c . We will see in section 3.5 an example of an approximate symmetry enhancement without a fixed point, which may have a similar origin. It's easy to imagine even more complicated scenarios but we will stop here.

³⁰As a technical comment, we note that the actual fate of the BZ fixed point in this scenario at $x < x'$ depends on the G' quantum numbers of the operator \mathcal{O} which breaks G' to G and induces a flow between BZ and BZ' . If these quantum numbers are such that they allow a nonzero three-point function $f_{\mathcal{O}\mathcal{O}\mathcal{O}} \sim \langle \mathcal{O}\mathcal{O}\mathcal{O} \rangle$ then the beta-function for the perturbing coupling λ_{\perp} will have the schematic form $-\epsilon\lambda_{\perp} + f_{\mathcal{O}\mathcal{O}\mathcal{O}}\lambda_{\perp}^2$ where $\epsilon \sim x - x'$ and a real BZ fixed point will exist on both sides of x' . Suppose on the other hand that \mathcal{O} is odd under some \mathbb{Z}_2 subgroup of G' , so that $f_{\mathcal{O}\mathcal{O}\mathcal{O}}$ vanishes. The couplings λ_{\perp} and $-\lambda_{\perp}$ are now equivalent and the beta-function has the form $-\epsilon\lambda_{\perp} + O(\lambda_{\perp}^3)$. Now fixed point at $x < x'$ lives at negative λ_{\perp}^2 which may e.g. lead to violations of unitarity.

3.4.4 The conformal window in holographic QCD

The question of the conformal window in large N QCD has been studied also in holographic bottom-up models [165–167].³¹ These models consider QCD in the Veneziano limit, $N_f \rightarrow \infty$ with x fixed: they consist of a five dimensional bulk theory with a dilaton and a tachyon, transforming respectively in the singlet and the bifundamental of the flavor group. The boundary duals of these bulk fields are $\text{tr}F^2$ and the fermionic bilinear respectively.

As usual in holographic RG, boundary evolution from the UV to the IR corresponds to bulk evolution from the near boundary region to the center, see for example [168]. The authors of [165–167] make ansatz for the potentials of these fields subject to some constraints: in the UV, close to the boundary, these potentials must behave so that the beta functions for the boundary couplings reproduce the perturbative QCD beta functions. There are further conditions on the deep IR asymptotics of the potential related to having confinement and a linear glueball spectrum in the gapped phase. Once an ansatz for these potentials is selected, one can numerically study the evolution from the UV to the IR.

The authors find that an IR conformal fixed point exists for $x_c \leq x < 11/2$; the precise value of x_c depends on details of the chosen potential but is in general $x_c \sim 4$. The value of x_c is determined to be the point where the dimension of the fermion bilinear becomes $d/2 = 2$; as mentioned earlier, this is a peculiarity of the large N limit, which does not need to hold at small N .

For $x \lesssim x_c$, it's seen that the theory flows to some confining phase, but the dilaton exhibits a walking regime (see for example figure 7 of [165]). While we know that, close to the boundary, the dilaton is dual to the gauge coupling, deeper in the bulk this represents some effective coupling which is some linear combination of the singlet couplings of the theory. This does not imply that the walking coupling is the gauge coupling, and we find no contradiction with our claim of appendix B.3 that at infinite N , the walking coupling should be that of the fermion quadrilinear.

Complex CFTs make their appearance in [165–167] as boundary duals of theories violating the Breitenlohner-Freedman (BF) bound [169]. In AdS_{d+1} , in the case of scalar fields, we have a relation between bulk mass and boundary scaling dimension

$$\Delta(\Delta - d) = m^2, \tag{3.4.4}$$

where we set the radius of AdS to unity. For masses violating the BF bound, i.e. $m^2 \leq -d^2/4$, the above equation admits two complex solutions for Δ . Notice that for $x = x_c$, the fermion bilinear has dimension $d/2$ and it saturates the BF bound. For $x \leq x_c$, it makes sense to consider the two complex solutions for Δ as two complex CFTs. These are well defined saddle points, which are however subleading to the spontaneously symmetry-broken confining phase to which the theory flows in the IR.

³¹The authors consider both finite and zero temperature, but we will focus only on the latter.

3.5. Deconfined criticality: a further example of walking?

Another interesting feature of this model is that it gives us the opportunity to compute the spectrum for $x < x_c$ [166, 167]. The authors find that, for $x < x_c$, the spectrum is always gapped, except for the pions which are the Goldstone bosons of the spontaneously broken chiral symmetry, and as $x \rightarrow x_c^-$ all other masses go to zero, with their ratios being finite. This is in agreement with our claim in section 3.4.2, that walking theories in general do not have a light dilaton in the spectrum. In general, in this setup it's possible to study explicitly the behavior of the masses below the conformal windows, and it's seen that they scale like $\log m \sim -1/\sqrt{x_c - x}$ in the $x \rightarrow x_c^-$ limit, as expected.

3.5 Deconfined criticality: a further example of walking?

Here we will discuss an interesting 3d RG flow which, while not fully understood, seems to exhibit phenomena plausibly explainable by walking. This discussion is largely based on sections V.E.2 and V.E.4 of [17] where further details and references can be found.

This RG flow has been originally brought up in condensed matter literature in relation with the Néel-Valence Bond Solid (VBS) transition and the phenomenon of “deconfined criticality” [32]. Without going into condensed matter details, in field-theoretical language one studies the 3d Abelian Higgs model (also called bosonic QED₃), which is the theory of a 3d $U(1)$ gauge field coupled to N complex scalars ϕ_i with an $SU(N)$ invariant potential $m^2|\phi|^2 + \lambda(|\phi|^2)^2$. For this discussion we focus on $N = 2$ which is the most interesting and best-studied case, although $N > 2$ is also interesting.

The global symmetry of this theory is $SO(3) \times U(1)_T$. The $SO(3) = SU(2)/\mathbb{Z}_2$ part of the global symmetry descends from the $SU(2)$ symmetry of the scalar potential (one has to divide by \mathbb{Z}_2 since the center part of $SU(2)$ corresponds to a gauge transformation). The $U(1)_T$ part of the global symmetry is topological, called $U(1)_T$ to distinguish it from the gauge group. The operators charged under it are $U(1)$ gauge field flux defects, called monopoles.

In the above theory, by varying the UV mass m^2 , one induces a phase transition between a Coulomb and a Higgs phase of the gauge field. This transition is supposed to describe the critical properties of the Néel-VBS transition in certain $(2+1)$ d quantum antiferromagnets. One interesting question is whether this transition is continuous or first-order.

From Monte Carlo studies performed by various groups, the following picture transpires [33, 34]. First, no signs of a conventional first-order transitions are seen: it is either continuous, or perhaps a very weakly first-order (the correlation length being at least several hundred lattice spacings). Second, quite unexpectedly, near the phase transition the system is seen to possess a global symmetry enhancement from $SO(3) \times U(1)$ to $SO(5)$. For example, the Néel order parameter operator transforming as a fundamental of $SO(3)$ turns out to have the same scaling dimension $\Delta_\Phi = 0.625(15)$ as the lowest charge monopole, which suggests that they may be combined into a Φ in the fundamental of $SO(5)$. For other impressive tests of $SO(5)$ enhancement see [33, 34].

Assuming we have both a continuous phase transition and $SO(5)$ symmetry enhancement, one can ask about dimensions of lowest scalar operators S and T transforming as a singlet and a symmetric traceless tensor of $SO(5)$. The T is known to be relevant of dimension ~ 1.5 [34], its various component being interpreted as the charge two monopole and the mass term $m^2|\phi|^2$ which drives the transition. On the other hand S has to be irrelevant, because otherwise the transition would not be reached.

Now, it turns out that this expectation comes into a clash with rigorous bounds computed from conformal bootstrap under the assumption of unitarity and $SO(5)$ invariance [35, 170]. Namely, these bounds imply that the irrelevance of S requires $\Delta_\Phi > 0.76$ [171], in conflict with the above measurement $\Delta_\Phi = 0.625(15)$

The clash would be resolved if we assume that the phase transition is weakly first-order due to a walking behavior of the RG flow. The CFT controlling this flow being non-unitary and moreover complex, rigorous bootstrap bounds do not apply. The observed scaling exponents are then attributed to the approximately scale-invariant part of the RG trajectory. If this interpretation is correct, we are led to conclude that walking RG flow manages to relax the bound on Δ_Φ quite significantly, from 0.76 for unitary theories down to the observed 0.625(15).

It's not our goal here to discuss various pro and contra in favor of this scenario. The hypothesis of a weakly first-order phase transition via walking mechanism was put forward in [33] even before the above bootstrap evidence emerged, as one of the ways to explain some unusual finite-size scaling effects observed in their Monte Carlo simulations, and it was also discussed further in [132]. In 4 we will discuss peculiar form of deviations from scale invariance (drifting scaling dimensions) present in walking RG flows, possibly related to the unusual Monte Carlo effects seen in [33].

Finally, we mention two related condensed matter transitions which seem to exhibit similar physics. First, there is the $N_f = 2$ fermionic QED₃, for which the situation is as murky as for the Néel-VBS: a continuous/weakly first-order dilemma, symmetry enhancement from $SU(2) \times U(1)$ to $SO(4)$, and a clash with bootstrap bounds, see section V.E.4 of [17]. Second, there exists an easy-plane version of the Néel-VBS transition studied via numerical simulations in [172],[173]. In this case the situation is clearer: there is a weakly first-order phase transition due to walking behavior, as well as symmetry enhancement from $SO(3) \times \mathbb{Z}_2$ to $SO(4)$. It would be interesting to understand better these examples.

Notice that in this work we discuss walking flows with rotational invariance. This should be relevant for statistical physics examples of deconfined criticality. One may ask how our picture would be modified for quantum deconfined criticality, where the phase transition is driven by quantum fluctuations in anti-ferromagnets. The difference is that in this case we also expect scale-dependent deviations from rotational invariance, parametrized by 'running of the speed of light'.³² Running of the speed of light does not spoil our picture, but some of our

³²We are grateful to Silviu Pufu for raising this interesting point.

RG computations need to be modified. When we perturb complex CFTs, as in section 3.6.3, we will have to add a marginal coupling to the T_{00} component of the stress tensor into the RG equations. Interplay between this additional coupling and the walking coupling λ will lead to new effects, but we believe our basic picture should be preserved. It would be interesting to work this out in detail.

3.6 Complex CFTs

We have provided the reader with several examples of physical systems which show walking behavior. Both QCD with $x = N_f/N_c \lesssim x_c$ and the Potts model with $Q \gtrsim Q_c$ at the critical temperature have a large separation between the UV and the IR scale and a region of approximate scale invariance. As mentioned in section 3.2.2, RG behavior of walking systems is controlled by complex fixed points with small imaginary parameters. There we introduced complex fixed points to study the beta-function of the form (3.2.3):

$$\beta(\lambda) = -y - \lambda^2, \quad (3.6.1)$$

which for $y > 0$ has fixed points $\mathcal{C}, \bar{\mathcal{C}}$ at complex values of the coupling constant $\lambda = \pm i\sqrt{y}$. At these fixed points the operator controlling the RG flow has anomalous dimension given in (3.2.4), namely

$$\Delta = d - 2i\sqrt{y}, \quad \lambda = i\sqrt{y}, \quad (3.6.2)$$

$$\Delta = d + 2i\sqrt{y}, \quad \lambda = -i\sqrt{y}. \quad (3.6.3)$$

In this section we will proceed to study such complex fixed points in more detail.

We emphasize that each of these operators belongs only to the indicated fixed point but not to the other one. To have this feature it was crucial to consider an RG flow in the space of complex couplings. To appreciate this last point better it is instructive to consider a different system of beta-functions for two real coupling constants:

$$\begin{aligned} \beta_u &= 2\sqrt{y}v, \\ \beta_v &= -2\sqrt{y}u. \end{aligned} \quad (3.6.4)$$

This system of beta-functions may seem exotic, and indeed field theories that produce this kind of behavior are rather involved. In the classification which we will promulgate below they will count as real theories, albeit non-unitary. The motivation to call such theories real is that the coupling constants stay real, and moreover if one works in the basis of operators that correspond to couplings u and v , correlation functions are also manifestly real. We will present some examples below, but for now let us study these equations as an abstract toy model.

In case at hand there is a single fixed point for $u = v = 0$ and there are two close-to-marginal operators at this fixed point with dimensions $d \pm 2i\sqrt{y}$. In spite of the appearance of complex

anomalous dimensions, which clearly indicates non-unitarity, the crucial difference of the fixed point of (3.6.4) from those of (3.6.1) is that both above complex-conjugate operators belong to it, while as mentioned each fixed point of (3.6.1) has a single complex operator.

We will turn this distinction into a more formal statement in the next section, where we give some more details, definitions and examples of complex and real theories.

3.6.1 Real vs complex QFTs

3.6.1.1 RG evolution

Let us start with the discussion of general QFTs and specify to CFTs later.³³ We would like to formalize the distinction between real and complex QFTs. It's best to proceed from examples. Consider e.g. a perturbative Lagrangian theory of multiple real scalar fields. We can complexify coupling constants, considering them living in \mathbb{C}^M where M is the total number of couplings. In this setup we can consider the subspace $\mathcal{R} = \mathbb{R}^M$ of all couplings real. We would like to call theories corresponding to this subspace real. Notice that this subspace is preserved by RG evolution, so this looks like a natural definition.

For theories of real scalars in integer spacetime dimension d , the class of real theories coincides with that of unitary theories. However in general a real QFT does not have to be unitary. To see a simple example, let us couple scalars with vector fields, with all couplings real. The theory is still real, but as is well known it will be unitary only in a restricted class of theories respecting gauge invariance.

A general comment about complexifying RG evolution is in order. We assume that a coupling basis exists, such that beta-functions $\beta_a = dg_a/dt$ are locally analytic functions of complexified couplings with real coefficients: $\beta_a(\{g_b^*\}) = \beta_a^*(\{g_b\})$. This guarantees that the subspace of real couplings \mathcal{R} is RG-preserved. Notice that it would be incorrect to think of the map $g_a \rightarrow g_a^*$ as *simply* an example of a \mathbb{Z}_2 symmetry under which the imaginary parts of all couplings are odd; it's much more than that. Of course we can split each coupling into real and imaginary part $g_a = \sigma_a + i\tau_a$ and view RG evolution as happening in \mathbb{R}^{2M} . If we impose that τ_a are odd under a \mathbb{Z}_2 , this would also explain why \mathcal{R} is preserved, but the above assumption of analyticity with real coefficients is much more constraining. Compare for example the beta-function $\beta(g) = g^2$ which in terms of real and imaginary parts reads

$$\beta_\sigma = \sigma^2 - \tau^2, \quad \beta_\tau = 2\sigma\tau. \quad (3.6.5)$$

On the contrary imposing only \mathbb{Z}_2 would allow quadratic beta-functions of the same functional form but with arbitrary relative coefficients.

³³The reader interested primarily in complex CFTs can jump directly to section 3.6.2.

3.6.1.2 Correlation functions

Definition of real vs complex theories in terms of RG evolution is intuitively clear, but we would like to have a definition that may be applicable to theories which contain fields that are intrinsically complex, as well as theories which do not necessarily admit a Lagrangian description. Such a definition can be given in terms of correlation functions: we will call a theory real if it contains a set of operators \mathcal{O}_i whose correlation functions are real at all distances.

A slightly more nuanced but practically almost equivalent definition is as follows. For simplicity let us focus on theories which have parity invariance and let's talk only about bosonic operators. The theory is called real if there is an involutive map $*$ which acts on local operator labels and puts in correspondence to each local³⁴ operator A_i an operator A_i^* such that the correlation functions of A 's and A^* 's, while in general complex, are complex conjugate of each other:

$$\langle A_1(x_1)A_2(x_2)\dots A_n(x_n) \rangle^* = \langle A_1^*(x_1)A_2^*(x_2)\dots A_n^*(x_n) \rangle. \quad (3.6.6)$$

Hopefully it will not be confusing that we use the same symbol $*$ as a complex conjugation acting on numbers, as well as a map acting on names of operators. Real operators are those whose correlation functions are real, and so according to the above definition we have $A^* = A$ for such operators.³⁵

On the contrary, if the map $*$ with the above properties does not exist, then the theory is classified as complex.

Notice that the above definition makes sense separately of any quantization interpretation. So the operation $*$ does not have to be thought of as a conjugation of operators acting in some Hilbert space. If we know all correlation functions of the theory, we can inspect them and decide if the map $*$: $A \mapsto A^*$ exists.

However if we do have a parity-invariant unitary theory realized in a Hilbert space, then it's easy to see that it would be classified as real according to the above definition with $\mathcal{O}^* = (-1)^{p_{\mathcal{O}}} \mathcal{O}^\dagger$ where $p_{\mathcal{O}}$ is the parity of \mathcal{O} . Let us split $x = (\tau, \mathbf{x})$ and use quantization by planes in the τ direction, so that $\mathcal{O}(\tau, \mathbf{x})^\dagger = \mathcal{O}^\dagger(-\tau, \mathbf{x})$ and so

$$\langle \mathcal{O}_1(x_1)\dots \mathcal{O}_n(x_n) \rangle^* = \langle \mathcal{O}_1^\dagger(-\tau_1, \mathbf{x}_1)\dots \mathcal{O}_n^\dagger(-\tau_n, \mathbf{x}_n) \rangle. \quad (3.6.7)$$

Using parity transformation we can now flip all τ 's and go back to the equation of the form (3.6.6) where the operators in the r.h.s. and l.h.s. are at the same positions.

So, all unitary theories are real but of course unitary theories in Euclidean space satisfy a crucial additional assumption, the reflection positivity, which is the positivity constraint on

³⁴Here as in the rest of the chapter we focus for simplicity on local operators, however the conjugation relation in a real theory should exist also for non-local operators. We thank Silviu Pufu for inquiring.

³⁵For any A the operators $A + A^*$ and $i(A - A^*)$ will be real.

($2n$)-point functions:

$$\langle \mathcal{O}_1^\dagger(-\tau_1, \mathbf{x}_1) \mathcal{O}_2^\dagger(-\tau_2, \mathbf{x}_2) \dots \mathcal{O}_2(\tau_2, \mathbf{x}_2) \mathcal{O}_1(\tau_1, \mathbf{x}_1) \rangle \geq 0. \quad (3.6.8)$$

We refer the reader to e.g. [174] for precise definition of reflection positivity. Reflection positive theories can be analytically continued to Minkowski space in a consistent way.

On the space of complex QFT's it is natural to define the complex conjugation map such that for any operator A_i present in the original theory the complex conjugate theory contains operator A_i^* and correlation functions of the operators in two theories are related by Eq. (3.6.6). Then real theories are the fixed points of the conjugation map.

3.6.1.3 Examples

Let us now give some examples of real yet non-unitary Euclidean theories. One example was already mentioned: theories of multiple scalars and vectors without gauge invariance, coupled with real couplings.

A more subtle example is a real scalar ϕ with potential $V(\phi) = ih\phi + i\lambda\phi^3$. This potential satisfies $V(-\phi) = V(\phi)^*$. This theory will be real according to the correlation function definition, with $\mathcal{O} = i\phi$ being a real operator.³⁶ We will encounter the IR fixed point of this theory in section 3.6.2.1 as a real but non-unitary CFT – the Lee-Yang minimal model $\mathcal{M}_{2,5}$.

As the next example, consider $O(N)$ models analytically continued to non-integer N . Correlation functions stay real, at least in perturbation theory, but these theories are non-unitary [175].

Finally, consider theories of real scalars with real couplings, analytically continued to non-integer Euclidean dimensions d , *à la* Wilson-Fisher. Such theories have been shown to be non-unitary in [79, 176]. It would be nice to clarify to which extent they are nonperturbatively well-defined.

3.6.2 Real vs complex CFTs

We now proceed to discuss real and complex CFTs. Since the structure of CFTs is more constrained we will be able to make our definitions more concrete. Real (complex) CFTs can arise as fixed points of real (complex) RG flows. We will discuss the consequences of reality on the spectrum of a CFT, and provide the reader with some examples.

A CFT is defined by its conformal data: the set of all operator dimensions and all OPE coefficients. Following the discussion of the previous section, if a CFT is real, and an operator \mathcal{O}

³⁶Such theories are sometimes called PT-invariant. Literature on PT-invariant theories is sometimes hard to read because valid results on Euclidean PT-invariant theories are often interspersed with highly suspect claims that such theories may somehow be relevant also for real-time, Lorentzian physics, in spite of being non-unitary.

with complex scaling dimension Δ is part of the theory, then also \mathcal{O}^* , with scaling dimension Δ^* , must be part of the theory. Some operators will have real scaling dimensions, while operators with complex scaling dimensions can exist only in complex conjugate pairs in order for \mathcal{O}^* to exist.³⁷

OPE coefficients must satisfy relations that follow from (3.6.6) applied to three-point functions, in particular OPE coefficients of three real operators must be real.³⁸

If instead we consider a complex CFT, operators with complex scaling dimension can appear without their complex conjugated partner being present in the theory. Similarly OPE coefficients can be complex numbers not subject to any obvious constraints. Central charge of complex CFTs can be a complex number, as we will see in 4. Despite the fact that conformal data is complex, complex CFTs still fulfill other usual properties: conformal symmetry, operator product expansion, and crossing.

3.6.2.1 Examples

We will now review some examples. As we saw above, all unitary CFTs are real. Let us consider examples of real but non-unitary CFTs, in order to highlight the difference between reality and unitarity.

Consider first 2d examples. The simplest example is the Lee-Yang minimal model $\mathcal{M}_{2,5}$ which appears as an IR fixed point of a theory of 2d scalar with purely imaginary cubic coupling [177, 178], see section 3.6.1.3. This CFT has real spectrum, with a single Virasoro primary ϕ of dimension $h = \bar{h} = -1/5$ and real central charge $c = -22/5$. That h and c are negative is a clear sign of non-unitarity. In the usual normalization the OPE coefficient $C_{\phi\phi\phi}$ is purely imaginary. The real field is $\tilde{\phi} = i\phi$, with a real OPE coefficient $C_{\tilde{\phi}\tilde{\phi}\tilde{\phi}}$. This CFT is thus real non-unitary.

The previous example generalizes to all non-unitary minimal models $\mathcal{M}_{p,q}$. Recall that $\mathcal{M}_{m,m+1}$ are unitary while for $|p - q| > 1$ the minimal models $\mathcal{M}_{p,q}$ are non-unitary. We consider integer p, q so that there is a finite Kac table and a finite number of primaries. In spite of being non-unitary, all primary fields in these theories have real scaling dimensions $h_{r,s}$ and the central charge is real. The OPE coefficients in minimal models were investigated by Dotsenko and Fateev [179, 180]. It follows from their work that pairwise products of OPE coefficients $C_{ijk}C_{klm}$, for which they give explicit formulas, are real. This means that either all OPE coefficients are real or purely imaginary, in which case they are made real multiplying all fields by i . So these non-unitary minimal models are real CFTs.

Continuing the list of 2d examples, critical Potts model with Q non-integer and $Q < Q_c$ will

³⁷Notice that when dealing with a real *QFT*, we could always pass from any operator to its real and imaginary part (footnote 35) which are real operators. For real *CFTs* this is not a natural thing to do, because if \mathcal{O} is an operator of complex scaling dimension, its real and imaginary part will not have a well-defined scaling dimension.

³⁸Note that in unitary CFTs OPE coefficients are known to satisfy reality constraints, see [17]. Here we are describing a context when it is natural to impose reality of OPE coefficients even if the CFT is not unitary.

be real but non-unitary. That they are non-unitary can be seen very easily from their central charge and the spectrum, which are exactly known as we will discuss in 4. Also the random cluster measure which is the microscopic origin of these critical point is known not to have reflection positivity [124]. On the other hand the random cluster description is manifestly real, and so it guarantees that the critical point if it exists should be a real CFT.

The same holds for the $O(n)$ model with non-integer n in 2d, which can be given a nonperturbative microscopic definitions as theories of loops, and is known to have a critical point for $n \in [-2, 2]$. Much is known about these CFTs, see e.g. [137]. These are also examples of real non-unitary CFTs.

These examples have purely real conformal data and can be hardly confused with complex theories. In this regard it is useful to bring up a CFT which is still real, but has pairs of complex conjugate operator dimensions. It turns out that Wilson-Fisher fixed point in $d = 4 - \epsilon$ dimensions is a theory of this sort [176].³⁹ The Wilson-Fisher fixed point in $d = 4 - \epsilon$ is a textbook example of a weakly coupled fixed point. It is described by a massless boson perturbed by a quartic interaction term with a real coupling. In $d = 4$ the theory is unitary: all states have positive norm; however, when we move to $d = 4 - \epsilon$ the situation changes. There are some *evanescent operators* which have zero norm in integer dimension, but can have negative norm in fractional dimension: it follows that the theory at the Wilson-Fisher fixed point is non-unitary. This is also reflected in the spectrum of the theory: because of the negative norm states it is possible for some operators to acquire a complex anomalous dimension. This happens for some of these evanescent operators, and complex scaling dimensions always appear in complex conjugate pairs, as expected in a real CFT. The existence of these complex operators was a bit hard to notice, since at first-order in ϵ they appear at very high dimension ($\Delta = 23$) [176].

Another curious physical example of a real theory with pairs of complex operator dimensions is a long-range disorder fixed point studied in [182].

Continuing with higher-dimensional examples, it is worth mentioning that the Lee-Yang CFT described above can be studied for any $2 \leq d < 6$, as a fixed point of the cubic scalar theory with imaginary coupling, and we expect it to be real for all d in this range. Close to the upper critical dimension, in $d = 6 - \epsilon$, the theory can be studied perturbatively. It would be interesting to see if the spectrum of the theory is completely real in $d = 6 - \epsilon$ as it is in $d = 2$, or if operator pair with complex conjugate dimensions occur.

Finally let us discuss examples of complex CFTs. These examples are less frequent in the literature than real non-unitary theories, and there seems to be no general consensus if they are physical and/or well defined. Our first example is $\mathcal{N} = 4$ SYM: since the beta-function vanishes for all values of g^2 , it appears that if we give g^2 an imaginary part, we should obtain a complex CFT.⁴⁰ Notice that this procedure is fundamentally different from considering

³⁹See also [79] for prior work and [181] for a related fermionic example.

⁴⁰In the planar limit of $\mathcal{N} = 4$ SYM, scaling dimensions of operators appear to be analytic functions of the 't

the theory as a function of the complexified couplings $\tau, \bar{\tau} = \frac{\theta}{2\pi} \pm \frac{4\pi i}{g^2}$, with θ the theta-angle. Taking g^2 complex means that we are considering the situation when $\bar{\tau} \neq \tau^*$.⁴¹ More generally, we can consider a supersymmetric CFTs possessing a set of exactly marginal couplings λ_i , and consider it as a function of complexified couplings $\lambda_i \in \mathbb{C}^M$, which gives rise to complex CFTs. Partition functions for such complex deformations were discussed in [185]. On the other hand Ref. [186] considered SCFTs perturbed by complex mass deformations, which in our language corresponds to complex QFTs.⁴²

In studies of RG flows of multi-scalar theories using the ϵ -expansion and $1/N$ -expansion, it's not unusual to encounter RG fixed points at complex couplings, which should be interpretable as complex CFTs living in non-integer dimension d . Many such examples have appeared recently in the work of Simone Giombi, Igor Klebanov and collaborators [187–190], with complex fixed points arising from real fixed points which annihilate and go into the complex plane when varying the number of fields N or the dimension d . While these works view complex operator dimensions as a sign of instability, and refer to complex fixed points as “unstable CFTs”, more optimistically these theories could actually be nonperturbatively well-defined Euclidean CFTs.

A further example are the fishnet theories [191], obtained as deformations of $\mathcal{N} = 4$ SYM at large N and in some special double limit of the coupling and of the twists. These deformations break supersymmetry, and the fishnet theories are non-supersymmetric fixed points with complex anomalous dimensions and no pair of complex conjugate operators [192] — they appear to be complex theories according to our definition.

Our final example is the complex fixed point for the Potts model with $Q > Q_c$, to be studied in detail in 4. It allows for many explicit computations which significantly clarify the concept of complex CFT.

3.6.3 Complex CFTs and walking

We have seen in section 3.2.2 that the walking beta-function has two zeros at complex coupling, and walking behavior of a theory can be understood as the flow passing in between these complex fixed points, when they are close to the real axis. Now we would like to reverse the logic and show how, by starting from a pair of CFTs in the complex plane of the coupling, we can describe the real walking theory. From the practical point of view, this section is perhaps the most important one in this chapter: while the rest of our work was devoted mostly to clarifying misunderstandings (some of the them our own) and laying conceptual foundations, here we will propose a concrete calculational scheme.

Hooft coupling $\lambda, \lambda^2 = g^2 N_c / (16\pi^2)$, in the disk $|\lambda| < 1/4$ (see e.g. [183], Eq. (67)). We thank Carlo Meneghelli and Pedro Vieira for discussions.

⁴¹Note in this respect the limit $\bar{\tau} \rightarrow -i\infty$ with τ fixed considered in [184], although there it was interpreted as taking $g \rightarrow 0$ and theta-angle imaginary and large. We thank Nikita Nekrasov for discussions.

⁴²We thanks Silviu Pufu for discussions.

Let us start with two complex theories, \mathcal{C} and $\bar{\mathcal{C}}$, which are related by complex conjugation, meaning that the spectrum of $\bar{\mathcal{C}}$ is the complex conjugate of the spectrum of \mathcal{C} . A similar condition holds for OPE coefficients. We will formalize the condition that these two theories are close to being real, by requiring that scaling dimension and OPE coefficients have an imaginary part of order $O(\epsilon)$, where $\epsilon \ll 1$. We will assume that this condition should hold at least for low-lying operators.⁴³ Furthermore, we assume that the spectrum of \mathcal{C} contains one almost marginal operator \mathcal{O} of dimension $\Delta_{\mathcal{O}} = d - i\epsilon + O(\epsilon^2)$, which is a singlet under the global symmetry group. We emphasize once again that the operator of the complex conjugate dimension then belongs to $\bar{\mathcal{C}}$, and is not a part of \mathcal{C} .

We will develop a form of conformal perturbation theory (CPT) where we perturb \mathcal{C} by \mathcal{O} . Usually, CPT is used to describe RG trajectories which either flow out from a CFT or flow into it. The difference here is that we will use CPT to describe an RG trajectory which approaches CFT but does not necessarily touch it, as in Fig. 3.2. Apart from this difference of interpretation, formally we proceed as usual in CPT, perturbing the action of \mathcal{C} by adding operator \mathcal{O} with some (in general complex) coupling g :

$$S_{\mathcal{C}} + g \int d^d x \mathcal{O}(x). \quad (3.6.9)$$

For nonzero g , the scale invariance of the theory is in general broken and the coupling g will run. The one loop beta-function is given by the standard result (see e.g. [21])

$$\beta_g = -i\epsilon g + \frac{1}{2} S_d C_{\mathcal{O}\mathcal{O}\mathcal{O}} g^2 + \dots, \quad (3.6.10)$$

with S_d the volume of the d -dimensional unit sphere and $C_{\mathcal{O}\mathcal{O}\mathcal{O}}$ the OPE coefficient extracted from the three-point (3pt) function $\langle \mathcal{O}\mathcal{O}\mathcal{O} \rangle$. In general $C_{\mathcal{O}\mathcal{O}\mathcal{O}}$ is complex, but at the order we will be working here, we can neglect its $O(\epsilon)$ imaginary part and treat it as real.

We see that the above beta-function has two fixed points: the trivial $g = 0$, and the nontrivial at $g = g_{FP} = i \frac{2\epsilon}{S_d C_{\mathcal{O}\mathcal{O}\mathcal{O}}}$, which we denote \mathcal{C}_{FP} . Since there is only one almost marginal singlet operator, and \mathcal{C} and $\bar{\mathcal{C}}$ are close to each other, it appears reasonable to identify \mathcal{C}_{FP} with $\bar{\mathcal{C}}$. One simple check of this identification is to compute the scaling dimension of the operator \mathcal{O} at this fixed point:

$$[\mathcal{O}]_{g=g_{FP}} = d + \beta'_g(g_{FP}) = d + i\epsilon + O(\epsilon^2). \quad (3.6.11)$$

We see that the imaginary part flipped sign as expected.

What about the other operators? Along the flow, a generic operator ϕ acquires an anomalous dimension (see e.g. [21])

$$\gamma_{\phi}(g) = S_d C_{\phi\phi\mathcal{O}} g + O(g^2). \quad (3.6.12)$$

⁴³As we said before, a general real theory could have operators with complex scaling dimension, provided that they appear in complex conjugate pairs. We are assuming here that \mathcal{C} and $\bar{\mathcal{C}}$ are close to a more restricted real theory, where all operator dimensions are real, at least in the low-dimension part of the spectrum.

Its scaling dimension at the fixed point is $\Delta_\phi^{\mathcal{C}} + \gamma_\phi(g_{FP})$. To identify it with the dimension of the same operator at $\bar{\mathcal{C}}$, the imaginary part must flip sign (we call it the Im-flip condition). For operator \mathcal{O} this happened automatically because of the way the coefficient $C_{\mathcal{O}\mathcal{O}\mathcal{O}}$ controlled the calculation, but for a generic operator this requires a non-trivial relation between OPE coefficients and scaling dimensions. At one loop we should have (all quantities refer to CFT \mathcal{C}):

$$\frac{\text{Im}\Delta_\phi}{C_{\phi\phi\mathcal{O}}} = \frac{\text{Im}\Delta_\mathcal{O}}{C_{\mathcal{O}\mathcal{O}\mathcal{O}}}, \quad (3.6.13)$$

up to corrections higher order in ϵ .

Here's an intuitive argument in favor of (3.6.13). Assume for a second that it does not hold for some operator ϕ . Then the dimension of ϕ at the fixed point will be different from Δ_ϕ^* , and hence \mathcal{C}_{FP} cannot coincide with $\bar{\mathcal{C}}$. So assuming such a scenario, we have four nearby complex CFTs: $\mathcal{C}, \bar{\mathcal{C}}, \mathcal{C}_{FP}, \bar{\mathcal{C}}_{FP}$, as opposed to only \mathcal{C} and $\bar{\mathcal{C}}$. This proliferation of CFTs seems rather unlikely. It is more economical to assume that in fact $\mathcal{C}_{FP} = \bar{\mathcal{C}}$, which requires (3.6.13). Hopefully in the future (3.6.13) will be derived from general CFT principles (like OPE and crossing) applied to the pair of complex CFTs, although at the moment we don't have such a proof. In 4, we will give an explicit example where this relation is satisfied by several operators.

Now we would like to recover the real walking theory. Intuitively, it corresponds to the RG trajectory which passes in the middle between the two complex CFTs. We should land on this trajectory by adding half of the coupling that takes us from \mathcal{C} to $\bar{\mathcal{C}}$. Adding the operator \mathcal{O} with a coupling $g = \frac{g_{FP}}{2} - \lambda$, the above beta-function re-expressed in terms of λ takes the form:

$$\beta_\lambda = -\frac{\epsilon^2}{2S_d C_{\mathcal{O}\mathcal{O}\mathcal{O}}} - \frac{S_d C_{\mathcal{O}\mathcal{O}\mathcal{O}}}{2} \lambda^2 + \dots \quad (3.6.14)$$

We see that to the considered order all imaginary terms cancel: the coupling λ , if it starts real, will remain real during the RG evolution. Rescaling λ , we bring the beta-function to the walking beta-function (3.2.3) with $y = \epsilon^2/4$. Since y does not depend on $C_{\mathcal{O}\mathcal{O}\mathcal{O}}$, the generated hierarchy (3.2.7) in this one-loop order is independent of the OPE coefficient.

To further check that the theory described by the flow (3.6.14) is indeed real, we should compute correlation functions of local operators and show that they are real. For 2pt function this will be done in chapter 4, where we will also compute deviations from scale invariance interpreted as "drifting scaling dimensions".

Finally, the following comment on the validity of CPT is in order. To land on the real trajectory, we need to perturb with the coupling $g_{FP}/2$, which is proportional to the imaginary part of the dimension of \mathcal{O} . Consequently, the latter needs to be small in order for the perturbation theory to be under control. Higher order calculations performed in 4 will demonstrate that it is actually the square of the imaginary part that serves as an expansion parameter for real physical quantities, which somewhat improves the convergence properties of CPT.

To summarize, in this section we sketched a technique whereby, once the conformal data of the complex CFTs is known, CPT can be used to make predictions for correlation functions in the walking regime. We limited ourselves to the leading-order CPT for simplicity, but one can go to higher orders provided that the conformal data of the complex CFT is known to $O(\epsilon^2)$ or even exactly. To put the perturbative computation under control (in the walking regime), it was convenient to assume that there is a family of CFTs depending on the continuous parameter ϵ . If instead the complex CFTs are isolated, meaning that there is no such continuous parameter, one can still do an expansion provided that $(\Delta_{\mathcal{O}} - d)^2$ is numerically small.⁴⁴

3.7 Conclusions

To conclude, let us briefly summarize the main results of this chapter. We introduced a new type of conformal field theories that we call complex since they correspond to fixed points of RG flows that exist at complex values of coupling constants. We argued that these theories can be well defined, and that one can work with them in the same way as one does with usual real CFTs. Importantly, these complex fixed points actually control RG flows of some real and unitary *gapped* physical theories. This happens if the parameters of a complex CFT have small imaginary parts and the real RG flow, which we actually are interested in, is forced to pass close to it. As usual, in the proximity of a fixed point the RG flow becomes slow which leads to various interesting phenomenological properties, like a large hierarchy of scales and a large correlation length. The corresponding RG behavior is referred to as walking.

Examples of applications of complex CFTs include certain gauge theories near the end of the conformal window, as well as various condensed matter systems that exhibit weakly first-order phase transitions. Previous approaches to describing these systems, however, centered their discussion around real fixed points that exist only if certain parameters of the theory are altered. We claim that a better-controlled approximation and more physical understanding arises with our method. In this chapter we focused mostly on drawing the general physical picture, and showed how to back it up with elementary computations. Further evidence will be provided in chapter 4 in which we study a very clean and amenable to detailed calculations example of walking RG — the two-dimensional Potts model with number of states Q larger than four. There we construct explicitly the corresponding complex CFT and check that its perturbation indeed describes the model of interest.

We reckon that thinking in terms of complex CFTs will improve our understanding of various models studied in high energy particle physics, as well as of condensed matter systems.

⁴⁴For subtleties related to such an expansion see the recent discussion in section 3.4 in [90].

4 The $Q > 4$ Potts model

4.1 Introduction

In the previous chapter we reviewed walking as a mechanism of generating hierarchies, and pointed out several examples of physical systems which realize it. One example are 4d and 3d gauge theories, where the walking mechanism is realized, conjecturally, below the lower end of the conformal window. Another example is the Q -state Potts model which has a conformal phase at $Q \leq Q_c(d)$, and the walking mechanism governs the physics of a weakly first-order transition just above Q_c . Abundant evidence, especially in $d = 2$ where $Q_c = 4$, allows to firmly establish walking in the Potts model.

Another goal of chapter 3 was to highlight the concept of ‘complex CFTs’, an unusual class of conformal field theories which describe fixed points of RG flow occurring at complex coupling. These complex CFTs control walking RG flow passing near them, in a way similar to how a UV fixed-point CFT controls the beginning of the RG trajectory arising from it via a relevant perturbation.

This chapter will develop further the connection between walking and complex CFTs, by studying in depth the 2d Potts model at $Q > 4$. While CFTs describing the conformal phase of the 2d Potts model at $Q \leq 4$ have been studied intensely [122, 137, 193], as far as we know, our work is the first one discussing the complex CFTs at $Q > 4$.

We start in section 4.2 reviewing 2d Potts model results relevant for our purposes. We discuss the spin and cluster formulations of the model, transition to the height representation, and the Coulomb gas construction for the conformal phase at $Q \leq 4$. We present the partition function of the model on the torus, and obtain from it the spectrum of low-lying operators. We explain the way to obtain some of the OPE coefficients of the theory by imposing crossing and using Virasoro symmetry. We also speculate about possible implementations of the permutation symmetry with non-integer number of elements.

In section 4.3 we analytically continue the conformal Potts theory in Q to real $Q > 4$, which

leads to complex conformal theories. In section 4.4 we reconstruct the real $Q > 4$ theory at the first-order phase transition by means of conformal perturbation theory around the complex CFT. We present several one- and two-loop consistency checks, and in particular compute drifting scaling dimensions – a characteristic feature of two-point functions in theories exhibiting walking RG behavior.

Several technical points are relegated to the appendices. Appendix C.4 reviews some representation theory of the permutation group and discusses a few operators transforming in its higher representations. Appendix C.5 reviews some basic results in the orbifold construction of the $Q = 4$ theory.

4.2 2d Potts model for $Q \leq 4$

In this paper we deal with the 2d Potts model with Q states. An elementary introduction to this model was already given in chapter 3. Here we will repeat definitions for completeness and provide a few further details. Almost everything we say in this section will be well known to the experts on the 2d Potts model and the related loop models. Still, by our own experience it's not always easy to parse the results scattered throughout the literature, so we will provide a self-contained exposition of the needed facts. One place where our point of view differs from the existing literature is concerning Kondev's argument, see footnote 16.

Consider first the lattice formulation, working on a square lattice for definiteness. For integer Q we have a model of spins s_i living on the lattice sites, which can be in Q states labeled $1, \dots, Q$, and which have ferromagnetic nearest-neighbor interaction $-\beta\delta_{s_i, s_j}$, preserving S_Q global symmetry.

This model can be rewritten in terms of probability distribution of random graphs X living on the same lattice (called the Fortuin-Kasteleyn, or cluster representation). The graphs X include all lattice sites and some of the bonds, and the weight of a given graph is given by $\nu^{b(X)} Q^{c(X)}$ where $b(X)$ is the number of bonds and $c(X)$ is the number of connected components (clusters). The two definitions give an identical partition function for integer Q if $\nu = e^\beta - 1$. Notably, the second definition also makes sense for non-integer Q and allows to analytically continue the model in Q . Here we will consider real $Q > 0$.

The model has an order-disorder phase transition located at $\nu = \sqrt{Q}$, which is continuous for $Q \leq Q_c = 4$. The CFT describing this transition is called the critical Potts model.

One can also define the dilute Potts model where certain sites of the lattice are kept vacant. Varying both the fugacity of the vacancies and the temperature, the dilute model has a tricritical point for $Q \leq 4$. (It also has a critical point which is the same as for the original Potts model.) The CFTs describing the tricritical and critical Potts model are different for $Q < 4$ and coincide for $Q = 4$.

For integer $Q = 2, 3, 4$ the CFTs describing the tricritical and critical Potts model are unitary

and exactly solvable (for $Q = 2, 3$ these are unitary minimal models, while for $Q = 4$ it's an orbifold of compactified free boson, see appendix C.5). For non-integer $0 < Q < 4$ as well as $Q = 1$ these CFTs are real (in the sense that all the observables are real, see section 3.6) but non-unitary. As we will see below, the spectrum of local operators of the tricritical and critical Potts models is exactly known for all $0 < Q \leq 4$. However, not all the OPE coefficients among these operators are exactly known for Q different from 2,3,4. So these CFTs have not been exactly solved.¹

4.2.1 Lattice transfer matrix and local operators

The cluster definition of the Potts model for non-integer Q being nonlocal, it may seem puzzling how a local CFT may describe its phase transition. This section will clarify the physical meaning of CFT operators in the cluster definition. This discussion is a bit technical, and the reader interested merely in the applications of the Potts model to the subject of complex CFTs, rather than in the physics of the Potts model itself, can skip to Eq. (4.2.18) where we begin to present the results for the torus partition function.

Recall that in the familiar integer Q case, when we can describe the Potts model in terms of spins, local lattice operators are obtained by fixing the values of a certain number of spin variables at nearby points. A general lattice operator will have the form

$$\delta(s(x_1) = a_1) \cdots \delta(s(x_n) = a_n) \tag{4.2.1}$$

where $s(x_1), \dots, s(x_n)$ are spin variables at nearby lattice points and a_1, \dots, a_n are fixed values. These operators can be further grouped into irreducible representations (irreps) of S_Q symmetry (see e.g. [196]).

In this case, the correspondence between lattice operators and local CFT operators is as follows. At the critical point we have local CFT operators with well-defined scaling dimension and spin, transforming in an irrep of S_Q . Each lattice operator can be expanded into CFT operators. Going in the opposite direction, for each local CFT operator we can find a local lattice operator so that their correlation functions agree at distances large compared to the lattice spacing.

Another way to make contact between the lattice and the CFT is to consider the model on the cylinder $S^1 \times \mathbb{R}$, i.e. with one dimension compactified on a circle of length L , and the other thought of as (Euclidean) time. States propagating along the cylinder have energies $(2\pi/L)\Delta_i$, where Δ_i are scaling dimensions of the CFT operators (up to a constant shift $-c/12$ due to the conformal anomaly). These energies can be measured on the lattice by constructing the transfer matrix and measuring its eigenvalues (see below).

Going next to the cluster description applicable also for non-integer Q , the simplest nontrivial

¹See [194] and [195] for recent progress on the $Q = 1$ case (percolation) using a numerical conformal bootstrap approach.

observable is the probability that two distant points x and y are in the same cluster. This probability is the cluster analogue of the spin-spin correlation function. One can also consider more complicated events, e.g. probability that two groups of n nearby points x_1, \dots, x_n and y_1, \dots, y_n belong pairwise to n different clusters. Such probabilities are cluster analogues of two-point (2pt) functions of operators made of several spins for integer Q (see e.g. [197]). So, roughly, a local operator creates a localized disturbance in the cluster distribution. One type of disturbance is to emit a certain number of clusters. For integer Q , these operators correspond in the spin description to operators transforming nontrivially under S_Q . On the other hand, disturbances which don't emit clusters correspond to operators which are singlets under S_Q .

In local spin models, in particular in the Potts model for integer Q , it is standard to extract scaling dimensions of local operators by analyzing eigenvalues of the transfer matrix T_{spin} on a cylinder (i.e. on a lattice with periodic boundary conditions in one direction). Analogously, dimensions of scaling operators for non-integer Q can be extracted from a transfer matrix T_{cluster} in the cluster representation.² This T_{cluster} differs from T_{spin} in a few aspects, in particular they act on rather different spaces of states. The familiar T_{spin} acts in the space of spin states in a given time slice τ . On the other hand, T_{cluster} acts in a vector space spanned by *connectivity states*, which refer to two time slices, the initial 0 and the final τ , and are defined as follows. Suppose we already built the partition function on the cylinder from time 0 up to τ and we want to add another layer to the lattice $\tau \rightarrow \tau + 1$. To do this we only need to know how the $2L$ lattice sites $\{1, 2, \dots, L\}$ at time 0 and $\{1', 2', \dots, L'\}$ at time τ are connected among each other by clusters. A connectivity state is a partition P of these $2L$ sites into groups connected by clusters. For example the situation in Fig. 4.1 corresponds to $P = \{\{2\}, \{1, 1', 3\}, \{2', 3'\}\}$. The transfer matrix T_{cluster} maps state P_τ to a linear combination of states $P_{\tau+1}$, and can be constructed using two basic operations: join and detach. The join operation J_{xy} joins two clusters to which x, y belong, while the detach operation D_x detaches point x from its cluster (this process has weight Q if x was already by itself).

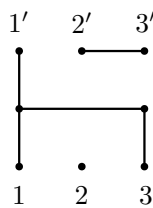


Figure 4.1 – This graph corresponds to the connectivity state described by a partition $P = \{\{2\}, \{1, 1', 3\}, \{2', 3'\}\}$.

An important characteristic of a state P is the number of bridges b , defined as clusters which connect time 0 and time τ ($b = 1$ in Fig. 4.1). Clearly, the number of bridges can either remain constant or decrease under the action of T_{cluster} , giving this transfer matrix an upper-block-

²This formalism goes back to [198]. Our discussion is based on [199–201]. We are grateful to Jesper Jacobsen for explanations.

triangular structure [200]. We are interested in the eigenvalues of T_{cluster} , which correspond, in the large L limit, to the dimensions of local operators. To each eigenvalue λ we can associate the maximal number of bridges present in the eigenvector, b_λ . To compute the eigenvalues, we can first diagonalize the blocks T_b of the transfer matrix which leave the number of bridges constant and equal to b . The full transfer matrix will then have the same eigenvalues, the part of the eigenvectors with $b' < b$ uniquely reconstructable from the part with b bridges using the block-triangular structure.³

In this language, the eigenvalues with $b_\lambda = 0$ correspond to the ‘singlet’ sector of the theory. For integer Q , these eigenvalues correspond to states which are singlets under S_Q . From the leading eigenvalue we extract the ground state energy (the central charge), from the subleading ones the dimensions of operators ε and ε' which will appear below, etc. On the other hand, the eigenvalues with $b_\lambda > 0$ correspond to operators ‘transforming nontrivially under the symmetry’ (borrowing classification from integer Q). For example, the spin operator will correspond to the first eigenvalue in the sector with $b_\lambda = 1$.

Let us discuss briefly how the transfer matrix is used to compute the Potts partition function on a torus, i.e. with periodic boundary conditions in both directions. At integer Q , the partition function is given by

$$Z = \text{Tr} (T_{\text{spin}})^N, \quad (4.2.2)$$

where N is the time-direction extent of the torus. In terms of transfer matrix eigenvalues λ this can be written as

$$Z = \sum_{\lambda} M_{\lambda} \lambda^N, \quad (4.2.3)$$

where M_{λ} are integer eigenvalue multiplicities. At integer Q we have S_Q symmetry, and M_{λ} ’s are dimensions of (possibly reducible) representations of S_Q .

The analogue of (4.2.2) for non-integer Q looks more complicated:

$$Z = \text{Tr} [G(T_{\text{cluster}})^N], \quad (4.2.4)$$

where G is a gluing operator which makes the torus out of the cylinder and takes into account that clusters can be reconnected nontrivially during this operation. Thus we can still write (4.2.3), but now M_{λ} ’s are products of eigenvalue multiplicities times matrix elements of the gluing operator. In particular, M_{λ} will not in general be an integer nor even positive. The coefficients M_{λ} can be evaluated combinatorially [203] and are polynomials in Q . We will have more to say about them below when we will discuss the partition function in the continuum limit using the Coulomb gas method.

Notice that by construction Eq. (4.2.4) should agree with Eq. (4.2.2) for integer Q , although

³Here we are assuming that eigenvalues are non-degenerate among different blocks T_b . Otherwise the full transfer matrix may not be diagonalizable, rather reducible to a Jordan normal form. This more complicated situation corresponds in the continuum limit to logarithmic CFTs. It is realized in the limit $Q \rightarrow 1$ describing percolation [202].

this is not manifest because the cluster transfer matrix is not obviously related to the spin transfer matrix. In fact for large integer Q , Eq. (4.2.4) provides a more efficient way to evaluate the partition function of the Potts model than Eq. (4.2.2), because the Hilbert space dimension is much smaller.

Finally, we note that while the above discussion focused on the Potts model, it can be adapted to the diluted Potts model by allowing for vacancies. In particular, it is possible to study operator dimensions of the tricritical Potts model by means of a cluster transfer matrix [136].

4.2.2 Symmetry

What is the symmetry of the Potts model? For integer Q , it's S_Q , while for non-integer Q it should be some sort of analytic continuation of S_Q . Here as in chapter 3 we will take an intuitive approach to symmetry for non-integer Q – as something which exists and which will be clarified in future work. For example, we will try to expand partition function multiplicities into dimensions of representations of S_Q analytically continued to non-integer Q , although clearly there is no such thing as a vector space of non-integer dimension. Another consequence of the symmetry is that Q doesn't renormalize, even if non-integer. So Q is viewed as a fixed parameter characterizing the theory, not as a coupling constant. This will be important when we study RG flows in perturbed Potts models. Readers bewildered by non-integer Q may adopt the point of view that only integer Q is 'physical', while the intermediate Q is just a trick to do the analytic continuation. We don't endorse such a restricted point of view, but it can be a helpful crutch.

4.2.3 Height representation

The cluster representation was applicable to the Potts model in any number of dimensions. Here we will describe the loop and the height representations, which are specific for 2d. These representations are the key to the torus partition function calculation explained in the next section.

The loop representation is obtained by drawing loops surrounding clusters on the 'medial lattice' whose sites are midpoints of the bonds on the original lattice. Each loop is given weight \sqrt{Q} , and at the critical temperature the partition functions of the Potts model and of the loop model coincide (see e.g. [137], Eq. (4.5)), if one works on a finite lattice with free boundary conditions as in Fig. 4.2.

One then further passes from the loop model to a height model (also called solid-on-solid model). This is accomplished by splitting the loop weight into two terms corresponding to two possible loop orientations. Each loop orientation gets a complex weight $e^{\pm 4iu}$ obtained by multiplying factors $e^{\pm iu}$ for each left/right term (the total number of turns counted with

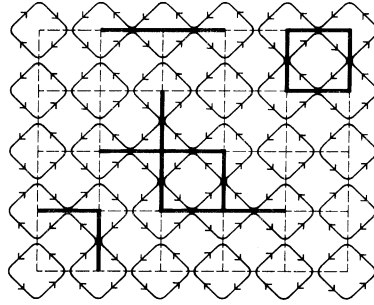


Figure 4.2 – Passing from a cluster configuration to an oriented loop configuration (figure from [137]).

sign being 4), and u is chosen so that

$$\sqrt{Q} = 2 \cos(4u), \quad (4.2.5)$$

summing over the two orientations. One then defines the height function ϕ starting from zero boundary condition and changing it by $\pm\phi_0$, where $\phi_0 = \pi/2$ by convention, when crossing any loop, so that larger height is always on the left of the arrow. The resulting height model, for $Q \leq 4$, is known to renormalize at long distances to the gaussian fixed point

$$\frac{g}{4\pi} \int d^2x (\nabla\phi)^2, \quad (4.2.6)$$

where the coupling g is related to Q by

$$Q = 2 + 2 \cos \frac{\pi g}{2}, \quad (4.2.7)$$

the branch $2 < g \leq 4$ chosen for the considered critical Potts model. This nontrivial result (see [193] for a review, as well as [137], Eq. (2.19)) is the foundation on which the rest of the construction is built.

For the tricritical Potts model the height representation is harder to build and we will not discuss it [204]. Once the dust settles, it turns out that the tricritical Potts model also renormalizes to the gaussian fixed point, the only difference being that one has to choose another solution branch of (4.2.7), namely $4 \leq g < 6$.

In summary, we have

$$g(Q) = 4 + \frac{2}{\pi} \cos^{-1} \left(\frac{Q-2}{2} \right). \quad (4.2.8)$$

with \cos^{-1} in the interval $[-\pi, 0]$ on the critical and $[0, \pi]$ on the tricritical branches at $Q \leq 4$, see Fig. 4.3.

It might be surprising that the oriented loop model with complex weights led to the gaussian model (4.2.6) with real weights. One explanation is that we can map the oriented loop model

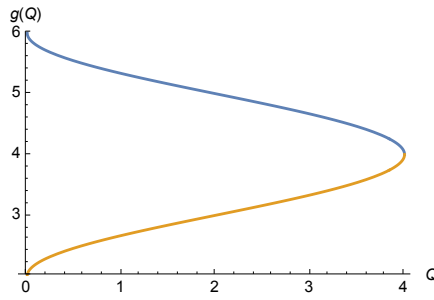


Figure 4.3 – Coupling constant as a function of $Q \leq 4$ for the critical (lower branch, orange) and tricritical (upper branch, blue) Potts model.

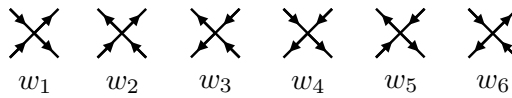


Figure 4.4 – Vertices of the 6-vertex model.

on the F -model, which is a 6-vertex model with positive weights. The mapping consists in putting vertices on the medial lattice, with two arrows pointing inwards and two pointing outwards. The F -model vertices are shown in Fig. 4.4, with weights

$$w_1 = w_2 = w_3 = w_4 = 1, \quad w_5 = w_6 = e^{2iu} + e^{-2iu}. \quad (4.2.9)$$

These assignments are in accord with the fact that vertices 1 to 4 can be uniquely decomposed into two loop strands (and $1 = e^{iu} e^{-iu}$), while for vertices 5 and 6 there are two possible decompositions, see Fig. 4.5. The height function for the F -model is the same as for the oriented loop model, and in the continuum limit the F -model renormalizes onto the free scalar boson (4.2.6).

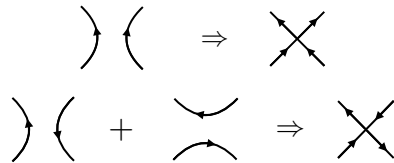


Figure 4.5 – Passing from the oriented loop model to the F -model.

In the above discussion we were a bit cavalier about the boundaries. Suppose we are working on a simply connected domain like a rectangle. Along the boundary, we have to use boundary vertices shown in Fig. 4.6, and decide which weight to assign to them. In the F -model, it is natural to give weight 1 to the boundary vertices, which is called free boundary conditions for the 6-vertex model, and corresponds to using the Dirichlet boundary conditions for the corresponding height field. With this assignment, the F -model renormalizes onto the free scalar boson (4.2.6) with the Dirichlet boundary conditions.

On the other hand, to reproduce correctly the weight of the oriented loops, boundary vertices

in the Potts model should be given weights $e^{\pm iu}$.⁴ The product of these weights equals

$$e^{iu(C_+ - C_-)} \tag{4.2.10}$$

where C_{\pm} are parts of the perimeter occupied by left/right going loops. To illustrate the importance of this factor, consider the partition function. The F -model partition function will reduce in the continuum limit to the partition function of the free scalar boson (4.2.6) with Dirichlet boundary conditions. The Potts model partition function will be much more nontrivial, since we have to include factor (4.2.10) into the path integral.



Figure 4.6 – Boundary vertices, assigned weight 1 in the F -model, and weights $e^{\pm iu}$ in the Potts model.

4.2.4 Long cylinder partition function and the Coulomb gas

In the next section we will consider the torus partition function, where we won't have to deal with the above complications due to the boundary terms, but there will be other complications due to loops going around the torus. Here we would like to discuss partition function on the cylinder of circumference L and length T . Were we to keep the rule that each oriented loop gets a weight obtained by multiplying $e^{\pm iu}$ for every left/right turn, we would get weight 1 instead of $e^{\pm 4iu}$ to loops circling around the cylinder, so that the unoriented loops get weight 2 instead of \sqrt{Q} . This discrepancy should be corrected as follows. Let us impose for definiteness the zero boundary condition on ϕ at the time 0 boundary of the cylinder. Then, on the lattice, at time T , ϕ will take a constant value given by $n(\pi/2)$ where n is the number of oriented loops circling around the cylinder (counted with opposite sign for two opposite orientations). Changing the weight of such loops from 1 to $e^{\pm 4iu}$ can thus be accomplished multiplying the partition function with an extra factor

$$e^{ie_0\phi(T)}, \tag{4.2.11}$$

where $e_0 = 4u/(\pi/2)$, which gives

$$e_0 = 2 - g/2. \tag{4.2.12}$$

This is usually described as ‘placing charges $\pm e_0$ at two opposite ends of the cylinder’. The whole construction is known as ‘Coulomb gas’.⁵

To evaluate the Potts model partition function on the cylinder, we thus have to combine three ingredients: the F -model in the bulk which renormalizes to the free scalar boson, and the

⁴We thank Hubert Saleur for explaining this point to us.

⁵The resulting formalism is similar to the Dotsenko-Fateev Coulomb gas construction [179], although the logic is different: here the extra charges are forced on us by the physics, while in [179] one adds extra charges at infinity by hand and studies the structure of the resulting theory.

factors (4.2.10) and (4.2.11). For a finite aspect ratio T/L this is a nontrivial task which was accomplished in [205, 206].⁶ However the computation can be performed rather easily in the long cylinder limit $T \gg L$, which is enough to extract the central charge and operator dimensions. In this limit the two boundaries of the cylinder don't talk to each other and so the factor (4.2.10) just gives some overall rescaling of the partition function. In addition we expect that the typical value of $\phi(T)$ will be large, and so we can treat the boundary condition $\phi(T)$ as a continuous variable rather than quantized. So we are led to evaluating the path integral

$$\int [D\phi] e^{-S+i e_0 \phi(T)} \quad (4.2.13)$$

with boundary conditions $\phi(0) = 0$, $\phi(T) = h = \text{const.}$ and S as in (4.2.6). We split ϕ into the classical component ϕ_{cl} and the fluctuation $\delta\phi$ satisfying the Dirichlet boundary conditions. We first integrate over $\delta\phi$, and then over h , the latter integral being

$$\int dh e^{-S_{\text{cl}}(h)+i e_0 h}, \quad S_{\text{cl}}(h) = \frac{g}{4\pi} (h/T)^2 LT. \quad (4.2.14)$$

This gives an extra factor $e^{-(\pi e_0^2/g)(T/L)}$ in the partition function, which is interpreted as the reduction of the central charge c from the free scalar boson value $c = 1$ to

$$c_{\text{Potts}} = 1 - \frac{6e_0^2}{g} \quad (4.2.15a)$$

$$= 1 - 6 \frac{(2-g/2)^2}{g} = 13 - 6 \left(\frac{g}{4} + \frac{4}{g} \right). \quad (4.2.15b)$$

Recall that the partition function should scale as $Z \sim e^{(\pi c/6)(T/L)}$ for $T \gg L$.

Let us proceed to discuss the operator spectrum. One interesting class of operators are the electric vertex operators $\mathcal{V}_e = e^{ie\phi}$. The set of allowed electric charges can be determined by the following argument. In the oriented loop model description, if we change orientation of a loop, the height inside will change by $2\phi_0 = \pi$. On the other hand in terms of clusters the loop orientation has no observable meaning. This means that any vertex operator playing a role in the Potts model should be invariant under such a change, i.e. $e \in 2\mathbb{Z}$.⁷

Scaling dimensions of these vertex operators can be predicted by a path integral argument based on (4.2.13). Namely, we insert an extra factor $e^{ie\phi(T)}$ and compute the partition function on a long cylinder. The change in the free energy compared to $e = 0$ gives the scaling

⁶On the contrary the partition function of the F -model on the cylinder is trivial to evaluate: one computes the gaussian path integral as a function of the height difference $\phi(T)$, and sums over $\phi(T) = n(\pi/2)$ [205]. Notice that it is legitimate to use the gaussian action (4.2.6) to compare relative weights of sectors not only for $\phi(T) \gg 1$ but also for $\phi(T) = O(1)$.

⁷Another argument which gives the same prediction is as follows. In the large volume limit, the distribution of ϕ at any point x will become periodic with period $2\phi_0$ because of succession of many loops surrounding x which can take any orientation. Correlation functions of vertex operators which are not invariant under $\phi \rightarrow \phi + 2\phi_0$ will thus vanish in the infinite volume limit.

Parameter	Meaning	Relation
u	parameter of the oriented loop model	$\sqrt{Q} = 2 \cos(4u)$
g	coupling of the gaussian height model (critical $2 < g \leq 4$, tricritical $4 \leq g < 6$)	$Q = 2 + 2 \cos \frac{\pi g}{2}$
e_0	Coulomb gas charge	$e_0 = 2 - g/2$
c_{Potts}	CFT central charge	Eq. (4.2.15)
t	parameter in Eq. (4.2.31) for Kac-degenerate dimensions	$t = \max(g/4, 4/g) \geq 1$
m	index of the minimal model \mathcal{M}_m with the same central charge	$t = (m + 1)/m$

Table 4.1 – Main relations between parameters characterizing the Q -state Potts model. See section 4.2.3 for u, g , section 4.2.4 for e_0, c_{Potts} , and section 4.2.5 for t, m .

dimension:

$$\Delta(\mathcal{V}_e) = \frac{1}{2g} ((e_0 + e)^2 - e_0^2). \quad (4.2.16)$$

While Eqs. (4.2.15a) and (4.2.16) are standard for free scalar boson CFTs with background charge (see e.g. [207], section 9), we chose for completeness to include their direct derivation starting from (4.2.13) in the above review. It's also very important to emphasize that only some aspects of the Potts model can be understood from the Coulomb gas descriptions.

Main relations between parameters characterizing the Q -state Potts model are summarized in Table 4.1.

4.2.5 Torus partition function

The full partition function Z_Q of the Q -state Potts model on the torus was found in the classic paper [137]. Let us describe the result and how it was obtained. The basic building block is the partition function of the free boson (4.2.6) with frustrated boundary conditions around the two cycles of the torus:

$$Z_{m,m'}(g) = \int_{\delta_1 \phi = 2\pi m, \delta_2 \phi = 2\pi m'} [D\phi] e^{-S}. \quad (4.2.17)$$

Summing these over frustration multiples of f , one defines the partition function of the compactified boson with compactification radius f :

$$Z_c[g, f] = f \sum_{m, m' \in f\mathbb{Z}} Z_{m,m'}(g). \quad (4.2.18)$$

This quantity has expansion in terms of the usual torus modulus $q = e^{2\pi i\tau}$ and \bar{q} :

$$Z_c[g, f] = \frac{1}{\eta(q)\eta(\bar{q})} \sum_{\substack{e \in \mathbb{Z} \\ m \in \mathbb{Z} \\ f}} q^{x_{em}} \bar{q}^{\bar{x}_{em}}, \quad (4.2.19)$$

where $\eta(q) = q^{\frac{1}{24}} \mathcal{P}(q)$ is the Dedekind eta function, $\mathcal{P}(q) = \prod_{N=1}^{\infty} (1 - q^N)$. The weights x_{em} , \bar{x}_{em} are labeled by electric and magnetic charges e and m :

$$x_{em}, \bar{x}_{em} = \frac{1}{4} (e/\sqrt{g} \pm m\sqrt{g})^2, \quad (4.2.20)$$

so that the scaling dimension and spin of the corresponding operators are given by:

$$x_{em} + \bar{x}_{em} = \frac{e^2}{2g} + \frac{g}{2} m^2, \quad x_{em} - \bar{x}_{em} = em. \quad (4.2.21)$$

We also need a modification of the compactified partition function (4.2.18) given by the following equation:

$$\hat{Z}[g, e_0] = \sum_{M', M \in \mathbb{Z}} Z_{M'/2, M/2}(g) \cos(\pi e_0 M' \wedge M), \quad (4.2.22)$$

where $a \wedge b = \gcd(a, b)$ is the greatest common divisor, with $a \wedge 0 = a$ by convention, introduced for the following reason. As for the cylinder case above, the F -model (which renormalizes to the free scalar boson) does not correctly reproduce the weights of noncontractible loop. The factor $\cos(\pi e_0 M' \wedge M)$ corrects for this mismatch, analogously to inserting the charges $\pm e_0$ at the ends of the cylinder in section 4.2.4.

The so defined $\hat{Z}[g, e_0]$ can be expanded in series in q and \bar{q} [137]:

$$\hat{Z}[g, e_0] = \frac{1}{\eta(q)\eta(\bar{q})} \left[\sum_{P \in \mathbb{Z}} (q\bar{q})^{x_{e_0+2P,0}} + \sum_{\substack{M, N=1 \\ N \text{ divides } M}}^{\infty} \Lambda(M, N) \sum_{\substack{P \in \mathbb{Z} \\ P \wedge N=1}} q^{x_{2P/N, M/2}} \bar{q}^{\bar{x}_{2P/N, M/2}} \right]. \quad (4.2.23)$$

Coefficients $\Lambda(M, N)$ are given by Eq. (3.24) of [137]. In general they depend on the factorization of M and N into prime integers. Below we will only need the following two partial cases for $M = 1$ or $M > 1$ prime:

$$\Lambda(M, 1) = 2 \left(\frac{\cos(\pi e_0 M) - \cos(\pi e_0)}{M} + \cos \pi e_0 \right), \quad (4.2.24)$$

$$\Lambda(M, M) = 2 \left(\frac{\cos(\pi e_0 M) - \cos(\pi e_0)}{M} \right) \quad (M \neq 1). \quad (4.2.25)$$

$\Lambda(M, N)$ are polynomials in Q with rational coefficients, which implies that multiplicities $M_{h, \bar{h}}$ will also be polynomial in Q .

In terms of the defined objects, the torus partition function of the Potts model takes the form:⁸

$$\mathbf{Z}_Q = \hat{Z}[g, e_0] + \frac{1}{2}(Q-1)(Z_c[g, 1] - Z_c[g, 1/2]). \quad (4.2.26)$$

Basically, $\hat{Z}[g, e_0]$ provides most of the answer, while the second term corrects a mismatch between the Potts model and the loop model for clusters having the cross topology, see [137] for details. We recall that g is related to Q by (4.2.7), choosing $2 < g \leq 4$ ($4 \leq g < 6$) for the critical (tricritical) case, and e_0 is given by (4.2.12).

As mentioned, the $Q = 2, 3$ critical and tricritical Potts theories are unitary minimal models, while $Q = 4$ can be described as an orbifold theory, as we review briefly in appendix C.5. In all these cases partition function can be computed independently and the result agrees with (4.2.26) [137].

4.2.6 Spectrum of primaries for $Q \leq 4$

We will now use the torus partition function to discuss the spectrum of primaries of the critical and tricritical Potts model. Recall that the torus partition function of any CFT can be written as

$$Z = (q\bar{q})^{-\frac{c}{24}} \text{Tr} q^{L_0} \bar{q}^{\bar{L}_0}, \quad (4.2.27)$$

with Hamiltonian $H = L_0 + \bar{L}_0 - c/12$ and momentum $P = L_0 - \bar{L}_0$. Expanding Z in q, \bar{q} one can read off the spectrum of all states present in the theory and their multiplicities:

$$Z = (q\bar{q})^{-\frac{c}{24}} \sum_{h, \bar{h} \in \text{all}} M_{h\bar{h}} q^h \bar{q}^{\bar{h}}. \quad (4.2.28)$$

Furthermore, the partition function is also expandable into Virasoro characters χ_h of primaries:

$$Z(q, \bar{q}) = (q\bar{q})^{-\frac{c}{24}} \sum_{h, \bar{h} \in \text{primaries}} N_{h\bar{h}} \chi_h(q) \chi_{\bar{h}}(\bar{q}), \quad (4.2.29)$$

the sum being over the weights h, \bar{h} of the primaries, with $N_{h, \bar{h}}$ their multiplicities. On the other hand the sum in (4.2.28) is over both primaries and descendants, so that sum contains many more terms, and with different multiplicities.

Below we will encounter two types of Virasoro characters. First, for generic h (non-degenerate primary), the character is given by⁹

$$\chi_h(q) = q^h / \mathcal{P}(q). \quad (4.2.30)$$

Second, there will be cases when h is a Kac degenerate representation $h = h_{r,s}$. For the central

⁸Notice that one should not confuse electric and magnetic charges e, m of the states in this expression with the Coulomb gas charge of operator \mathcal{V}_e in (4.2.16). In particular the constraint $e \in 2\mathbb{Z}$, does not apply to e .

⁹We don't include the factor $q^{-c/24}$ into the character.

charge as in (4.2.15) these are given by (see [207], Eq. (7.31))

$$h_{r,s} = \frac{t}{4}(r^2 - 1) + \frac{1}{4t}(s^2 - 1) + \frac{1 - rs}{2}, \quad t = \max(g/4, 4/g), \quad (4.2.31)$$

with r, s positive integers.^{10,11} The representation is then degenerate at level rs , the null descendant having weight $h_{r,-s}$. Below we will mostly focus on the generic Q case, when this descendant itself is not degenerate.¹² In this case the character of the $h_{r,s}$ primary is given by:

$$\chi_{h_{r,s}}(q) = (q^{h_{r,s}} - q^{h_{r,-s}}) / \mathcal{P}(q). \quad (4.2.33)$$

A particular case of (4.2.33) occurs for the unit operator: $h = 0 = h_{1,1}$, when

$$\chi_0(q) = (1 - q) / \mathcal{P}(q). \quad (4.2.34)$$

From (4.2.26), (4.2.19), (4.2.23) we get expansion (4.2.28) of the Potts model partition function. Notice, however, that ‘multiplicities’ $M_{h,\bar{h}}$ are given by polynomials in Q , so they are in general not integer, unless Q is integer.¹³ This may sound puzzling since normally multiplicities are integer. To understand the origin of this subtlety, let us go back to the lattice partition function from section 4.2.1. In the continuum limit, the factors $q^h \bar{q}^{\bar{h}}$ in (4.2.28) originate from the eigenvalue factors λ^N on the lattice in (4.2.3), while the multiplicities $M_{h,\bar{h}}$ are the weights M_λ in (4.2.3). As discussed in section 4.2.1 these weights for non-integer Q do not just count the eigenvalues, but involve a matrix element of a gluing operator, which explains why they don’t have to be integers nor even positive.¹⁴

Up to the prefactor $1/[\eta(q)\eta(\bar{q})]$, the obtained expansion of \mathbf{Z}_Q consists of terms of the form $q^{x_{em}} \bar{q}^{\bar{x}_{em}}$, times multiplicities. We will introduce notation $\mathcal{O}_{e,m}$ for the state corresponding to such a term. Its conformal weight is given by

$$h = x_{em} + \frac{c-1}{24}, \quad \bar{h} = \bar{x}_{em} + \frac{c-1}{24}. \quad (4.2.35)$$

First, we have states with $e = e_0 + 2P$ ($P \in \mathbb{Z}$) and $m = 0$, coming from the first term in $\hat{Z}[g, e_0]$.

¹⁰The two branches $t = g/4$ and $t = 4/g$ are related by interchanging r and s . By choosing always $t > 1$ we ensure that for $t = (m+1)/m$ the weight numbering will agree with the form

$$h_{r,s} = \frac{[(m+1)r - ms]^2 - 1}{4m(m+1)}, \quad (4.2.32)$$

conventional in the unitary minimal models. This will be convenient in section 4.4.

¹¹Notice that not all operators appearing in partition function are Kac-degenerate. In some literature on the Potts model weights of non-degenerate operators are also represented as $h_{r,s}$ with r, s non-integer. This will not be done in our work, where notation $h_{r,s}$ will be used only with r, s integer.

¹²On the other hand, in minimal models $\mathcal{M}_{p,p'}$ we have $h_{r,-s} = h_{p'+r, p-s}$ and so it may be degenerate. The character then takes a more complicated form than (4.2.33).

¹³These multiplicities have also been studied in [208].

¹⁴Note that negativity of some weights is not a direct consequence of the model being non-unitary. For example, while the Lee-Yang model is non-unitary, its torus partition function decomposes into characters with positive integer weights.

Notice that $\mathcal{O}_{e_0+2P,0} = \mathcal{V}_{2P}$, the vertex operator of the same dimension introduced in the Coulomb gas description. This identification is not accidental, the Coulomb gas scaling dimension (4.2.16) and the term $\propto (q\bar{q})^{x_{e_0+2P,0}}$ in \mathbf{Z}_Q having essentially the same path-integral origin.

Second, we have states with e and m both rational numbers, coming from $Z_c[g, f]$ and from the second term in $\hat{Z}[g, e_0]$. We should identify $\mathcal{O}_{e,m} \equiv \mathcal{O}_{-e,-m}$ since they have the same conformal weights. These states do not have an obvious Coulomb gas interpretation.

In this notation, \mathbf{Z}_Q takes the form of the sum of nondegenerate characters (4.2.30) of states $\mathcal{O}_{e,m}$. Does this mean they are all primaries? Not so fast. We have to watch out that some $\mathcal{O}_{e,m}$ are Kac-degenerate. More work is then needed to reorganize the decomposition in terms of Virasoro characters, during which process some states may drop out from the list of primaries. We also need to check for more banal *spectrum coincidences*, which may lead to total cancellation of multiplicities. To study these degeneracies we write h, \bar{h} as $r_1 g^{-1} + r_2 g + r_3$ with r_i rational:

$$\begin{aligned} \mathcal{V}_{2P} \equiv \mathcal{O}_{e_0+2P,0}: \quad h = \bar{h} = P(P+2)g^{-1} - P/2, \\ \mathcal{O}_{e,m}: \quad h, \bar{h} = \left(\frac{e^2}{4} - 1\right)g^{-1} + \left(\frac{m^2}{4} - \frac{1}{16}\right)g + \frac{1}{2} \pm em/2. \end{aligned} \quad (4.2.36)$$

Apart from $\mathcal{O}_{e,m} \equiv \mathcal{O}_{-e,-m}$ mentioned above, there is only one spectrum coincidence which holds for any Q : it is between \mathcal{V}_{-2} and the operators $\mathcal{O}_{0,\pm 1/2}$. The total multiplicity comes out $-(Q-1) + 2 \cos \pi e_0 + 1 = 0$, so these states do not actually exist.¹⁵

The first Kac degeneracy occurs for the operator \mathcal{V}_0 . It has dimension 0 and is identified with the unit operator; clearly it is Kac-degenerate. The full unit operator character is (see Eq. (4.2.34))

$$\chi_0(q)\chi_0(\bar{q}) = (1-q)(1-\bar{q})/[\mathcal{P}(q)\mathcal{P}(\bar{q})]. \quad (4.2.37)$$

We have to see how this character emerges from combining various nondegenerate characters. Expanding the numerator, the first term $1/[\mathcal{P}(q)\mathcal{P}(\bar{q})]$ is precisely the contribution of \mathcal{V}_0 . One missing term, $q\bar{q}/[\mathcal{P}(q)\mathcal{P}(\bar{q})]$, comes from \mathcal{V}_{-4} , of scaling dimension 2, which as a consequence does not exist as a primary operator.¹⁶

The other missing term in the unit operator character is the cross term $(-q - \bar{q})/[\mathcal{P}(q)\mathcal{P}(\bar{q})]$. This comes from the operators $\mathcal{O}_{e,m}$ with $e = \pm 2$, $m = \pm 1/2$ which have spin 1 and dimension

¹⁵We exclude as contrived the possibility that a state exists but does not contribute to the partition function for any Q .

¹⁶In fact, even more is true. Were we to expand the partition function in powers of q, \bar{q} (including the Dedekind factors), we would see that the theory does not contain *any* scalar of dimension 2, primary or descendant. This is in contradiction with the discussion of Kondev [209], who argued that operator $\mathcal{V}_{-4} = e^{-i4h}$ must be ‘exactly marginal’, and used this to determine the relation between Q and g , instead of borrowing the F -model result (4.2.7). While the calculation behind Kondev’s argument is correct, physical interpretation should be changed because as we showed the operator he calls ‘exactly marginal’ does not even exist. A different interpretation is explained in appendix A of [4].

1 for any g . These operators appear in the second term in (4.2.23) ($M = N = P = 1$) as well as in $Z_c[g, 1/2]$. Their total coefficient is $2 \cos(\pi e_0) - (Q - 1) = -1$ as needed. The conclusion is that we reproduce correctly the character of the unit operator, while operators \mathcal{V}_{-4} and $\mathcal{O}_{\pm 2, \pm 1/2}$ drop out from the spectrum of primaries.

We will now carry out similar analysis for a few more prominent low-lying primary operators. We will see more examples of Kac-degenerate states, and degenerate characters arising as sums of non-degenerate ones. We will not, however, attempt to rewrite the full partition function in terms of Virasoro characters.

Singlets

The operators \mathcal{V}_{2P} occur in the first term of $\hat{Z}[g, e_0]$ with multiplicity 1 for any Q , and therefore we will refer to them as ‘singlets’. As discussed above the case $P = 0$ corresponds to the unit operator, and $P = -1, -2$ do not exist. The lightest non-unit operators are for $P = 1, 2$, which we call the energy operator ε and the subleading energy operator ε' . On the tricritical branch both ε and ε' are relevant, while on the critical branch only ε is relevant. When the two branches meet we have $\Delta_{\varepsilon'} = 2$.

Comparing (4.2.36) with (4.2.31), we see that all \mathcal{V}_{2P} , $P \geq 0$, are Kac-degenerate. In fact $h = h_{1, P+1}$ on the tricritical or $h = h_{P+1, 1}$ on the critical branch. One can show that just like for the unit operator the terms in \mathbf{Z}_Q recombine nicely to give the degenerate characters $\chi_{h_{r,s}}(q)\chi_{h_{r,s}}(\bar{q})$. The scalar term $\propto q^{h_{r,s}}\bar{q}^{h_{r,s}}$ comes from $\mathcal{V}_{2P'}$ with $P' = -P - 2$, whose multiplicity is also 1. The spin-1 terms $-q^{h_{r,s}}\bar{q}^{h_{r,s}} - q^{h_{r,-s}}\bar{q}^{h_{r,s}}$ come from $\mathcal{O}_{e,m}$ with $e = \pm 2(P+1)$ and $\pm m = 1/2$, with precisely the right coefficient. The ability to rewrite the partition function in this form means that the operators $\mathcal{V}_{2P'}$ and $\mathcal{O}_{\pm 2(P+1), \pm 1/2}$ do not appear in the spectrum of primaries.¹⁷

As mentioned the operators $\mathcal{V}_{2P} \equiv \mathcal{O}_{e_0+2P, 0}$ should be identified with electric vertex operators $e^{ie\phi}$ with $e = 2P$ whose dimension was computed using Coulomb gas method in (4.2.16). The above discussion establishes that for $P \geq 0$ these vertex operators are primaries.

As far as $\mathcal{V}_{2P'}$ with negative charge $P' \leq -1$, the above discussion is summarized as follows. For $P' = -1$ this operator simply does not exist since multiplicity is exactly zero. For $P' \leq -3$ a scalar operator of such dimension exists, but is interpreted as not a primary but as a descendant of the positive charge primary \mathcal{V}_{2P} , $P = -P' - 2$, at level $(P+1, P+1)$. The latter reasoning formally applies also for $P' = -2$, but since the unit operator has no descendants at the level $(1, 1)$, this means that \mathcal{V}_{-4} does not exist. This may be a surprise from the point of view of the Coulomb gas construction, but that’s what the torus partition function tells us.¹⁸

¹⁷One might contemplate the possibility that primaries of such dimension actually secretly exist, but their contribution to the torus partition function, as well as to the annulus partition function [206], is exactly zero for all Q . Perhaps these may be null descendants of Kac-degenerate primaries, not necessarily identically vanishing in non-unitary theories. We discard such a possibility as unduly contrived.

¹⁸Additional evidence for the absence of these operators can be obtained from the cylinder partition function [206], Eq. (2). Organizing it in characters, one sees that negative electric charge operators are absent from the list

Vectors

We will call ‘vectors’ operators of multiplicity $Q - 1$, the dimension of the lowest nontrivial representation of S_Q . The lowest such operators are $\mathcal{O}_{e,0}$ with $e = \pm 1, \pm 3$, which come from $Z_c[g, 1]$. These are the spin and the subleading spin operators σ and σ' . For generic Q these operators are non-degenerate primaries.

Higher representations

An interesting light operator is $\mathcal{O}_{0,1}$, from the $P = 0, M = 2, N = 1$ term in the second sum of $\hat{Z}[g, e_0]$. Using (4.2.25), its multiplicity is

$$\cos \pi e_0 + \cos 2\pi e_0 = \frac{Q(Q-3)}{2}. \quad (4.2.38)$$

This matches the dimension of an S_Q representation given by the Young tableau with two rows with $Q - 2$ and 2 boxes in them, which for integer Q exists only for $Q \geq 4$. Notice that this multiplicity becomes negative for $Q < 3$. Again, for generic Q this operator is a non-degenerate primary.

See appendix C.4 for operators corresponding to even larger Young tableaux. For any Young tableau Y , the corresponding representation exists for all sufficiently large Q and has dimension $D_Y(Q)$ which is a polynomial in Q . One can take this polynomial and analytically continue it to $Q \leq 4$. In all cases that we checked, multiplicities of operators predicted by (4.2.26) are decomposable into sums of $D_Y(Q)$ with coefficients which are positive Q -independent integers (appendix C.4).¹⁹ It is not fully obvious why this should be the case. Of course for integer Q we have true S_Q symmetry and so the decomposition of multiplicities in dimensions of irreps of S_Q should be possible for each individual Q . The nontrivial part is that such a decomposition extends to non-integer Q with Q -independent coefficients.

In the above discussion we focused on generic Q . For $Q = 2, 3, 4$ the discussion needs to be modified. First of all the theory has a local spin description, so all multiplicities must be positive integers. In addition, for $Q = 2, 3$, the theories are minimal models and contain a finite number of primary fields. (On the contrary, for generic Q we have infinitely many primaries.) Various terms in the partition function must then recombine, to either cancel or form characters of degenerate primaries in the minimal models, which are more complicated than (4.2.33). Similar complicated cancellations have to happen for an infinite set of Q 's which give a rational central charge $c = c_m = 1 - 6/[(m+1)m]$ corresponding to the unitary minimal models, even though the spectrum of the Potts model will have only partial overlap with the corresponding minimal model unless $Q = 2, 3$ (see section 4.4).

A very simple example of such a cancellations happens for the operator with multiplicity

of primaries.

¹⁹Ref. [137] contains a tangential remark to the contrary for the analogous case of the $O(n)$ model, which appears to be an error. In any case, this minor discrepancy does not affect any of their other conclusions. We thank Hubert Saleur for a discussion.

(4.2.38). For $Q = 3$ this operator simply disappears. For $Q = 2$, its multiplicity is negative. However, for $Q = 2$ this operator is degenerate with the vector operator $\mathcal{O}_{\pm 3,0}$ along the critical branch and with $\mathcal{O}_{\pm 5,0}$ for the tricritical branch. The total multiplicity is zero: this operator does not exist for $Q = 2$.

The spectrum of several light scalar operators and their multiplicities are summarized on Fig. 4.7.

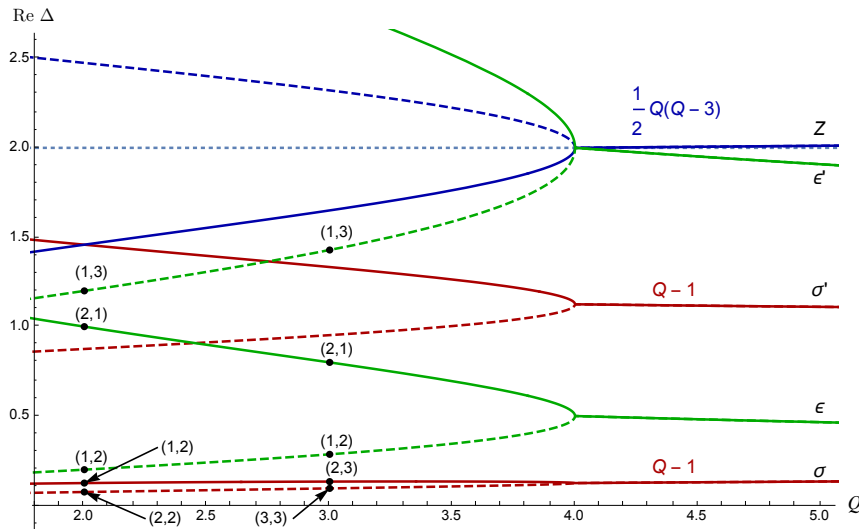


Figure 4.7 – Dimensions of light scalar operators as functions of Q . The $Q \leq 4$ region corresponds to the critical (solid) and tricritical (dashed) Potts models. Singlet operators are in green, other multiplicities are marked. $\Delta = 2$ is the marginality line. The (r, s) positions in the Kac table are shown for ε , ε' , as well as for σ which is degenerate for $Q = 2, 3$. Notice that ε and ε' remain Kac-degenerate with the same integer (r, s) also for non-integer Q , while this is not true for the other shown operators. For $Q > 4$ we show the real parts of the analytically continued dimensions, see section 4.3.

4.3 Analytic continuation to $Q > 4$

The 2d Potts model at criticality is normally discussed only for $Q \leq 4$. For $Q > 4$, the phase transition is first-order, and one does not expect to find any fixed points. As far as real fixed points are concerned this expectation is correct.²⁰ However, instead there exists a pair of complex fixed points. In the previous section we saw that critical and tricritical Potts models become identical at $Q = 4$. Following the discussion in section 3.6 it is convenient to visualize these fixed points as CFTs moving in the theory space as the parameter Q is varied, see Fig. 4.8.

²⁰In [210], some S_Q invariant CFTs with $4 < Q \lesssim 5.56$ were predicted to exist using the massless scattering theory method. Their theories are real and presumably can be realized as continuous phase transitions in the antiferromagnetic Potts model. There is no relation to the theories considered here. We thank Gesualdo Delfino for discussions.

The fixed points have the same symmetries and annihilate at $Q = 4$. Chapter 3 reviewed the abundant evidence from prior work [30, 31, 127, 131] that in the vicinity of this point, the beta-function controlling the RG flow is of the form (3.2.3) with $y \sim Q - 4$, suggesting the existence of two fixed points at couplings $\lambda \sim \pm i\sqrt{Q-4}$.

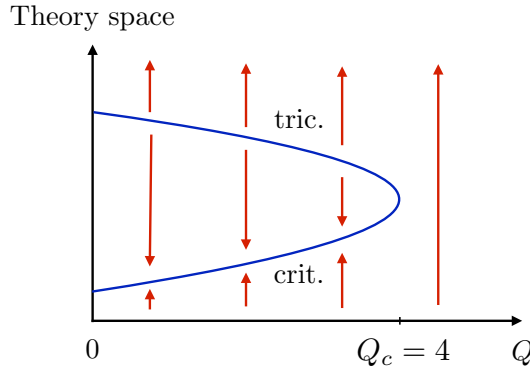


Figure 4.8 – Annihilation of critical and tricritical fixed points.

In section 3.6 we discussed some examples of perturbative complex theories defined by Lagrangians with complex coupling constants. The Potts model is a strongly coupled theory and consequently we don't expect to find any perturbative description. The $Q > 4$ complex Potts CFTs can in principle be constructed with the help of lattice models reviewed in section 4.2.1, either the spin or the cluster one, if one complexifies coupling constants in these models and tunes them to the critical values. To find these fixed points on the lattice, one will need to tune two complex couplings, which can be taken e.g. the temperature and the vacancy fugacity in the diluted Potts model (see footnote 25 below).

Here we will pursue an alternative method to explore the $Q > 4$ CFTs — by means of analytic continuation from $Q \leq 4$. In the previous section we discussed operator dimensions and their multiplicities in the torus partition function, which for $Q \leq 4$ are explicit analytic functions of Q . It is reasonable to assume that observables in the complex CFTs at $Q > 4$ will agree with the analytic continuation of the corresponding observable form $Q \leq 4$. In this paper we will only consider analytic continuation in the neighborhood of the real Q axis. We will perform a set of consistency checks that complex CFTs at real $Q > 4$ defined by means of such analytic continuation indeed describe the complex fixed points of the Potts model. In the future it would be interesting to explore analytically continued CFTs far away from the real Q axis, and to understand their physical meaning if any.

Analytic continuation is easiest for the central charge and the scaling dimensions, since these can be expressed as rational functions of g , Eqs. (4.2.15), (4.2.36). We will keep these expressions, but we will analytically continue $g(Q)$, given by Eq. (4.2.8), from $Q \leq 4$ to $Q > 4$.

For $Q \rightarrow 4^-$ we have $g(Q) \approx 4 \pm (2/\pi)\sqrt{4-Q}$. For $Q > 4$, $g(Q)$ develops a branch cut singularity,

$g(Q) \approx 4 \pm i(2/\pi)\sqrt{Q-4}$. The exact expression is

$$g(Q) = 4 \pm i \frac{2}{\pi} \log \frac{Q-2 + \sqrt{Q(Q-4)}}{2} \quad (Q > 4). \quad (4.3.1)$$

Notice that the real part of g remains constant. We will call \mathcal{C} the complex CFT corresponding to the $+$ branch, while the other branch is $\bar{\mathcal{C}}$.

Equivalently, we perform analytic continuation from the tricritical branch going around the branch point $Q = 4$ from below in the complex Q plane, so that $\sqrt{4-Q}$ for $Q < 4$ goes to $i\sqrt{Q-4}$ for $Q > 4$, where both square roots are positive. The choice between analytic continuation from the tricritical and critical branch is arbitrary²¹ — continuing from the critical branch with the same contour, or from the tricritical branch in the opposite direction, would get $\bar{\mathcal{C}}$ instead of \mathcal{C} . That is, the real parts of all scaling dimensions would be the same, and the imaginary parts would change signs. This is why there are two CFTs for $Q > 4$, one being the complex conjugate of the other. Finally, if one goes around the $Q = 4$ point in the complex plane and comes back to real $Q < 4$ the tricritical theory becomes the critical one and vice versa.

The real parts of analytically continued dimensions of a few low-dimension operators can be read off from the right side of Fig. 4.7. Analogously to the dimensions, the central charge (4.2.15) of the Potts CFT develops an imaginary part for $Q > 4$, the central charges of $\bar{\mathcal{C}}$ and \mathcal{C} being complex conjugate.

We see that the $Q > 4$ Potts CFTs contain operators with complex scaling dimensions, and the corresponding conjugate operators are not present in the same theory. In terminology of section 3.6, this means that these CFTs are complex, as opposed to real. Moreover there are two complex theories with opposite imaginary parts of all observables, and the size of these imaginary parts is controlled by the parameter $\sqrt{Q-4}$. In such a situation, the real RG flow squeezed between the two complex CFTs exhibits the walking behavior, as explained in chapter 3.

Turning next to the multiplicities of primary operators $M_{h,\bar{h}}$ (see section 4.2.6), they are polynomials in Q and their analytic continuation is straightforward. In particular, they stay real for any real Q . As mentioned, it appears that $M_{h,\bar{h}}$ can be represented as a sum of dimensions of irreducible representations of S_Q analytically continued in Q , with Q -independent positive integer coefficients. In particular, when we specialize to integer $Q \geq 5$, we expect complex Potts CFTs to have a true S_Q symmetry. For example, there should exist a pair of S_5 -symmetric complex CFTs of central charge

$$c = 13 - 6 \left(\frac{g(5)}{4} + \frac{4}{g(5)} \right) \approx 1.138 \pm 0.021 i. \quad (4.3.2)$$

²¹It is somewhat more convenient to continue from the tricritical branch, as it contains the relevant operator $\varepsilon' = \phi_{1,3}$, crucial for our computations below, which drives the RG flow from the tricritical to the critical branch. On the critical branch we have $\varepsilon' = \phi_{3,1}$ which is irrelevant.

To summarize, we started with the analytic expression for the torus partition function of the critical Potts model with real $Q < 4$ and analytically continued operator dimensions and multiplicities to $Q > 4$. This is equivalent to the analytic continuation of the partition function itself. In particular all the partition function properties for $Q < 4$, like modular invariance, continue to hold for $Q > 4$. The information extracted from the partition function is consistent with our conjecture about the existence of complex fixed points at $Q > 4$. Further checks involving OPE coefficients will be given below.

4.4 Walking RG flow in $Q > 4$ Potts models

We will now use the knowledge of the complex CFTs \mathcal{C} and $\bar{\mathcal{C}}$ to study the walking RG flow in the Potts model for $Q \gtrsim 4$. Basic framework of how to do this was presented in section 3.6. The real flow trajectory passes halfway between the two complex CFTs. The part of the trajectory close to the CFTs exhibits approximately scale-invariant behavior, and can be accessed using a form of conformal perturbation theory (CPT). Here we will demonstrate this framework by concrete computations.

CPT computations require operator dimensions in our complex CFTs, known from the partition function. We will also need OPE coefficients as well as some integrals of the 4pt functions (see [21] for a review of first-order and [88, 90, 211] for second-order CPT). In practice we will only need to know those up to some fixed order in $Q - 4$ since, as we will see momentarily, the imaginary part of the coupling constant in the walking region will itself be proportional to $Q - 4$. We would like to stress, however, that conceptually our procedure is quite different from expanding around the $Q = 4$ fixed point. One may imagine that conformal data at the complex fixed point is known exactly, and we are expanding only in the coupling constant of perturbation around this fixed point. In this sense our expansion is a usual CPT, albeit as we will see with a complex coupling. Instead expansion in $Q - 4$ around the $Q = 4$ Potts model is on a less obvious footing since $Q - 4$ itself isn't a coupling constant, but merely a parameter. In particular, models with different Q have different symmetries and expansion around $Q = 4$ requires deforming the symmetry, a feature that we would like to avoid.

Although the Potts models at general Q are not exactly solved apart from their spectrum, some additional conformal data needed for CPT can be determined for arbitrary Q for the following reason. Comparing (4.2.31) and (4.2.36), some of the light fields present in the Potts model belong to degenerate conformal families for any Q , and consequently their correlation functions satisfy certain differential equations [12]. In principle, this fixes the correlators up to a few constants that can be determined by requiring proper crossing symmetry properties, although in practice this procedure is still rather complicated.

There is, however, another helpful trick. For a discrete infinite set of Q 's between 2 and 4 (called the Beraha numbers) the Potts model central charge agrees with that of the diagonal

minimal models $\mathcal{M}_m \equiv \mathcal{M}(m+1, m)$, $c_m = 1 - 6/[m(m+1)]$.²² We have (see Fig. 4.9)

$$\text{Tricritical:} \quad Q = 2 + 2 \cos \frac{2\pi}{m}, \quad m = \frac{2\pi}{\arccos\left(\frac{Q}{2} - 1\right)}, \quad (4.4.1)$$

$$\text{Critical:} \quad Q = 2 + 2 \cos \frac{2\pi}{m+1}, \quad m = \frac{2\pi}{\arccos\left(\frac{Q}{2} - 1\right)} - 1. \quad (4.4.2)$$

What is the significance of this agreement? As is well known, the tricritical and critical $Q = 2$ Potts (i.e. Ising) are actually identical to $m = 4$ and $m = 3$, but for other Q 's for which m is an integer, there is no exact coincidence. E.g. the $Q = 3$ Potts models are nondiagonal minimal models – they contain only a subset of Kac-table operators, and with nontrivial multiplicities, as well as primaries with spin.

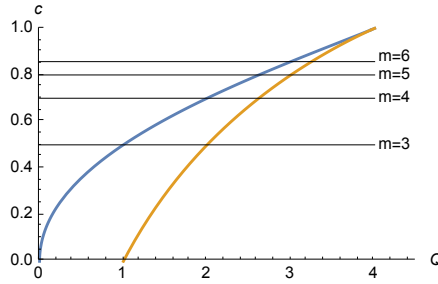


Figure 4.9 – Central charge of the critical (yellow) and tricritical (blue) Potts model as a function of Q . The central charge of several unitary minimal models is indicated by horizontal lines.

Still, there are some operators, singlets under S_Q , which occur in all minimal models and in all Potts models. It is easy to argue, in some cases, that their correlators should agree in both models. The reason is that both these correlators satisfy the same differential equations. The recipe is the following: one should first obtain the holomorphic and antiholomorphic differential equations, which correlators in both the minimal model and in the Potts model satisfy. From these equations, it's possible to see which Virasoro primary operators, with or without spin, can be exchanged. Then, one needs to check which of these operators are part of the critical Potts model, *i.e.* they appear in the torus partition function. Finally, one obtains the OPE coefficients of these allowed exchanged operators by imposing crossing symmetry of the four point function.²³ It follows that, if there is no room for the exchange of spinning primaries, then the unique crossing symmetric solution is the diagonal minimal model results computed in [179, 212] (see also [89] and [213] for some more compact expressions).

As an example, it's possible to study the four point functions $\langle \varepsilon' \varepsilon' \varepsilon' \varepsilon' \rangle$ and $\langle \varepsilon \varepsilon \varepsilon' \varepsilon' \rangle$, and check that, for general values of Q , no spinning operators can be exchanged in both the s and the

²²Recall that the diagonal (or A -series) minimal models only contain scalar primaries $h = \bar{h} = h_{r,s}$ with multiplicity 1.

²³In principle, crossing can give us families of solutions, rather than a unique one. If that is the case, one should look at other correlators involving the same field. For the cases we checked, a single correlator was enough.

t-channel. Therefore the $C_{\varepsilon'\varepsilon'\varepsilon'}$ and $C_{\varepsilon'\varepsilon\varepsilon}$ OPE coefficients for a given value of Q have to be the same as those of the diagonal minimal model for the corresponding value of m .

Additional source of information is $Q = 4$, since the 4-state Potts model is known to be described by the free boson compactified on S_1/\mathbb{Z}_2 [214], and direct computations are possible. To guard against possible subtleties and to obtain information about operators not present in the minimal models, we crosscheck some of the results at $Q = 4$ (appendix C.5). In fact for some of our considerations knowing the values of OPE coefficients at $Q = 4$ will be just enough, while for others higher orders in $Q - 4$ are needed, requiring the analytic continuation from the minimal models.

4.4.1 One-loop beta-function

Based on the agreement of dimensions noticed in section 4.2.6, we have identification [179]:

$$\text{Critical: } \varepsilon = \mathcal{O}_{e_0+2,0} = \phi_{2,1}, \quad (4.4.3)$$

$$\varepsilon' = \mathcal{O}_{e_0+4,0} = \phi_{3,1}, \quad (4.4.4)$$

$$\text{Tricritical: } \varepsilon = \mathcal{O}_{e_0+2,0} = \phi_{1,2}, \quad (4.4.5)$$

$$\varepsilon' = \mathcal{O}_{e_0+4,0} = \phi_{1,3}, \quad (4.4.6)$$

as also indicated in Fig. 4.7. We are most interested in ε' , the subleading energy operator. This singlet operator is irrelevant at the critical point and relevant at the tricritical point for $Q < 4$. Operator $\phi_{1,3}$ is known to produce the RG flow between consecutive minimal models [20]. We therefore make an extremely plausible assumption that operator ε' drives the flow from the tricritical Potts to the critical Potts for any $Q < 4$.²⁴ For $Q = 4$ the two CFTs collide, and ε' becomes marginal.

Now consider analytic continuation to $Q > 4$. The dimension of ε'

$$\Delta_{\varepsilon'}^{\mathcal{C}} = 16/g(Q) - 2, \quad (4.4.7)$$

acquires an imaginary part, negative in the complex theory \mathcal{C} (it would be positive in $\bar{\mathcal{C}}$), as well as a negative corrections to the real part (see Fig. 4.10). Near $Q = 4$ we have

$$\Delta_{\varepsilon'}^{\mathcal{C}} = 2 - 2i\frac{\varepsilon}{\pi} - \frac{\varepsilon^2}{\pi^2} + \dots \quad (\varepsilon = \sqrt{Q-4}). \quad (4.4.8)$$

We consider a family of RG flows perturbing \mathcal{C} by

$$g_0 \int d^2x \varepsilon'(x), \quad (4.4.9)$$

²⁴This is not fully obvious since as mentioned the spectrum of the Potts models only partly overlaps with that of the diagonal minimal models.

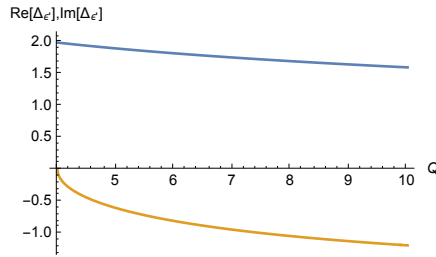


Figure 4.10 – Real and imaginary part of $\Delta_{\epsilon'}$ as a function of Q .

for various initial values of g_0 .

Note: From now on g_0 and g will refer to the bare and renormalized CPT coupling in expansion around \mathcal{C} , to agree with the notation in chapter 3. These couplings have nothing to do with the Coulomb gas coupling from section 4.2, which was denoted there g or $g(Q)$. The latter coupling will not appear in the rest of the chapter. Hopefully this will not create confusion.

The theory \mathcal{C} also contains a strongly relevant singlet operator, analytic continuation of ε , whose coefficient is tuned to zero. We expect these flows to have topology shown in Fig. 4.11. Notice that because of the negative $O(\varepsilon^2)$ correction to $\Delta_{\varepsilon'}^{\mathcal{C}}$ and $\Delta_{\varepsilon'}^{\bar{\mathcal{C}}}$, the trajectories starting at \mathcal{C} or $\bar{\mathcal{C}}$ slowly unwind. This effect was not considered in chapter 3, where the correction to the real part was neglected, leading to oversimplified flow topology shown in Fig. 3.2.²⁵

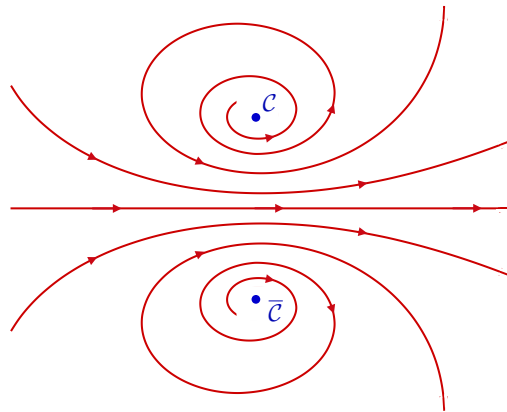


Figure 4.11 – RG flow topology expected in the complexified Potts model at $Q > 4$.

The part of the RG trajectories close to \mathcal{C} and $\bar{\mathcal{C}}$ can be studied in CPT. This concerns in particular the trajectory which does not even begin at \mathcal{C} or $\bar{\mathcal{C}}$ but follows the horizontal line halfway between them. According to the discussion of chapter 3, this trajectory describes the

²⁵Hence, to realize the complex fixed points $\mathcal{C}, \bar{\mathcal{C}}$ on the lattice, one has to finetune the couplings of both ε and ε' . In total one needs to tune two complex, or four real couplings, making lattice studies of the complex fixed points in the Potts model somewhat nontrivial.

walking RG flow.²⁶

Let us recall how one can move between \mathcal{C} and $\bar{\mathcal{C}}$, as well as study the walking RG trajectory, using leading order CPT (section 3.6). The one-loop beta-function reads [21]

$$\beta(g) = \kappa g + \pi C_{\mathcal{E}'\mathcal{E}'\mathcal{E}'} g^2, \quad (4.4.10)$$

where $\kappa = \Delta_{\mathcal{E}'}^{\mathcal{C}} - 2$,²⁷ and g is the renormalized coupling constant which appears in the expressions for beta-functions and anomalous dimensions, as opposed to the bare coupling g_0 used in (4.4.9). At one loop we only need κ at $O(\epsilon)$ and $C_{\mathcal{E}'\mathcal{E}'\mathcal{E}'}$ at $O(1)$. For later uses we cite $C_{\mathcal{E}'\mathcal{E}'\mathcal{E}'}$ including the first subleading term:²⁸

$$C_{\mathcal{E}'\mathcal{E}'\mathcal{E}'} = \frac{4}{\sqrt{3}} - \frac{2i\sqrt{3}}{\pi}\epsilon + O(\epsilon^2). \quad (4.4.11)$$

The beta-function vanishes at $g = 0$ and at

$$g = g_{FP} = -\kappa / (\pi C_{\mathcal{E}'\mathcal{E}'\mathcal{E}'}) = i \frac{\sqrt{3}\epsilon}{2\pi^2} + \dots \quad (4.4.12)$$

Notice that g_{FP} is purely imaginary at the considered leading order. This second fixed point should correspond to $\bar{\mathcal{C}}$. The first check of this identification is the ‘Im-flip’: the imaginary part of dimension of \mathcal{E}' changes sign when going from \mathcal{C} to $\bar{\mathcal{C}}$. As shown in 3.6 this is completely general at this order, and we don’t repeat the argument. However, we will see below several other checks of this identification, possible in the situation at hand.

Furthermore, the walking trajectory corresponds to g of the form

$$g = g_{FP}/2 - \lambda, \quad (4.4.13)$$

with λ real. Reality of λ is preserved since in terms of λ the beta-function is real:

$$\beta_\lambda = -\beta(g_{FP}/2 - \lambda) = -\frac{\sqrt{3}\epsilon^2}{4\pi^3} - \frac{4\pi}{\sqrt{3}}\lambda^2. \quad (4.4.14)$$

For small ϵ , this is the walking beta-function of the form (3.2.3) (up to rescaling λ). In particular, we can obtain the correlation length in the $Q > Q_c$ Potts models:

$$\xi_{\text{Potts}} = \exp\left(\int_{\lambda_{\text{IR}}}^{\lambda_{\text{UV}}} \frac{d\lambda}{\beta_\lambda}\right) \approx \text{const.} \exp\left(\frac{\pi^2}{\epsilon}\right), \quad (4.4.15)$$

where we integrated from $\lambda_{\text{UV}} = -O(1)$ to $\lambda_{\text{IR}} = +O(1)$. This agrees with the leading behavior

²⁶In general the real RG flow doesn’t have to follow an exact straight line, in fact this property is scheme dependent as we discuss in sections 4.4.4. Topology of the RG flow, however, doesn’t depend upon the choice of scheme.

²⁷In chapter 3 we used $\kappa = -i\epsilon$, but here ϵ stands for $\sqrt{Q-4}$.

²⁸The expression we used is given in the Appendix A of [89]. There this particular OPE coefficient is expressed as a finite product and hence as an analytic function of m . (ρ of [89] is related to m as $\rho = m/(m+1)$).

of the exact result for ξ_{Potts} , found in [131] via the Bethe ansatz. As discussed in section 3.6, at this order this prediction does not actually depend on knowing the OPE coefficient $C_{\epsilon'\epsilon'\epsilon'}$, which cancels out of the answer, but only on κ .²⁹ However, the ratios of $C_{\epsilon'\epsilon'\epsilon'}$ to other OPE coefficients is significant as we will now see. Curiously, with an appropriate choice of an expansion parameter, the one-loop answer for ξ_{Potts} turns out to be exact to all orders in perturbation theory, see the discussion around Eq. (4.4.45).

4.4.2 Im-flip for other operators

We will now perform the Im-flip check for other operators. At one loop, the anomalous dimension of a generic operator ϕ is given by

$$\gamma_\phi(g) = 2\pi C_{\phi\phi\epsilon'} g, \quad (4.4.16)$$

and the Im-flip condition (3.6.13) reads:

$$\frac{\text{Im}\Delta_\phi^C}{C_{\phi\phi\epsilon'}} = \frac{\text{Im}\Delta_{\epsilon'}^C}{C_{\epsilon'\epsilon'\epsilon'}} = -\frac{\sqrt{3}}{2\pi}, \quad (4.4.17)$$

We will consider the following operators

- The energy operator ϵ :

$$\Delta_\epsilon^C = \frac{1}{2} - \frac{3i\epsilon}{4\pi} - \frac{3\epsilon^2}{8\pi^2} + \dots, \quad (4.4.18)$$

$$C_{\epsilon\epsilon\epsilon'} = \frac{\sqrt{3}}{2} - \frac{i\sqrt{3}\epsilon}{4\pi} + \dots \quad (4.4.19)$$

- The spin operator σ :

$$\Delta_\sigma^C = \frac{1}{8} - \frac{i\epsilon}{16\pi} + \dots, \quad (4.4.20)$$

$$C_{\sigma\sigma\epsilon'} = \frac{1}{8\sqrt{3}} + \dots \quad (4.4.21)$$

Apart from orbifold at $Q = 4$, this OPE coefficient can be computed exactly for any Q identifying $\sigma = \mathcal{O}_{\pm 1,0} = \phi_{\frac{m}{2}, \frac{m}{2}}$ on the tricritical branch and continuing from the minimal models with m even. Analytic continuation is straightforward because the Dotsenko-Fateev expression for $C(\phi_{\frac{m}{2}, \frac{m}{2}}, \phi_{\frac{m}{2}, \frac{m}{2}}, \phi_{1,3})$ contains a finite m -independent number of terms. This gives an OPE coefficient whose $m \rightarrow \infty$ limit agrees with the orbifold result. We won't need the subleading in ϵ terms so we don't quote them.

- The operator $Z \equiv \mathcal{O}_{0,1}$, contained in the Potts model with multiplicity $\frac{Q(Q-3)}{2}$, see section

²⁹This can be seen already from the fact that $C_{\epsilon'\epsilon'\epsilon'}$ can be scaled out of the beta-function (4.4.10) by rescaling g .

4.2.6:

$$\Delta_Z^C = 2 + \frac{i\epsilon}{\pi} + \dots, \quad (4.4.22)$$

$$C_{ZZ\epsilon'} = -\frac{2}{\sqrt{3}} + \dots, \quad (4.4.23)$$

which does not appear in any of the minimal models,³⁰ but we can determine the $Q = 4$ OPE coefficient via the orbifold. Notice that the imaginary parts of Δ_Z^C and of $C_{ZZ\epsilon'}$ have the opposite sign compared to the all the other cases computed so far. This is related to the fact that Z is irrelevant in the UV (on the tricritical branch for $Q < 4$), and relevant in the IR (i.e. on the critical branch), see Fig. 4.7.

As a sanity check, the Im-flip condition (4.4.17) is satisfied for all these operators by inspection. The success of this check can be traced to the fact that for $Q < 4$ we have the flow from tricritical to critical Potts models triggered by the same operator, $\phi_{1,3}$. Im-flip condition for $Q > 4$ is the analytically continued counterpart of the condition that ensures an appropriate change in the scaling dimensions of operators along this flow.

4.4.3 Drifting scaling dimensions

In this section we will use CPT to compute observables in the real physical theory in the range of distances corresponding to the walking regime, that is for $g = \frac{g_{FP}}{2} - \lambda$ with λ small. We will discuss below the range of λ for which our calculation is under control.

Consider the 2pt functions of some primary operator ϕ . In the walking regime, we expect that the correlation functions exhibit approximate power-law scaling. To quantify this idea, we will define the drifting dimension of an operator ϕ as

$$\delta_\phi(r) = -\frac{1}{2} \frac{1}{G_\phi(r)} \frac{\partial G_\phi(r)}{\partial \log r}, \quad (4.4.24)$$

where G_ϕ is the 2pt function $\langle \phi(r)\phi(0) \rangle$. For a conformal theory, $\delta_\phi(r)$ would be just a constant equal to the scaling dimension, but in the walking regime it will be scale-dependent. In principle, it should be possible to measure the drifting dimensions, or at least closely related quantities, on the lattice as we mention below.

We compute $\delta_\phi(r)$ via the Callan-Symanzik (CS) equation. Restoring the dependence of the 2pt function on the renormalization scale μ and the renormalized coupling g , the CS equation for $G_\phi(r, g, \mu)$ reads:

$$[\mu\partial_\mu + \beta(g)\partial_g + 2\gamma_\phi(g)] G_\phi(r, g, \mu) = 0. \quad (4.4.25)$$

To proceed we introduce the dimensionless variable $\tau = \mu r$ and factor out the fixed-point

³⁰For Q such that m is integer, this operator is actually Kac-degenerate with $r = m - 2$ and $s = m + 1$, however this is outside of the range of s allowed for \mathcal{M}_m .

scaling of G_ϕ :

$$G_\phi(r, g, \mu) = \frac{c(\tau, g)}{r^{2\Delta_\phi^C}}. \quad (4.4.26)$$

Solution of the CS equation for c takes the well-known form:

$$c(\tau, g) = \hat{c}(\bar{g}(\tau, g)) \exp \left[-2 \int_1^\tau d \log \tau' \gamma_\phi(\bar{g}(\tau', g)) \right] \quad (4.4.27)$$

where $\bar{g}(\tau, g)$ is the running coupling with the initial conditions $\bar{g} = g$ at $\tau = 1$. We focus on the real RG trajectory $\bar{g} = g_{FP}/2 - \bar{\lambda}$ with initial condition $\bar{\lambda} = 0$ for definiteness. The running coupling satisfies $\tau \partial_\tau \bar{g} = -\beta(\bar{g})$, or equivalently $\tau \partial_\tau \bar{\lambda} = -\beta_\lambda(\bar{\lambda})$ with β_λ given in (4.4.14). Integrating this equation we find:

$$\bar{\lambda} = \frac{\sqrt{3}\epsilon}{4\pi^2} \tan \left(\frac{\epsilon \log \tau}{\pi} \right). \quad (4.4.28)$$

The one-loop contribution to \hat{c} , comes from the integrated 3pt function $\int d^2x \langle \phi \phi \phi' \epsilon'(x) \rangle$. After subtracting the $1/\epsilon$ pole, the $O(1)$ part of this integral vanishes,³¹ so that

$$\hat{c} = 1 + O(i\epsilon)\bar{\lambda} + \dots \quad (4.4.29)$$

At the one-loop order we can ignore the correction and set $\hat{c} = 1$. We will comment on this purely imaginary $O(\bar{\lambda})$ correction in section 4.4.4.

Using (4.4.16) we have

$$\gamma_\phi \left(\frac{g_{FP}}{2} - \lambda \right) = \pi C_{\phi\phi\epsilon'} g_{FP} - 2\pi C_{\phi\phi\epsilon'} \lambda. \quad (4.4.30)$$

It is easy to see that due to (4.4.17), the constant part of the anomalous dimension cancels exactly the imaginary part of Δ_ϕ^C in $1/r^{2\Delta_\phi^C}$. Consequently, modulo an overall r -independent constant, G_ϕ will be real at this order, see below. Substituting (4.4.28) into (4.4.30) and doing the simple integral in (4.4.27) we finally get (denoting $\mu = 1/r_0$ where convenient)

$$G_\phi(r) = C(\mu) \frac{\left(\cos \frac{\epsilon \log r / r_0}{\pi} \right)^{-\sqrt{3}C_{\phi\phi\epsilon'}}}{r^{2\text{Re}\Delta_\phi^C}}. \quad (4.4.31)$$

where $C(\mu) = \mu^{2i\text{Im}\Delta_\phi^C}$. While this factor is in general complex, we can absorb it defining the rescaled real operator ϕ_R by

$$\phi_R = \mu^{-i\text{Im}\Delta_\phi^C} \phi. \quad (4.4.32)$$

The two point function of ϕ_R is then real in the real theory. We conjecture that the same rescaling renders all higher n -point functions real as well, but at the moment this remains

³¹The relevant integral takes the form $\int d^2x / (|x|^{2+\kappa} |x-y|^{2+\kappa}) = w(\kappa)^2 / w(2\kappa) |y|^{2+2\kappa}$ where $w(\kappa)$ is the factor which arises when going to the Fourier transform $1/|x|^{2+\kappa} \rightarrow w(\kappa) |p|^\kappa$. In the small κ limit $w(\kappa) \sim 1/\kappa + O(1)$ but it's easy to see that the $O(1)$ term will always disappear from the specific combination $w(\kappa)^2 / w(2\kappa)$.

one of the future checks of our proposal. Real operators that have real correlation functions are thus related to operators naturally used in CPT by complex normalization factors which depend on the renormalization scale. We should not be surprised that this redefinition is needed to identify real operators, as it corresponds to an ambiguity in the choice of basis of the operators present in the complex theory \mathcal{C} .

Using (4.4.31), we compute the drifting dimension:

$$\delta_\phi(r) = \text{Re} \Delta_\phi^{\mathcal{C}} - \frac{\sqrt{3}\epsilon}{2\pi} C_{\phi\phi\epsilon'} \tan\left(\frac{\epsilon \ln r / r_0}{\pi}\right), \quad (4.4.33)$$

expressed in terms of the leading in ϵ values of the OPE coefficient and the operator dimension. For several operators ϕ of interest this complex CFT data was given in section 4.4.2.

Let us now discuss the range of validity of Eq. (4.4.33). First of all, there will be correction to (4.4.33) coming from ignoring the higher-order term in the beta-function and anomalous dimension. Since the leading-order result for the deviation $\delta_\phi(r) - \Delta_\phi^{\mathcal{C}}$ is of order of the running coupling $\bar{\lambda}(r)$, we see that we can trust it as long as this deviation remains $\ll 1$ (for example there is no constraint that the deviation should remain $O(\epsilon)$ as one might have naively expected). This condition allows the argument of tangent in (4.4.33) to become $O(1)$ as long as it does not get within $O(\epsilon)$ to $\pi/2$. Another set of corrections to (4.4.33) will arise from the expansion of the CFT data in ϵ , which are non-zero even at $\lambda = 0$.

To show a concrete example, we plotted in Fig. 4.12 the drifting dimension of the energy operator δ_ϵ , as a function of the normalized logarithmic scale $x = \epsilon \log(r/r_0)$ for a few values of Q . We also indicate a (very rough) estimate of the theoretical error on this quantity. To estimate the λ -independent correction $[\delta_\epsilon]_\epsilon$ we used the order ϵ^2 contribution to $\Delta_\epsilon^{\mathcal{C}}$ given in (4.4.18). On the other hand, the higher-loop correction was estimated as a relative correction to the non-trivial part of the drifting dimension proportional to the ratio of two-loop and one-loop terms in the beta-function (4.4.39) below, that is $[\delta_\epsilon]_\lambda = (\delta_\epsilon(r) - \text{Re} \Delta_\epsilon^{\mathcal{C}}) \frac{\beta^{(2)}}{\beta^{(1)}}$. We then add the corrections as mean squares $[\delta_\epsilon]_{\text{total}} = \sqrt{[\delta_\epsilon]_\epsilon^2 + [\delta_\epsilon]_\lambda^2}$. Of course this is not meant to be a rigorous procedure, but just an estimate of the magnitude and qualitative behavior of the error.

Analogously to the drifting scaling dimension $\delta_\epsilon(r)$ one can define a drifting exponent $\nu(r)$ as

$$\nu(r) = \frac{1}{d - \delta_\epsilon(r)}. \quad (4.4.34)$$

Recently a quantity similar to $\nu(r)$ was measured by means of lattice Monte Carlo simulations [133]. Some features of their Fig. 3 suggest qualitative agreement with (4.4.33), however, there is also some discrepancy. There is no immediate problem because the quantity they measured was not exactly (4.4.34), and different reasonable definitions of drifting exponents may not agree with each other. Notice in this regard that detailed behavior of drifting exponents is distinct even for two different definitions used in [133]. In the future it would be interesting to

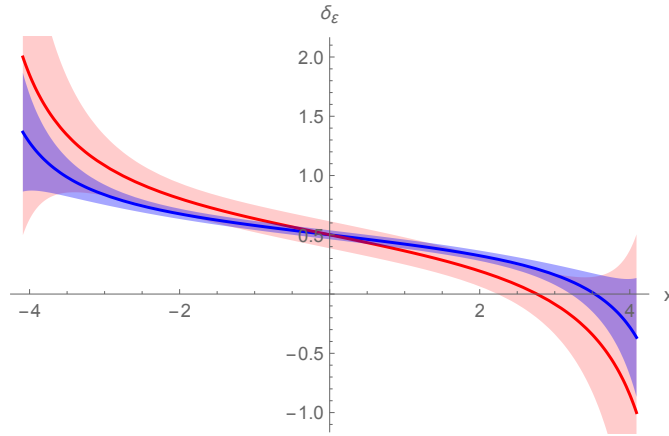


Figure 4.12 – Drifting scaling dimension δ_ϵ given by the equation (4.4.33) as a function of $x = \epsilon \log(r/r_0)$ and an estimate of the theoretical uncertainty for $Q = 5$ (blue) and 7 (red).

measure a quantity more directly related to (4.4.33) on the lattice. We believe that it should also be possible to perform an analytic calculation of finite-volume observables, such as those measured in [133], with the help of CPT around complex Potts model, but we leave this computation for the future.

The dependence of drifting dimensions on $\log r$ shown in Fig. 4.12, with an inflexion point at $r = r_0$, is pretty peculiar. It should be possible to use this dependence to differentiate the walking scenario from a more conventional scenario of nearly-scale invariant RG flow, namely the flow which slowly approaches an IR fixed point along a weakly irrelevant direction, with the schematic beta-function

$$\beta \sim \epsilon \lambda + \lambda^2. \tag{4.4.35}$$

For this flow, deviations of drifting dimensions from IR CFT limits will go like $\sim 1/\log(r)$ in the region $\epsilon \lesssim \lambda \ll 1$, smoothly transitioning to a $const./r^\epsilon$ behavior at distances where $\lambda \lesssim \epsilon$. This functional dependence is clearly distinct from (4.4.33), in particular there is no inflection, and with enough precision it should be possible to distinguish the two scenarios.

Finally let us mention that drifting exponents do not seem related by simple analytic continuation to any $Q < 4$ quantity. To compute them it was important to first analytically continue the conformal data and then develop the CPT around the complex fixed point. We also stress that even if the exact values of CFT dimensions or OPE coefficients are not known, as for example is the case in all higher-dimensional examples of walking discussed in chapter 3, the characteristic form of the drifting dimensions given by Eq. (4.4.33) stays the same and as such can be considered the smoking gun of the walking behavior.

4.4.4 Two-loop beta-function

Now we would like to go one order higher in ϵ and do perturbation theory up to two loops. We therefore need to address the question of scheme dependence. Up to two loops, we have a beta-function of the form

$$\beta^{2\text{-loop}} = \beta_1 g + \beta_2 g^2 + \beta_3 g^3. \quad (4.4.36)$$

Different schemes correspond to changes $g \rightarrow g + \alpha g^2 + \dots$. As is well known, if $\beta_1 = 0$, the two-loop beta-function is scheme independent. However, in our case $\beta_1 \neq 0$, so we need to specify the scheme.

We will use the ‘OPE scheme’ [88], also used in [89].³² The two-loop beta-function in this scheme takes the following form:

$$\beta^{2\text{-loop}} = \kappa(\epsilon)g + \pi C_{\epsilon'\epsilon'\epsilon'}(\epsilon)g^2 - \frac{\pi}{3}I_{\epsilon'}g^3, \quad (4.4.37)$$

where as indicated we include the ϵ -dependence of κ and of the OPE coefficient $C_{\epsilon'\epsilon'\epsilon'}$.³³ Taking into account that $g_{FP} = O(\epsilon)$, at the two-loop order we should keep terms of total degree up to three in ϵ and g , which means that we will need κ at $O(\epsilon^2)$ and $C_{\epsilon'\epsilon'\epsilon'}$ at $O(\epsilon)$, see (4.4.8),(4.4.11).

The two-loop coefficient $I_{\epsilon'}$, needed at $O(1)$, originates from the “triple” OPE of the field ϵ' , i.e. divergences arising when three insertions of the field ϵ' are close together. At this order it can be extracted from the integrated 4pt function $\int d^2z \langle \epsilon'(0)\epsilon'(z)\epsilon'(1)\epsilon'(\infty) \rangle$ of the $Q = 4$ Potts model. However, one has to be careful and subtract extra divergences, which are related to the ordinary OPE of the field ϵ' with itself or with other relevant operators. Taking into account all the subtractions, we have $I_{\epsilon'} = -8\pi$.³⁴

Computing the zero of the two-loop beta-function corresponding to $\bar{\mathcal{C}}$, it turns out that it's still given by (4.4.12), with no corrections at $O(\epsilon^2)$. This is a nice feature of the OPE scheme: were we to change $g \rightarrow g + \alpha g^2$ then $\text{Re } g_{FP} \neq 0$, losing the intuitive picture of \mathcal{C} and $\bar{\mathcal{C}}$ sitting symmetrically around the real RG flow as in Fig. 4.11. That g_{FP} remains purely imaginary is one of the reasons we chose the ‘OPE scheme’, the other being that the real RG stays a straight line passing halfway between the two complex fixed points, Eq. (4.4.13), see below. These desirable features would be lost at two loops in most schemes, e.g. in the scheme of [90].

Next we compute the dimension of ϵ' at the $\bar{\mathcal{C}}$ fixed point, which comes out complex conjugate

³²Eq. (4.4.39) equals (-2) times Eq. (2.19) of [89] due to different normalization of beta-function used in that work..

³³This is different e.g. from the scheme followed by [90], where the OPE coefficient in (4.4.37) is evaluated at $\epsilon = 0$. The two schemes are related by a coupling redefinition $g \rightarrow g + \alpha g^2$, which, at this order, only shifts the ϵg^2 term of the beta function. At this order, it does not change the value of $I_{\epsilon'}$.

³⁴This result was first obtained in [215] and then in [89], and we checked it numerically applying methods of [2, 90] to the 4pt function $\langle \epsilon'\epsilon'\epsilon'\epsilon' \rangle$ given in appendix C of [89]. Minor modifications are required compared to [2], as it was tailored to a flow driven by an operator with a vanishing 3pt function.

of ε' in \mathcal{C} , as it should:

$$2 + \beta'(g)|_{g=g_{FP}} = 2 + \frac{2i\epsilon}{\pi} - \frac{\epsilon^2}{\pi^2}, \quad (4.4.38)$$

We now study the real walking RG trajectory. We claim that in our scheme it still given by $g = \frac{g_{FP}}{2} - \lambda$. To check this, we express the beta-function in terms of λ and see that it comes out real:

$$\beta_\lambda^{2\text{-loop}}(\lambda) = -\frac{\sqrt{3}\epsilon^2}{4\pi^3} - \frac{4\pi}{\sqrt{3}}\lambda^2 + \frac{\epsilon^2}{2\pi^2}\lambda + \frac{8\pi^2}{3}\lambda^3. \quad (4.4.39)$$

It can also be checked that the anomalous dimension of ε' has a constant imaginary part, which cancels exactly the imaginary part of its scaling dimension at \mathcal{C} :

$$\Delta_{\varepsilon'}(\lambda) = 2 + \beta'(g)|_{g=\frac{g_{FP}}{2}-\lambda} = 2 + \frac{\epsilon^2}{2\pi^2} - \frac{8\pi\lambda}{\sqrt{3}} + 8\pi^2\lambda^2. \quad (4.4.40)$$

So in the OPE scheme, the real walking theory still corresponds to the line $\text{Im } g = 0$ in the space of complex couplings $g \in \mathbb{C}$. While the Im-flip of ε' at $\bar{\mathcal{C}}$ and cancellation of its imaginary part of the dimension on the real walking theory were automatic at one-loop, at two loops the check of these conditions explicitly involved the values of the OPE coefficients and integrated 4pt function $I_{\varepsilon'}$.

We can also consider other operators. For a generic operator ϕ , the two-loop anomalous dimension is

$$\gamma_\phi(g) = 2\pi C_{\phi\phi\varepsilon'}g - \pi I_\phi g^2. \quad (4.4.41)$$

As a check, for $\phi = \varepsilon'$ this agrees with $\Delta_{\varepsilon'}(g) = 2 + \beta'(g)$. At the considered order we need to keep terms with total degree up to two in g and ϵ . The I_ϕ is extracted from $\int d^2z \langle \phi(0)\varepsilon'(1)\varepsilon'(z)\phi(\infty) \rangle$ in the same way as previously explained for $I_{\varepsilon'}$.

Unfortunately the only other operator for which we currently have access to the 4pt function $\langle \phi\varepsilon'\varepsilon'\phi \rangle$ is $\phi = \varepsilon$ [89]. $C_{\varepsilon\varepsilon\varepsilon'}$ is given in (4.4.19), and we have $I_\varepsilon = -\pi$. Again it is easy to check the Im-flip at $\bar{\mathcal{C}}$ up to $O(\epsilon^2)$, as well as reality of the dimension of ε on the real axis:

$$\Delta_\varepsilon(g_{FP}) = \Delta_\varepsilon^{\mathcal{C}} + \gamma_\varepsilon(g_{FP}) = \frac{1}{2} + \frac{3i\epsilon}{4\pi} - \frac{3\epsilon^2}{8\pi^2} + \dots = \Delta_\varepsilon^{\bar{\mathcal{C}}}, \quad (4.4.42)$$

$$\Delta_\varepsilon\left(\frac{g_{FP}}{2} - \lambda\right) = \Delta_\varepsilon^{\mathcal{C}} + \gamma_\varepsilon\left(\frac{g_{FP}}{2} - \lambda\right) = \frac{1}{2} - \frac{3\epsilon^2}{16\pi^2} - \sqrt{3}\pi\lambda + \pi^2\lambda^2 + \dots \quad (4.4.43)$$

Although we won't do this, we could use the given two-loop beta-function and the functions $\Delta_\phi\left(\frac{g_{FP}}{2} - \lambda\right)$ to extend the drifting dimension analysis of section 4.4.3 to the two-loop order. The provided information is sufficient to evaluate the integral \int_1^r in (4.4.27), giving correction to drifting dimensions of relative order $O(1)\bar{\lambda}$. Since we verified that the functions entering the integral are real, the correction will be real, as expected in a real walking theory. The correction from $O(i\epsilon)\bar{\lambda}$ term in \hat{c} in (4.4.29) is subleading. Since it is imaginary, we expect it to cancel with the imaginary part of the two-loop term in \hat{c} , although we have not checked.

4.4.5 General arguments about the real flow

We saw in section 4.4.1 that to the one-loop order in CPT reality of the theory at $g = g_{FP}/2 - \lambda$ is almost automatic. Let us now present some arguments why we expect to find a real theory to all orders in perturbation theory. In chapter 3 we defined the complex conjugation map that acts on the space of QFTs, or equivalently on the space of RG flows. A real theory is then a fixed point of this map. At one loop we had the line of purely imaginary g that connected \mathcal{C} and $\bar{\mathcal{C}}$ and that was mapped into itself by the conjugation. Obviously any continuous map of an interval into itself has a fixed point. In general we expect that higher order corrections will deform the conjugation map in some continuous fashion, but under such deformations the fixed point is expected to remain. In general a continuous involution³⁵ possesses fixed points as long as the topology of the space on which it acts is relatively simple, see e.g. [216] and references therein for the precise theorem formulations. Since the topology of the space of theories in the vicinity of \mathcal{C} and $\bar{\mathcal{C}}$ is trivial to leading order in CPT, it is likely to stay such under small deformations. Consequently the real theory should continue to exist in higher orders of perturbation theory.

In spite of this general argument, the above calculations showed that at the technical level emergence of the real observables is quite non-trivial. In section 4.4.4 we saw that quantities that do not directly correspond to physical observables, like anomalous dimensions and beta-functions, may actually be complex, and that this property depends on the choice of scheme. Calculation of section 4.4.3 demonstrated that, even at the one-loop order, one is required to use certain complex normalization constants in the definition of real operators. Nevertheless, both calculations do support the statement that the real theory exists and can be accessed by the deformation of the complex CFT.

4.4.6 The range of Q for which the walking behavior persists

Having studied some higher-order results we can now try to gain some more intuition on the values of the parameter Q for which we expect to see the walking behavior and consequently large correlation length in the Potts model. A rigorous discussion is possible in the limit $Q \rightarrow 4$, when the imaginary parts of operator dimensions go to zero, but this is not the only physically interesting regime, and moreover large values of the correlation length suggest that the walking regime extends all the way to $Q \sim 10$, see Table 3.1. As it often happens, the $Q - 4$ expansion can be extended to large values of Q after various factors of π are taken into account. First of all, we see factors π and π^2 in the one- and two-loop terms of the beta-function (4.4.37) or (4.4.39). These factors have purely geometric origin — they arise from angular integration, and the n -loop term will similarly carry factor π^n . This shows that a natural coupling constant

³⁵Involution is a map which square is the identity, a condition that complex conjugation clearly satisfies.

along the real RG flow is $\tilde{\lambda} = \pi\lambda$.³⁶ In terms of this variable the beta-function reads

$$\beta_{\tilde{\lambda}} = -\frac{\sqrt{3}\epsilon^2}{4\pi^2} - \frac{4}{\sqrt{3}}\tilde{\lambda}^2 + \frac{\epsilon^2}{2\pi^2}\tilde{\lambda} + \frac{8}{3}\tilde{\lambda}^3. \quad (4.4.44)$$

We see that $\tilde{\lambda}^2$ and $\tilde{\lambda}^3$ coefficients became $O(1)$ numbers and we expect this to persist to higher orders in this normalization. We can also observe that the coefficients of different powers of $\tilde{\lambda}$ admit an expansion in ϵ^2/π^2 . It is the same expansion that we have seen above for complex CFT data, except that along the real flow only even powers of $i\epsilon/\pi$ enter. The fact that physical observables are expandable in even powers of ϵ follows from the fact that they are always real quantities, while the factors of $1/\pi$ can be traced back to (4.3.1) and should not be confused with the geometric π rescaling performed above.

Consequently we expect the beta-function to maintain approximately the same form while the expansion parameter remains small: $\epsilon^2/\pi^2 \ll 1$. This identification of the expansion parameter makes it not so surprising that the picture obtained in small ϵ expansion remains reliable even for $\epsilon \sim \sqrt{6}$ corresponding to $Q \sim 10$. More generally, for perturbation around any complex CFT, the expansion will be controlled by the square of the imaginary part of the CFT dimension of the perturbing operator. In case at hand $(\text{Im } \Delta_{\epsilon'})^2 \sim 4\epsilon^2/\pi^2$, and it appears that an extra factor of 4 does not affect the range of the validity of perturbation theory.

If we study the dependence of the complex CFT data on ϵ to higher orders than above, we realize that an even more natural expansion parameter is $4/|m|^2$, which agrees with ϵ^2/π^2 to the first nontrivial order, see Fig. 4.13. Here $m = m(Q)$ is the ‘minimal model’ numbering parameter whose relation to Q is given by (4.4.1), so that $g(Q) = 4 + 4/m(Q)$, $m(Q)$ is real for $Q \leq 4$ and becomes purely imaginary for $Q > 4$.

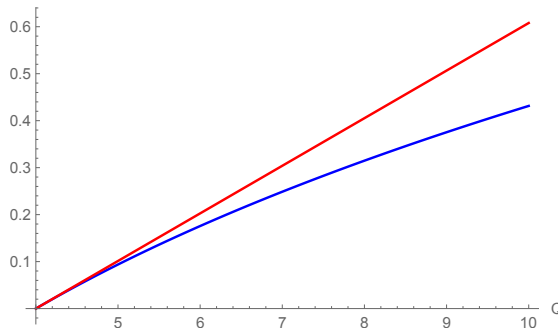


Figure 4.13 – Expansion parameters $\frac{\epsilon^2}{\pi^2}$ (red) and $\frac{4}{|m|^2}$ (blue).

At this point it would be nice to compute some physical observable along the walking flow, like a drifting dimension, to higher order in ϵ/π or $1/m$ and to confirm the suggested behavior. Unfortunately, such a computation appears to be rather tedious since the first nontrivial correction is expected at relative order $1/m^2$, requiring to compute at NNLO (three loops).

³⁶This is similar to counting $1/(16\pi^2)$ factors appearing in Feynman-diagrammatic perturbation theory in 4d.

Alternatively, we could study the behavior of perturbation theory by expanding in the coupling constant some exact non-perturbative result. One such quantity is the correlation length on the square lattice computed exactly for any Q in [131]. Computation of this quantity in perturbation theory using Eq. (4.4.15) would include two types of corrections, those coming from the beta-function and those coming from the dependence of λ_{UV} and λ_{IR} on Q . Inspection of the exact answer, however, leads to a big surprise: if $1/m$ is used as an expansion parameter the answer turns out to be one-loop exact! Namely, expanded at small $1/|m|$ the exact correlation length reads³⁷

$$\xi_{\text{Potts}} = \frac{\sqrt{2}}{16} e^{\pi|m|/2} + O(e^{-\pi|m|/2}). \quad (4.4.45)$$

We see that all corrections to the one-loop answer are non-perturbative in $1/m$. As far as we know this observation has not been made before. This fact is absolutely non-manifest in our perturbation theory, and it suggests that there might be an even superior computational scheme. We leave exploration of this possibility for the future.

4.5 Conclusions

In this chapter we carried on with our proposal that walking behavior can be understood as an RG flow passing between two complex CFTs. Here we were able to provide an example where we have access to the complex CFTs, meaning that we know the operator spectrum and many of the OPE coefficients. The model we studied is the 2d Potts model, which undergoes a weakly first-order phase transition and walking behavior when the number of states Q is in the range $4 \lesssim Q \lesssim 10$. For $Q < 4$, on the other hand, the model has a critical and a tricritical point, and the corresponding partition functions on the torus, and hence the operator spectrum, are known [137]. We access the full complex CFT spectrum by analytically continuing these partition functions to $Q > 4$. We are also able to analytically continue some OPE coefficients involving Kac-degenerate operators, and determine a few others near $Q = 4$ via the orbifold construction of the $Q = 4$ Potts model.

We can then describe the real walking theory as the complex CFT perturbed by a nearly marginal operator, making predictions for observable quantities. Since the walking regime is only approximately scale invariant, 2pt functions exhibit small deviations from power laws, which we compute using perturbation theory. It would be interesting to check our results for drifting scaling dimensions with lattice measurements. These techniques also allow to compute the correlation length of the model for $Q \gtrsim 4$, in agreement with the result obtained using integrability.

The construction passes several purely theoretical consistency checks as well. It was anticipated in chapter 3 that the existence of two complex conjugate CFTs next to each other, as well as of the real theory in between them, requires certain conspiracies in the conformal data. Here we confirmed, up to the two-loop order, that these conspiracies indeed take place in the

³⁷See Eq. (4.46) of [131]; there is an obvious typo in (4.47).

complex Potts CFTs.

We would like to emphasize that our complex CFTs are not just some approximations which may break down upon closer look. On the contrary, they are perfectly nonperturbatively well defined theories which satisfy usual CFT axioms (OPE, crossing, modular-invariant partition function). Being non-unitary, they are naturally defined in Euclidean signature, and may not necessarily allow analytic continuation to Lorentzian signature.³⁸ We outlined how to look for them by studying the Potts model in the space of complexified couplings.

There is at least one more example of walking in two dimensions for which some exact information can be extracted about the complex CFTs, thus providing further tests and applications of our idea: the $O(n)$ model. Very similarly to the Potts model, for $-2 \leq n \leq 2$ there are two branches of fixed points, the critical and the low-temperature fixed point (which is in general non-trivial). At $n = n_c = 2$ the two fixed points merge and go into the complex plane. At $n > 2$ there is no phase transition, nevertheless, for $n \gtrsim 2$ we expect to find a massive theory without any tunable parameter with large correlation length due to walking RG behavior. Many of our techniques can be applied to the $O(n)$ model in an analogous way. This theory, especially for n integer, has been extensively studied in the past, however, to the best of our knowledge, the walking behavior has not been emphasized (see however [217]). Notice that the walking behavior for $n \gtrsim 2$ would be a distinct phenomenon from the slow logarithmic running of the nonlinear sigma-model coupling at short distances. It remains to be seen how far above $n_c = 2$ the walking regime extends, and whether any vestiges of walking remain visible at $n = 3$.

Walking can also be realized in higher dimensions, and in chapter 3 we presented several examples: 3d and 4d gauge theories below conformal window, the three-state Potts model in 3d, and possibly deconfined criticality transitions. Certainly there are others. In these theories it is harder to make quantitative predictions, since the analytic computations of the properties of corresponding complex CFTs are less feasible. Still, the mechanism governing the RG behavior is the same. Our ability to derive the properties of the walking flow from given conformal data is independent of the number of dimensions. Hence several our results, like the form of the walking 2pt function, can be immediately transcribed for the higher-dimensional cases.

³⁸The Osterwalder-Shrader theorem allowing analytic continuation from Euclidean to Lorentzian only works for reflection-positive, i.e. unitary, theories.

Conclusions and outlook

In this thesis we have presented studies of strongly coupled QFTs. In the first part, we considered non-local CFTs, specifically the critical long range Ising (LRI) model. This theory is characterized by different regimes depending on the parameter s , which determines how fast the long range interactions in the spin model decay. For s low enough the model is trivial, but for $s > d/2$ it is interacting. We have developed a way to show that the intermediate regime is conformally invariant to all orders of perturbation theory in an expansion in $\epsilon \sim s - d/2$, despite the absence of a stress tensor in the theory. We have achieved this by considering a defect CFT living in an auxiliary higher-dimensional space. This theory is local and has a stress tensor, so it is straightforward to obtain the Ward identities for the special conformal transformations. Then we can simply restrict ourselves to the defect and show that the Ward identities imply that the original theory is conformally invariant.

Then we focused on the crossover between the intermediate, long-range, regime and the “short range” regime which happens for some value of $s = s^*$. Before our work, many aspects of this crossover were not clear, because the standard picture predicted that for $s \geq s^*$ the CFT would just be described by the local short range Ising (SRI) CFT. We found a more natural picture, where the short range regime is described by the local SRI CFT plus a decoupled GFF. What follows is that we can study the intermediate regime by starting from this short range regime and adding a perturbation which couples the two subsectors. The fact that the intermediate regime can be obtained as the end point of another flow, *i.e.* a Gaussian theory perturbed by a quartic coupling, means that we have an IR duality. The two flows ending in the LRI fixed point are under perturbative control in different situations, and give us the great computational power of finding the critical exponents of the strongly coupled CFT close to the crossover.

While we focused only on the long range Ising model, it’s clear that our mechanism can easily describe other long range models. For example, we could couple the $O(N)$ CFT to some GFF sector and, provided that some term of the beta function has the correct sign, we would end up with a unitary, non-local, $O(N)$ invariant CFT. In this sense we have shown that, while there’s not that many local CFTs, it’s easy to construct continuous families of non-local CFTs.

The second part of this thesis concerned walking behavior, a phenomenon which plays a role in both high energy physics and statistical mechanics. We mentioned several known examples

and some likely candidate of walking theories and tried to correct some misconceptions that are present in the literature. We discussed the concept of complex CFTs, which can be thought of as non-unitary theories living at imaginary values of the coupling, and understood the walking behavior as an RG flow passing close to these complex CFTs.

Knowledge of the conformal data of these complex CFTs allows us to describe observables of the walking theory in perturbation theory. We've shown this exactly in the two dimensional Potts model with $Q \gtrsim 4$. For $0 < Q \leq 4$, the spectrum of this model is known exactly, and OPE coefficients can be obtained in general by requiring crossing symmetry of the theory. By analytically continuing to $Q > 4$, we can obtain the conformal data of the complex CFTs. For example, we were able to obtain the leading behavior in $Q - 4$ of the correlation length at the critical temperature, as well as corrections to two point functions by using conformal perturbation theory.

Another interesting question concerns other systems which show walking behavior. For example, there is evidence that the Néel/VBS phase transition is a weakly first order phase transition. A more approachable system, however, is the two dimensional $O(n)$ model for $n \gtrsim 2$. The $O(n)$ model has a richer spectrum than the Potts model: for example, it has a conserved current due to the continuous symmetry group. It is therefore very important to understand what it means to have this symmetry at non-integer n in order to approach this problem.

A future research direction would also be to systematically investigate what are the constraints from crossing symmetry in the case of a complex CFT living close to the real axis of the coupling. The bootstrap program taught us that, in the case of unitary CFTs, big portions of theory space are incompatible with crossing symmetry. It would be interesting to see what happens to these bounds and constraints as we start breaking unitarity weakly.

Appendices **Part III**

A Further facts about the Long Range Ising model

A.1 Relative normalization of the ϕ and ϕ^3 OPE coefficients

In this section we investigate the consequence of the nonlocal equation of motion (1.3.21) for OPE coefficients and operator normalizations. We will be working in the IR theory. With a small redefinition of the constants involved we can write (1.3.21) as

$$\int d^d y \frac{1}{|x-y|^{2(d-\Delta_\phi)}} \phi(y) = C \phi^3(x), \quad C = -\frac{g_0}{3!} (2\pi)^{2d} w_{d-s} w_{d+s} > 0. \quad (\text{A.1.1})$$

Let us first investigate the consequences of the equation of motion for three point functions. Using (A.1.1), and Symanzik's star integral formula [218], we can easily deduce that if

$$\langle \phi(x) \mathcal{O}_1(y) \mathcal{O}_2(z) \rangle = \frac{\lambda_{12\phi}}{|x-y|^{\Delta_\phi+\Delta_1-\Delta_2} |x-z|^{\Delta_\phi-\Delta_1+\Delta_2} |y-z|^{-\Delta_\phi+\Delta_1+\Delta_2}}, \quad (\text{A.1.2})$$

then

$$\langle \phi^3(x) \mathcal{O}_1(y) \mathcal{O}_2(z) \rangle = \frac{\lambda_{12\phi^3}}{|x-y|^{\Delta_{\phi^3}+\Delta_1-\Delta_2} |x-z|^{\Delta_{\phi^3}-\Delta_1+\Delta_2} |y-z|^{-\Delta_{\phi^3}+\Delta_1+\Delta_2}}, \quad (\text{A.1.3})$$

with $\Delta_{\phi^3} \equiv d - \Delta_\phi$ and with a relative three point function coefficient given by

$$\frac{\lambda_{12\phi^3}}{\lambda_{12\phi}} = \frac{M_3}{C}, \quad M_3 = \pi^{d/2} \frac{\Gamma(\frac{1}{2}(d - \Delta_\phi + \Delta_{12})) \Gamma(\frac{1}{2}(d - \Delta_\phi - \Delta_{12})) \Gamma(\Delta_\phi - d/2)}{\Gamma(d - \Delta_\phi) \Gamma(\frac{1}{2}(\Delta_\phi + \Delta_{12})) \Gamma(\frac{1}{2}(\Delta_\phi - \Delta_{12}))}. \quad (\text{A.1.4})$$

Here we introduced $\Delta_{12} \equiv \Delta_1 - \Delta_2$. Notice that this computation provides an alternative derivation of the scaling dimension Δ_{ϕ^3} in the IR theory, which was derived from the two point function in the main text. Notice also that the gaussian limit $\epsilon \rightarrow 0$ is smooth because in this limit λ is only nonzero if $\Delta_\phi = \pm \Delta_{12} - 2k$, and the zero in M_3 precisely cancels the overall $1/g_0 \sim 1/\epsilon$.

The above three point functions are rather meaningless without knowledge of the two point

Appendix A. Further facts about the Long Range Ising model

functions of the operators involved. The two point function of ϕ takes the form

$$\langle \phi(x)\phi(0) \rangle = \frac{1 + \rho(\epsilon)}{|x|^{2\Delta_\phi}}. \quad (\text{A.1.5})$$

The function ρ is a nontrivial function of ϵ which behaves as ϵ^2 for small ϵ . The two point function of ϕ^3 is then given by the analogue of (1.3.37), which in the current conventions takes the form

$$\langle \phi^3(x)\phi^3(0) \rangle = \int d^d y \int d^d z \frac{\rho(\epsilon)/C^2}{|x-y|^{2(d-\Delta_\phi)}|z|^{2(d-\Delta_\phi)}|y-z|^{2\Delta_\phi}}. \quad (\text{A.1.6})$$

Notice that we subtracted the tree-level part from the two point function of ϕ , cf. the discussion below equation (1.3.37). The resulting two point function is therefore proportional to ρ . The integral as written is actually singular, but we can view it as a formal expression that has a well-defined and finite meaning in momentum space. It then evaluates to

$$\langle \phi^3(x)\phi^3(0) \rangle = \frac{\rho(\epsilon)M_2/C^2}{|x|^{2\Delta_{\phi^3}}} \quad (\text{A.1.7})$$

with

$$M_2 = \frac{\pi^d \Gamma(d/2 - \Delta_\phi) \Gamma(\Delta_\phi - d/2)}{\Gamma(d - \Delta_\phi) \Gamma(\Delta_\phi)}. \quad (\text{A.1.8})$$

We emphasize that the gaussian limit is again smooth.

Substituting $\Delta_\phi = (d - \epsilon)/4$ in (A.1.8) we find that $M_2 < 0$ in a finite interval around $\epsilon = 0$, for all physical values of d . The coefficient ρ is then also expected to be negative, so that altogether the coefficient of (A.1.7) comes out positive. Indeed we expect the LRI to be described by a unitary, or reflection positive in the Euclidean, conformal field theory.¹ We see from (1.3.26) that ρ is negative to the first nontrivial order in perturbation theory, which is in agreement with expectations.

Meaningful three point functions involve the unit normalized operators

$$\tilde{\phi}(x) \equiv \frac{1}{\sqrt{1 + \rho(\epsilon)}} \phi(x), \quad \tilde{\phi}^3(x) \equiv \frac{1}{\sqrt{\rho(\epsilon)M_2/C^2}} \phi^3(x), \quad (\text{A.1.9})$$

in terms of which we find that

$$\frac{\lambda_{12\tilde{\phi}^3}}{\lambda_{12\tilde{\phi}}} = \frac{M_3 \sqrt{1 + \rho(\epsilon)}}{\sqrt{\rho(\epsilon)M_2}}. \quad (\text{A.1.10})$$

We see that C drops out, but the relative three point functions still involve ρ which we can only compute perturbatively.

Notice however that we can take further ratios to get rid of the unknown ρ . Namely, if we

¹The gaussian theory is unitary as long as Δ_ϕ is above the scalar unitarity bound $d/2 - 1$, i.e. if $s < 2$. This condition is satisfied throughout region 2, see Fig. 1.1. We expect that perturbing a unitary theory by a hermitian operator ϕ^4 with a real coupling will give rise to a unitary theory.

A.2. Selected prior work on the long-range Ising model

consider two OPEs $\mathcal{O}_1 \times \mathcal{O}_2$ and $\mathcal{O}'_1 \times \mathcal{O}'_2$, then

$$\frac{\lambda_{12\tilde{\phi}^3} / \lambda_{12\tilde{\phi}}}{\lambda_{1'2'\tilde{\phi}^3} / \lambda_{1'2'\tilde{\phi}}} = \frac{M_3}{M'_3}. \quad (\text{A.1.11})$$

This equation may be used in a variety of ways in conformal bootstrap analyses involving multiple correlators.

It is interesting to consider the limit $s \rightarrow s_*$ where the LRI should transition to the SRI. The SRI does not have an operator corresponding to our $\tilde{\phi}^3$. However from (A.1.10) we see that there is no decoupling of the $\tilde{\phi}^3$ operator unless $\rho = -1$, which would imply that ϕ becomes null and also decouples. Barring this decoupling, a transition from LRI to SRI should be discontinuous. However, the transition is from LRI to SRI+GFF and is indeed continuous.

A.2 Selected prior work on the long-range Ising model

A.2.1 Physics

The study of the long-range Ising model has started in earnest in [22], where also the effective description based on the ϕ^4 -flow has been proposed. That reference has erroneously put the crossover to short range at $s = 2$. This was corrected by [23, 24], leading to what we called the “standard picture”, which has since been supported by theoretical studies [36, 37] and by lattice Monte Carlo simulations [38].

More recently some debate restarted about the nature of the long-range to short-range crossover. Lattice Monte Carlo simulations in [219] observed deviations from the standard picture near the crossover (see also [220]) However, Ref. [219] may have underestimated systematic errors due to possible logarithmic corrections to scaling near the crossover [221]. From our perspective these logarithmic corrections are associated with the operator $\sigma\chi$, marginally irrelevant at the crossover (see section 2.2.3).

Ref. [51] analyzed the problem using the functional renormalization group and also found support for the standard picture.

As a side remark, some of this recent literature likes to phrase the conclusions in terms of the so called “effective dimension” $D_{\text{eff}}(s)$ such that the LRFP in d dimensions is supposed to have the same critical exponents as the SRFP in D_{eff} dimensions. We would like to use this occasion to stress that this “effective dimension” is clearly not a fundamental notion, bound to work only for a few exponents and only in low orders of perturbation theory.

Many of the above-mentioned papers also considered the $O(N)$ generalization of the long-range Ising model. Recently, Ref. [103] analyzed the crossover in the large N approximation. They argued that the IR normalization of the 2pt function of ϕ vanishes as $s \rightarrow s_*$. While we do not fully understand the details of their argument, the conclusion agrees with our picture,

Appendix A. Further facts about the Long Range Ising model

as discussed in section 2.4.2. See also [222] for a recent discussion of the large N limit in this model.

A.2.2 Rigorous results

The ϕ^4 -flow has been studied via rigorous renormalization group analysis in $d = 1, 2, 3$ in [59–61, 223]. These works show that an infrared fixed point exists nonperturbatively at least for sufficiently small $\epsilon > 0$. For some critical exponents, dependence on ϵ in this region of small ϵ has also been rigorously investigated. Ref. [61] announced a proof that ϕ does not acquire anomalous dimension. Ref. [223] showed that the susceptibility and the specific heat critical exponents take, at leading order in ϵ , values expected from the ϵ -expansion predictions for γ_ϕ and γ_{ϕ^2} (this reference considers the general $O(n)$ case, including $n = 0$ corresponding to self-avoiding walks).

Long-range Ising model can also be studied directly from the lattice Hamiltonian, without relying on the renormalization group. It is known that the model has a phase transition separating a low- β phase with vanishing magnetization from a high- β phase where the magnetization is nonzero. Moreover the transition is continuous, in the sense that magnetization vanishes as β_c is approached from above. The above statements have been proved rigorously for $d = 1$, $0 < s < 1$ and for $d = 2, 3$, $0 < s < 2$, which includes the range $0 < s < 2 - \eta_{\text{SR}}$ we are interested in ([110], section 1.4). Incidentally, the same paper also proved for the first time continuity of the phase transition in the *short-range* Ising model for $d = 3$.

Another rigorous result worth mentioning is that the spin-spin correlator of the long-range Ising model decays at $\beta < \beta_c$ with the exponent $d + s$. See [63], Eq. (2.8). Many other rigorous results about the long-range Ising model on the lattice are reviewed in that paper.

B Further facts about walking

B.1 Tuning and weakly first-order phase transitions

First-order phase transitions have several characteristics, but the one which will be most useful to us is that the correlation length ξ for fluctuations of the order parameter remains finite at such a transition. Some first-order transitions are classified as weak. Once again there are various characterizations of what this means. A useful for us definition is that the correlation length at a weak first-order (WFO) phase transition becomes very large with respect to the microscopic length scale (e.g. the lattice spacing): $\xi \gg a$.

Continuous phase transitions, which have $\xi = \infty$, are understood by RG theory as nontrivial fixed points of RG flow,¹ usually described by CFTs. WFO transitions are in a sense “almost continuous”, and one expects the RG theory to say something about them. An RG flow trajectory which corresponds to a WFO transition is long (so that a hierarchy $\xi \gg a$ results), but it does not lead to a CFT fixed point, because otherwise the transition would be continuous.

How such an RG trajectory can arise? Walking is one possibility. However, weakness of some first-order phase transitions is explained via the tuning scenario, as we will now review.

In this scenario a CFT fixed point exists, but an RG flow near-misses it because of an extra relevant coupling turned on, see Fig. B.1. Here we see a flow in the space of three couplings, g_P , g_R (both relevant) and irrelevant g_I , which play different physical roles. We assume that g_P is the control parameter which is tuned in the UV to reach the transition. As such it's a relevant perturbation of the CFT. The g_R represents another relevant perturbation of the CFT, while g_I stands collectively for all irrelevant perturbations.

If $g_R = 0$ in the UV, then by tuning g_P we can get onto a trajectory which ends in a CFT — this would be a continuous transition. Suppose instead that our system has a nonzero value of g_R in the UV. Then we end up on the red trajectory which misses the CFT. That trajectory may end up at another CFT (in which case the transition is still continuous but in a different

¹We call by trivial the fixed points describing the ordered and disordered phases with finite correlation lengths.

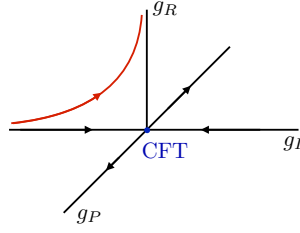


Figure B.1 – The tuning mechanism for a weakly first-order phase transition.

universality class). But it might as well happen that the red trajectory ends in a gapped theory — then the transition is first-order.²

Now imagine that we tune g_R to be very small in the UV. Then the RG trajectory will spend a lot of RG time near the CFT, until eventually ending in a gapped phase. In this case the first-order transition will be weak. The RG flow duration depends on how strongly relevant the g_R perturbation is near the CFT. If the scaling dimension of that perturbation is $\Delta_R < d$, then by the standard RG reasoning we expect the hierarchy

$$\xi/a \sim g_R^{-1/(d-\Delta_R)}, \quad (\text{B.1.1})$$

where we express g_R in dimensionless units at the lattice scale. This way of generating a WFO phase transition is precisely the tuning mechanism from section 3.2.1, see Eq. (3.2.2).

As in section 3.2.1, there are two ways to get a very large number in the r.h.s. of (B.1.1):

1. If $d - \Delta_R = O(1)$, we have to take g_R very small.
2. If, on the other hand, our CFT has a property that $d - \Delta_R \ll 1$, then it's enough to take g_R somewhat smaller than one. E.g. if $d - \Delta_R = 0.25$ and $g_R = 0.25$ we get $\xi/a \sim 256$ which starts being a large number. This latter possibility is what we called ‘mild tuning’ in section 3.2.1.

To illustrate possibility 1, consider the Ising model, for definiteness in 3d, in a small nonzero magnetic field. We pick g_P magnetic field, g_R deviation from the critical temperature T_c . If $g_R = 0$, then for $g_P = 0$ we have a second order transition, governed by the critical 3d Ising CFT. The leading operator which couples to g_R is the energy operator ε , of dimension $\Delta_R \approx 1.41$. For $g_R < 0$ the transition becomes first-order. Since $d - \Delta_R = O(1)$, the transition is weak only if g_R is very small.

To illustrate possibility 2, consider the CFT \mathcal{C}_0 consisting of N decoupled critical 3d Ising CFTs. The global symmetry of this fixed point is the *cubic group*, generated by independent \mathbb{Z}_2

²We assume that the trajectories for $g_P < 0$ and $g_P > 0$ flow to two different phases, otherwise there is no phase transition to talk about.

transformations of each copy and by permutations of the copies. We are interested in RG flows which preserve this symmetry at the microscopic level. There are only two relevant singlet operators:

$$\mathcal{O}_P = \varepsilon_1 + \dots + \varepsilon_N, \quad \mathcal{O}_R = \sum_{i < j} \varepsilon_i \varepsilon_j, \quad (\text{B.1.2})$$

where ε_i are the energy perturbations of each Ising CFT.³ The dimension of ε being ≈ 1.41 , we have $\Delta_R \approx 2.82$. We get a transition varying g_P . Consider the nature of the transition as a function of g_R . If $g_R = 0$ the transition is continuous. Consider what happens if $g_R \neq 0$, depending on the sign. If $g_R > 0$, the RG trajectory misses the CFT \mathcal{C}_0 . It is known that in that case it leads to another CFT, which is the critical $O(2)$ model for $N = 2$, and the so-called ‘‘cubic fixed point’’ for $N \geq 3$. If $g_R < 0$, the trajectory also misses \mathcal{C}_0 and leads to a gapped phase — this will be a first-order transition. Since $d - \Delta_R \ll 1$, a moderate tuning in g_R will suffice for systems with this symmetry to exhibit a *weakly* first-order phase transition.

The just given example is important for understanding why some antiferromagnets with multicomponent order parameters exhibit first-order phase transitions [164, 225]. This first-order phase transition is referred to in the literature as ‘‘fluctuation driven’’, for the following reason. In the Landau-Ginzburg description, we would describe the above RG flow in terms of a multicomponent scalar theory with the mass term

$$m^2(\varphi_1^2 + \dots + \varphi_N^2) = m^2 \vec{\varphi}^2 \quad (\text{B.1.3})$$

and two quartic interactions allowed by the cubic symmetry

$$u(\vec{\varphi}^2)^2 + v(\varphi_1^4 + \dots + \varphi_N^4). \quad (\text{B.1.4})$$

The decoupled fixed point has $u = 0$, $v = v_0 > 0$ and some critical value of m^2 . Perturbing by g_R corresponds to turning on a small u . If $|u| \ll v_0$, of whatever sign, the quartic potential is stable, and the Landau theory predicts a second-order phase transition. However, RG analysis, which is under perturbative control in $d = 4 - \epsilon$ dimensions, shows that $u < 0$, however small, grows more negative so that eventually the flow leads to an unstable potential, with the conclusion that the transition is actually first-order. This is the origin of the ‘‘fluctuation driven’’ terminology, included here for historical reasons. If one thinks nonperturbatively, this terminology does not play much of a role.

B.2 Walking vs BKT transition

Let us briefly review the BKT transition and explain why, while superficially it shares some similarity with the basic scenario of walking as presented in section 3.2, there are also some important differences of principle.

BKT-like transition arises when three conditions are satisfied:

³We constructed this example inspired by [224].

Appendix B. Further facts about walking

- there is a one-parameter family of CFTs $\mathcal{T}(K)$ related by an exactly marginal deformation (coupling) K , singlet of the global symmetry group. Let's call the corresponding singlet scalar operator \mathcal{O}_0 , of dimension $\Delta_0 = d$ for any K ;
- along this family, there is another singlet scalar operator, call it \mathcal{O}_1 , whose scaling dimension $\Delta_1(K)$ varies monotonically with K and crosses from relevant to irrelevant at $K = K_c$.
- the leading nontrivial operator which occurs in the OPE $\mathcal{O}_1 \times \mathcal{O}_1$ is \mathcal{O}_0 , so that the OPE coefficient $C_{110} \sim \langle \mathcal{O}_1 \mathcal{O}_1 \mathcal{O}_0 \rangle$ is nonzero.

In the original BKT transition, as reviewed e.g. in [21], we have $d = 2$ and the family $\mathcal{T}(K)$ is the massless scalar boson θ compactified on $[0, 2\pi]$ and with the action $\frac{1}{2}K \int d^2x (\nabla\theta)^2$. So \mathcal{O}_0 is just the operator multiplying K in the action. It is the singlet of the global $U(1)$ symmetry of the CFT.⁴ On the other hand \mathcal{O}_1 is the vortex operator which inserts a defect, its scaling dimension being $\Delta_1(K) = \pi K$, and $K_c = 2/\pi$.⁵ The OPE coefficient C_{110} is indeed nonzero in this case.

Let us go back to the general setup and consider the consequences. By shifting and rescaling K we can assume that $K_c = 0$ and $\Delta_1 = d + K + O(K^2)$ near $K = 0$. We perturb $\mathcal{T}(0)$ by $K\mathcal{O}_0 + y\mathcal{O}_1$ and study the RG flow, which to the lowest order in K, y has the form:

$$\beta_K = \frac{1}{2}S_d C_{110} y^2, \quad \beta_y = Ky. \quad (\text{B.2.1})$$

Notice that since K is exactly marginal, its beta-function vanishes in absence of y perturbation. Further rescaling the couplings to absorb the OPE coefficient, the new beta-functions take the simple form:

$$\beta_K = y^2, \quad \beta_y = Ky. \quad (\text{B.2.2})$$

The RG flow diagram is in Fig. B.2. Consider the flows starting at $K_0 > 0$ and at $y_0 > 0$. If $y_0 < K_0$ then we end at a CFT, while for $y_0 > K_0$ we flow 'to the unknown' (presumably some gapped phase). When the microscopic theory is varied along the 'micro' line, transition between the two regimes will happen at some non-universal value $K = K_*$. This is the BKT transition.

To study the flow to the unknown, we introduce two combinations of the couplings $u = y^2 - K^2$ and $v = y + K$, in terms of which the RG equations take the form

$$\beta_u = 0, \quad \beta_v = \frac{1}{2}v^2 + \frac{1}{2}u. \quad (\text{B.2.3})$$

The first equation means that u stays constant in this one-loop approximation, while in the second equation we recognize our walking beta-function equation (3.2.3) with v and u some trivial rescalings of λ and y . Let us fix then $u > 0$ and consider a flow of v which starts at some positive $v = v_0 \ll 1$ and heads towards $v = 0$. Differently from the walking scenario [117], the

⁴More precisely, the global symmetry is $U(1)_L \times U(1)_R$.

⁵More precisely, \mathcal{O}_1 is the sum of the charge-1 vortex and antivortex operators.

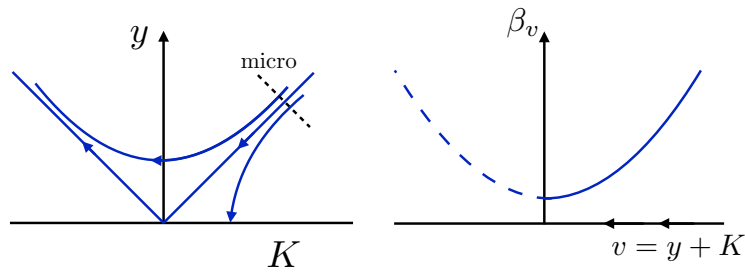


Figure B.2 – *Left*: the RG flow diagram for the BKT transition. *Right*: the beta-function for the coupling combination v .

flow terminates at $v \sim u$, at which point $y - K = u/v = O(1)$ and we go out of the regime of validity of the original beta-functions (B.2.2). We get only one half of the walking RG trajectory, and the arising exponential hierarchy is given by the equation of the form (3.2.7) with an extra $\frac{1}{2}$ in the exponent.

The main differences between walking and the BKT transition are as follows. One key difference is that the true couplings which control the weakness of the perturbation around $\mathcal{T}(0)$ are K and y , not their combinations u , v which make the RG equations assume a simple form. That's why RG in the BKT transition breaks down for v close to 0, while it's perfectly fine and weakly coupled in the walking RG running for $\lambda \sim 0$. The second difference is that the combination u of the couplings, which enters as a fixed parameter into β_v , only remains constant in the one-loop approximation. This was not so for the walking beta-function (3.2.3), where the analogous parameter y was not renormalized to any order. A deeper structural reason for the latter difference is that in the BKT transitions, the CFTs $\mathcal{T}(K)$ all have the same symmetry and are related by an exactly marginal deformation (and hence parameter K can flow). All of these CFTs, be that for $K < K_c$ or $K > K_c$, are unitary and nothing goes into the complex plane. On the contrary, in the considered examples of the walking scenario the family of CFTs all have a different global symmetry and are not related by an exactly marginal deformation.

Notice as well that the leading exponent in the BKT scaling is not universal since there is no universal relation between the parameters of the microscopic theory and the coupling u , while on the other hand, the leading exponent in (3.2.7) is universal, it depends only on the CFT data. For the above reasons, we propose to avoid calling hierarchy (3.2.7) 'BKT scaling' when discussing the walking scenario. We propose to refer to it as the 'walking scaling'.

B.3 Walking in large- N theories

In this section we discuss an example of walking behavior in field theories with large- N counting. As in the examples discussed in the main text we assume existence of two families of fixed points that depend on a parameter, x , and that merge for some critical value of this parameter, x_c . We also assume that at least when the parameter is close to its critical value

Appendix B. Further facts about walking

there exists an RG flow connecting the fixed points. At large N , the corresponding flow was studied in [226] by means of the Hubbard-Stratonovich transformation, where it was shown that it exists as long as one of the CFTs contains a double-trace operator which is weakly relevant. Here we give a simple description using conformal perturbation theory (CPT) that is valid in the vicinity of the merger point. Let us call the operator which triggers the flow $[\mathcal{O}\mathcal{O}]$, and denote its dimension $d + \gamma_{UV}$ at the UV fixed point and $d + \gamma_{IR}$ at the IR one. Then $\gamma_{UV} < 0 < \gamma_{IR}$ and they go to zero when $x = x_c$. First of all, let us show that the operator responsible for the flow has to be a double-trace operator.⁶ To do this, recall the leading-order formula for the change in anomalous dimensions:

$$\gamma_{IR} - \gamma_{UV} = 2S_d g_{FP} C_{[\mathcal{O}\mathcal{O}][\mathcal{O}\mathcal{O}]}^{[\mathcal{O}\mathcal{O}]}, \quad (\text{B.3.1})$$

where g_{FP} is the value of the coupling constant at which the IR CFT is reached. If instead of $[\mathcal{O}\mathcal{O}]$ we tried to use some single-trace operator, say operator \mathcal{O} from which we are “building” $[\mathcal{O}\mathcal{O}]$, its OPE coefficients of the form $C_{\Phi\Phi}^{\mathcal{O}}$, where Φ is any operator, including \mathcal{O} itself, would be suppressed by $1/N$. Correspondingly, g_{FP} would have to be at least of order N and the flow wouldn’t be perturbative. Here we are assuming that at least some anomalous dimensions in two CFTs are different at the $O(1)$ order in $1/N$. Instead, the double-trace operator OPE coefficients $C_{[\mathcal{O}\mathcal{O}][\mathcal{O}\mathcal{O}]}^{[\mathcal{O}\mathcal{O}]}$ and $C_{\mathcal{O}\mathcal{O}}^{[\mathcal{O}\mathcal{O}]}$ are $O(1)$ and as long as γ ’s are small we expect to be able to control the flow within CPT around the UV fixed point.

There is one simple cross-check that we can make at the leading order. Dimension of \mathcal{O} is given by

$$\dim(\mathcal{O}) = \frac{d}{2} + \frac{1}{2}\gamma_{UV(IR)} + O(1/N) \quad (\text{B.3.2})$$

and for consistency we need $C_{[\mathcal{O}\mathcal{O}][\mathcal{O}\mathcal{O}]}^{[\mathcal{O}\mathcal{O}]} = 2C_{\mathcal{O}\mathcal{O}}^{[\mathcal{O}\mathcal{O}]} + O(1/N)$, so that \mathcal{O} gets the right dimension for the same value of g . Since to leading order the OPE coefficients can be calculated by Wick contractions it is easy to check that this relation indeed holds for canonically normalized operators.

Arguments above simply relied on some sort of $1/N$ expansion. In particular, they apply to gauge theory in the large N_c, N_f limit holding $x = N_f/N_c$ fixed. This is the large N limit of the Banks-Zaks-like theories discussed in section 3.4. In this context we arrive at the following conclusion. For $x = x_{AF}$ when the BZ fixed point is free all operators with low dimensions can be easily classified. If we are looking for an operator that for $x = x_c$ becomes marginal and controls the walking behavior for $x < x_c$ then at large N this operator must be a double-trace singlet. As it was advocated in [117], good candidates are four-fermion operators which for $x = x_{AF}$ have dimension 6.

If this picture is right, the schematic behavior of operator dimensions at the BZ fixed point in $d = 4$ in the range $x_c < x < x_{AF}$ has, in the strict $N_c = \infty$ limit, schematic form shown in Fig. B.3. Since $(\bar{\psi}\psi)^2$ starts at dimension 6 and is expected to become marginal at $x = x_c$, there

⁶In theories with large N_c and N_f we will use single-traceness condition with respect to both N_c and N_f .

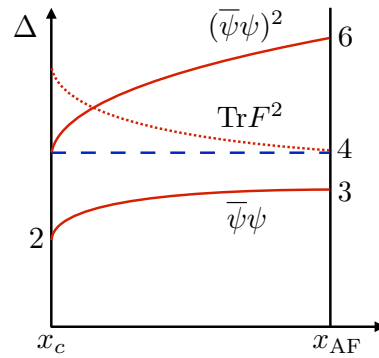


Figure B.3 – Schematic behavior of the operator dimensions at the BZ fixed point as a function of $x = N_f/N_c$, at $N_c = \infty$. The dimension of $(\bar{\psi}\psi)^2$ is twice that of $\bar{\psi}\psi$. All dimensions have a square-root singularity at $x = x_c$.

should be a level crossing between this operator and $\text{tr} F^2$. An alternative picture in which it's $\text{tr} F^2$ becomes marginal is, as we said, disfavored because the three-point function of this single-trace operator vanishes at $N_c = \infty$, and so it's unsuitable for generating a flow from QCD* to BZ with expected properties.

Of course at finite but large N_c we expect that level crossing in Fig. B.3 will be resolved by a small amount. In this case, the operator which becomes marginal at $x = x_c$ is continuously connected to $\text{tr} F^2$, but it still makes sense to label it as double trace $(\bar{\psi}\psi)^2$ because its properties are similar to those of the latter in $N_c = \infty$ limit.

C Further facts about the Potts model

In this section we collect a few further facts about the Potts model which, while not central to our main line of reasoning, may turn out useful for non-experts.

C.1 ‘Breakdown’ of Landau-Ginzburg paradigm

Historically, the first successful approach to phase transitions was the Landau-Ginzburg (LG) paradigm [227]. Although from modern perspective, limitations of this paradigm are well known, it remains a highly influential stepping stone in our thinking about the physics of phase transitions. The basic assumption of LG paradigm is that one can describe continuous phase transitions by considering the fluctuations of the order parameter. One considers an effective Lagrangian built out of the order parameter, which respects the same symmetries of the model and is supposed to describe the coarse-grained physics of it. In the original formulation, one applies the mean field approximation by neglecting fluctuations, and studies the order of the transition. For example, for the Ising model the order parameter is a scalar φ odd under the \mathbb{Z}_2 symmetry. We end up with a Lagrangian given by even powers of φ , and this correctly predicts a second-order phase transition. For the Potts model with $Q \geq 3$, limiting ourselves to integer Q for this discussion, the situation is different. The order parameter is the magnetization φ_a , a vector under S_Q , with $a = 1, \dots, Q$, and subject to the constraint $\sum_a \varphi_a = 0$. The symmetry S_Q acts by shuffling the indices a around, and it is possible to construct a cubic term which is singlet under S_Q . Since all the terms not forbidden by the symmetry have to be included in our effective description, this term has to be considered. Within the original LG rules, the presence of the cubic term would imply that the phase transition is first-order for all $Q \geq 3$. That this prediction is not correct in the case of $Q = 3, 4$ and $d = 2$ is a breakdown of the Landau-Ginzburg theory. In the case at hand the breakdown is usually explained by saying that the fluctuations of the order parameter are significant, and so what was first-order transition in mean field description becomes second-order in reality.

The words ‘LG description’ are sometimes used in the theory of critical phenomena in a way different from the above [228]. Namely, one considers a UV-complete QFT built out of scalar

Appendix C. Further facts about the Potts model

fields with relevant interactions which, for some value of the couplings, flows in the IR to a CFT of interest (the same CFT may describe the continuous phase transition of a lattice model). Such an LG description exists for all unitary minimal models [228], for the Yang-Lee CFT $\mathcal{M}_{2,5}$ [178], as well as for some other non-unitary minimal models [229]. For 2d $Q = 3, 4$ Potts model, natural candidates for such LG descriptions are the S_Q -symmetric Lagrangians considered in [230, 231] which contain both cubic and quartic interaction terms.

C.2 First-order phase transition at large Q

Consider the Potts model in d dimensions with $Q \gg 1$. We will argue that the phase transition is first-order. Consider first the zero-temperature ($\nu = \infty$) fully ordered state which in the cluster definition corresponds to the lattice-filling X , and the infinite-temperature ($\nu = 0$) fully disordered state corresponding to the empty X . The free energies per site of these two states are:

$$f_{\text{Ord}} = d \log \nu, \quad f_{\text{Dis}} = \log Q. \quad (\text{C.2.1})$$

Assuming that these states adequately describe physics all the way to the transition (which will be argued to be the case for $Q \gg 1$), we determine the approximate transition temperature by equating these two free energies: $\nu_c \approx Q^{1/d}$.¹ To show that this guess is self-consistent, we do the low-temperature expansion around the ordered state and the high-temperature expansion around the disordered state. Normally these expansions would converge only for very large and very small ν respectively. But for $Q \gg 1$ they actually converge all the way to the transition. At low expansion orders the smallness of corrections is easy to check. E.g. the first correction to the disordered state comes from X having one bond, and is suppressed by ν/Q , which remains $\ll 1$ for $\nu \lesssim \nu_c$. On the other hand the first few correction terms to the ordered state correspond to removing $k \leq 2d - 1$ bonds and are suppressed by $1/\nu^k$, which is $\ll 1$ throughout the region $\nu \gtrsim \nu_c$. At $k = 2d$ we can finally create one more cluster—an isolated point. This gives a contribution $\sim Q/\nu^{2d}$, still suppressed. This can be made systematic by writing down the full $1/Q$ expansion series around the ordered and disordered state.² This argument can be made mathematically rigorous using the Pirogov-Sinai theory, see [238] and [125], section 7.5.

To summarize, the fully ordered and fully disordered state survive, up to small correction, all the way to the transition temperature where they coexist. Both of these states clearly have $O(1)$ correlation length. Finiteness of the correlation length and phase coexistence mean that the transition is first-order at large Q .

¹In $d = 2$ this guess turns out to be exact for any Q , as follows from the self-duality of the model.

²The $1/Q$ expansion in the Potts model was originally discussed in [232–236]. See especially Eqs. (7), (8) in [237].

C.3 Generalization to $d > 2$

We have seen that, in $d = 2$, the order of the transition depends on the value of Q . It is believed that, in a general number of dimension d , the transition is second-order for $0 < Q \leq Q_c(d)$ and first-order for $Q > Q_c(d)$. As we have seen, $Q_c(2) = 4$.³ In three dimensions, it is known the transition is continuous for $Q = 2$ and (weakly) first-order for $Q = 3$.⁴ The value of Q_c was found to be $Q_c(3) \approx 2.45$ in some Monte Carlo studies [241]. For $d \geq 4$, it is known that $Q_c(d) = 2$.

When it comes to the critical and tricritical fixed point annihilating, there is evidence from RG that it happens in $d \neq 2$ similarly to 2d [242, 243]. It seems thus reasonable to assume that in 3d the two fixed points annihilate at $Q = Q_c(3) \approx 2.45$. One difference of $d > 2$ from 2d is that there exist a value $Q_m(d)$ such that at $Q = Q_m(d)$ the line of tricritical fixed points meets the gaussian (free) line [242]. In 3d, we expect $Q_m(3) = 2$, in accord with the upper critical dimension for the Ising tricritical point being $d = 3$. See Fig. C.1 for the conjectured summary of the situation in $d = 3$.

For the $Q = 3$ 3d Potts model the transition is weakly first-order, with the correlation length still largish, $\xi \sim 10$ [244]. The complex CFT picture developed in our work may be relevant in this case.

One could wonder if it's possible to start from a gaussian fixed point and vary the value of Q in order to get a weakly coupled interacting theory, for example for the tricritical Potts model for $Q = 2 + \delta$, $d = 3$ or the critical Potts model for $Q = 2 - \delta$, $d = 4$, with δ small. In the latter context, this question was examined in [243], and the answer is negative. It was found that, in $d = 4$, the theory in the limit $Q \rightarrow 2^-$ reduces to two decoupled sector, one being a free theory describing the Ising model, and a strongly coupled second sector describing the Potts fields. While it is true that at $Q = 2 - \delta$ the two sectors interact weakly, the full theory is not perturbative. Using this framework, Ref. [243] developed a theory describing the critical and tricritical fixed points merger in $d = 4 - \epsilon$ dimensions.

C.4 Representations of S_Q and the operator spectrum

Irreps of S_Q are in one-to-one correspondence with Young tableaux Y with Q boxes, and their dimension $D_Y(Q)$ is given by the hook rule [245]:

$$D_Y(Q) = \frac{Q!}{\prod_{\text{boxes}} \text{hook length}}. \tag{C.4.1}$$

³This has been proven rigorously [239, 240].

⁴See [121] for the older evidence of a first-order transition in $d = 3$, $Q = 3$.

Appendix C. Further facts about the Potts model

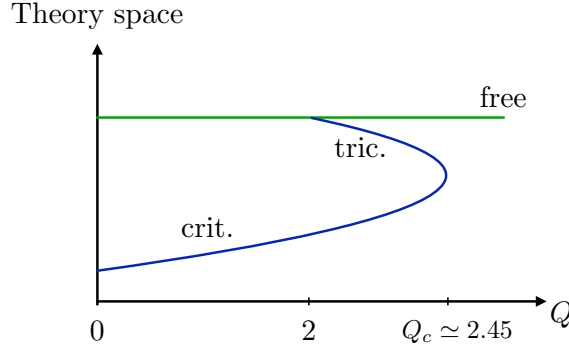


Figure C.1 – Critical and tricritical Potts model for $d = 3$ as a function of $Q > 0$. The two fixed points annihilate at $Q \approx 2.45$. At $Q = 2$ the tricritical line intersects with the line of gaussian fixed points (see the text).

The hook length for one given box is the number of boxes below it, plus the number of boxes to its right, plus one. For example, the irrep

$$\begin{array}{|c|c|c|c|c|} \hline \square & \square & \square & \square & \square \\ \hline \end{array} \quad (C.4.2)$$

Q boxes

has dimension $\frac{Q!}{Q!} = 1$, and is the singlet representation of S_Q . The irrep

$$\begin{array}{|c|c|c|c|c|} \hline \square & \square & \square & \square & \square \\ \hline \square & & & & \\ \hline \end{array} \quad (C.4.3)$$

Q-1 boxes

has dimension $\frac{Q!}{Q(Q-2)!} = Q - 1$ and is the vector representation.⁵

By the hook rule, $D_Y(Q)$ is a polynomial in Q with integer single zeros. Now we list the dimension of a few irreps of S_Q . Denote by $[a_1, a_2, \dots, a_n]$ the Young tableau with a_1 boxes in the first row, a_2 boxes in the second row, etc., so that $\sum_i a_i = Q$. Then we have $((a)_n$ is the Pochhammer symbol)

$$D_{[Q]} = 1, \quad (C.4.4)$$

$$D_{[Q-n, n]} = \frac{(Q-n+2)_{n-1}}{n!} (Q-2n+1) \quad \text{with } n \leq \left\lfloor \frac{Q}{2} \right\rfloor, \quad (C.4.5)$$

$$D_{[Q-n, 1, \dots, 1]} = \frac{(Q-n)_n}{n!} \quad \text{with } n < Q, \quad (C.4.6)$$

$$D_{[Q-4, 2, 1, 1]} = \frac{Q(Q-2)(Q-3)(Q-5)}{8}. \quad (C.4.7)$$

⁵ S_Q acts naturally on the Q -dimensional vector space with the basis ϕ_a ($a = 1, \dots, Q$), by permuting the indices. This representation is reducible and decomposes into singlet $\sum_a \phi_a$, and $(Q-1)$ -dimensional vector $\tilde{\phi}_a = \phi_a - \frac{1}{Q} \sum_b \phi_b$, $\sum_a \tilde{\phi}_a = 0$.

C.4. Representations of S_Q and the operator spectrum

We now test the observation from section 4.2.6: *Multiplicities $M_{h,\bar{h}}$ can be decomposed as sums of dimensions of irreps of S_Q , analytically continued in Q , with Q -independent positive integer coefficients.* This is nontrivial: $M_{h,\bar{h}}$ is a polynomial in Q , but not every polynomial has the stated property. The simplest counterexample would be $M_{h,\bar{h}} = Q - 2$. Notice that it would still be consistent with having true S_Q symmetry for integer $Q \geq 2$, were we to relax the request for Q -independence of the expansion coefficients and let the number of singlets scale with Q as $Q - 2$. The latter realization of the symmetry, however, appears less elegant.

A few operators whose multiplicities coincide with a dimension of a single irrep ($\mathbb{1}, \varepsilon, \varepsilon', \sigma, \sigma', \mathcal{O}_{0,1}$) were discussed in section 4.2.6. One more example is the spin-1 operator $\mathcal{O}_{1,1}$, whose multiplicity is

$$\Lambda(2,2) + Q - 1 = \frac{1}{2}(Q-1)(Q-2) = D_{[Q-2,1,1]} = D_{[Q-2,2]} + 1. \quad (\text{C.4.8})$$

The latter identity means that $\mathcal{O}_{1,1}$ multiplet may also decompose into two irreps.

In more complicated case more than one irrep is required. E.g. consider the scalar $\mathcal{O}_{0,3/2}$, which comes from the term with $M = 3, N = 1, P = 0$ in the second term of (4.2.23), as well as from $Z_c[g, 1/2]$. This operator has multiplicity $\Lambda(3,1) - (Q-1) = \frac{(Q^2 - 5Q + 3)(Q-1)}{3}$. This quantity is clearly not the dimension of an irrep of S_Q , since it has zeros at non-integer values of Q . However it can be decomposed as a sum of dimension of irreps of S_Q . We have two possibilities:

$$\frac{(Q^2 - 5Q + 3)(Q-1)}{3} = D_{[Q-3,1,1,1]} + D_{[Q-3,3]} = D_{[Q-1,1]} + 2D_{[Q-3,3]}. \quad (\text{C.4.9})$$

Another interesting operator is $\mathcal{O}_{0,2}$, which arises from the $M = 4, P = 0, N = 1$ term of (4.2.23). Its multiplicity is $\Lambda(4,1) = \frac{1}{4}Q(Q-2)(Q-3)^2$ which has a double zero and hence is not a dimension of an irrep of S_Q . Here's one of several possible decompositions as a sum of irreps:

$$\frac{Q(Q-2)(Q-3)^2}{4} = 3D_{[Q-3,1,1,1]} + D_{[Q-4,2,1,1]} + 3D_{[Q-4,1,1,1]}. \quad (\text{C.4.10})$$

Whenever there are multiple possible decompositions, we cannot currently decide which one is physically preferred. Hopefully this can be done in the future by defining some sort of twisted partition function, which would give different weights to different irreps, or by studying the structure of the 3pt functions.

Let's finally mention what happens for $Q = 2, 3, 4$. As mentioned in section 4.2.6, all multiplicities for these Q should be positive. The case of operator $\mathcal{O}_{0,1}$, which might appear to have negative multiplicity for $Q = 2$, was already discussed in section 4.2.6. Similarly, operator $\mathcal{O}_{0,3/2}$ appears to have negative multiplicity for $Q = 2, 3, 4$, but this is resolved by degeneracies with other operators of the theory.⁶ These are examples of a general phenomenon: for $Q = 2, 3, 4$

⁶On the critical branch it is degenerate with $\mathcal{O}_{e_0+4,0}$, $\mathcal{O}_{\pm 5,0}$ and $\mathcal{O}_{e_0\pm 6,0}$, for $Q = 2, 3, 4$ correspondingly. The same happens on the tricritical branch, but with different operators ($\mathcal{O}_{e_0+8,0}$, $\mathcal{O}_{\pm 7,0}$ and $\mathcal{O}_{e_0\pm 6,0}$).

Appendix C. Further facts about the Potts model

partition function (4.2.26) can be transformed to a simpler form [137], showing manifestly that the theory contains primaries with positive multiplicities only.

C.5 $Q = 4$ Potts model as an orbifold free boson

The $Q = 4$ Potts model can be described as free scalar boson compactified on S_1/\mathbb{Z}_2 with radius $R = 1/\sqrt{2}$, see e.g. [214] whose notation we will follow. Local operators in this theory are built from holomorphic and anti-holomorphic components of the scalar field ϕ and $\bar{\phi}$.⁷

First, let us identify the operator ε' in this description. In total there are three marginal operators [214]:

$$L = \partial\phi\bar{\partial}\bar{\phi}, \quad V_1 = V_{0,4}^+ = \sqrt{2} \cos\left(\sqrt{2}(\phi - \bar{\phi})\right), \quad V_2 = V_{1,0}^+ = \sqrt{2} \cos\left(\sqrt{2}(\phi + \bar{\phi})\right). \quad (\text{C.5.1})$$

Consequently ε' must be a linear combination of these. To determine which one, let us use the $\varepsilon \times \varepsilon$ OPE. Since the remaining marginal operators transform non-trivially under S_4 and ε is a singlet, the only dimension 2 operator that can appear in this OPE is ε' . The energy operator itself can be easily identified in the orbifold theory: $\varepsilon = V_{0,2}^+$, since this is the only operator of dimension 1/2.

OPEs of vertex operators and L are well known (see e.g. [246]). In particular:

$$L \times V_{n,m}^+ \sim \left(\frac{n^2}{R^2} - \frac{m^2 R^2}{4} \right) V_{n,m}^+, \quad V_{n,m}^+ \times V_{n',m'}^+ \sim \frac{1}{\sqrt{2}} V_{n+n',m+m'}^+. \quad (\text{C.5.2})$$

We get

$$V_{0,2}^+ \times V_{0,2}^+ \sim \frac{1}{\sqrt{2}} V_{0,4}^+ - \frac{1}{2} L = C_{\varepsilon\varepsilon\varepsilon'} \varepsilon', \quad (\text{C.5.3})$$

where

$$\varepsilon' = \frac{\sqrt{2}}{\sqrt{3}} V_{0,4}^+ - \frac{1}{\sqrt{3}} L \quad (\text{C.5.4})$$

is unit-normalized, and $C_{\varepsilon\varepsilon\varepsilon'} = \frac{\sqrt{3}}{2}$ agrees with (4.4.19). Using (C.5.4), we also confirm the $O(\varepsilon^0)$ term in (4.4.11).

Combinations of L , V_1 and V_2 orthogonal to ε' are the remaining marginal operators:

$$Z_1 = V_2, \quad Z_2 = \frac{2}{\sqrt{3}} L + \frac{1}{\sqrt{3}} V_1. \quad (\text{C.5.5})$$

This leads to $\varepsilon' \times Z_i \sim -\frac{2}{\sqrt{3}} Z_i$, and hence to (4.4.23).

⁷Notice that this is not the same scalar field as the height field denoted by the same letter in section 4.2.3. It is tempting to say that the two fields are related by some sort of T-duality, but the precise relation is unclear to us due to the necessity to orbifold. In a simpler case of the $O(2)$ model, the height field used in [137] is indeed the T-dual of the usual compactified boson.

C.5. $Q = 4$ Potts model as an orbifold free boson

Turning to the spin operator, one of its components is identified with $V_{0,1}^+$ (the other two residing in the twisted sector). Using (C.5.2) we get

$$V_{0,1}^+ \times V_{0,1}^+ \sim -\frac{1}{8}L, \quad (\text{C.5.6})$$

which after taking the inner product with ε' leads to (4.4.21).

D Technicalities

D.1 Integrals for γ_ϵ and γ_T

In the computation of γ_ϵ in $d = 2$ we encountered a vanishing integral

$$\int_{\mathbb{C}} d^2 z f(z, \bar{z}) = \int_{\mathbb{C}} d^2 z \frac{1}{|1-z|^4} \left(\frac{|1+z|^2}{4|z|} - 1 \right) = 0, \quad (\text{D.1.1})$$

Let us give an analytic proof of this fact. It is important to remember that this integral is not absolutely convergent, and needs to be computed with circular cutoffs around 0, 1 and infinity. We divide the complex plane into three regions (see Fig. D.1):

$$\begin{aligned} R_1 &= \{z : \epsilon < |z| < 1 - \delta\}, \\ A &= \{z : 1 - \delta < |z| < 1 + \delta, |z - 1| > \epsilon\}, \\ R_2 &= \{z : 1 + \delta < |z| < \epsilon^{-1}\}. \end{aligned} \quad (\text{D.1.2})$$

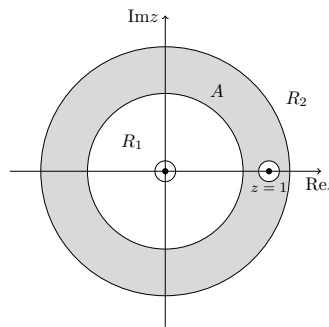


Figure D.1 – The three integration regions (D.1.2).

We need to compute the integral for small but finite values of ϵ and then take $\epsilon \rightarrow 0$ limit. The quantity δ is introduced for convenience. In principle the sum of three integrals does not depend on it, but we will see that all three integrals will simplify for $\delta \ll 1$, so we will take a

Appendix D. Technicalities

limit $\delta \rightarrow 0$ (after $\epsilon \rightarrow 0$). It will turn out that the contribution of the region A approaches a nonzero constant for $\delta \rightarrow 0$. It's easy to forget about this contribution and get a wrong answer.

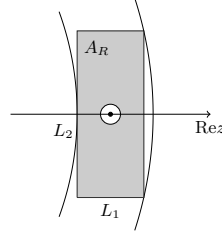


Figure D.2 – Deformation of the region A , which yields the same result in the $\delta \rightarrow 0$ limit.

The integrals over R_1 and R_2 can be computed by writing

$$\int d^2 z f(z, \bar{z}) = \int r dr d\theta f(re^{i\theta}, re^{i\theta}) = \int r dr \oint \frac{d\rho}{i\rho} f(r\rho, r/\rho) \quad (\text{D.1.3})$$

and doing the ρ integrals by residues. This way one obtains:

$$\begin{aligned} \lim_{\epsilon \rightarrow 0} \int_{R_1} d^2 z f(z, \bar{z}) &= \frac{\pi}{8} + O(\delta), \\ \lim_{\epsilon \rightarrow 0} \int_{R_2} d^2 z f(z, \bar{z}) &= \frac{\pi}{8} + O(\delta). \end{aligned} \quad (\text{D.1.4})$$

We are left with computing the integral over the region A . When the limit $\delta \rightarrow 0$ is taken, and the annulus shrinks, the integral will give a non zero contribution because of the singularity at $z = 1$. We can restrict the integration region A to a rectangle around $z = 1$, as the regions where the integrand is not singular yield a zero contribution in the $\delta \rightarrow 0$ limit. We consider therefore the region in Fig. D.2.

We expand the integrand around $z = 1$ and keep only the divergent terms, since only they contribute in the $\delta \rightarrow 0$ limit. Doing the shift $z \rightarrow 1 + z$ and defining the region shown in Fig. D.2, $A_R = \left\{ z : -\frac{L_1}{2} < \text{Re } z < \frac{L_1}{2}, -\frac{L_2}{2} < \text{Im } z < \frac{L_2}{2}, |z| > \epsilon \right\}$, we have

$$\lim_{\delta \rightarrow 0} \lim_{\epsilon \rightarrow 0} \int_A d^2 z f(z, \bar{z}) = \lim_{\delta \rightarrow 0} \lim_{\epsilon \rightarrow 0} \int_{A_R} d^2 z \left(\frac{1}{8z^2} + \frac{1}{8\bar{z}^2} \right). \quad (\text{D.1.5})$$

It's straightforward to carry out the integration of the r.h.s., and one obtains

$$\int_{A_R} d^2 z \left(\frac{1}{8z^2} + \frac{1}{8\bar{z}^2} \right) = \frac{1}{4} \left(\pi - 4 \tan^{-1} \frac{L_2}{L_1} \right). \quad (\text{D.1.6})$$

The result does not depend on the cutoff ϵ once we carry out the angular integration. In order to take the $\delta \rightarrow 0$ limit we need to understand how L_1 and L_2 scale with δ . We see that $L_1 \sim \delta$ and $L_2 \sim \sqrt{\delta}$, therefore $\tan^{-1} L_2/L_1 \rightarrow \pi/2$ when $\delta \rightarrow 0$. Therefore, using (D.1.5),

$$\lim_{\delta \rightarrow 0} \lim_{\epsilon \rightarrow 0} \int_A d^2 z f(z, \bar{z}) = -\frac{\pi}{4}. \quad (\text{D.1.7})$$

Combining this result with (D.1.4),

$$\int_{\mathbb{C}} d^2 z f(z, \bar{z}) = \lim_{\delta \rightarrow 0} \lim_{\epsilon \rightarrow 0} \left(\int_{R_1} + \int_A + \int_{R_2} \right) f(z, \bar{z}) d^2 z = 0. \quad (\text{D.1.8})$$

The same line of reasoning gives the result (2.3.24) for the anomalous dimension of the stress tensor. Given the integral

$$\int_{\mathbb{C}} d^2 z g(z, \bar{z}) = \int_{\mathbb{C}} d^2 z \frac{1}{(1 - \bar{z})^2} \frac{(z^2 + 30z + 1)}{z^2}, \quad (\text{D.1.9})$$

the contributions of the three regions (D.1.2), in the limit $\epsilon \rightarrow 0$ and $\delta \rightarrow 0$, are

$$\int_{R_1} d^2 z g(z, \bar{z}) = \int_{R_2} d^2 z g(z, \bar{z}) = \pi, \quad \int_A d^2 z g(z, \bar{z}) = -32\pi. \quad (\text{D.1.10})$$

This gives us the result (2.3.24).

Bibliography

- [1] M. F. Paulos, S. Rychkov, B. C. van Rees, and B. Zan, “Conformal Invariance in the Long-Range Ising Model,” *Nucl. Phys.* **B902** (2016) 246–291, [arXiv:1509.00008 \[hep-th\]](#).
- [2] C. Behan, L. Rastelli, S. Rychkov, and B. Zan, “A scaling theory for the long-range to short-range crossover and an infrared duality,” *J. Phys.* **A50** no. 35, (2017) 354002, [arXiv:1703.05325 \[hep-th\]](#).
- [3] V. Gorbenko, S. Rychkov, and B. Zan, “Walking, Weak first-order transitions, and Complex CFTs,” *JHEP* **10** (2018) 108, [arXiv:1807.11512 \[hep-th\]](#).
- [4] V. Gorbenko, S. Rychkov, and B. Zan, “Walking, Weak first-order transitions, and Complex CFTs II. Two-dimensional Potts model at $Q > 4$,” *SciPost Phys.* **5** no. 5, (2018) 050, [arXiv:1808.04380 \[hep-th\]](#).
- [5] J. Polchinski, “Scale and Conformal Invariance in Quantum Field Theory,” *Nucl.Phys.* **B303** (1988) 226.
- [6] M. A. Luty, J. Polchinski, and R. Rattazzi, “The a -theorem and the Asymptotics of 4D Quantum Field Theory,” *JHEP* **1301** (2013) 152, [arXiv:1204.5221 \[hep-th\]](#).
- [7] A. Dymarsky, Z. Komargodski, A. Schwimmer, and S. Theisen, “On Scale and Conformal Invariance in Four Dimensions,” [arXiv:1309.2921 \[hep-th\]](#).
- [8] S. El-Showk, Y. Nakayama, and S. Rychkov, “What Maxwell Theory in $D \neq 4$ teaches us about scale and conformal invariance,” *Nucl.Phys.* **B848** (2011) 578–593, [arXiv:1101.5385 \[hep-th\]](#).
- [9] K. G. Wilson and M. E. Fisher, “Critical exponents in 3.99 dimensions,” *Phys. Rev. Lett.* **28** (1972) 240–243.
- [10] S. Ferrara, A. F. Grillo, and R. Gatto, “Tensor representations of conformal algebra and conformally covariant operator product expansion,” *Annals Phys.* **76** (1973) 161–188.
- [11] A. M. Polyakov, “Nonhamiltonian approach to conformal quantum field theory,” *Zh. Eksp. Teor. Fiz.* **66** (1974) 23–42. [Sov. Phys. JETP39,9(1974)].
- [12] A. Belavin, A. M. Polyakov, and A. Zamolodchikov, “Infinite Conformal Symmetry in Two-Dimensional Quantum Field Theory,” *Nucl.Phys.* **B241** (1984) 333–380.
- [13] R. Rattazzi, V. S. Rychkov, E. Tonni, and A. Vichi, “Bounding scalar operator dimensions in 4D CFT,” *JHEP* **0812** (2008) 031, [arXiv:0807.0004 \[hep-th\]](#).

Bibliography

- [14] S. El-Showk, M. F. Paulos, D. Poland, S. Rychkov, D. Simmons-Duffin, and A. Vichi, “Solving the 3D Ising Model with the Conformal Bootstrap,” *Phys.Rev.* **D86** (2012) 025022, [arXiv:1203.6064 \[hep-th\]](#).
- [15] F. Kos, D. Poland, D. Simmons-Duffin, and A. Vichi, “Precision islands in the Ising and $O(N)$ models,” *JHEP* **08** (2016) 036, [arXiv:1603.04436 \[hep-th\]](#).
- [16] D. Simmons-Duffin, “The Lightcone Bootstrap and the Spectrum of the 3d Ising CFT,” *JHEP* **03** (2017) 086, [arXiv:1612.08471 \[hep-th\]](#).
- [17] D. Poland, S. Rychkov, and A. Vichi, “The Conformal Bootstrap: Theory, Numerical Techniques, and Applications,” *Rev. Mod. Phys.* **91** no. 1, (2019) 015002, [arXiv:1805.04405 \[hep-th\]](#).
- [18] A. L. Fitzpatrick, J. Kaplan, D. Poland, and D. Simmons-Duffin, “The Analytic Bootstrap and AdS Superhorizon Locality,” *JHEP* **12** (2013) 004, [arXiv:1212.3616 \[hep-th\]](#).
- [19] Z. Komargodski and A. Zhiboedov, “Convexity and Liberation at Large Spin,” *JHEP* **11** (2013) 140, [arXiv:1212.4103 \[hep-th\]](#).
- [20] A. B. Zamolodchikov, “Renormalization Group and Perturbation Theory Near Fixed Points in Two-Dimensional Field Theory,” *Sov. J. Nucl. Phys.* **46** (1987) 1090. [*Yad. Fiz.*46,1819(1987)].
- [21] J. L. Cardy, *Scaling and renormalization in statistical physics*. Cambridge, UK: Univ. Pr. (1996) 238 p.
- [22] M. E. Fisher, S.-k. Ma, and B. Nickel, “Critical Exponents for Long-Range Interactions,” *Phys.Rev.Lett.* **29** (1972) 917–920.
- [23] J. Sak, “Recursion relations and fixed points for ferromagnets with long-range interactions,” *Phys. Rev. B* **8** (1973) 281–285.
- [24] J. Sak, “Low-temperature renormalization group for ferromagnets with long-range interactions,” *Phys. Rev. B* **15** (1977) 4344–4347.
- [25] N. Seiberg, “Electric - magnetic duality in supersymmetric nonAbelian gauge theories,” *Nucl. Phys.* **B435** (1995) 129–146, [arXiv:hep-th/9411149 \[hep-th\]](#).
- [26] E. Farhi and L. Susskind, “Technicolor,” *Phys. Rept.* **74** (1981) 277.
- [27] B. Holdom, “Raising the Sideways Scale,” *Phys. Rev.* **D24** (1981) 1441.
- [28] K. Yamawaki, M. Bando, and K.-i. Matumoto, “Scale Invariant Technicolor Model and a Technidilaton,” *Phys. Rev. Lett.* **56** (1986) 1335.
- [29] T. W. Appelquist, D. Karabali, and L. C. R. Wijewardhana, “Chiral Hierarchies and the Flavor Changing Neutral Current Problem in Technicolor,” *Phys. Rev. Lett.* **57** (1986) 957.
- [30] J. L. Cardy, M. Nauenberg, and D. J. Scalapino, “Scaling theory of the Potts-model multicritical point,” *Phys. Rev. B* **22** (1980) 2560–2568.
- [31] M. Nauenberg and D. J. Scalapino, “Singularities and Scaling Functions at the Potts-Model Multicritical Point,” *Phys. Rev. Lett.* **44** (1980) 837–840.

- [32] T. Senthil, L. Balents, S. Sachdev, A. Vishwanath, and M. P. A. Fisher, “Quantum criticality beyond the Landau-Ginzburg-Wilson paradigm,” *Phys. Rev. B* **70** (2004) 144407.
- [33] A. Nahum, J. T. Chalker, P. Serna, M. Ortuño, and A. M. Somoza, “Deconfined Quantum Criticality, Scaling Violations, and Classical Loop Models,” *Phys. Rev. X* **5** no. 4, (2015) 041048, [arXiv:1506.06798](#) [[cond-mat.str-el](#)].
- [34] A. Nahum, P. Serna, J. T. Chalker, M. Ortuño, and A. M. Somoza, “Emergent $SO(5)$ Symmetry at the Néel to Valence-Bond-Solid Transition,” *Phys. Rev. Lett.* **115** no. 26, (2015) 267203, [arXiv:1508.06668](#) [[cond-mat.str-el](#)].
- [35] Y. Nakayama and T. Ohtsuki, “Necessary Condition for Emergent Symmetry from the Conformal Bootstrap,” *Phys. Rev. Lett.* **117** no. 13, (2016) 131601, [arXiv:1602.07295](#) [[cond-mat.str-el](#)].
- [36] J. Honkonen and M. Y. Nalimov, “Crossover Between Field Theories With Short Range And Long Range Exchange Or Correlations,” *J.Phys.* **A22** (1989) 751–763.
- [37] J. Honkonen, “Critical behavior of the long range $(\phi^2)^2$ model in the short range limit,” *J.Phys.* **A23** (1990) 825–831.
- [38] E. Luijten and H. W. J. Blöte, “Boundary between long-range and short-range critical behavior in systems with algebraic interactions,” *Phys. Rev. Lett.* **89** (2002) 025703, [arXiv:cond-mat/0112472](#) [[cond-mat.stat-mech](#)].
- [39] J. Le Guillou and J. Zinn-Justin, “Accurate critical exponents for Ising like systems in noninteger dimensions,” *J. Physique* **48** (1987) 19–24.
- [40] S. El-Showk, M. Paulos, D. Poland, S. Rychkov, D. Simmons-Duffin, and A. Vichi, “Conformal Field Theories in Fractional Dimensions,” *Phys. Rev. Lett.* **112** (2014) 141601, [arXiv:1309.5089](#) [[hep-th](#)].
- [41] D. Simmons-Duffin, “A Semidefinite Program Solver for the Conformal Bootstrap,” *JHEP* **06** (2015) 174, [arXiv:1502.02033](#) [[hep-th](#)].
- [42] S. Rychkov, “Conformal Bootstrap in Three Dimensions?,” [arXiv:1111.2115](#) [[hep-th](#)].
- [43] S. El-Showk and M. F. Paulos, “Bootstrapping Conformal Field Theories with the Extremal Functional Method,” *Phys.Rev.Lett.* **111** no. 24, (2013) 241601, [arXiv:1211.2810](#) [[hep-th](#)].
- [44] S. El-Showk, M. F. Paulos, D. Poland, S. Rychkov, D. Simmons-Duffin, and A. Vichi, “Solving the 3d Ising Model with the Conformal Bootstrap II. c -Minimization and Precise Critical Exponents,” *J.Stat.Phys.* **157** (2014) 869, [arXiv:1403.4545](#) [[hep-th](#)].
- [45] F. Kos, D. Poland, and D. Simmons-Duffin, “Bootstrapping Mixed Correlators in the 3D Ising Model,” *JHEP* **1411** (2014) 109, [arXiv:1406.4858](#) [[hep-th](#)].
- [46] F. Gliozzi, “More constraining conformal bootstrap,” *Phys.Rev.Lett.* **111** (2013) 161602, [arXiv:1307.3111](#).
- [47] F. Gliozzi and A. Rago, “Critical exponents of the 3d Ising and related models from Conformal Bootstrap,” *JHEP* **1410** (2014) 042, [arXiv:1403.6003](#) [[hep-th](#)].

Bibliography

- [48] F. Gliozzi, P. Liendo, M. Meineri, and A. Rago, “Boundary and Interface CFTs from the Conformal Bootstrap,” *JHEP* **05** (2015) 036, [arXiv:1502.07217 \[hep-th\]](#).
- [49] C. Behan, “Bootstrapping the long-range Ising model in three dimensions,” [arXiv:1810.07199 \[hep-th\]](#).
- [50] S. El-Showk. unpublished.
- [51] N. Defenu, A. Trombettoni, and A. Codello, “Fixed-point structure and effective fractional dimensionality for $O(N)$ models with long-range interactions,” *Phys. Rev. E* **92** (2015) 052113, [arXiv:1409.8322 \[cond-mat.stat-mech\]](#).
- [52] J. C. Collins, *Renormalization*. Cambridge University Press, 1986.
- [53] S. Weinberg, “High-energy behavior in quantum field theory,” *Phys. Rev.* **118** (1960) 838–849.
- [54] R. Ticciati, *Quantum Field Theory for Mathematicians*. Cambridge University Press, 1999.
- [55] Zavyalov, O.I., *Perenormirovannye diagrammy Feinmana (Renormalised Feynman diagrams)*. Moscow: Nauka, 1979. (in Russian).
- [56] H. Kleinert and V. Schulte-Frohlinde, *Critical properties of ϕ^4 theories*. World Scientific, 2001. 489 p.
- [57] Vasil’ev, A.N., *The field theoretic renormalization group in critical behavior theory and stochastic dynamics*. CRC Press, 2004. 681 p.
- [58] L. S. Brown, “Dimensional Regularization of Composite Operators in Scalar Field Theory,” *Annals Phys.* **126** (1980) 135.
- [59] D. C. Brydges, P. K. Mitter, and B. Scoppola, “Critical $\Phi_{3,\epsilon}^4$,” *Commun. Math. Phys.* **240** (2003) 281–327, [arXiv:hep-th/0206040 \[hep-th\]](#).
- [60] A. Abdesselam, “A Complete Renormalization Group Trajectory Between Two Fixed Points,” *Commun. Math. Phys.* **276** (2007) 727–772, [arXiv:math-ph/0610018 \[math-ph\]](#).
- [61] P. K. Mitter, “Long range ferromagnets: Renormalization group analysis,” <https://hal.archives-ouvertes.fr/cel-01239463>. presented in a talk at LPTHE, Université Pierre et Marie Curie, Paris, 24.10.2013.
- [62] P. K. Mitter. personal communication.
- [63] M. Aizenman and R. Fernández, “Critical exponents for long-range interactions,” *Letters in Mathematical Physics* **16** (1988) 39–49.
- [64] S. Rychkov and Z. M. Tan, “The ϵ -expansion from conformal field theory,” *J. Phys.* **A48** no. 29, (2015) 29FT01, [arXiv:1505.00963 \[hep-th\]](#).
- [65] A. M. Polyakov, “Conformal symmetry of critical fluctuations,” *JETP Lett.* **12** (1970) 381–383.
- [66] M. Rajabpour, “Conformal symmetry in non-local field theories,” *JHEP* **1106** (2011) 076, [arXiv:1103.3625 \[hep-th\]](#).

- [67] K. J. Wiese, “Classification of perturbations for membranes with bending rigidity,” *Phys. Lett.* **B387** (1996) 57–63, [arXiv:cond-mat/9607192](#) [cond-mat].
- [68] V. S. Rychkov and A. Vichi, “Universal Constraints on Conformal Operator Dimensions,” *Phys.Rev.* **D80** (2009) 045006, [arXiv:0905.2211](#) [hep-th].
- [69] D. Dorigoni and V. S. Rychkov, “Scale Invariance + Unitarity \implies Conformal Invariance?,” [arXiv:0910.1087](#) [hep-th].
- [70] L. Caffarelli and L. Silvestre, “An extension problem related to the fractional laplacian,” *Communications in Partial Differential Equations* **32** (2007) 1245–1260, [arXiv:math/0608640](#) [math.AP].
- [71] G. Parisi, “Conformal invariance in perturbation theory,” *Phys. Lett.* **B39** (1972) 643–645.
- [72] S. Sarkar, “Dimensional Regularization and Broken Conformal Ward Identities,” *Nucl. Phys.* **B83** (1974) 108.
- [73] V. M. Braun, G. P. Korchemsky, and D. Mueller, “The Uses of conformal symmetry in QCD,” *Prog. Part. Nucl. Phys.* **51** (2003) 311–398, [arXiv:hep-ph/0306057](#) [hep-ph].
- [74] Y. Nakayama, “Scale invariance vs conformal invariance,” *Phys.Rept.* **569** (2015) 1–93, [arXiv:1302.0884](#) [hep-th].
- [75] J.-F. Fortin, B. Grinstein, and A. Stergiou, “Limit Cycles and Conformal Invariance,” *JHEP* **01** (2013) 184, [arXiv:1208.3674](#) [hep-th].
- [76] S. Rychkov, “EPFL Lectures on Conformal Field Theory in $D \geq 3$ Dimensions,” https://sites.google.com/site/slavyrychkov/CFT_LECTURES_Rychkov.pdf. December 2012.
- [77] S. Rychkov, “Quantum field theory without Lagrangians,” www.youtube.com/watch?v=nzikm3AbZwC. Talk at “A Passion for Particles”, a conference in honor of Riccardo Barbieri, 19-20 December 2013.
- [78] S. Meneses, J. Penedones, S. Rychkov, J. M. Viana Parente Lopes, and P. Yvernay, “A structural test for the conformal invariance of the critical 3d Ising model,” *JHEP* **04** (2019) 115, [arXiv:1802.02319](#) [hep-th].
- [79] M. Hogervorst, S. Rychkov, and B. C. van Rees, “Truncated conformal space approach in d dimensions: A cheap alternative to lattice field theory?,” *Phys. Rev.* **D91** (2015) 025005, [arXiv:1409.1581](#) [hep-th].
- [80] A. Codello, N. Defenu, and G. D’Odorico, “Critical exponents of $O(N)$ models in fractional dimensions,” *Phys. Rev.* **D91** no. 10, (2015) 105003, [arXiv:1410.3308](#) [hep-th].
- [81] Y. Nakayama, “Is boundary conformal in CFT?,” *Phys. Rev.* **D87** no. 4, (2013) 046005, [arXiv:1210.6439](#) [hep-th].
- [82] V. Riva and J. L. Cardy, “Scale and conformal invariance in field theory: A Physical counterexample,” *Phys. Lett.* **B622** (2005) 339–342, [arXiv:hep-th/0504197](#) [hep-th].
- [83] F. A. Dolan and H. Osborn, “Conformal four point functions and the operator product expansion,” *Nucl. Phys.* **B599** (2001) 459–496, [arXiv:hep-th/0011040](#) [hep-th].

Bibliography

- [84] M. E. Peskin, “Mandelstam-’t Hooft duality in abelian lattice models,” *Annals of Physics* **113** (1978) 122–152.
- [85] C. Dasgupta and B. I. Halperin, “Phase transition in a lattice model of superconductivity,” *Phys. Rev. Lett.* **47** (1981) 1556–1560.
- [86] J. Cardy, “Conformal Field Theory and Statistical Mechanics,” in *Les Houches, Session XLIX, 1988, Fields, Strings and Critical Phenomena*, E. Brézin and J. Zinn-Justin, ed. Elsevier, 1989.
- [87] A. Cappelli, J. I. Latorre, and X. Vilasis-Cardona, “Renormalization group patterns and C theorem in more than two-dimensions,” *Nucl. Phys.* **B376** (1992) 510–538, [arXiv:hep-th/9109041 \[hep-th\]](#).
- [88] M. R. Gaberdiel, A. Konechny, and C. Schmidt-Colinet, “Conformal perturbation theory beyond the leading order,” *J. Phys.* **A42** (2009) 105402, [arXiv:0811.3149 \[hep-th\]](#).
- [89] R. Poghossian, “Two Dimensional Renormalization Group Flows in Next to Leading Order,” *JHEP* **01** (2014) 167, [arXiv:1303.3015 \[hep-th\]](#).
- [90] Z. Komargodski and D. Simmons-Duffin, “The Random-Bond Ising Model in 2.01 and 3 Dimensions,” *J. Phys.* **A50** no. 15, (2017) 154001, [arXiv:1603.04444 \[hep-th\]](#).
- [91] S. Rychkov, D. Simmons-Duffin, and B. Zan, “Non-gaussianity of the critical 3d Ising model,” *SciPost Phys.* **2** no. 1, (2017) 001, [arXiv:1612.02436 \[hep-th\]](#).
- [92] M. Hogervorst and S. Rychkov, “Radial Coordinates for Conformal Blocks,” *Phys. Rev.* **D87** (2013) 106004, [arXiv:1303.1111 \[hep-th\]](#).
- [93] F. Kos, D. Poland, and D. Simmons-Duffin, “Bootstrapping the $O(N)$ vector models,” *JHEP* **06** (2014) 091, [arXiv:1307.6856 \[hep-th\]](#).
- [94] M. S. Costa, T. Hansen, J. Penedones, and E. Trevisani, “Radial expansion for spinning conformal blocks,” *JHEP* **07** (2016) 057, [arXiv:1603.05552 \[hep-th\]](#).
- [95] D. Pappadopulo, S. Rychkov, J. Espin, and R. Rattazzi, “OPE Convergence in Conformal Field Theory,” *Phys. Rev.* **D86** (2012) 105043, [arXiv:1208.6449 \[hep-th\]](#).
- [96] S. Rychkov and P. Yvernay, “Remarks on the Convergence Properties of the Conformal Block Expansion,” *Phys. Lett.* **B753** (2016) 682–686, [arXiv:1510.08486 \[hep-th\]](#).
- [97] M. P. Mattis, “Correlations in Two-dimensional Critical Theories,” *Nucl. Phys.* **B285** (1987) 671–686.
- [98] E. D. Skvortsov, “On (Un)Broken Higher-Spin Symmetry in Vector Models,” in *Proceedings, International Workshop on Higher Spin Gauge Theories: Singapore, November 4-6, 2015*, pp. 103–137. 2017. [arXiv:1512.05994 \[hep-th\]](#).
- [99] S. Giombi and V. Kirilin, “Anomalous dimensions in CFT with weakly broken higher spin symmetry,” *JHEP* **11** (2016) 068, [arXiv:1601.01310 \[hep-th\]](#).
- [100] K. Roumpedakis, “Leading Order Anomalous Dimensions at the Wilson-Fisher Fixed Point from CFT,” *JHEP* **07** (2017) 109, [arXiv:1612.08115 \[hep-th\]](#).

- [101] H. Osborn and A. C. Petkou, “Implications of conformal invariance in field theories for general dimensions,” *Annals Phys.* **231** (1994) 311–362, [arXiv:hep-th/9307010](#) [hep-th].
- [102] R. Rattazzi, S. Rychkov, and A. Vichi, “Central Charge Bounds in 4D Conformal Field Theory,” *Phys. Rev.* **D83** (2011) 046011, [arXiv:1009.2725](#) [hep-th].
- [103] E. Brezin, G. Parisi, and F. Ricci-Tersenghi, “The crossover region between long-range and short-range interactions for the critical exponents,” *J. of Stat. Phys.* **157** no. 4-5, (2014) 855–868, [arXiv:1407.3358](#) [cond-mat.stat-mech].
- [104] M. Billó, M. Caselle, D. Gaiotto, F. Gliozzi, M. Meineri, and R. Pellegrini, “Line defects in the 3d Ising model,” *JHEP* **07** (2013) 055, [arXiv:1304.4110](#) [hep-th].
- [105] D. Gaiotto, D. Mazac, and M. F. Paulos, “Bootstrapping the 3d Ising twist defect,” *JHEP* **03** (2014) 100, [arXiv:1310.5078](#) [hep-th].
- [106] D. Mazáč and E. Trevisani. work in progress.
- [107] M. F. Paulos, J. Penedones, J. Toledo, B. C. van Rees, and P. Vieira, “The S-matrix Bootstrap I: QFT in AdS,” [arXiv:1607.06109](#) [hep-th].
- [108] Y. Holovatch, “Critical exponents of Ising-like systems in general dimensions,” *Theoretical and Mathematical Physics* **96** no. 3, (1993) 1099–1109.
- [109] F. J. Dyson, “Existence of a phase-transition in a one-dimensional ising ferromagnet,” *Comm. Math. Phys.* **12** no. 2, (1969) 91–107.
- [110] M. Aizenman, H. Duminil-Copin, and V. Sidoravicius, “Random Currents and Continuity of Ising Model’s Spontaneous Magnetization,” *Comm. Math. Phys.* **334** (2015) 719–742, [arXiv:1311.1937](#) [math-ph].
- [111] D. J. Thouless, “Long-Range Order in One-Dimensional Ising Systems,” *Phys. Rev.* **187** (1969) 732–733.
- [112] M. Aizenman, J. T. Chayes, L. Chayes, and C. M. Newman, “Discontinuity of the magnetization in one-dimensional $1/|x - y|^2$ Ising and Potts models,” *J. Stat. Phys.* **50** (1988) 1–40.
- [113] P. W. Anderson and G. Yuval, “Some numerical results on the Kondo problem and the inverse square one-dimensional Ising model,” *J. of Phys. C* **4** (1971) 607–620.
- [114] J. Bhattacharjee, S. Chakravarty, J. L. Richardson, and D. J. Scalapino, “Some properties of a one-dimensional Ising chain with an inverse-square interaction,” *Phys. Rev. B* (1981) 3862–3865.
- [115] J. M. Kosterlitz, “Phase transitions in long-range ferromagnetic chains,” *Phys. Rev. Lett.* **37** (Dec, 1976) 1577–1580. <https://link.aps.org/doi/10.1103/PhysRevLett.37.1577>.
- [116] K. Binder and E. Luijten, “Monte carlo tests of renormalization-group predictions for critical phenomena in ising models,” *Physics Reports* **344** no. 4, (2001) 179 – 253. <http://www.sciencedirect.com/science/article/pii/S0370157300001277>. Renormalization group theory in the new millennium.
- [117] D. B. Kaplan, J.-W. Lee, D. T. Son, and M. A. Stephanov, “Conformality Lost,” *Phys. Rev.* **D80** (2009) 125005, [arXiv:0905.4752](#) [hep-th].

Bibliography

- [118] M. A. Luty, “Strong Conformal Dynamics at the LHC and on the Lattice,” *JHEP* **04** (2009) 050, [arXiv:0806.1235 \[hep-ph\]](#).
- [119] M. A. Luty and T. Okui, “Conformal technicolor,” *JHEP* **09** (2006) 070, [arXiv:hep-ph/0409274 \[hep-ph\]](#).
- [120] G. ’t Hooft, “Naturalness, chiral symmetry, and spontaneous chiral symmetry breaking,” *NATO Sci. Ser. B* **59** (1980) 135–157.
- [121] F. Y. Wu, “The Potts model,” *Rev. Mod. Phys.* **54** (1982) 235–268.
- [122] J. L. Jacobsen, “Loop Models and Boundary CFT,” in *Conformal Invariance: an Introduction to Loops, Interfaces and Stochastic Loewner Evolution*, M. Henkel and D. Karevski, eds., pp. 141–183. Springer Berlin Heidelberg, 2012.
- [123] C. Fortuin and P. Kasteleyn, “On the random-cluster model,” *Physica* **57** no. 4, (1972) 536 – 564.
- [124] M. Biskup, “Reflection Positivity of the Random-Cluster Measure Invalidated for Noninteger q ,” *J. of Stat. Phys.* **92** no. 3, (1998) 369–375.
- [125] G. Grimmett, *The Random-Cluster Model*. Grundlehren der mathematischen Wissenschaften. Springer Berlin Heidelberg, 2006.
- [126] R. J. Baxter, “Potts model at critical temperature,” *J. Phys.* **C6** (1973) L445–L448.
- [127] B. Nienhuis, A. N. Berker, E. K. Riedel, and M. Schick, “First- and Second-Order Phase Transitions in Potts Models: Renormalization-Group Solution,” *Phys. Rev. Lett.* **43** (1979) 737–740.
- [128] E. Vernier, J. Lykke Jacobsen, and J. Salas, “Q-colourings of the triangular lattice: exact exponents and conformal field theory,” *J. of Phys. A* **49** no. 17, (2016) 174004, [arXiv:1509.02804 \[cond-mat.stat-mech\]](#).
- [129] R. J. Baxter, *Exactly solved models in statistical mechanics*. Academic Press, 1982.
- [130] H. Saleur, “Zeroes of chromatic polynomials: a new approach to Beraha conjecture using quantum groups,” *Comm. Math. Phys.* **132** no. 3, (1990) 657–679. <https://projecteuclid.org:443/euclid.cmp/1104201233>.
- [131] E. Buffenoir and S. Wallon, “The correlation length of the Potts model at the first-order transition point,” *J. Phys. A* **26** no. 13, (1993) 3045.
- [132] C. Wang, A. Nahum, M. A. Metlitski, C. Xu, and T. Senthil, “Deconfined quantum critical points: symmetries and dualities,” *Phys. Rev. X* **7** no. 3, (2017) 031051, [arXiv:1703.02426 \[cond-mat.str-el\]](#).
- [133] S. Iino, S. Morita, A. W. Sandvik, and N. Kawashima, “Detecting signals of weakly first-order phase transitions in two-dimensional Potts models,” *arXiv e-prints* (Jan., 2018), [arXiv:1801.02786 \[cond-mat.stat-mech\]](#).
- [134] M. Blume, V. J. Emery, and R. B. Griffiths, “Ising Model for the λ Transition and Phase Separation in He³-He⁴ Mixtures,” *Phys. Rev. A* **4** (1971) 1071–1077.

-
- [135] A. N. Berker and M. Wortis, “Blume-Emery-Griffiths-Potts model in two dimensions: Phase diagram and critical properties from a position-space renormalization group,” *Phys. Rev. B* **14** (1976) 4946–4963.
- [136] X. Qian, Y. Deng, and H. W. J. Blöte, “Dilute Potts model in two dimensions,” *Phys. Rev. E* **72** (2005) 056132.
- [137] P. Di Francesco, H. Saleur, and J. B. Zuber, “Relations between the Coulomb gas picture and conformal invariance of two-dimensional critical models,” *J. Stat. Phys.* **49** no. 1, (1987) 57–79.
- [138] M. P. M. den Nijs, “A relation between the temperature exponents of the eight-vertex and q -state Potts model,” *J of Phys A* **12** no. 10, (1979) 1857.
- [139] J. L. Black and V. J. Emery, “Critical properties of two-dimensional models,” *Phys. Rev. B* **23** (1981) 429–432.
- [140] B. Nienhuis, “Analytical calculation of two leading exponents of the dilute potts model,” *J Phys A* **15** no. 1, (1982) 199.
- [141] A. A. Belavin and A. A. Migdal, “Calculation of anomalous dimensions in non-abelian gauge field theories,” *JETP Letters* **19** (1974) 181. [article pdf](#).
- [142] W. E. Caswell, “Asymptotic Behavior of Nonabelian Gauge Theories to Two Loop Order,” *Phys. Rev. Lett.* **33** (1974) 244.
- [143] T. Banks and A. Zaks, “On the Phase Structure of Vector-Like Gauge Theories with Massless Fermions,” *Nucl. Phys.* **B196** (1982) 189–204.
- [144] D. Nogradi and A. Patella, “Strong dynamics, composite Higgs and the conformal window,” *Int. J. Mod. Phys.* **A31** no. 22, (2016) 1643003, [arXiv:1607.07638 \[hep-lat\]](#).
- [145] S. Giombi, I. R. Klebanov, and G. Tarnopolsky, “Conformal QED_d, F -Theorem and the ϵ Expansion,” *J. Phys.* **A49** no. 13, (2016) 135403, [arXiv:1508.06354 \[hep-th\]](#).
- [146] S. Gukov, “RG Flows and Bifurcations,” *Nucl. Phys.* **B919** (2017) 583–638, [arXiv:1608.06638 \[hep-th\]](#).
- [147] N. Karthik and R. Narayanan, “Scale-invariance of parity-invariant three-dimensional QED,” *Phys. Rev.* **D94** no. 6, (2016) 065026, [arXiv:1606.04109 \[hep-th\]](#).
- [148] N. Karthik and R. Narayanan, “Scale-invariance and scale-breaking in parity-invariant three-dimensional QCD,” *Phys. Rev.* **D97** no. 5, (2018) 054510, [arXiv:1801.02637 \[hep-th\]](#).
- [149] H. Gies and J. Jaeckel, “Chiral phase structure of QCD with many flavors,” *Eur. Phys. J.* **C46** (2006) 433–438, [arXiv:hep-ph/0507171 \[hep-ph\]](#).
- [150] V. A. Miransky, “Dynamics of spontaneous chiral symmetry breaking and the continuum limit in quantum electrodynamics,” *Nuovo Cim.* **90** no. 2, (1985) 149–170.
- [151] A. Dymarsky, I. R. Klebanov, and R. Roiban, “Perturbative search for fixed lines in large N gauge theories,” *JHEP* **08** (2005) 011, [arXiv:hep-th/0505099 \[hep-th\]](#).
- [152] A. G. Cohen and H. Georgi, “Walking Beyond the Rainbow,” *Nucl. Phys.* **B314** (1989) 7–24.

Bibliography

- [153] D. Poland, D. Simmons-Duffin, and A. Vichi, “Carving Out the Space of 4D CFTs,” *JHEP* **05** (2012) 110, [arXiv:1109.5176 \[hep-th\]](#).
- [154] T. DeGrand, “Lattice tests of beyond Standard Model dynamics,” *Rev. Mod. Phys.* **88** (2016) 015001, [arXiv:1510.05018 \[hep-ph\]](#).
- [155] F. Coradeschi, P. Lodone, D. Pappadopulo, R. Rattazzi, and L. Vitale, “A naturally light dilaton,” *JHEP* **11** (2013) 057, [arXiv:1306.4601 \[hep-th\]](#).
- [156] M. Baggio, N. Bobev, S. M. Chester, E. Lauria, and S. S. Pufu, “Decoding a Three-Dimensional Conformal Manifold,” *JHEP* **02** (2018) 062, [arXiv:1712.02698 \[hep-th\]](#).
- [157] W. A. Bardeen, M. Moshe, and M. Bander, “Spontaneous Breaking of Scale Invariance and the Ultraviolet Fixed Point in $O(n)$ Symmetric (ϕ^6 in Three-Dimensions) Theory,” *Phys. Rev. Lett.* **52** (1984) 1188.
- [158] E. David, D. A. Kessler, and H. Neuberger, “A Study of $(\phi^2)^3$ in Three-dimensions at $N = \infty$,” *Nucl. Phys.* **B257** (1985) 695–728.
- [159] H. Omid, G. W. Semenoff, and L. C. R. Wijewardhana, “Light dilaton in the large N tricritical $O(N)$ model,” *Phys. Rev.* **D94** no. 12, (2016) 125017, [arXiv:1605.00750 \[hep-th\]](#).
- [160] G. Delfino and J. L. Cardy, “The Field theory of the $q \rightarrow 4^+$ Potts model,” *Phys. Lett.* **B483** (2000) 303–308, [arXiv:hep-th/0002122 \[hep-th\]](#).
- [161] **Lattice Strong Dynamics** Collaboration, T. Appelquist *et al.*, “Nonperturbative investigations of $SU(3)$ gauge theory with eight dynamical flavors,” [arXiv:1807.08411 \[hep-lat\]](#).
- [162] T. A. Ryttov and R. Shrock, “Physics of the non-Abelian Coulomb phase: Insights from Padé approximants,” *Phys. Rev.* **D97** no. 2, (2018) 025004, [arXiv:1710.06944 \[hep-th\]](#).
- [163] A. Aharony, “Critical behavior of anisotropic cubic systems,” *Phys. Rev. B* **8** (1973) 4270–4273.
- [164] A. Pelissetto and E. Vicari, “Critical phenomena and renormalization-group theory,” *Phys. Rept.* **368** (2002) 549–727, [arXiv:cond-mat/0012164](#).
- [165] M. Jarvinen and E. Kiritsis, “Holographic Models for QCD in the Veneziano Limit,” *JHEP* **03** (2012) 002, [arXiv:1112.1261 \[hep-ph\]](#).
- [166] D. Arean, I. Iatrakis, M. Jarvinen, and E. Kiritsis, “V-QCD: Spectra, the dilaton and the S-parameter,” *Phys. Lett.* **B720** (2013) 219–223, [arXiv:1211.6125 \[hep-ph\]](#).
- [167] D. Arean, I. Iatrakis, M. Jarvinen, and E. Kiritsis, “The discontinuities of conformal transitions and mass spectra of V-QCD,” *JHEP* **11** (2013) 068, [arXiv:1309.2286 \[hep-ph\]](#).
- [168] V. Balasubramanian and P. Kraus, “Space-time and the holographic renormalization group,” *Phys. Rev. Lett.* **83** (1999) 3605–3608, [arXiv:hep-th/9903190 \[hep-th\]](#).
- [169] P. Breitenlohner and D. Z. Freedman, “Stability in Gauged Extended Supergravity,” *Annals Phys.* **144** (1982) 249.
- [170] D. Simmons-Duffin. private communication (2016).
- [171] Y. Nakayama. private communication (2016).

- [172] B. Zhao, P. Weinberg, and A. W. Sandvik, “Symmetry enhanced first-order phase transition in a two-dimensional quantum magnet,” [arXiv:1804.07115](#).
- [173] P. Serna and A. Nahum, “Emergence and spontaneous breaking of approximate $O(4)$ symmetry at a weakly first-order deconfined phase transition,” [arXiv:1805.03759](#) [[cond-mat.str-el](#)].
- [174] R. Haag, *Local quantum physics: Fields, particles, algebras*. Berlin, Germany: Springer, 356 p. (Texts and monographs in physics), 1992.
- [175] J. Maldacena and A. Zhiboedov, “Constraining Conformal Field Theories with A Higher Spin Symmetry,” *J. Phys.* **A46** (2013) 214011, [arXiv:1112.1016](#) [[hep-th](#)].
- [176] M. Hogervorst, S. Rychkov, and B. C. van Rees, “Unitarity violation at the Wilson-Fisher fixed point in $4 - \epsilon$ dimensions,” [arXiv:1512.00013](#) [[hep-th](#)].
- [177] M. E. Fisher, “Yang-Lee Edge Singularity and ϕ^3 Field Theory,” *Phys. Rev. Lett.* **40** (1978) 1610–1613.
- [178] J. L. Cardy, “Conformal Invariance and the Yang-lee Edge Singularity in Two-dimensions,” *Phys. Rev. Lett.* **54** (1985) 1354–1356.
- [179] V. S. Dotsenko and V. A. Fateev, “Conformal Algebra and Multipoint Correlation Functions in Two-Dimensional Statistical Models,” *Nucl. Phys.* **B240** (1984) 312.
- [180] V. S. Dotsenko and V. A. Fateev, “Four Point Correlation Functions and the Operator Algebra in the Two-Dimensional Conformal Invariant Theories with the Central Charge $c < 1$,” *Nucl. Phys.* **B251** (1985) 691–734.
- [181] L. Di Pietro and E. Stamou, “Operator mixing in the ϵ -expansion: Scheme and evanescent-operator independence,” *Phys. Rev.* **D97** no. 6, (2018) 065007, [arXiv:1708.03739](#) [[hep-th](#)].
- [182] A. Weinrib and B. I. Halperin, “Critical phenomena in systems with long-range-correlated quenched disorder,” *Phys. Rev.* **B27** (1983) 413–427.
- [183] S. Leurent and D. Volin, “Multiple zeta functions and double wrapping in planar $N = 4$ SYM,” *Nucl. Phys.* **B875** (2013) 757–789, [arXiv:1302.1135](#) [[hep-th](#)].
- [184] E. Frenkel, A. Losev, and N. Nekrasov, “Instantons beyond topological theory. I,” [arXiv:hep-th/0610149](#) [[hep-th](#)].
- [185] E. Gerchkovitz, J. Gomis, and Z. Komargodski, “Sphere Partition Functions and the Zamolodchikov Metric,” *JHEP* **11** (2014) 001, [arXiv:1405.7271](#) [[hep-th](#)].
- [186] N. Bobev, H. Elvang, U. Kol, T. Olson, and S. S. Pufu, “Holography for $\mathcal{N} = 1^2$ on S^4 ,” *JHEP* **10** (2016) 095, [arXiv:1605.00656](#) [[hep-th](#)].
- [187] L. Fei, S. Giombi, and I. R. Klebanov, “Critical $O(N)$ models in $6 - \epsilon$ dimensions,” *Phys. Rev.* **D90** no. 2, (2014) 025018, [arXiv:1404.1094](#) [[hep-th](#)].
- [188] L. Fei, S. Giombi, I. R. Klebanov, and G. Tarnopolsky, “Three loop analysis of the critical $O(N)$ models in $6 - \epsilon$ dimensions,” *Phys. Rev.* **D91** no. 4, (2015) 045011, [arXiv:1411.1099](#) [[hep-th](#)].

Bibliography

- [189] S. Giombi, I. R. Klebanov, and G. Tarnopolsky, “Bosonic tensor models at large N and small ϵ ,” *Phys. Rev. D* **96** no. 10, (2017) 106014, [arXiv:1707.03866 \[hep-th\]](#).
- [190] S. Giombi, I. R. Klebanov, F. Popov, S. Prakash, and G. Tarnopolsky, “Prismatic Large N Models for Bosonic Tensors,” [arXiv:1808.04344 \[hep-th\]](#).
- [191] Ö. Gürdoğan and V. Kazakov, “New Integrable 4D Quantum Field Theories from Strongly Deformed Planar $\mathcal{N} = 4$ Supersymmetric Yang-Mills Theory,” *Phys. Rev. Lett.* **117** no. 20, (2016) 201602, [arXiv:1512.06704 \[hep-th\]](#). [Addendum: *Phys. Rev. Lett.* **117**,no.25,259903(2016)].
- [192] D. Grabner, N. Gromov, V. Kazakov, and G. Korchemsky, “Strongly γ -Deformed $\mathcal{N} = 4$ Supersymmetric Yang-Mills Theory as an Integrable Conformal Field Theory,” *Phys. Rev. Lett.* **120** no. 11, (2018) 111601, [arXiv:1711.04786 \[hep-th\]](#).
- [193] B. Nienhuis, “Coulomb Gas Formulation of Two-dimensional Phase Transitions,” in *Phase Transitions and Critical Phenomena*, C. Domb and J. Lebowitz, eds., vol. 11. Academic Press, 1987.
- [194] M. Picco, S. Ribault, and R. Santachiara, “A conformal bootstrap approach to critical percolation in two dimensions,” *SciPost Phys.* **1** no. 1, (2016) 009, [arXiv:1607.07224 \[hep-th\]](#).
- [195] J. L. Jacobsen and H. Saleur, “Bootstrap approach to geometrical four-point functions in the two-dimensional critical Q -state Potts model: A study of the s -channel spectra,” [arXiv:1809.02191 \[math-ph\]](#).
- [196] R. Couvreur, J. Lykke Jacobsen, and R. Vasseur, “Non-scalar operators for the Potts model in arbitrary dimension,” *J. Phys.* **A50** no. 47, (2017) 474001, [arXiv:1704.02186 \[cond-mat.stat-mech\]](#).
- [197] G. Delfino and J. Viti, “Potts q -color field theory and scaling random cluster model,” *Nucl. Phys.* **B852** (2011) 149–173, [arXiv:1104.4323 \[hep-th\]](#).
- [198] H. Blöte and M. Nightingale, “Critical behaviour of the two-dimensional Potts model with a continuous number of states; A finite size scaling analysis,” *Physica A* **112** no. 3, (1982) 405 – 465.
- [199] J. Salas and A. D. Sokal, “Transfer Matrices and Partition-Function Zeros for Antiferromagnetic Potts Models. I. General Theory and Square-Lattice Chromatic Polynomial,” *J. Stat. Phys.* **104** no. 3, (2001) 609–699.
- [200] J.-F. Richard and J. L. Jacobsen, “Character decomposition of Potts model partition functions, I: Cyclic geometry,” *Nucl. Phys. B* **750** (2006) 250–264, [math-ph/0605016](#).
- [201] J. L. Jacobsen and J. Salas, “Phase diagram of the chromatic polynomial on a torus,” *Nucl. Phys.* **B783** (2007) 238–296, [arXiv:cond-mat/0703228 \[cond-mat.stat-mech\]](#).
- [202] R. Vasseur, J. Lykke Jacobsen, and H. Saleur, “Logarithmic observables in critical percolation,” *J. Stat. Mech.* **7** (2012) L07001, [arXiv:1206.2312 \[cond-mat.stat-mech\]](#).
- [203] J.-F. Richard and J. L. Jacobsen, “Eigenvalue amplitudes of the Potts model on a torus,” *Nucl. Phys. B* **769** (2007) 256–274, [math-ph/0608055](#).
- [204] B. Nienhuis, “Analytical calculation of two leading exponents of the dilute Potts model,” *J. Phys. A* **15** no. 1, (1982) 199.

- [205] H. Saleur and M. Bauer, “On Some Relations Between Local Height Probabilities and Conformal Invariance,” *Nucl. Phys.* **B320** (1989) 591–624.
- [206] J. L. Cardy, “The $O(n)$ model on the annulus,” *J. Statist. Phys.* **125** (2006) 1, [arXiv:math-ph/0604043](#) [math-ph].
- [207] P. Di Francesco, P. Mathieu, and D. Senechal, *Conformal Field Theory*. Springer-Verlag, New York, 1997.
- [208] N. Read and H. Saleur, “Exact spectra of conformal supersymmetric nonlinear sigma models in two-dimensions,” *Nucl. Phys.* **B613** (2001) 409, [arXiv:hep-th/0106124](#) [hep-th].
- [209] J. Kondev, “Liouville field theory of fluctuating loops,” *Phys. Rev. Lett.* **78** (1997) 4320–4323, [arXiv:cond-mat/9703113](#) [cond-mat].
- [210] G. Delfino and E. Tartaglia, “Classifying Potts critical lines,” *Phys. Rev.* **E96** no. 4, (2017) 042137, [arXiv:1707.00998](#) [cond-mat.stat-mech].
- [211] A. W. W. Ludwig and K. J. Wiese, “The 4-loop β -function in the 2D non-Abelian Thirring model, and comparison with its conjectured ‘exact’ form,” *Nucl. Phys.* **B661** (2003) 577–607, [arXiv:cond-mat/0211531](#) [cond-mat].
- [212] V. S. Dotsenko and V. A. Fateev, “Operator Algebra of Two-Dimensional Conformal Theories with Central Charge $c \leq 1$,” *Phys. Lett.* **154B** (1985) 291–295.
- [213] I. Esterlis, A. L. Fitzpatrick, and D. Ramirez, “Closure of the Operator Product Expansion in the Non-Unitary Bootstrap,” *JHEP* **11** (2016) 030, [arXiv:1606.07458](#) [hep-th].
- [214] R. Dijkgraaf, E. P. Verlinde, and H. L. Verlinde, “ $C = 1$ Conformal Field Theories on Riemann Surfaces,” *Commun. Math. Phys.* **115** (1988) 649–690.
- [215] M. Lässig, “Geometry of the renormalization group with an application in two dimensions,” *Nuclear Physics B* **334** no. 3, (1990) 652 – 668. <http://www.sciencedirect.com/science/article/pii/0550321390903166>.
- [216] J. Jaworowski, “On antipodal sets on the sphere and on continuous involutions,” *Fundamenta Mathematicae* **43** no. 2, (1956) 241–254.
- [217] J. L. Cardy and H. W. Hamber, “The $O(n)$ Heisenberg Model Close to $n = d = 2$,” *Phys. Rev. Lett.* **45** (1980) 499. [Erratum: *Phys. Rev. Lett.* 45,1217(1980)].
- [218] K. Symanzik, “On Calculations in conformal invariant field theories,” *Lett.Nuovo Cim.* **3** (1972) 734–738.
- [219] M. Picco, “Critical behavior of the Ising model with long range interactions,” [arXiv:1207.1018](#) [cond-mat.stat-mech].
- [220] T. Blanchard, M. Picco, and M. Rajabpour, “Influence of long-range interactions on the critical behavior of the Ising model,” *Europhys.Lett.* **101** (2013) 56003, [arXiv:1211.6758](#) [cond-mat.stat-mech].
- [221] M. C. Angelini, G. Parisi, and F. Ricci-Tersenghi, “Relations between short-range and long-range ising models,” *Phys. Rev. E* **89** (2014) 062120, [arXiv:1401.6805](#) [cond-mat.stat-mech].

Bibliography

- [222] S. S. Gubser, C. Jepsen, S. Parikh, and B. Trundy, “O(N) and O(N) and O(N),” [arXiv:1703.04202 \[hep-th\]](#).
- [223] G. Slade, “Critical exponents for long-range $O(n)$ models below the upper critical dimension,” [arXiv:1611.06169 \[math-ph\]](#).
- [224] Z. Komargodski, “Space of CFTs.” Exercise 1, 2017. <http://bootstrap.ictp-saifr.org/wp-content/uploads/2017/05/CPT-Exercise-1.pdf>.
- [225] K. Binder, “Theory of first-order phase transitions,” *Reports on Progress in Physics* **50** no. 7, (1987) 783.
- [226] S. S. Gubser and I. R. Klebanov, “A Universal result on central charges in the presence of double trace deformations,” *Nucl. Phys.* **B656** (2003) 23–36, [arXiv:hep-th/0212138 \[hep-th\]](#).
- [227] L. Landau and E. Lifshitz, *Statistical Physics*. Elsevier Science, 2013.
- [228] A. B. Zamolodchikov, “Conformal Symmetry and Multicritical Points in Two-Dimensional Quantum Field Theory.,” *Sov. J. Nucl. Phys.* **44** (1986) 529–533. [*Yad. Fiz.*44,821(1986)].
- [229] N. Amoruso, “Renormalization group flows between non-unitary conformal models.” Master thesis, Università di Bologna, 2016. <http://amslaurea.unibo.it/11308/>.
- [230] R. K. P. Zia and D. J. Wallace, “Critical Behavior of the Continuous N Component Potts Model,” *J. Phys.* **A8** (1975) 1495–1507.
- [231] D. Amit, “Renormalization of the Potts model,” *J. of Phys.* **A 9** no. 9, (1976) 1441.
- [232] P. H. Ginsparg, Y. Y. Goldschmidt, and J.-B. Zuber, “Large q Expansions for q State Gauge Matter Potts Models in Lagrangian Form,” *Nucl. Phys.* **B170** (1980) 409–432.
- [233] J. Kogut and D. Sinclair, “ $1/q$ -expansions for the lagrangian formulation of three-dimensional potts models,” *Solid State Communications* **41** no. 2, (1982) 187 – 190.
- [234] J. B. Kogut and D. Sinclair, “ $1/q$ expansions for potts models in all dimensions,” *Physics Letters A* **86** no. 1, (1981) 38 – 42.
- [235] D. Kim, “ $1/q$ -expansion for the magnetization discontinuity of potts model in two dimensions,” *Physics Letters A* **87** no. 3, (1981) 127 – 129.
- [236] H. Park and D. Kim, “Large q expansion of the Potts model susceptibility and magnetization in Two and Three dimensions,” *J. Korean Phys. Soc.* **15** no. 2, (1982) 55–60. <http://chris.kias.re.kr/papers/jkps-dkim82.pdf>.
- [237] T. Bhattacharya, R. Lacaze, and A. Morel, “Large q expansion of the 2D q -states Potts model,” *J. Phys. I(France)* **7** (1997) 81–103, [arXiv:hep-lat/9601012 \[hep-lat\]](#).
- [238] L. Laanait, A. Messenger, S. Miracle-Sole, J. Ruiz, and S. Shlosman, “Interfaces in the Potts model I: Pirogov-Sinai theory of the Fortuin-Kasteleyn representation,” *Comm. in Math. Phys.* **140** no. 1, (1991) 81–91.
- [239] H. Duminil-Copin, V. Sidoravicius, and V. Tassion, “Continuity of the phase transition for planar random-cluster and Potts models with $1 \leq q \leq 4$,” [arXiv:1505.04159 \[math.PR\]](#).

- [240] H. Duminil-Copin, M. Gagnebin, M. Harel, I. Manolescu, and V. Tassion, “Discontinuity of the phase transition for the planar random-cluster and Potts models with $q > 4$,” [arXiv:1611.09877 \[math.PR\]](#).
- [241] J. Lee and J. M. Kosterlitz, “Three-dimensional q -state Potts model: Monte Carlo study near $q = 3$,” *Phys. Rev. B* **43** (1991) 1268–1271.
- [242] B. Nienhuis, E. K. Riedel, and M. Schick, “ q -state potts model in general dimension,” *Phys. Rev. B* **23** (1981) 6055–6060.
- [243] K. E. Newman, E. K. Riedel, and S. Muto, “ Q -State Potts Model by Wilson’s Exact Renormalization Group Equation,” *Phys. Rev.* **B29** (1984) 302–313.
- [244] W. Janke and R. Villanova, “Three-dimensional 3-state potts model revisited with new techniques,” *Nuclear Physics B* **489** no. 3, (1997) 679 – 696.
- [245] H. Georgi, *Lie Algebras In Particle Physics: from Isospin To Unified Theories*. Frontiers in Physics. Avalon Publishing, 1999.
- [246] L. P. Kadanoff and A. C. Brown, “Correlation functions on the critical lines of the Baxter and Ashkin-Teller models,” *Annals Phys.* **121** (1979) 318–342.

Acknowledgements

When the first draft of this thesis was finally assembled, I thought "well, it didn't go so bad". So many different elements had to come together in order to make this last four years stimulating and enjoyable, both from the point of view of physics and of life in general, that I'm still surprised it worked out so smoothly.

It's not easy to quantify the importance that Slava Rychkov, my supervisor, had during these years. Not all good scientists are good supervisors, but I was lucky to find someone who is able to combine scientific excellence with an enormous dedication towards his students. Thanks to him I not only have a much clearer idea of science, but also of what it takes to be a good scientist. His approachability and his understanding of what was the best way to advise me made him an ideal supervisor for me (all of this despite the fact that I don't like rock climbing).

A special thanks goes also to my other supervisor, Riccardo Rattazzi, that definitely got the short end of the stick by being the person that I bothered when bureaucratic issues arised rather than when I had some interesting physics problem at hand. He played a vital role in making sure that my second half of the PhD occurred in one of the best possible ways (and place), with both my physics and non-physics life benefiting greatly from this.

I have enjoyed both discussions about physics and just about anything else with many other collaborators and fellow students. In Paris, I have to thank Emilio, Apratim and Miguel. In Lausanne, I have to thank Lorenzo, Marco, Denis, Andrea, Alessandro, my almost flatmate Kin, Marc and a few more. Many people in the Bootstrap collaboration also would deserve a proper thanking.

It has always been hard for me to forget that there is more to life than physics. With a life where we have completely abandoned any kind of geographical stability and moving every few years is forced on us, it can feel like finding one own's corner of the world is a hopeless or even pointless task. In my experience, this has been proven wrong by the people I met and shared times and places with. The biggest culprits have been the Ritals of Paris, that is Simone, Noemi, Michele, Mattia, Gaia, Adele, Sarina, Giulio, Jasmine, Martino, Andrea, Cate, Olivia, Duccio, Cosimo and many more. I learned a lot from you and, among all the pastis, you were the first reason why I was able to think about this grey metropolis as home. Turns out that, if you look well enough, there are also some non-italians in Paris, and they can be pretty sweet too. I have to thank Yanis, Michael, Eva, Mauri, Magu, for the spicy food, concerts, trips and beers. Of the people that passed through Lausanne, I have to thank Olivier a.k.a. Cayson, Marco, Tiziano and Asja.

In last acknowledgements I had to write, I talked a lot about some people which are still present in my life, four years later. I'm talking about Eugenio, Carlo, Freddy, Barginia, Elena, Robi and others from the

Acknowledgements

Amsterdam gang. My friendship with each one of you still goes on despite the distance, and you have no idea how much security this gives me in view of my future journeys.

It has been more than six years since I left Bologna, my hometown. I never had any doubts that these are not the kinds of roots to be easily canceled by a few years abroad, but every time I go back I find myself wondering whether leaving it, without any concrete plan to ever come back, was the right choice. And this is due to all the friends for which distance has never been an insurmountable obstacle. I would have to thank you all, but there are too many of you, really. But please know that if crossing this ocean is so difficult for me, it's mostly because of you all.

Some more abstract entities or collectives of people have played a significant role in these few years. I need to mention King Gizzard and the Lizard Wizard for being the main soundtrack of these years, the ASPA in Montreuil for making combat sports a better experience and for the bruised ribs, and the Sharknado movie series for lowering my intellectual standards way below where they should be.

And finally, there's those from which it all started. My parents who, among other things, first instilled in me and then seconded a curiosity to see the world, and then never complained too much any time their son, who lives far away, forgot to call them. My sister, who I look up to very much. And my grandma, who passed away when the first pages of this manuscript were being put together.

Paris, June 2019

*"Oh, if the trip and the plan come apart in your hand
You can turn it on yourself, you ridiculous clown
You forgot what you meant when you read what you said
And you always knew you were tired, but then
Where are your friends tonight?"*

– LCD Soundsystems, All My Friends

Bernardo Zan – Curriculum Vitae

Date of Birth	7 September 1990	Email	bernardo.zan@epfl.ch
Place of Birth	Bologna, Italy	ORCID	0000-0002-5218-5540
Nationality	Italian		

Education

- Oct 2015 - Present** **Doctoral studies in Theoretical Physics**
Theoretical Particle Physics Laboratory, Institute of Physics
École polytechnique fédérale de Lausanne, Switzerland
Thesis Director: Prof. Riccardo Rattazzi
Thesis Co-director: Prof. Vyacheslav Rychkov, ENS, Paris
Thesis title: “*Studies in strongly coupled quantum field theories and renormalization group flows*”
- Oct 2015 - Sep 2017** **Cooperative Associate**
CERN, Geneva
- Feb 2013 - Jun 2015** **Master in Theoretical Physics, cum laude**
Institute for Theoretical Physics, Universiteit van Amsterdam
Master Project: “*Investigating the ER=EPR correspondence: a field theory study of long wormholes*”. Advisor: Prof. Jan de Boer
GPA: 9.2/10
- Sep 2009 - Oct 2012** **Bachelor in Physics, cum laude**
University of Bologna
Final grade: 110/110
GPA: 29.7/30

Publications

- M. F. Paulos, S. Rychkov, B. C. van Rees, and B. Zan, “Conformal Invariance in the Long-Range Ising Model,” *Nucl. Phys.* **B902** (2016) 246–291, arXiv:1509.00008 [hep-th]
- S. Rychkov, D. Simmons-Duffin, and B. Zan, “Non-gaussianity of the critical 3d Ising model,” *SciPost Phys.* **2** (2017) 001, arXiv:1612.02436 [hep-th]
- C. Behan, L. Rastelli, S. Rychkov, and B. Zan, “Long-range critical exponents near the short-range crossover,” *Phys. Rev. Lett.* **118** no. 24, (2017) 241601, arXiv:1703.03430 [cond-mat.stat-mech]
- C. Behan, L. Rastelli, S. Rychkov, and B. Zan, “A scaling theory for the long-range to short-range crossover and an infrared duality,” *J. Phys.* **A50** no. 35, (2017) 354002, arXiv:1703.05325 [hep-th]
- V. Gorbenko, S. Rychkov, and B. Zan, “Walking, Weak first-order transitions, and Complex CFTs,” *JHEP* **10** (2018) 108, arXiv:1807.11512 [hep-th]
- V. Gorbenko, S. Rychkov, and B. Zan, “Walking, Weak first-order transitions, and Complex CFTs II. Two-dimensional Potts model at $Q > 4$,” *SciPost Phys.* **5** no. 5, (2018) 050, arXiv:1808.04380 [hep-th]
- M. F. Paulos and B. Zan, “A functional approach to the numerical conformal bootstrap,” arXiv:1904.03193 [hep-th]

Talks

	"A scaling theory from the long-range to short-range crossover"
Jun 2017	Bootstrap 2017, Sao Paulo, Brazil:
	"Walking, weakly first order phase transitions and complex CFTs"
May 2018	DESY, Hamburg, Germany
Jun 2018	EPFL, Lausanne, Switzerland
Oct 2018	SISSA, Trieste, Italy
Oct 2018	Scuola Normale Superiore, Pisa, Italy
Oct 2018	UC Davis, Davis, US
Oct 2018	Stanford University, Palo Alto, US
Oct 2018	Johns Hopkins University, Baltimore, US
Oct 2018	Brown University, Providence, US
Oct 2018	Boston University, Boston, US
Nov 2018	Columbia University, New York, US
Nov 2018	Cornell University, Ithaca, US
Nov 2018	McGill University, Montreal, Canada
Nov 2018	Queen Mary University, London, UK
Dec 2018	Yale University, New Haven, US
Jan 2019	CERN, Geneva, Switzerland

Teaching activities

Nov 2013 - Dec 2014	Teaching assistant for the course Condensed Matter II University of Amsterdam
Feb 2014 - Mar 2014	Teaching assistant for the course Electrodynamics and theory of relativity II University of Amsterdam
Feb 2016 - Jun 2016	Teaching assistant for the course Statistical Physics II
Feb 2017 - Jun 2017	EPFL

Computer skills

Knowledge of Mathematica, Python, LaTeX, Linux, Office.

Languages

- Italian: native language
- English: fluent
- Spanish: intermediate
- French: intermediate

May 16, 2019

